R/V Mirai Cruise Report

MR19-03C

Arctic Challenge for Sustainability (ArCS)

Arctic Ocean, Bering Sea and North Pacific

28 September 2019 – 10 November 2019

Japan Agency for Marine-Earth Science and Technology (JAMSTEC)

Contents

1. Cruise Summary

1.1 Objectives

In recent year, sea-ice freeze-up has been delayed over the northern Bering Sea, and Chukchi Sea during autumn, causing decline of Arctic sea-ice extent in autumn and winter. The decrease in sea-ice extent leads to changes in atmosphere, ocean and ecosystem over the Arctic region. Those changes would influence on not only regional but also global climates.

The objectives of this cruise are as follows:

(1) To quantify of on-going changes in atmosphere, sea ice, ocean and ecosystem, including wave situation and environmental chemical cycle during autumn

(2) To understand process and interactions among atmosphere, sea ice, ocean and ecosystem

(3) To investigate the influence of the Arctic Ocean change on global climate during autumn

In addition to above, the Multidisciplinary drifting Observatory for the Study of Arctic Climate (MOSAiC) has been started since September 2019 to conduct year-round measurements by the German icebreaker Polarstern. The combination of MOSAiC and our cruise provides a great opportunity to investigate differences in atmospheric and oceanographic structures between sea ice and open water areas.

1.2 Basic information

Cruise ID:	MR19-03C
Name of vessel:	R/V Mirai
	L x B x D 118.02m x 19.0m x 13.2m
	Gross Tonnage: 8,706 tons
	Call Sign JNSR
Title of the cruise:	Arctic Challenge for Sustainability (ArCS)
Undertaking institute:	Japan Agency for Marine-Earth Science and Technology (JAMSTEC)
Chief scientist:	Kazutoshi Sato (Kitami Institute of Technology)
Cruise period:	27 September 2019 – 10 November 2019
Ports of call:	27 September 2019, Sekinehama (leave port)
	29 September 2019, Hachinohe (arrival in and leave port)
	10 November 2019, Hachinohe (arrival in port)
Research area:	The North Pacific Ocean, the Bering Sea, and the Arctic Ocean
Research Map:	

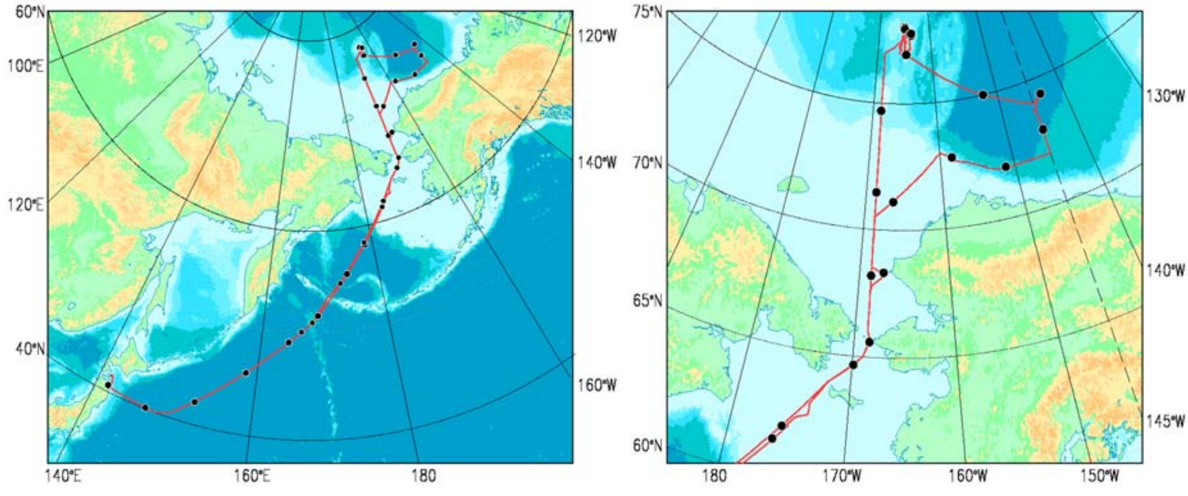

Figure 1.2: Cruise track and points at 00UTC for each day of MR19-03C.

1.3 Atmospheric and Oceanographic Overview during the cruise

Meteorological and oceanographic observations were made in the north Pacific ocean, the Bering Sea and the Arctic ocean on board the R/V Mirai from 28 September 2019 to 10 November 2019 as a part of the Arctic Challenge for Sustainability (ArCS) project (Figure 1.2). During this cruise, the R/V Mirai entered the northern Chukchi Sea (78.2°N). Because the sea ice extent during October in the Arctic Ocean was the minimum record since 2002, in particular Chukchi and Beaufort Seas. Based on the NCEP CFSR reanalysis data, the negative sea ice concentration anomaly is found over the Chukshi Sea compared with early 2000s (Figure 1.3-1 left). The monthly averaged sea surface temperature (SST) was abnormally high (> 2 ˚C) over the northern Chukchi Sea (Figure 1.3-1 right) during October, suggesting that the delay of freezing in the northern Chukchi Sea was expected.

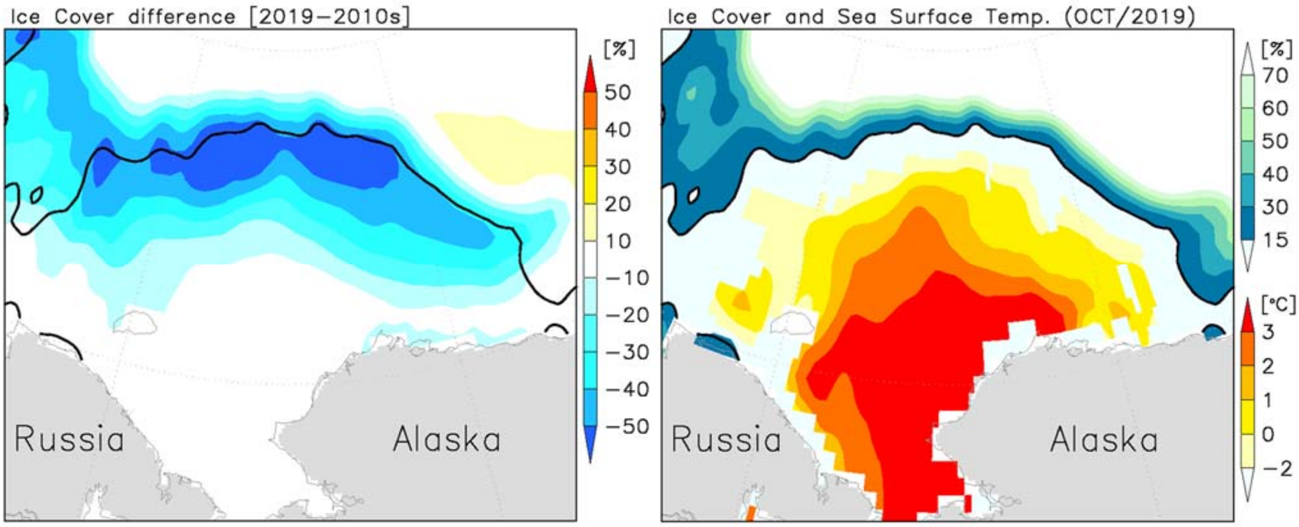

Figure 1.3-1: (Left) Difference map of ice cover between 2019 and 2010s during October (shaded) with ice area exceeding 15% on October 2019 (contor). (Right) Maps of averaged Ice cover and sea surface temperature during October 2019 derived from the NCEP CFSR reanalysis data.

To investigate the vertical structure of ocean and sample the water over the Arctic Ocean, we carried out CTD observation, (Table 1.3). In addition, Zooplankton samples were always collected by plankton nets with CTD observations. Over the southern Chukchi Sea, Smith-McIntyre sampler collected Sea bottom sediments. The tethered balloon observation conducted to measure the vertical profiles of particle number concentration, BC mass concentration and particle size distribution over the Pacific and Arctic oceans. Over the sea ice area, surface temperature and distributions of sea ice are monitored by drone observations. To measure wave height and upper ocean current, drifting buoys were deployed over the Canada basin and near Barrow.

After wave buoy deployments over the ice-free and ice-covered regions in the Canada Basin on 13 October, we made a daily repeat section over the northern Chukchi Sea (Figure 1.3-2). This repeat section consists of a station of marginal ice zone and open water zone. We had one station in the marginal ice zone and 3 or 4 stations over the open water area for each day. The position of the station of MIZ varied every day due to sea-ice advance/retreat. During repeat section period, the CTD, plankton and CPS observations were conducted in the open water area during nighttime every day. In contrast, the tethered balloon and drone observations were carried out over the marginal ice zone when wind speed is weaker than about 5 m/s. The radiosonde observations were conducted every 6-hour.

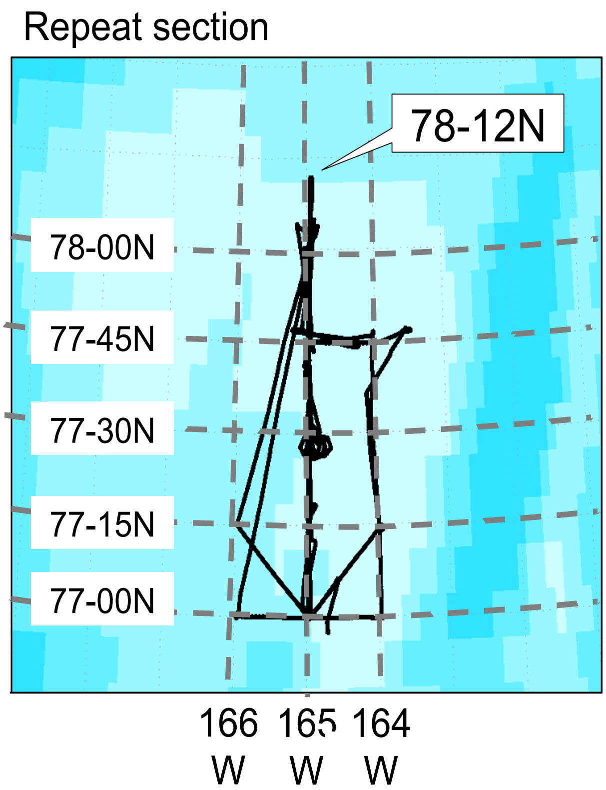

Figure 1.3-2: A map of repeat station.

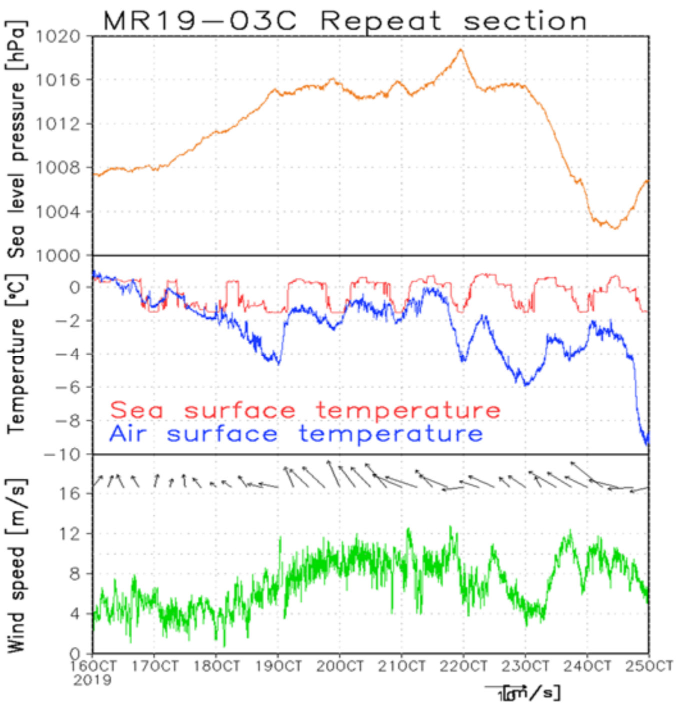

Figure 1.3-3: Time series of sea level pressure, surface temperatures of water and air, wind speeds, observed by RV Mirai during the repeat section.

There are two weather regimes (Figure 1.3-3). The first one is a moderate southerly wind condition with high air temperature (around -2˚C) from open water area (16-22 October). At the first day of the repeat section, small ice floes were found at the northern part (around 78˚N) of the repeat section (Figure 1.3-4). However, a warm air advection would reduce of sea ice formation. The second one is a moderate southwesterly wind condition with low air temperature (around -4˚C) from sea ice area (23-25 October). Overall, this repeat section provides unique opportunities to understand the recent delay of freezing during early autumn.

Figure 1.3-4: Photos taken at northernmost point in marginal ice zone for each day (on 16, 17, 18 and 19 November 2019) during repeat section.

To achieve this challenging cruise, precise weather and sea-ice forecasts are necessary for safe navigation and valuable observing activities. This cruise was supported by the operational forecasts provided from ECMWF and ECCC as a part of Year of Polar Prediction (YOPP). In addition to this, the Japanese National Institute of Polar Research (NIPR) has developed the Vessel Navigation Unit support System (VENUS) to receive and process the forecast data automatically on the ship. To decide the observing point and manage the cruise schedule, the chief scientist used these useful information, in particular near sea ice area.

Table 1.3: List of observation points of MR19-03C

								Activities						
Sta. no for schedule	Information							CTD	XCTD	RINKO	NORPAC net	Ring net	Closing net	Sediments net
sta. 000		50	0.00	N	166	7.63	E	○ (000-1,2)		○ (000)				
sta. 001		62	0.60	N	175	3.60	W							
sta. 002		62	3.00	N	175	12.60	W							
sta. 003		62	13.14	N	174	52.62	W							
sta. 004		62	23.40	N	174	34.20	W							
sta. 005		62	28.08	N	174	4.98	W							
sta. 006		62	33.60	N	173	33.00	W							
sta. 007		62	47.22	N	173	30.00	W							
sta. 008		63	2.00	N	173	27.60	W							
sta. 009		63	16.80	N	173	4.80	W							
sta. 010		63	36.24	N	172	35.46	W							
FP-1		64	40.13	N	169	55.15	W			○ (001)	○			○
sta. 011		65	38.00	N	168	28.00	W	○ (001)			○			
sta. 012		66	0.00	N	168	45.00	W	○ (002)						
sta. 013		66	30.00	N	168	45.00	W	○ (003)			○			
sta. 014		67	0.00	N	168	45.00	W	○ (004)			○		○	○
sta. 015		67	30.00	N	168	45.00	W		○					
sta. 016		68	0.00	N	168	45.00	W		○					
FT-1		68	9.91	N	168	45.38	W			○ (002)				
sta. 017		68	30.00	N	168	45.00	W		○					
sta. 018		69	0.00	N	168	45.00	W	○ (005)			○			○
sta. 019		69	30.00	N	168	45.00	W	○ (006)			○			
sta. 020		70	0.00	N	168	45.00	W	○ (007)						
sta. 021		70	30.00	N	168	45.00	W	○ (008)			○		○	○
sta. 022		71	0.00	N	167	0.00	W		○					
FT-2		71	6.54	N	166	30.65	W			○ (003)				
sta. 023		71	30.00	N	165	15.00	W		○					
sta. 024		72	0.00	N	163	30.00	W	○ (009)			○		○	○

sta. 025		72	30.00	N	161	45.00	W	○ (010)			○			
sta. 026		73	0.00	N	160	0.00	W	○ (011)			○			
sta. 027		72	50.00	N	158	45.00	W							
FT-3		72	46.90	N	158	22.49	W			○ (004)				
sta. 028		72	40.00	N	157	30.00	W							
sta. 029		72	30.00	N	156	15.00	W	○ (012)			○			
sta. 030		72	20.00	N	155	0.00	W	○ (013)			○			
sta. 031		72	10.00	N	153	45.00	W	○ (014)			○			
sta. 032		72	0.00	N	152	30.00	W							
FT-4		72	0.62	N	151	17.73	W			○ (005)				
sta. 033		72	0.00	N	150	0.00	W							
sta. 034		72	0.00	N	147	30.00	W	○ (015)	○		○			
sta. 035		72	0.00	N	145	0.00	W	○ (016)			○			
FT-5		72	58.53	N	144	55.52	W			○ (006)				
sta. 036		73	0.00	N	145	0.00	W							
sta. 037		74	0.00	N	145	0.00	W							
FT-6		74	20.08	N	143	30.89	W			○ (007)				
FP-2		74	46.09	N	150	30.13	W	○ (017)			○		○	
FT-7		74	59.96	N	152	16.15	W			○ (008)				
FP-3		76	27.95	N	161	38.51	W	○ (018)			○			
sta. 038		76	30.00	N	165	0.00	W							
FT-8		76	57.80	N	164	45.19	W			○ (009)				
sta. 39-1	Repaeat Day 1	77	0.00	N	165	0.00	W	○ (019-1)			○	○		
sta. 40-1	Repaeat Day 1	77	15.00	N	165	0.00	W	○ (020-1)						
FP-4	Repaeat Day 1	77	15.10	N	164	59.48	W			○ (010)				
FT-9 (MIZ-1)	Repaeat Day 1	78	3.94	N	164	56.89	W			○ (011)	○	○		
FP-5	Repaeat Day 1	77	53.38	N	164	59.98	W			○ (012)				

sta. 40-2	Repaeat Day 2	77	15.00	N	165	0.00	W	○ (020-2)			○	○		
sta. 41-1	Repaeat Day 2	77	30.00	N	165	0.00	W	○ (021-1)						
sta. 42-1	Repaeat Day 2	77	45.00	N	165	0.00	W	○ (022-1)			○			
FT-10 (MIZ-2)	Repaeat Day 2	78	0.28	N	164	59.05	W			○ (013)	○	○		
FP-6	Repaeat Day 2	77	45.12	N	165	0.00	W			○ (014)				
sta. 40-3	Repaeat Day 3	77	15.00	N	165	0.00	W	○ (020-3)			○	○		
sta. 41-2	Repaeat Day 3	77	30.00	N	165	0.00	W	○ (021-2)						
sta. 42-2	Repaeat Day 3	77	45.00	N	165	0.00	W	○ (022-2)			○			
FP-7	Repaeat Day 3	78	2.13	N	164	58.49	W	○ (022-2)						
FT-11 (MIZ-3)	Repaeat Day 3	78	3.87	N	165	10.12	W	○ (023)		○ (015)	○	○		
FP-8	Repaeat Day 3	77	45.21	N	164	59.79	W			○ (016)				
sta. 39-2	Repaeat Day 4	77	0.00	N	165	0.00	W	○ (019-2)			○	○		
sta. 40-4	Repaeat Day 4	77	15.00	N	165	0.00	W	○ (020-4)						
sta. 41-3	Repaeat Day 4	77	30.00	N	165	0.00	W	○ (021-3)			○			
FT-12 (MIZ-4)	Repaeat Day 4	78	3.06	N	164	59.60	W			○ (017)	○	○		
FP-9	Repaeat Day 4	77	45.16	N	165	0.32	W			○ (018)				
sta. 39-3	Repaeat Day 5	77	0.00	N	165	0.00	W	○ (019-3)			○	○		
sta. 40-5	Repaeat Day 5	77	15.00	N	165	0.00	W	○ (020-5)						
sta. 41-4	Repaeat Day 5	77	30.00	N	165	0.00	W	○ (021-4)			○			
FP-10	Repaeat Day 5	77	44.98	N	164	59.95	W			○ (019)				
FT-13 (MIZ-5)	Repaeat Day 5	78	0.92	N	164	58.44	W			○ (020)	○	○		
sta. 043	Repaeat Day 6	77	15.00	N	166	0.00	W	○ (024)			○	○		
sta. 39-4	Repaeat Day 6	77	0.00	N	165	0.00	W	○ (019-4)			○	○		
sta. 40-6	Repaeat Day 6	77	15.00	N	165	0.00	W	○ (020-6)						
sta. 41-5	Repaeat Day 6	77	30.00	N	165	0.00	W	○ (021-5)						

FP-11	Repaeat Day 6	77	44.87	N	164	59.98	W			○ (021)				
FT-14 (MIZ-6)	Repaeat Day 6	78	1.55	N	164	57.64	W			○ (022)	○	○		
sta. 044	Repaeat Day 7	77	0.00	N	166	0.00	W	○ (025)			○	○		
sta. 39-5	Repaeat Day 7	77	0.00	N	165	0.00	W	○ (019-5)			○	○		
sta. 40-7	Repaeat Day 7	77	15.00	N	165	0.00	W	○ (020-7)						
sta. 41-6	Repaeat Day 7	77	30.00	N	165	0.00	W	○ (021-6)						
FP-12	Repaeat Day 7	77	44.96	N	165	0.00	W			○ (023)				
FT-15 (MIZ-7)	Repaeat Day 7	77	46.14	N	164	5.42	W			○ (024)	○	○		
sta. 045	Repaeat Day 8	77	0.00	N	164	0.00	W	○ (026)			○	○		
sta. 39-6	Repaeat Day 8	77	0.00	N	165	0.00	W	○ (019-6)			○	○		
sta. 40-8	Repaeat Day 8	77	15.00	N	165	0.00	W	○ (020-8)						
sta. 41-7	Repaeat Day 8	77	30.00	N	165	0.00	W	○ (021-7)						
FP-13	Repaeat Day 8	77	44.98	N	165	0.31	W			○ (025)				
FT-16 (MIZ-8)	Repaeat Day 8	77	47.02	N	163	35.81	W			○ (026)	○	○		
sta. 046	Repaeat Day 9	77	15.00	N	164	0.00	W	○ (027)			○	○		
sta. 39-7	Repaeat Day 9	77	0.00	N	165	0.00	W	○ (019-7)			○	○		
sta. 40-9	Repaeat Day 9	77	15.00	N	165	0.00	W	○ (020-9)						
sta. 41-8	Repaeat Day 9	77	30.00	N	165	0.00	W	○ (021-8)						
FP-14	Repaeat Day 9	77	44.99	N	165	0.32	W			○ (027)				
FT-17 (MIZ-9)	Repaeat Day 9	77	47.62	N	163	40.60	W			○ (028)	○	○		
sta. 046		77	15.00	N	164	0.00	W							
sta. 047		77	30.00	N	168	45.00	W							
sta. 048		77	15.00	N	168	45.00	W							
sta. 049		77	0.00	N	168	45.00	W	○ (028)			○	○		
sta. 050		76	0.00	N	168	45.00	W		○					
sta. 051		75	0.00	N	168	45.00	W							
FT-18		74	41.30	N	168	45.66	W			○ (029)	○			

sta. 052		74	0.00	N	168	45.00	W	○ (029)			○	○		
sta. 053		73	30.00	N	168	45.00	W	○ (030)						
sta. 054		73	0.00	N	168	45.00	W	○ (031)			○	○		
sta. 055		72	30.00	N	168	45.00	W	○ (032)						
sta.056		72	0.00	N	168	45.00	W			○ (030-1, 2)	○			
sta.057 (FT-19)		71	30.00	N	168	45.00	W			○ (031)				
sta. 058		71	0.00	N	168	45.00	W			○ (032)	○	○		
sta. 059		70	30.00	N	168	45.00	W	○ (033)						
sta. 060		70	0.00	N	168	45.00	W	○ (034)			○	○		○
sta. 061		69	30.00	N	168	45.00	W	○ (035)			○	○		
sta. 062		69	0.00	N	168	45.00	W	○ (036)			○	○		
sta. 063		68	30.00	N	168	45.00	W			○ (033)	○	○		
FT-20		68	18.12	N	167	23.01	W			○ (034)				
sta. 064		68	18.00	N	166	56.10	W				○			
sta. 065		68	14.52	N	167	7.32	W							
sta. 066		68	11.10	N	167	18.48	W							
sta. 067		68	7.68	N	167	29.70	W							
sta. 068		68	0.78	N	167	52.02	W	○ (037)			○	○		○
sta. 069		67	53.88	N	168	14.10	W							
sta. 070		67	46.98	N	168	36.12	W	○ (038)			○	○		○
sta. 071		67	30.00	N	168	45.00	W	○ (039)			○			
sta. 072		67	0.00	N	168	45.00	W	○ (040)			○			
sta. 073		66	30.00	N	168	45.00	W	○ (041)						
sta. 074		66	0.00	N	168	45.00	W			○ (035)				
FT-21		65	36.85	N	168	28.79	W			○ (036)				
sta. 000-2		50	0.00	N	166	7.63	E	○ (000-3,4)	○	○ (037)				

1.4 List of participants

Table 1.4: List of participants of MR19-03C

No.	Name	Organization	Position
1	Kazutoshi Sato	Kitami Institute of Technology (KIT)	Assistant professor
2	Akihiko Murata	Japan Agency for Marine-Earth Science and Technology (JAMSTEC)	Superior researcher
3	Jun Inoue	National Institute of Polar Research (NIPR)	Associate professor
4	Jumpei Yamamoto	Tokyo University of Marine Science and Technology	Graduate student
5	Rio Maya	Tokyo University of Marine Science and Technology	Project researcher
6	Eri Yoshizawa	Korea Polar Research Institute	Research scientist
7	Tsubasa Kodaira	The University of Tokyo	Assistant professor
8	Ryo Kusakawa	The University of Tokyo	Graduate student
9	Eun Yae Son	The University of Tokyo	Graduate student
10	Kohei Matsuno	Hokkaido University	Assistant professor
11	Koki Tokuhiro	Hokkaido University	Graduate student
12	Fumihiko Kimura	Hokkaido University	Graduate student
13	Nao Sato	Hokkaido University	Graduate student
14	Hotaek Park	Japan Agency for Marine-Earth Science and Technology (JAMSTEC)	Senior scientist
15	Fumikazu Taketani	Japan Agency for Marine-Earth Science and Technology (JAMSTEC)	Senior scientist
16	Taro Maruo	Japan Agency for Marine-Earth Science and Technology (JAMSTEC) / University of Kobe	Research student / Graduate student
17	Minoru Hamana	Japan Agency for Marine-Earth Science and Technology (JAMSTEC)	Research scientist
18	Ryo Oyama	Nippon Marine Enterprises, Ltd. (NME)	Technical staff
19	Souichiro Sueyoshi	Nippon Marine Enterprises, Ltd. (NME)	Technical staff
20	Shinya Okumura	Nippon Marine Enterprises, Ltd. (NME)	Technical staff
21	Kazuho Yoshida	Nippon Marine Enterprises, Ltd. (NME)	Technical staff
22	Yutaro Murakami	Nippon Marine Enterprises, Ltd. (NME)	Technical staff
23	Masanori Enoki	Marine Works Japan Ltd. (MWJ)	Technical staff
24	Jun Matsuoka	Marine Works Japan Ltd. (MWJ)	Technical staff
25	Masahiro Orui	Marine Works Japan Ltd. (MWJ)	Technical staff
26	Shinichiro Yokogawa	Marine Works Japan Ltd. (MWJ)	Technical staff
27	Keitaro Matsumoto	Marine Works Japan Ltd. (MWJ)	Technical staff
28	Hiroshi Hoshino	Marine Works Japan Ltd. (MWJ)	Technical staff
29	Atsushi Ono	Marine Works Japan Ltd. (MWJ)	Technical staff
30	Tomomi Sone	Marine Works Japan Ltd. (MWJ)	Technical staff
31	Erii Irie	Marine Works Japan Ltd. (MWJ)	Technical staff
32	Yuko Miyoshi	Marine Works Japan Ltd. (MWJ)	Technical staff
33	Mikio Kitada	Marine Works Japan Ltd. (MWJ)	Technical staff
34	Shinsuke Toyota	Marine Works Japan Ltd. (MWJ)	Technical staff
35	Shungo Oshitani	Marine Works Japan Ltd. (MWJ)	Technical staff
36	Rio Kobayashi	Marine Works Japan Ltd. (MWJ)	Technical staff
37	Kanako Yoshida	Marine Works Japan Ltd. (MWJ)	Technical staff
38	Tun Htet Aung	Marine Works Japan Ltd. (MWJ)	Technical staff
39	David Snider	Martech Polar Consulting Ltd.	Ice Navigator

2. Meteorology

2.1 GPS Radiosonde

(1) Personnel

Jun Inoue	NIPR	- Principle Investigator (PI)
Kazutoshi Sato	KIT	
Jumpei Yamamoto	Tokyo University of Marine Science and Technology	
Hotaek Park	JAMSTEC	
Taro Maruo	JAMSTEC	
Ryo Oyama	NME	
Shinya Okumura	NME	
Kazuho Yoshida	NME	
Yutaro Murakami	NME	
Soichiro Sueyoshi	NME	

(2) Objectives

To understand the thermodynamic structure of the boundary layer, and migratory cyclones and anticyclones, GPS radiosonde observations were made from 12 UTC 30 September to 00 UTC 1 November. Obtained data will be used mainly for studies of clouds, validation of reanalysis data as well as satellite analysis, and data assimilation. They were also used for briefing information of drone flights (section 2.6) and tethered balloon launches (section 2.10.2).

(3) Parameters

Temperature, Humidity, Pressure, Wind speed and direction.

(4) Instruments and Methods

Two types of GPS radiosondes were used: Vaisala RS41-SG for 00 and 12 UTC launches, and Vaisala RS41-SGP for 06 and 18 UTC launches. The observing frequency over the Arctic Ocean (the north of the Bering Strait) was 4 times launches per day(00, 06, 12, and 18 UTC), and over the other areas (the Bering Sea, and North Pacific) was twice daily launches (00, and 12 UTC), respectively. We used software (MW41 Vaisala Sounding System; version 2.11.0), processor (SPS311), GPS antenna (GA20), UHF antenna (RB21) and balloon launcher (ASAP) made by VaisalaOyj. Prior to launch, humidity, air temperature, and pressure sensors were calibrated by using the calibrator system (RI41 and PTB330, Vaisala). In case the relative wind to the ship is not appropriate for the launch, the handy launch was selected. For every launch, TOTEX 350g balloon was used.

Several simultaneous observations with the Cloud Particle Sensor (CPS) sonde (section 2.2) were made mainly during night time (e.g. 06 UTC), which indicated in the remarks in the Table 2.1 as “CPS exp.”. Most of the data went into Global Telecommunication System (GTS)though the Japan Meteorological Agency immediately after each observation, and were used for the operational weather forecasts.

(5) Station List

Table 2.1 summarizes the log of the GPS radiosondes observations. Raw data was recorded as binary format during ascent. ASCII data was converted from raw data.

(6) Preliminary results

Locations of all radiosonde observations during the cruise are shown in Figure 2.1-1. A time-height cross section of observed air temperature and wind during the cruise are shown in Figure 2.1-2. During 16-25

October, a daily repeat section was made to understand differences in atmospheric and oceanic characteristics between the marginal ice zone and open ocean. The radiosonde observation was conducted at near the marginal ice zone (MIZ) at 00 UTC (the northernmost point in the section), while the observation at the southernmost observation was made at 18 UTC during the period.

The most of the period is characterized by southerly winds from low pressure systems over the Bering Sea, enhancing the intrusion of warm air masses into the north of Chukchi Sea. The tropopause height was recorded 11km which was abnormally high in this season and latitude (78˚N) over the MIZ. On the last day of this section (25 October), strong northerly winds with relatively cold airmass from the northern sea ice region was prevailed

(7) Data Archive

These data obtained in this cruise will be submitted to the Data Management Group of JAMSTEC, and will be opened to the public via "Data Research System for Whole Cruise Information in JAMSTEC (DARWIN)" in JAMSTEC web site. http://www.godac.jamstec.go.jp/darwin/e

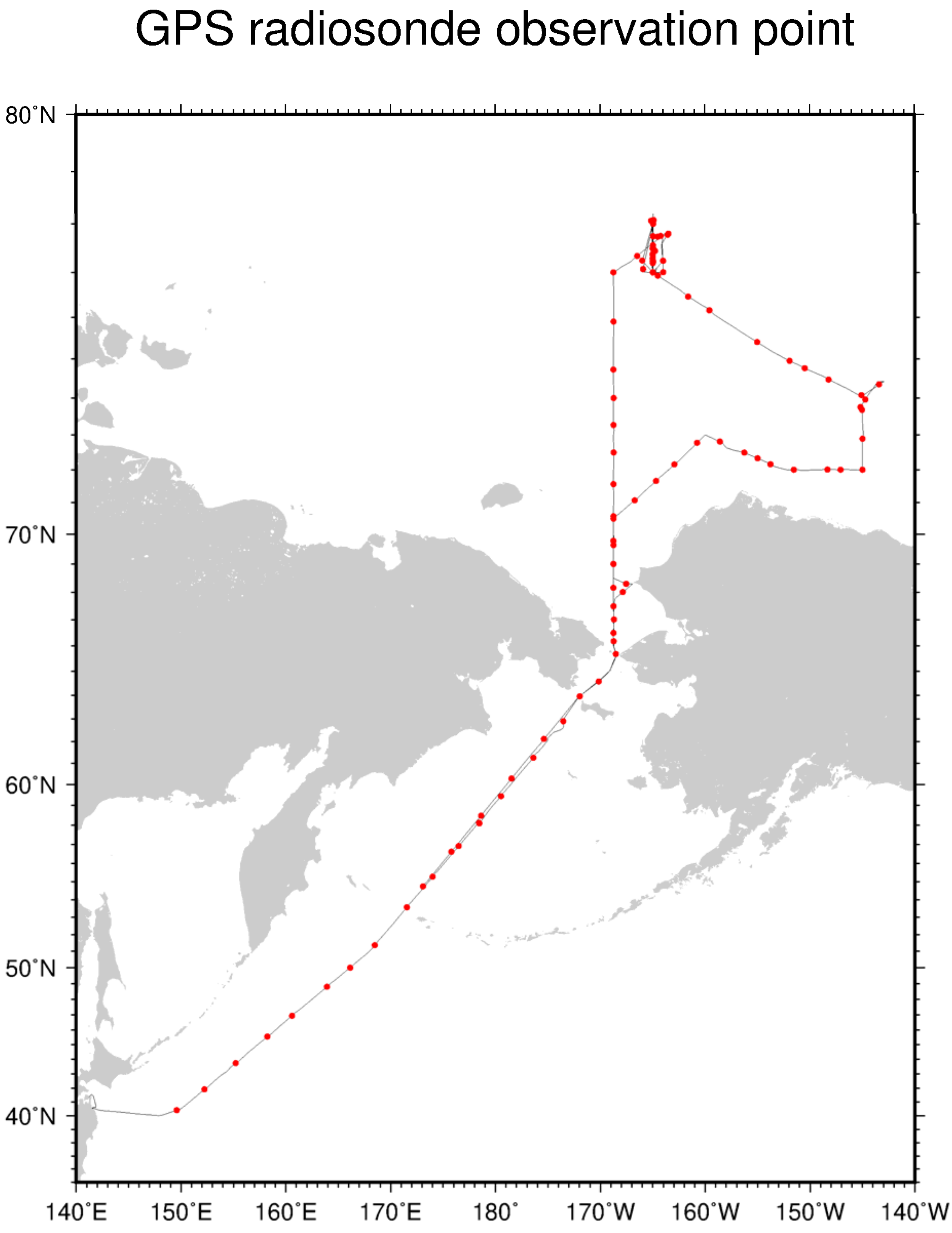

Figure 2.1-1: Sounding stations during the cruise.

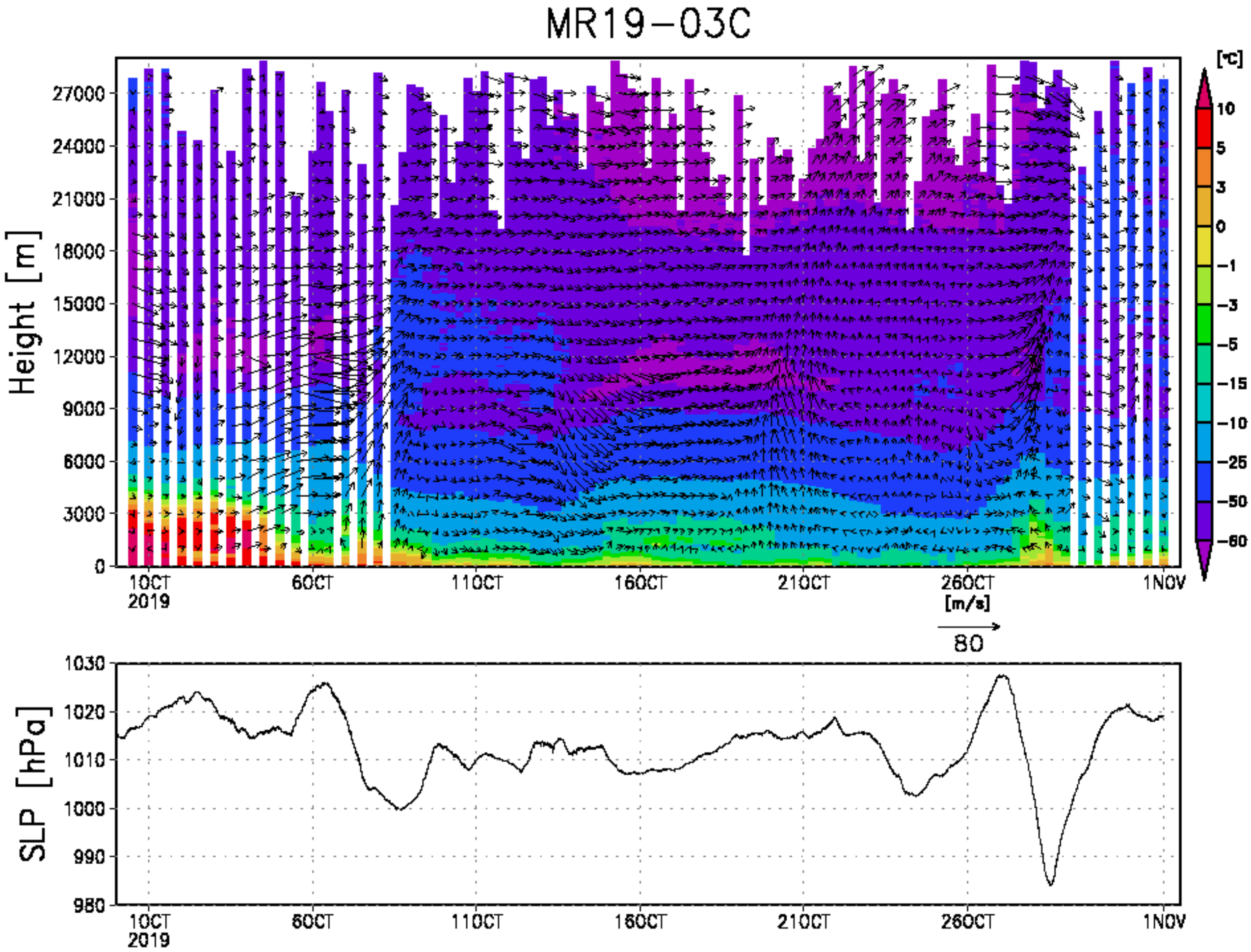

Figure 2.1-2: (a) Time-height cross section of air temperature (shade) and wind (vectors), and (b) time series of sea level pressure.

Table 2.1: Launch log

ID	Date	Latitude	Longitude	Psfc	Tsfc	RHsfc	WD	Wsp	SST	Max height			Cloud		remarks
	YYYYMM DDHH	degN	degE	hPa	degC	%	deg	m/s	degC	hPa	m	Duration	Amount	Type	
RS001	2019093012	40.405	149.586	1014.3	19.5	84	335	8.6	21.77	16.4	27906	6694	-	-	
RS002	2019100100	41.910	152.235	1016.5	19.1	74	63	6.9	19.58	15.2	28388	6475	9	Cu,Sc	
RS003	2019100112	43.744	155.215	1018.7	12.5	98	56	7.0	13.53	15.1	28406	6656	-	-	
RS004	2019100200	45.558	158.235	1020.6	9.7	83	44	5.5	11.29	26.1	24827	5456	10	St	
RS005	2019100212	46.937	160.596	1021.7	7.9	69	245	2.9	9.57	28.2	24334	5637	-	-	
RS006	2019100300	48.803	163.926	1019.1	8.3	78	241	11.1	9.43	18.1	27178	5600	10	Sc	
RS007	2019100312	49.991	166.129	1016.0	9.4	85	232	14.6	9.33	30.8	23760	5326	-	-	
RS008	2019100400	51.359	168.484	1013.2	9.9	96	234	14.5	9.87	14.9	28411	6206	10	St	
RS009	2019100412	53.579	171.543	1013.3	9.9	90	244	10.0	9.77	13.8	28862	7109	-	-	
RS010	2019100500	55.281	174.007	1014.2	8.4	85	171	6.1	9.94	15	28318	6233	10	Cu,Sc	
RS011	2019100512	56.916	176.484	1015.3	7.5	77	325	9.5	9.82	45.6	21206	4974	-	-	
RS012	2019100600	58.118	178.431	1022.0	6.1	55	338	1.6	9.52	30.7	23743	5146	1	As	
RS013	2019100602	58.081	178.454	1022.3	6.3	54	115	0.7	9.58	16.7	27675	6256	9	Sc,As	
RS014	2019100612	59.435	-179.475	1023.2	5.1	61	153	2.7	9.06	21.6	26005	6124	-	-	
RS015	2019100700	61.255	-176.396	1017.3	5.5	72	144	13.5	7.39	17.9	27201	6127	10	Cu,As	
RS016	2019100712	62.898	-173.539	1005.6	5.8	96	140	15.0	5.71	34.3	22987	5066	-	-	
RS017	2019100800	64.580	-170.164	1001.5	4.1	100	185	8.8	2.55	15.2	28198	6188	10	St	
RS018	2019100812	66.187	-168.743	998.3	5.6	90	206	12.6	5.60	48.9	20648	5233	-	-	
RS019	2019100818	67.013	-168.708	997.5	4.8	90	187	11.3	7.07	30.4	23702	5468.3	8	St, Sc	
RS020	2019100901	68.166	-168.756	998.8	3.7	96	185	4.5	3.62	16.6	27553	6179	10	-	
RS021	2019100906	68.994	-168.753	1000.7	4.4	90	15	4.6	5.92	17	27398	6243.56	-	-	
RS022	2019100912	69.634	-168.754	1005.3	3.2	81	24	13.4	5.06	19.3	26523	6318	-	-	
RS023	2019100918	70.497	-168.754	1010.2	0.0	83	348	9.0	5.35	54.3	19860	5087.37	9	Sc, St	
RS024	2019101000	71.074	-166.732	1010.4	1.5	60	337	10.5	5.28	21.8	25728	6079	10	-	
RS025	2019101006	71.664	-164.684	1009.0	1.8	66	288	13.2	6.14	39.2	21927	5524.86	-	Cu	
RS026	2019101012	72.157	-162.945	1008.0	0.7	84	272	10.6	4.01	27.2	24231	5574	-	-	
RS027	2019101018	72.778	-160.780	1005.7	1.8	79	299	8.6	3.27	15.2	27904	6230.57	6	As, Sc	
RS028	2019101100	72.811	-158.599	1007.5	0.4	90	324	6.4	1.94	17.1	27145	6237	4	Cu,As,Ac,Ci	
RS029	2019101106	72.499	-156.270	1008.8	0.2	77	301	5.5	1.82	14.2	28319	7517.73	-	-	
RS030	2019101112	72.333	-155.005	1008.4	0.6	88	275	6.7	1.86	50.2	20276	5342	-	-	
RS031	2019101118	72.158	-153.783	1007.6	1.5	78	251	8.5	5.89	58.3	19298	4500.94	6	Sc, As, St	

RS032	2019101200	72.000	-151.546	1007.2	1.5	81	260	7.3	1.88	14.4	28222	6199	6	St,Sc,Ac	
RS033	2019101206	72.002	-148.341	1005.8	0.3	95	226	11.7	1.10	26.8	24284	5597.04	-	-	
RS034	2019101212	72.000	-147.088	1006.3	-0.1	90	287	13.4	0.59	31.3	23269	5843	-	-	
RS035	2019101218	71.998	-145.002	1010.0	-2.0	75	313	11.9	0.67	15	27874	6653.2	7	Sc, As	
RS036	2019101300	72.892	-144.994	1011.2	-2.2	76	288	10.0	0.24	14.8	27937	6587	5	Sc, Cu	CPS-exp.
RS037	2019101306	73.685	-145.042	1010.9	-2.7	61	299	12.0	0.20	23	25143	6900.15	-	-	
RS038	2019101312	73.758	-145.191	1011.7	-2.2	67	313	9.6	0.20	16.3	27194	6256	-	-	
RS039	2019101318	73.960	-144.721	1010.3	-1.1	78	264	13.2	0.10	20.9	25685	5611.89	10	St	
RS040	2019101400	74.360	-143.413	1009.6	-1.2	92	270	11.5	-1.40	20	25922	5350	10	-	
RS041	2019101406	74.078	-145.100	1010.0	-1.0	82	263	10.9	-0.11	33.5	22721	4493.43	-	-	CPS-exp.
RS042	2019101412	74.481	-148.232	1010.2	-0.1	68	280	8.8	0.67	15.5	27474	6543	-	-	
RS043	2019101418	74.769	-150.502	1010.6	0.5	59	222	5.2	1.05	18	26552	6079.73	8	St	
RS044	2019101500	74.954	-151.953	1008.8	0.0	95	185	10.1	-0.09	22.4	25192	5606	10	St	
RS045	2019101506	75.411	-155.051	1006.5	0.8	85	229	8.0	-0.19	12.3	28875	7513.46	6	Sc	
RS046	2019101512	76.157	-159.610	1005.1	1.3	93	227	5.0	0.99	13.9	28101	6997	-	-	
RS047	2019101518	76.467	-161.639	1004.8	1.0	97	192	3.7	0.67	15.7	27308	6165.91	10	St	
RS048	2019101600	76.930	-164.525	1005.0	0.6	97	206	4.3	0.56	16.2	27079	5680	10	St	
RS049	2019101606	77.000	-164.997	1005.4	0.6	88	197	5.5	0.30	33	22734	4884.39	-	-	CPS-exp.
RS050	2019101612	77.240	-165.001	1005.5	0.1	93	147	4.6	0.34	14.2	27891	6803	-	-	
RS051	2019101618	77.229	-164.972	1005.7	-0.2	74	167	4.5	0.37	22.5	25046	6221.91	10	-	
RS052	2019101700	78.082	-164.932	1005.5	-1.1	86	167	5.9	-1.49	19.6	25876	5802	10	St	
RS053	2019101706	77.368	-164.998	1005.9	-0.1	73	169	4.0	0.39	48.3	20338	5553.63	-	-	CPS-exp.
RS054	2019101712	77.500	-165.001	1006.9	-0.6	75	165	3.4	-0.77	14.2	27846	6868	-	-	
RS055	2019101718	77.753	-164.965	1007.8	-1.5	83	138	6.3	-1.28	18.8	26135	6259.31	10	-	
RS056	2019101800	78.006	-164.982	1009.0	-1.8	76	130	3.7	-1.49	27.8	23716	5861	10	St	
RS057	2019101806	77.250	-165.000	1009.3	-2.0	80	142	3.6	0.32	38.7	21700	5024.45	-	-	CPS-exp.
RS058	2019101812	77.573	-164.987	1010.1	-2.6	77	162	3.4	-1.40	34.3	22424	5195	-	-	
RS059	2019101818	77.758	-164.992	1011.3	-3.8	85	104	5.6	-1.06	49.4	20183	4702.94	8	St	
RS060	2019101900	78.067	-165.170	1012.6	-4.3	89	92	7.3	-1.51	16.5	26917	6555	7	Sc,As	
RS061	2019101906	77.301	-165.011	1012.4	-1.3	80	162	7.0	0.23	73.1	17737	4219.53	-	-	CPS-exp.
RS062	2019101912	77.254	-164.994	1013.1	-1.6	80	132	10.2	0.31	29.8	23310	5838	-	-	
RS063	2019101918	77.456	-164.789	1013.0	-2.0	84	124	8.3	0.24	46.3	20583	4635.84	10	-	CPS-exp.
RS064	2019102000	78.050	-165.001	1013.3	-2.1	85	162	9.0	-1.53	24.5	24500	6308	10	Sc	CPS-exp.
RS065	2019102006	77.398	-165.002	1012.3	-0.9	73	152	8.4	0.24	29.2	23430	5509.77	-	-	CPS-exp.
RS066	2019102012	77.199	-165.001	1012.2	-1.0	88	130	9.8	0.28	27.2	23863	5439	-	-	
RS067	2019102018	77.454	-164.799	1012.4	-1.1	75	133	9.3	0.27	44.1	20891	4467.14	4	Sc, St	

RS068	2019102100	78.017	-164.969	1013.4	-1.9	92	111	8.1	-1.53	35.9	22154	5159	8	Sc	
RS069	2019102106	77.253	-166.002	1012.4	-0.9	92	118	8.7	0.35	27	23922	6369.82	-	-	CPS-exp.
RS070	2019102112	77.005	-164.997	1013.4	-0.3	72	149	7.6	0.65	24.8	24459	5330	-	-	
RS071	2019102118	77.502	-165.002	1014.4	-0.9	76	121	12.3	0.26	15.1	27469	5730.25	-	-	
RS072	2019102200	78.025	-164.964	1016.4	-4.4	84	86	7.1	-1.51	16.4	26955	5763	10	Sc	
RS073	2019102206	77.074	-165.942	1013.0	-2.2	75	107	5.7	0.65	22.7	24999	6325.03	-	-	
RS074	2019102212	77.001	-164.996	1012.8	-3.1	79	117	9.5	0.74	12.7	28576	6569	-	-	
RS075	2019102218	77.502	-164.991	1013.0	-4.8	71	141	4.7	0.13	30.5	23145	4742.23	8	St	
RS076	2019102221	77.749	-164.512	1013.2	-5.5	79	121	6.7	-1.19	30.1	23236	5443	-	-	
RS077	2019102300	77.764	-164.250	1013.0	-5.6	76	107	6.5	-1.51	13.3	28228	6099	10	Sc	
RS078	2019102306	77.003	-164.011	1011.6	-4.9	70	170	3.8	0.47	45.1	20732	4091.92	2	Sc	
RS079	2019102312	77.002	-164.994	1008.5	-3.0	84	127	8.6	0.58	16.3	26992	6137	-	-	
RS080	2019102318	77.507	-164.969	1005.0	-4.1	86	118	11.6	-0.13	14	27873	5526.95	-	-	
RS081	2019102400	77.787	-163.587	1003.3	-3.4	81	114	6.8	-1.49	23.3	24744	5436	10	Sc	
RS082	2019102406	77.247	-164.015	1000.4	-3.1	81	139	10.1	-0.10	56.8	19208	4349.79	-	-	CPS-exp.
RS083	2019102412	77.004	-165.001	1000.2	-2.8	84	92	7.1	0.68	36.1	22018	5434	-	-	
RS084	2019102418	77.512	-165.006	1001.9	-4.2	75	81	9.5	-0.17	19.7	25709	5488.08	7	-	
RS085	2019102500	77.809	-163.516	1004.3	-8.9	94	61	6.8	-1.48	18.5	26087	5418	10	Sc	
RS086	2019102506	77.351	-166.490	1004.3	-5.9	89	52	8.9	0.04	14	27794	6162.29	-	-	
RS087	2019102512	77.002	-168.761	1006.4	-6.8	85	32	6.7	0.65	26.4	23878	5676	-	-	
RS088	2019102518	75.900	-168.744	1007.3	-3.6	80	30	9.9	1.11	31.1	22906	4760.96	8	-	
RS089	2019102600	74.733	-168.759	1009.2	-1.6	74	27	6.6	1.58	23.7	24612	5329	7	Sc	
RS090	2019102606	74.000	-168.742	1013.6	-2.7	79	303	10.3	1.99	19.6	25839	6176.74	-	-	
RS091	2019102612	73.272	-168.752	1018.3	-1.6	58	253	7.9	1.65	33.4	22573	5438	2	Cu,Sc	
RS092	2019102618	72.501	-168.741	1021.8	-1.2	60	244	7.3	1.350	12.7	28626	6323.34	8	-	
RS093	2019102700	71.569	-168.744	1025.1	-0.9	64	252	5.3	3.880	38.6	21809	4871	10	Sc	
RS094	2019102706	70.573	-168.745	1024.3	-0.6	54	93	3.9	3.500	46.7	20705	4848.26	-	-	
RS095	2019102712	69.773	-168.756	1018.5	0.1	65	55	13.0	2.090	15.7	27541	6069	-	-	
RS096	2019102718	69.003	-168.755	1010.3	0.3	88	69	9.6	3.120	12.8	28895	5877.23	10	-	
RS097	2019102800	68.309	-167.540	1002.0	2.4	91	66	9.3	3.590	13.1	28790	6094	-	-	
RS098	2019102806	68.014	-167.867	991.0	2.6	93	44	14.5	2.650	20.2	26166	7203.35	-	-	
RS099	2019102812	67.502	-168.751	982.5	3.7	100	354	1.3	2.640	16.6	27443	6230	-	-	
RS100	2019102818	66.502	-168.748	987.2	1.5	97	271	10.8	4.570	14.5	28372	5947.98	10	-	
RS101	2019102900	65.688	-168.517	994.2	1.4	93	316	10.5	3.880	16.9	27404	6121	10	St	
RS102	2019102912	63.969	-171.970	1004.2	-1.5	79	24	7.3	3.710	35.1	22849	5519	-	-	
RS103	2019103000	62.112	-175.382	1012.8	-1.2	72	302	7.4	4.570	22	25984	5573	10	Sc	

RS104	2019103012	60.288	-178.476	1017.6	2.5	60	251	6.7	4.580	14.3	28832	6458	-	-	
RS105	2019103100	58.474	178.617	1018.4	2.7	62	138	5.0	5.390	17.4	27586	6944	10	Cu,Sc	
RS106	2019103112	56.615	175.787	1016.6	3.6	73	82	4.9	4.730	15.1	28486	6274	-	-	
RS107	2019110100	54.747	173.080	1016.7	3.6	75	24	1.1	6.470	16.8	27781	6688	8	Cu,Sc	

2.2 CPS sonde

(1) Personnel

Jun Inoue	NIPR	- PI
Kazutoshi Sato	KIT	
Taro Maruo	Kobe University	
Jumpei Yamamoto	Tokyo University of Marine Science and Technology	
Taketani Fumikazu	JAMSTEC	
Ryo Oyama	NME	
Soichiro Sueyoshi	NME	
Shinya Okumura	NME	
Kazuho Yoshida	NME	
Yutaro Murakami	NME	
Hattori Takehito	MIRAI Crew	

(2) Objectives

To understand the vertical profiles of Arctic cloud, we conducted Cloud Particle Sensor (CPS) sonde observations over the Arctic Ocean and Bering Sea. The CPS sonde, which is developed by Japanese Meisei Electric Co., Ltd. (Meisei), measures vertical distributions of cloud particles (number of density, size and the phase (water cloud or ice cloud)) in addition to the meteorological elements (Temperature, Relative Humidity, Height, Wind direction and Wind speed). This is a first trial of cloud particles observation over the Arctic Ocean on R/V Mirai during October.

(3) Parameters

Cloud particles (number of density, Particle size and Output signal voltage)
Wind speed and direction
Pressure
Temperature
Relative Humidity

(4) Instruments and methods

Twelve (12) CPSs were launched during 13 and 24 October 2019. The CPS sonde consists of CPS sonde and GPS radiosonde transmitter (RS-11G, Meisei). The CPS sonde was connected with 350g balloon (Totex TA-350), parachute and Vaisala radiosonde. We used MEISEI standard GPS sonde ground system (RD-08AC), software (MGPS-R) and 400MHz antenna.

(5) Station list or Observation log

See Table 2.2 “CPS sonde launch log with surface observation and maximum sounding height”.

(6) Preliminary results

Figure 2.2-1 shows Mirai tracks during MR19-03C and CPS sonde points over the Arctic Ocean. Figures 2.2-2 to 2.2-13 show vertical profiles of temperature and relative humidity obtained by RS-11G GPS radiosonde, and number of particle, degree of polarization and P output obtained by CPS sonde. We successfully observed 18 clouds including low, middle and high clouds.

(7) Data archive

These data obtained in this cruise will be submitted to the Data Management Group of JAMSTEC, and will be opened to the public via “Data Research System for Whole Cruise Information in JAMSTEC (DARWIN)” in JAMSTEC web site.

<http://www.godac.jamstec.go.jp/darwin/e>

(8) Remarks

To reduce helium for balloon, we launched Meisei RS-11G GPS radiosonde and CPS sonde with Vaisala GPS radiosonde (RS41-SPG) during MR19-03C cruise ("with CPS" in table 2.1). No.2 launch has no Relative Humidity data, because of trouble of receiving of data.

Table 2.2: CPS sonde launch log with surface observation and maximum sounding height.

No.	Date (YYYYMMDD) Time (HH:MM) UTC	Lat (degN) Lon (degW)	Psfc (hPa)	Tsfc (℃)	RHsfc (%)	WDsfc (deg) WSsfc (m/s)	Max Alt (m)
01	20191013 06:00	73.75 145.07	1010.9	-2.7	61	299 12.0	25121
02	20191014 06:00	74.07 145.23	1009.9	-1.0	82	263 10.9	22677
03	20191016 06:00	77.00 164.99	1004.5	0.6	88	197 5.5	22724
04	20191017 06:00	77.27 165.02	1005.9	-0.1	73	169 4.0	20307
05	20191018 06:00	72.25 164.99	1009.3	-2.0	80	142 3.6	21680
06	20191019 06:00	77.21 164.94	1012.4	-1.3	80	162 7.0	17737
07	20191019 18:00	77.46 165.01	1012.9	-2.0	84	124 8.3	20576
08	20191020 00:00	78.05 164.99	1013.3	-2.1	85	162 9.0	24522
09	20191020 06:00	77.31 164.93	1012.3	-0.9	73	152 8.4	23427
10	20191021 06:00	77.25 166.00	1012.4	-0.9	92	118 8.7	23902
11	20191022 06:00	77.00 166.00	1012.9	-2.2	75	107 5.7	24969
12	20191024 06:00	77.24 163.99	1000.4	-3.1	81	139 10.1	19183

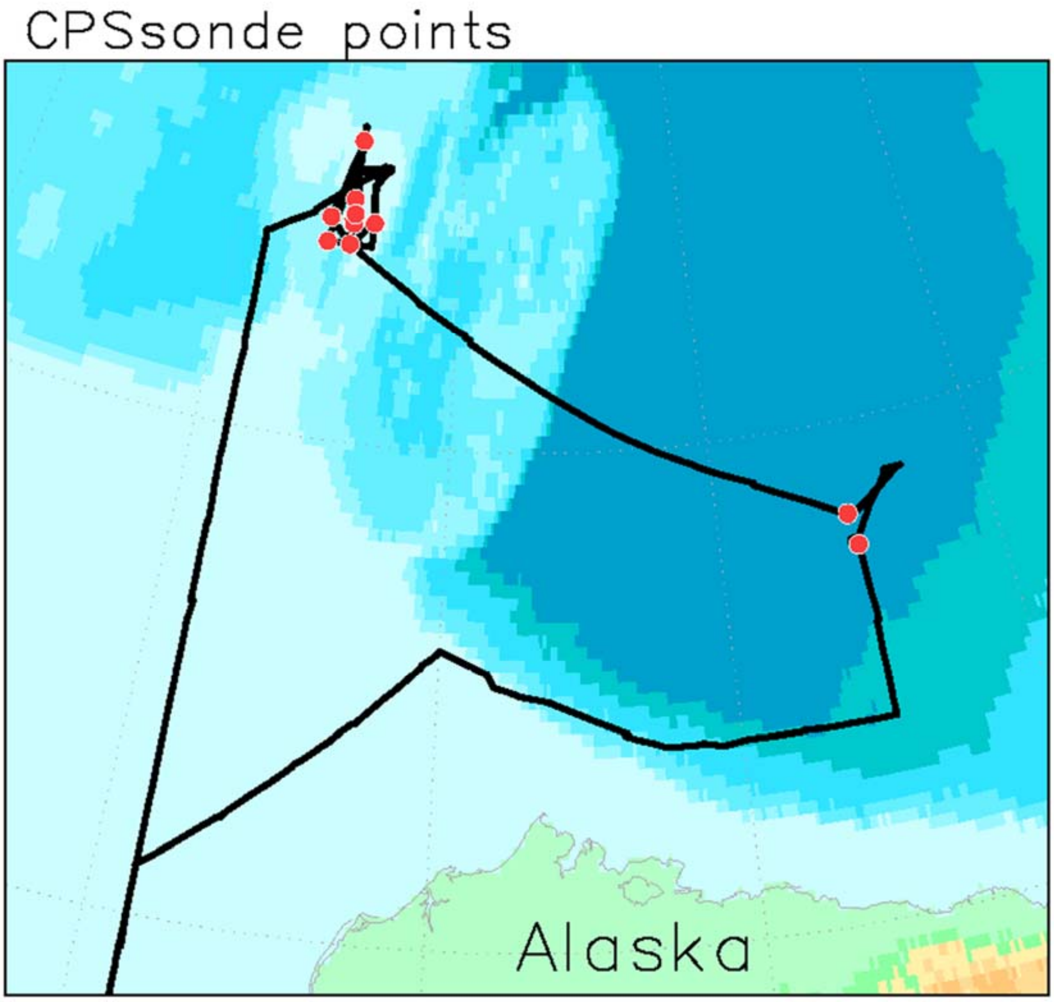

Figure 2.2-1: Mirai track (black line) and CPS sonde points (red dots) over the Arctic Ocean.

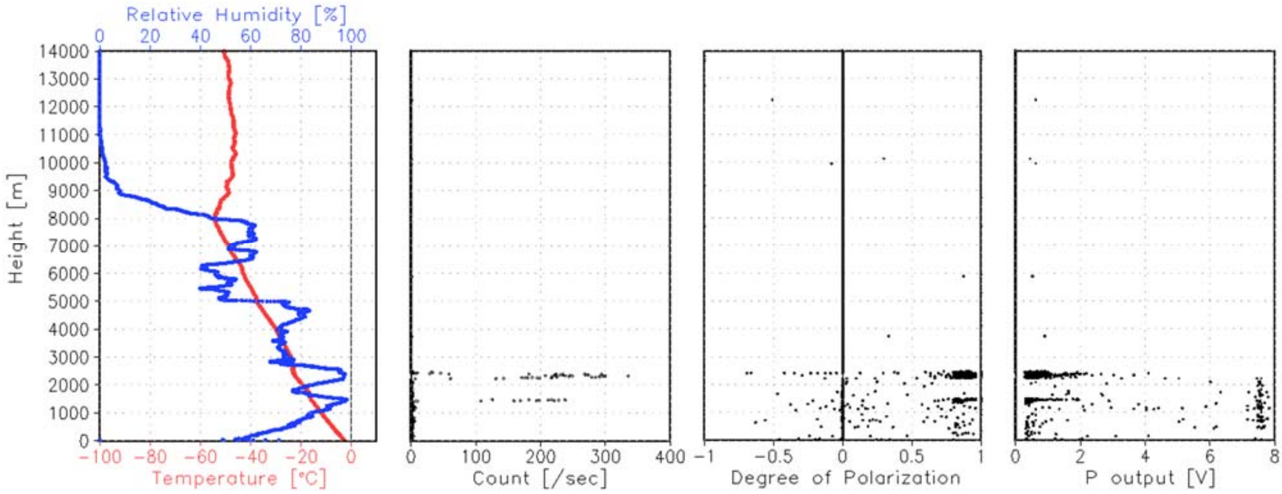

Figure 2.2-2: Vertical profiles of Temperature (red) and Humidity (blue) obtained by RS-11G radiosonde, and number of particle, degree of polarization and P output obtained by CPS sonde for No.1 launch (13 October).

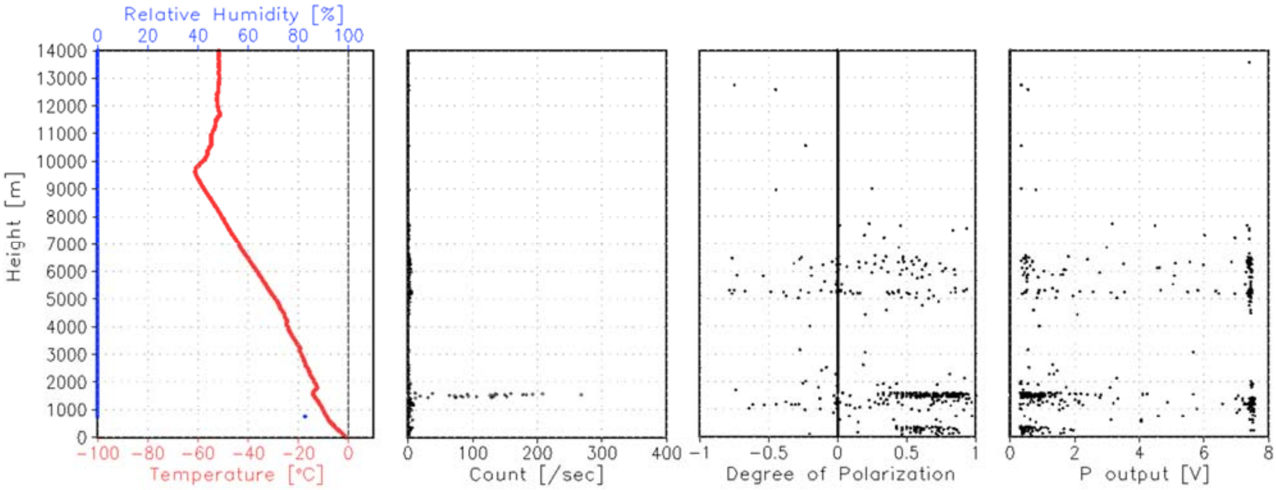

Figure 2.2-4: Same as in Figure 2.2-2, but for No.2 launch (14 October).

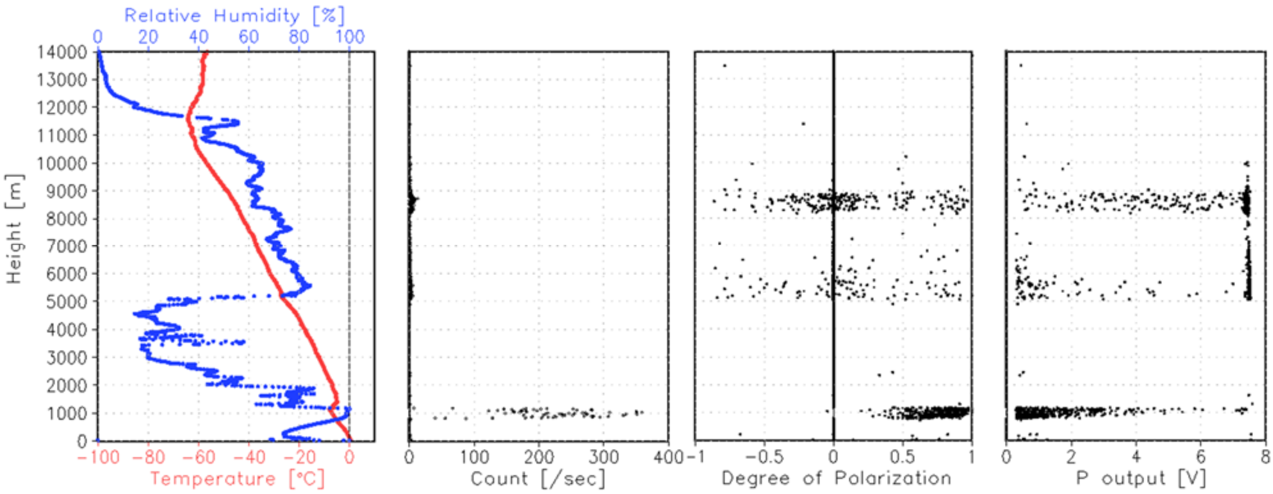

Figure 2.2-5: Same as in Figure 2.2-2, but for No.3 launch (16 October).

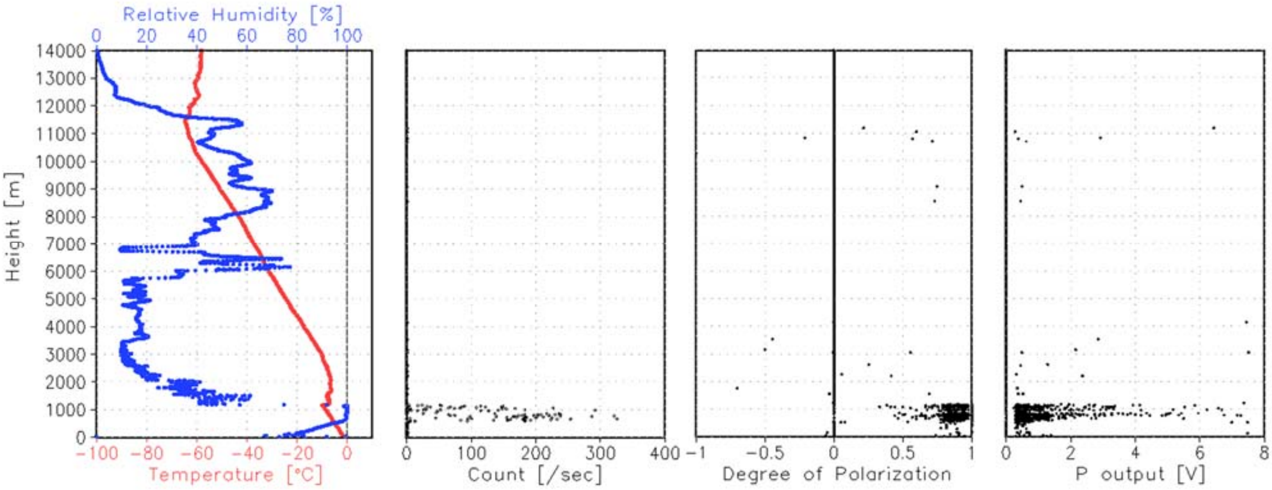

Figure 2.2-6: Same as in Figure 2.2-2, but for No.4 launch (17 October).

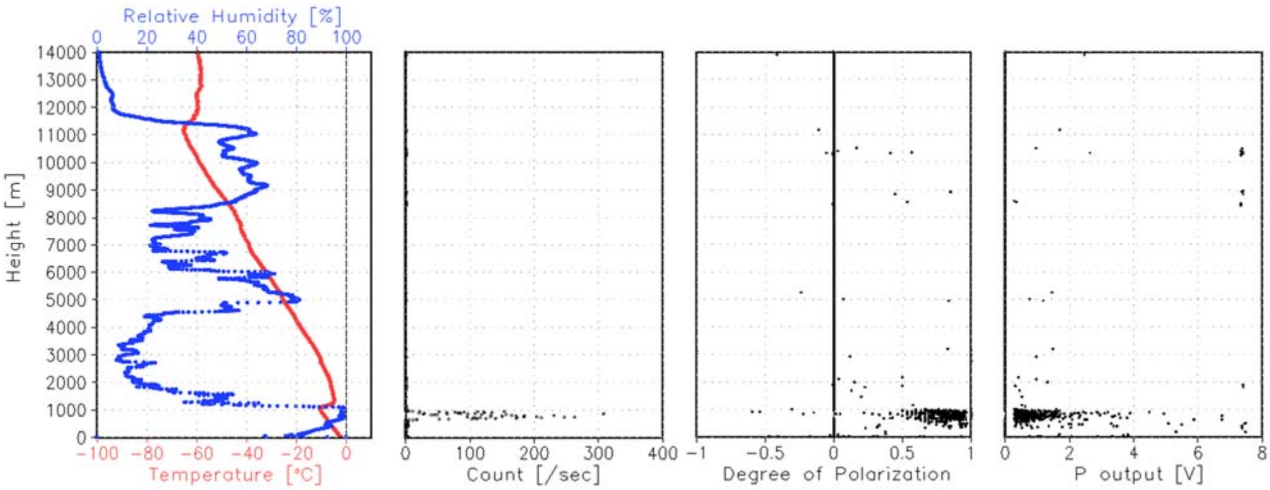

Figure 2.2-7: Same as in Figure 2.2-2, but for No.5 launch (18 October).

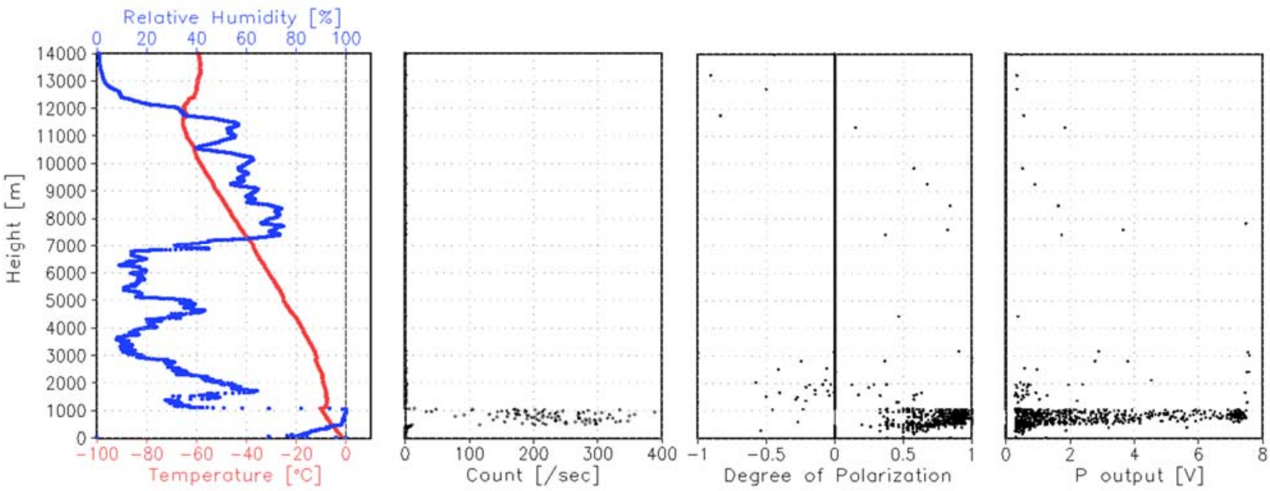

Figure 2.2-8: Same as in Figure 2.2-2, but for No.6 launch (06UTC 19 October).

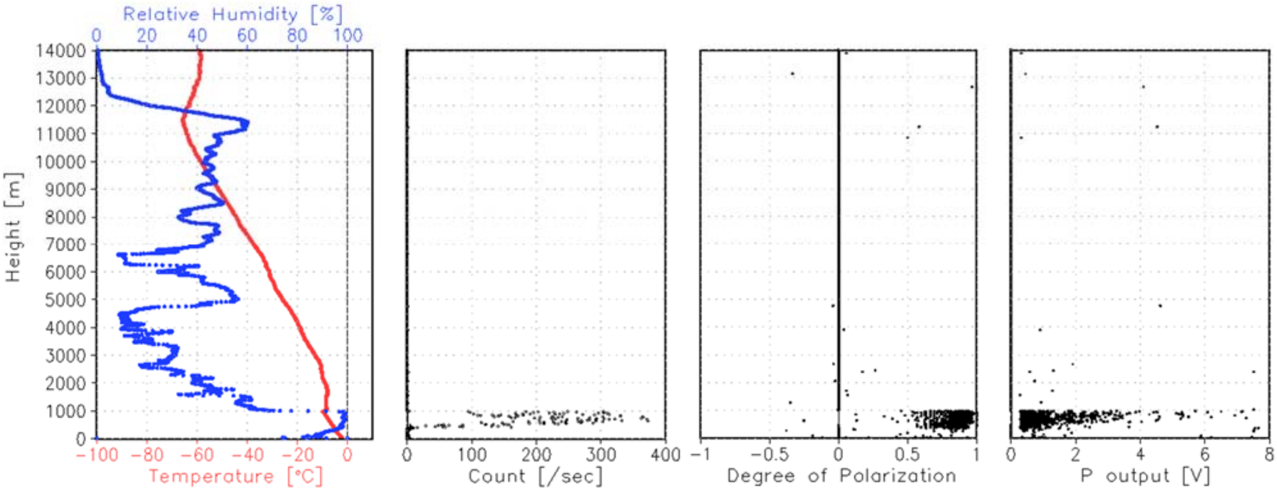

Figure 2.2-9: Same as in Figure 2.2-2, but for No.7 launch (18UTC 19 October).

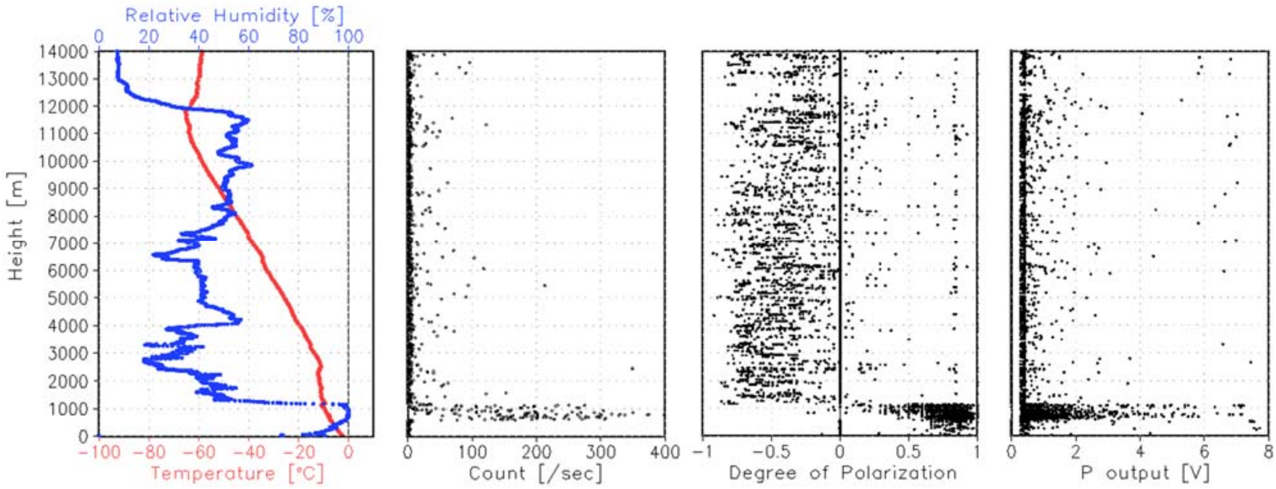

Figure 2.2-10: Same as in Figure 2.2-2, but for No.8 launch (00UTC 20 October).

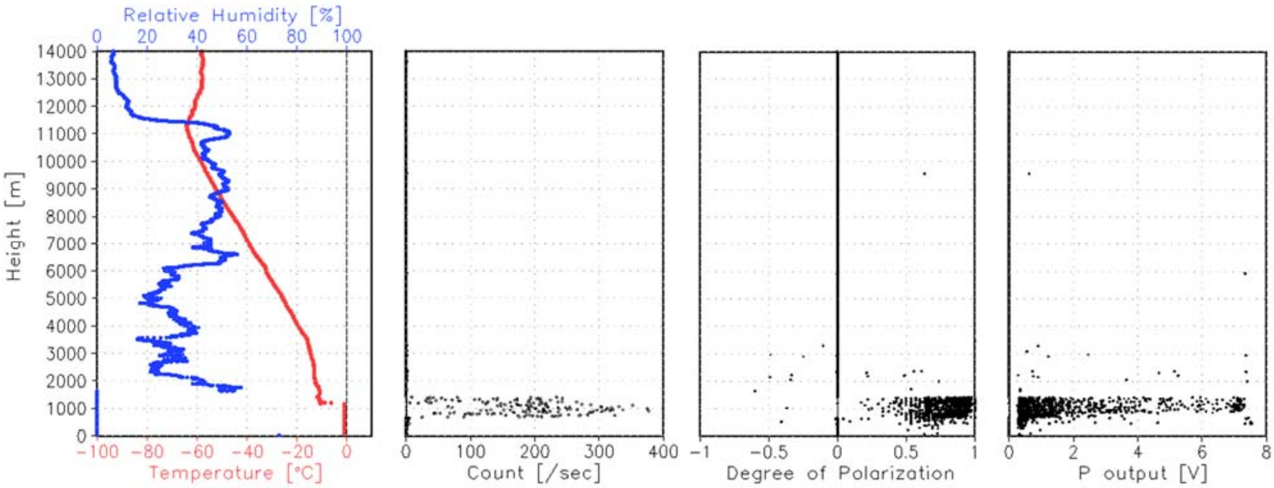

Figure 2.2-11: Same as in Figure 2.2-2, but for No.9 launch (06UTC 20 October).

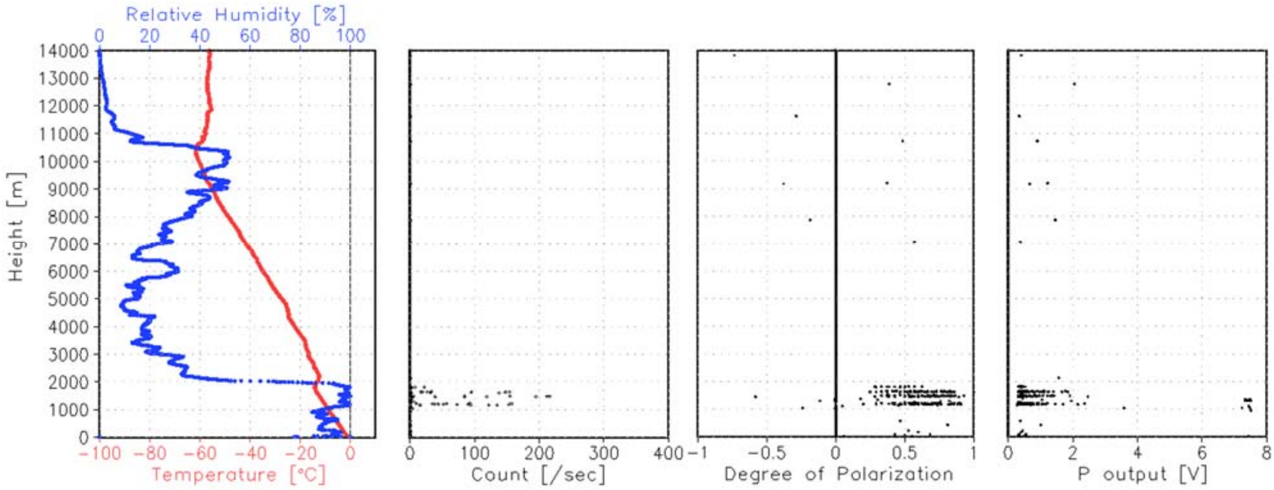

Figure 2.2-12: Same as in Figure 2.2-2, but for No.10 launch (21 October).

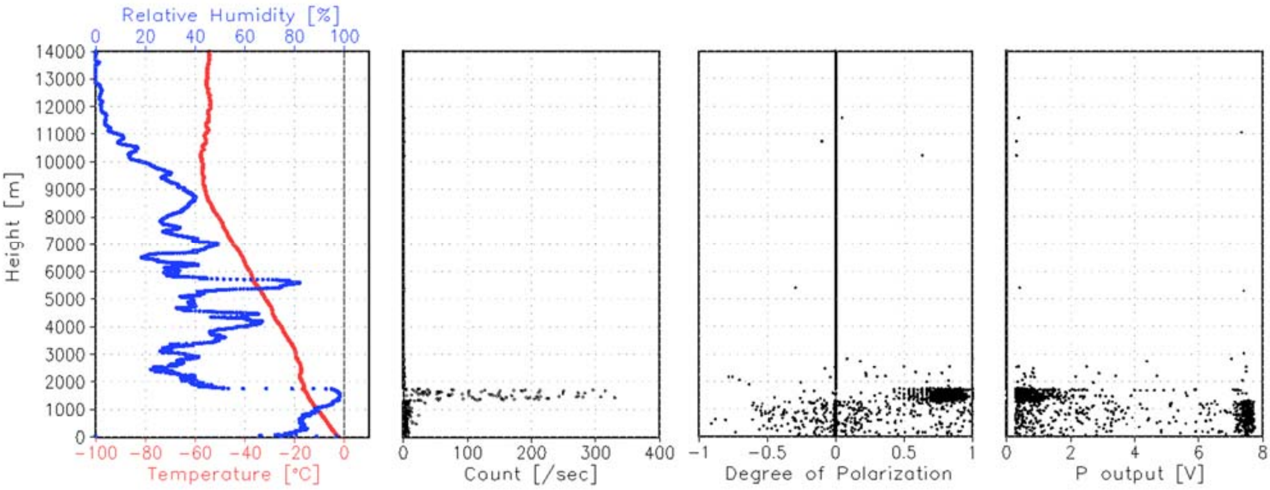

Figure 2.2-13: Same as in Figure 2.2-2, but for No.11 launch (22 October).

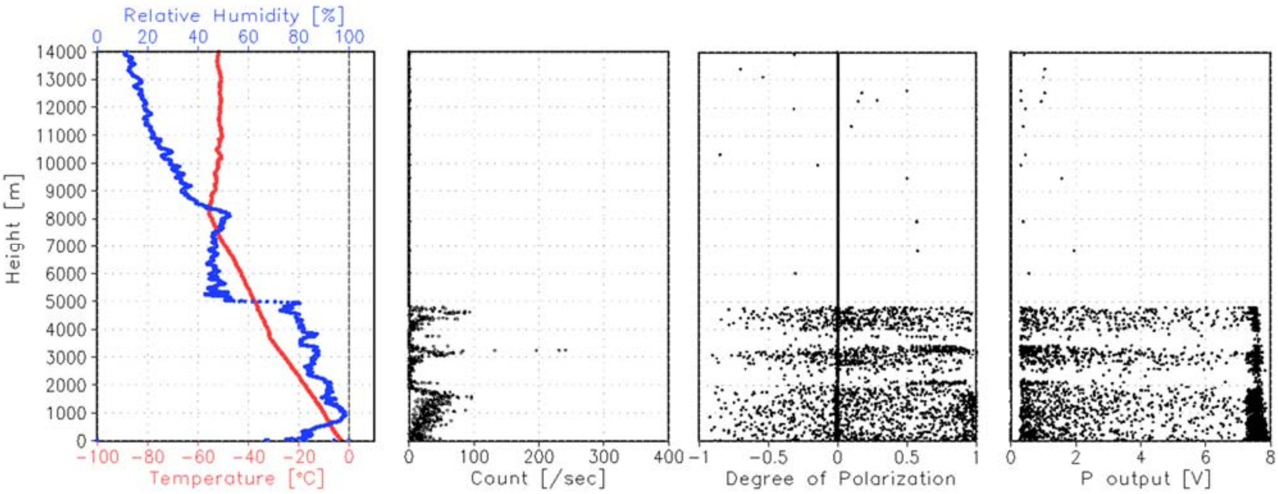

Figure 2.2-13: Same as in Figure 2.2-2, but for No.12 launch (24 October).

2.3 C-band Weather Radar

(1) Personnel

Kazutoshi Sato	KIT	- PI
Ryo Oyama	NME	
Souichiro Sueyoshi	NME	
Shinya Okumura	NME	
Kazuho Yoshida	NME	
Yutaro Murakami	NME	
Takehito Hattori	MIRAI Crew	

(2) Objectives

Low level clouds over the Arctic Ocean which usually dominate during early winter have a key role for sea/ice surface heat budget. In addition, cyclones which modify the sea-ice distributions are substantially important to understand the air-ice-sea interaction. To capture the broad cloud-precipitation systems and their temporal and spatial evolution over the Arctic Ocean, three-dimensional radar echo structure and wind fields of rain/snow clouds was obtained by C-band Doppler radar observation.

(3) Parameters

The C-band Weather radar observed three-dimensional radar echo structure and wind fields of rain/snow cloud.

Radar variables, which are converted from the power and phase of the backscattered signal at vertically-and horizontally-polarized channels, are as follows:

Radar reflectivity:	Z
Doppler velocity:	Vr
Spectrum width of Doppler velocity:	SW
Differential reflectivity:	ZDR
Differential propagation phase:	ΦDP
Specific differential phase:	KDP
Co-polar correlation coefficients:	ρHV

(4) Instruments and methods

The C-band Weather radar on board R/V Mirai is used. The basic specification of the radar is as follows:

Frequency:	5370 MHz (C-band)
Polarimetry:	Horizontal and vertical (simultaneously transmitted and received)
Transmitter:	Solid-state transmitter
Pulse Configuration:	Using pulse-compression
Output Power:	6 kW (H) + 6 kW (V)
Antenna Diameter:	4 meter
Beam Width:	1.0 degrees
INU (Inertial Navigation Unit):	PHINS (IXBLUE S.A.S.)

The antenna is controlled to point the commanded ground-relative direction, by controlling the azimuth and elevation to cancel the ship attitude (roll, pitch and yaw) detected by the INU. The Doppler velocity is also corrected by subtracting the ship motion in beam direction.

As the maintenance, internal parameters of the radar are checked and calibrated at the beginning and the end of the cruise. Meanwhile, the following parameters are checked daily; (1) frequency, (2) peak output power and (3) pulse width.

During the cruise, the radar was operated in two modes, which are shown in Tables 2.3-1 and 2.3-2, respectively. The radar was operated typically by repeating a volume scan with 17 PPIs (Plan Position Indicators) every 6-minute. A dual PRF (pulse repetition frequency) mode with the maximum range of typically 100 km was used for the volume scan. A surveillance PPI scan was performed every 30 minutes in a single PRF mode with the maximum range of 300 km. RHI (Range Height Indicator) scans were operated whenever detailed vertical structures are necessary in certain azimuth directions. On the way back from the Arctic Ocean, Vertical Point scans were added and performed due to collecting data for ZDR calibration.

(5) Station list or Observation log

The radar was operated continuously from 03:06UTC Sep. 30 to 08:00UTC Nov. 07.

(6) Preliminary results

The radar was operated continuously from Sep. 30 to Nov. 07 during the cruise. During the cruise, several precipitation systems passed near the R/V MIRAI. The C-band weather radar captured strong precipitation systems during MR19-03C. Figure 2.3 shows the temporal variation of the areal coverage of the radar echo within 100-km range on the PPI for precipitating events northward of 66°N (Top in figure 2.3). The strong echoes were captured when the low pressure systems approached R/V MIRAI (09, 23 and 28 October 2019). Strong snowfalls were observed near ice edges on 12 and 22 October 2019.

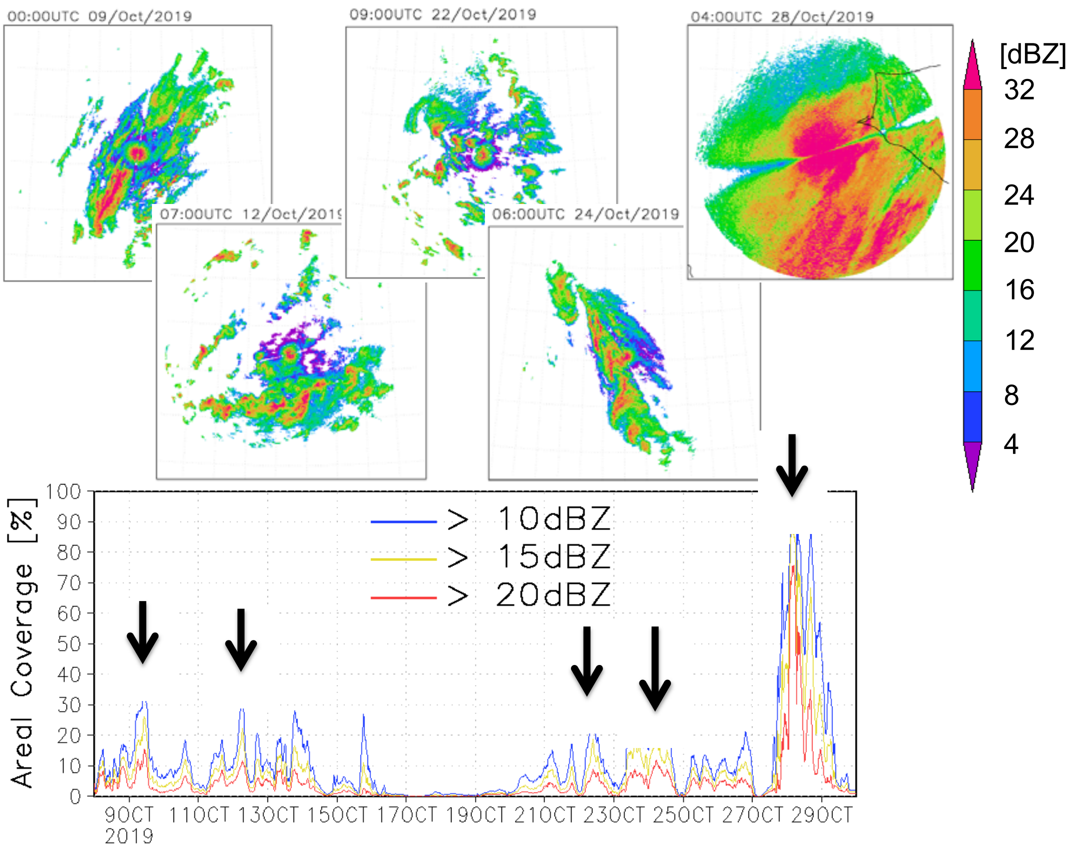

Figure 2.3: (Bottom) The temporal variations of the areal coverage of the echo exceeding threshold as 10 dBZ (blue), 15 dBZ (yellow) and 20 dBZ (red), within 100-km range distance on the PPI scans. (top) the six representing PPI images for characteristic precipitating event, obtained by the first PPI in the volume scan (at elevation angle of 0.5 degrees).

(7) Data archive

These data obtained in this cruise will be submitted to the Data Management Group of JAMSTEC, and will be opened to the public via "Data Research System for Whole Cruise Information in JAMSTEC (DARWIN)" in JAMSTEC web site.

<http://www.godac.jamstec.go.jp/darwin/e>

(8) Remarks (Times in UTC)

i) Observation mode

[Auto-1] (Scan parameters are shown in tables 2.3-1)

03:06UTC, 30 Sep. 2019 to 10:30UTC 31 Oct. 2019

[Auto-3] (Scan parameters are shown in tables 2.3-2)

10:36UTC, 31 Oct. 2019 to 08 Nov. 2019

ii) The following periods, data acquisition was suspended due to maintenance.

03:18 30 Sep. 2019 - 03:29 30 Sep. 2019

10:30 31 Oct. 2019 - 10:36 31 Oct. 2019

iii) Re-Unfolding correction of doppler velocity was not used during this cruise.

Table 2.3-1: Parameters for scan strategy in AUTO-1

<table>
<tr><th></th><th>Surveillance PPI Scan</th><th colspan="6">Volume Scan</th><th>RHI Scan</th></tr>
<tr><td>Repeated Cycle (min.)</td><td>30</td><td colspan="6">6</td><td>6</td></tr>
<tr><td>Times in One Cycle</td><td>1</td><td colspan="6">1</td><td>3</td></tr>
<tr><td>Pulse Width (long / short, in microsec)</td><td>200 / 2</td><td colspan="2">64 / 1</td><td colspan="2">32 / 1</td><td colspan="2">32 / 1</td><td>32 / 1</td></tr>
<tr><td>Scan Speed (deg/sec)</td><td>18</td><td colspan="2">18</td><td colspan="2">24</td><td colspan="2">36</td><td>9 (in el.)</td></tr>
<tr><td rowspan="2">PRF(s) (Hz)</td><td rowspan="2">400</td><td colspan="6">dual PRF (ray alternative)</td><td rowspan="2">1250</td></tr>
<tr><td>667</td><td>833</td><td>938</td><td>1250</td><td>1333</td><td>2000</td></tr>
<tr><td>Pulses / Ray</td><td>16</td><td>26</td><td>33</td><td>27</td><td>34</td><td>37</td><td>55</td><td>32</td></tr>
<tr><td>Ray Spacing (deg.)</td><td>0.7</td><td colspan="2">0.7</td><td colspan="2">0.7</td><td colspan="2">1.0</td><td>0.23</td></tr>
<tr><td>Azimuth</td><td colspan="7">Full Circle</td><td>Optional</td></tr>
<tr><td>Bin Spacing (m)</td><td colspan="8">150</td></tr>
<tr><td>Max. Range (km)</td><td>300</td><td colspan="2">150</td><td colspan="2">100</td><td colspan="2">60</td><td>100</td></tr>
<tr><td>Elevation Angle(s) (deg.)</td><td>0.5</td><td colspan="2">0.5</td><td colspan="2">1.0, 1.8, 2.6, 3.4, 4.2, 5.1, 6.2, 7.6, 9.7, 12.2 15.2</td><td colspan="2">18.7, 23.0, 27.9, 33.5, 40.0</td><td>-0.2 to 60.0</td></tr>
</table>

Table 2.3-2: Parameters for scan strategy in AUTO-3

	Surveillance PPI Scan	Volume Scan						RHI Scan	Vertical Point Scan
Repeated Cycle (min.)	30	6						12	
Times in One Cycle	1	1						3	3
Pulse Width (long / short, in microsec)	200 / 2	64 / 1		32 / 1		32 / 1		32 / 1	32/1
Scan Speed (deg/sec)	18	18		24		36		9 (in el.)	36
PRF(s) (Hz)	400	dual PRF (ray alternative)						1250	2000
		667	833	938	1250	1333	2000		
Pulses / Ray	16	26	33	27	34	37	55	32	64
Ray Spacing (deg.)	0.7	0.7		0.7		1.0		0.23	1.0
Azimuth	Full Circle							Optional	Full Circle
Bin Spacing (m)	150								
Max. Range (km)	300	150		100		60		100	60
Elevation Angle(s) (deg.)	0.5	0.5		1.0, 1.8, 2.6, 3.4, 4.2, 5.1, 6.2, 7.6, 9.7, 12.2 15.2		18.7, 23.0, 27.9, 33.5, 40.0		-0.2 to 60.0	90

2.4 Surface Meteorological Observations

(1) Personnel

Kazutoshi Sato	KIT	-PI
Ryo Oyama	NME	
Souichiro Sueyoshi	NME	
Shinya Okumura	NME	
Kazuho Yoshida	NME	
Yutaro Murakami	NME	
Takehito Hattori	MIRAI Crew	

(2) Objectives

Surface meteorological parameters are observed as a basic dataset of the meteorology. These parameters provide the temporal variation of the meteorological condition surrounding the ship.

(3) Instruments and methods

Surface meteorological parameters were observed during this cruise. In this cruise, we used two systems for the observation.

i. *MIRAI Surface Meteorological observation (SMet) system*

Instruments of SMet system are listed in Table 2.4-1 and measured parameters are listed in Table 2.4-2. Data were collected and processed by KOAC-7800 weather data processor made by Koshin-Denki, Japan. The data set consists of 6-second averaged data.

ii. *Shipboard Oceanographic and Atmospheric Radiation (SOAR) measurement system*

SOAR system designed by BNL (Brookhaven National Laboratory, USA) consists of major six parts.

a) Portable Radiation Package (PRP) designed by BNL – short and long wave downward radiation.
b) Additional short and long radiometers with ventilation units manufactured by Hukseflux, Netherlands – short and long wave downward radiation measurement adapted to cold areas in order to complement PRP measurement.
c) Analog meteorological data sampling with CR1000 logger manufactured by Campbell Scientific Inc. Canada – wind pressure, and rainfall (by a capacitive rain gauge) measurement.
d) Digital meteorological data sampling from individual sensors - air temperature, relative humidity and rainfall (by optical rain gauge (ORG)) measurement.
e) The Photosynthetically Available Radiation (PAR) sensor manufactured by Biospherical Instruments Inc. (USA) - PAR and Ultraviolet radiation (UV) measurement.
f) Scientific Computer System (SCS) developed by NOAA (National Oceanic and Atmospheric Administration, USA) – centralized data acquisition and logging of all data sets.

SCS recorded PRP, air temperature, relative humidity, CR1000, ORG and PAR data. SCS composed Event data (JamMet) from these data and ship's navigation data every 6 seconds. Instruments and their locations are listed in Table 2.4-3 and measured parameters are listed in Table 2.4-4.

For the quality control as post processing, we checked the following sensors, before and after the cruise.

i. Young Rain gauge (SMet and SOAR)
Inspect of the linearity of output value from the rain gauge sensor to change Input value by adding fixed quantity of test water.

ii. Barometer (SMet and SOAR)
Comparison with the portable barometer value, PTB220, VAISALA

iii. Thermometer (air temperature and relative humidity) (SMet and SOAR)
Comparison with the portable thermometer value, HM70, VAISALA

(4) Observation log
27 Sep. 2019 to 10 Nov. 2019

(5) Preliminary results
Figure. 2.4-1 shows the time series of the following parameters;
Wind (SOAR)
Air temperature (SMet)
Relative humidity (SMet)
Precipitation (SMet, ORG)
Short wave radiation (SOAR)
Long wave radiation (SMet)
Pressure (SMet)
Sea surface temperature (SMet)
Significant wave height (SMet; stern)

Figure. 2.4-2 and 2.4-3 show the time series of short and long wave radiation for comparing SOAR(PRP) to additional radiometers;

(6) Data archives
These data obtained in this cruise will be submitted to the Data Management Group of JAMSTEC, and will be opened to the public via "Data Research System for Whole Cruise Information in JAMSTEC (DARWIN)" in JAMSTEC web site.
<http://www.godac.jamstec.go.jp/darwin/e>

(7) Remarks (Times in UTC)

iv) The following period, Sea surface temperature of SMet data was available.
05:31UTC 29 Sep. 2019 - 23:55UTC 07 Nov. 2019

v) The following time, increasing of SMet capacitive rain gauge data were invalid due to test transmitting for MF/HF radio.
19:39UTC 29 Oct. 2019

vi) The following period, significant wave height and period data were invalid due to the logging PC trouble.
04:55UTC 07 Oct. 2019 - 05:55UTC 07 Oct. 2019

vii) The following periods, bow significant wave height and period data were invalid due to system trouble.
09:35UTC 01 Nov. 2019 - 23:34UTC 01 Nov. 2019

04:35UTC 02 Nov. 2019 - the end of the cruise.

viii) The following periods, SMet wind speed/direction were invalid due to sensor failure.
20:47UTC 10 Oct. 2019 - 20:56UTC 10 Oct. 2019
22:37UTC 10 Oct. 2019 - 22:50UTC 10 Oct. 2019
00:57UTC 19 Oct. 2019 - 02:49UTC 19 Oct. 2019

ix) The following periods, SMet wind speed/direction were measured by the ultrasonic anemometer on the aftermast.
20:56UTC 10 Oct. 2019 - 22:37UTC 10 Oct. 2019
22:50UTC 10 Oct. 2019 - 06:06UTC 12 Oct. 2019

x) The following period, SMet wind speed/direction were measured by KE-500, the wind vane anemometer on the foremast.
04:35UTC 19 Oct. 2019 - 00:00UTC 10 Nov. 2019

xi) The following days, SMet short wave radiation amount contains invalid value in nighttime, more than 0.01kW/m^2.
27 Sep. 2019 - 01 Oct. 2019
03 Oct. 2019 - 06 Oct. 2019

xii) The following period, SOAR data acquisition was suspended due to system maintenance.
06:33UTC 21 Oct. 2019 - 06:44UTC 21 Oct. 2019

xiii) The following period, ORG rain intensity of SOAR was invalid due to the sensor failure.
00:23UTC 14 Oct. 2019 - the end of the cruise

xiv) SOAR longwave radiation amount (PIR) has to be corrected by using right calibration coefficients which will be calibrated after the cruise, because PIR sensor was replaced before the beginning of this cruise.

xv) The following periods, SOAR longwave radiation amount (PIR) contained bias, because output of PIR case and/or dome thermistor for radiation correction fell below the temperature measurement limit(-5.6degC).
20:11UTC 22 Oct. 2019 - 03:27UTC 23 Oct. 2019
18:44UTC 24 Oct. 2019 - 07:17UTC 24 Oct. 2019
08:27UTC 25 Oct. 2019 - 14:10UTC 25 Oct. 2019

xvi) During this cruise, FRSR data was not acquired.

Table 2.4-1: Instruments and installation locations of SMet system

Sensors	Type	Manufacturer	Location(altitude from surface)
Anemometer(ultrasonic)	KS-5900	Koshin Denki, Japan	foremast (25 m)
			aftermast (37 m)
Anemometer(wind vane)	KE-500	Koshin Denki, Japan	foremast (24 m)
Tair/RH	HMP155	Vaisala, Finland	compass deck (21 m)
with 43408 Gill aspirated radiation shield		R.M. Young, USA	starboard and port side

Thermometer: SST	RFN2-0	Koshin Denki, Japan	4th deck (-1m, inlet -5m)
Barometer	Model-370	Setra System, USA	captain deck (13 m) weather obs. room
Rain gauge	50202	R. M. Young, USA	compass deck (19 m)
Optical rain gauge	ORG-815DR	Osi, USA	compass deck (19 m)
Radiometer (short wave)	MS-802	Eko Seiki, Japan	radar mast (28 m)
Radiometer (long wave)	MS-202	Eko Seiki, Japan	radar mast (28 m)
Wave height meter	WM-2	Tsurumi-seiki, Japan	bow (10 m) stern(8m)

Table 2.4-2: Parameters of MIRAI Surface Meteorological observation system

Parameter	Units	Remarks
1 Latitude	degree	
2 Longitude	degree	
3 Ship's speed	knot	Mirai log, DS-30 Furuno
4 Ship's heading	degree	Mirai Gyro, TOKYO-KEIKI, TG-8000
5 Relative wind speed	m/s	6sec./10min. averaged
6 Relative wind direction	degree	6sec./10min. averaged
7 True wind speed	m/s	6sec./10min. averaged
8 True wind direction	degree	6sec./10min. averaged
9 Barometric pressure	hPa	adjusted to sea surface level 6sec. averaged
10 Air temperature (starboard)	degC	6sec. averaged
11 Air temperature (port side)	degC	6sec. averaged
12 Dewpoint temperature (starboard)	degC	6sec. averaged
13 Dewpoint temperature (port side)	degC	6sec. averaged
14 Relative humidity (starboard)	%	6sec. averaged
15 Relative humidity (port side)	%	6sec. averaged
16 Sea surface temperature	degC	6sec. averaged
17 Rain rate (optical rain gauge)	mm/hr	hourly accumulation
18 Rain rate (capacitive rain gauge)	mm/hr	hourly accumulation
19 Down welling shortwave radiation	W/m^2	6sec. averaged
20 Down welling infra-red radiation	W/m^2	6sec. averaged
21 Significant wave height (bow)	m	hourly
22 Significant wave height (stern)	m	hourly
23 Significant wave period (bow)	second	hourly
24 Significant wave period (stern)	second	hourly

Table 2.4-3: Instruments and installation locations of SOAR system

Sensors (Meteorological)	Type	Manufacturer	Location (altitude from surface)
Anemometer	05106	R.M. Young, USA	foremast (25 m)
Barometer	PTB210	Vaisala, Finland	foremast (23 m)
with 61002 Gill pressure port, R.M. Young, USA			
Rain gauge	50202	R.M. Young, USA	foremast (24 m)
Tair/RH	HMP155	Vaisala, Finland	foremast (23 m)

with 43408 Gill aspirated radiation shield R.M. Young, USA

Optical rain gauge	ORG-815DR	Osi, USA	foremast (24 m)

Sensors (PRP)	Type	Manufacturer	Location (altitude from surface)
Radiometer (short wave)	PSP	Epply Labs, USA	foremast (25 m)
Radiometer (long wave)	PIR	Epply Labs, USA	foremast (25 m)
Fast rotating shadowband radiometer		Yankee, USA	foremast (25 m)

Sensors (PAR)	Type	Manufacturer	Location (altitude from surface)
PAR sensor	PUV-510	Biospherical Instruments Inc., USA	Navigation deck (18m)

Sensors (Additional Radiation)	Type	Manufacturer	Location (altitude from surface)
Radiometer (short wave)	SR-20	HukseFlux, Netherland	Compassdeck(20m)
with VU-01 Ventilation Unit		HukseFlux, Netherland	
Radiometer (long wave)	IR-20	HukseFlux, Netherland	Compassdeck(20m)
with VU-01 Ventilation Unit		HukseFlux, Netherland	

Table 2.4-4: Parameters of SOAR system

Parameter	Units	Remarks
1 Latitude	degree	
2 Longitude	degree	
3 SOG	knot	
4 COG	degree	
5 Relative wind speed	m/s	
6 Relative wind direction	degree	
7 Barometric pressure	hPa	
8 Air temperature	degC	
9 Relative humidity	%	
10 Rain rate (optical rain gauge)	mm/hr	
11 Precipitation (capacitive rain gauge)	mm	reset at 50 mm
12 Down welling shortwave radiation(PSP)	W/m^2	
13 Down welling infra-red radiation(PIR)	W/m^2	
14 Defuse irradiance	W/m^2	Not observed
15 PAR	microE/cm2/sec	
16 UV	microW/cm2/nm	
17 Additional Down welling shortwave radiation(SR20)	W/m^2	
18 Additional Down welling longwave radiation(IR20)	W/m^2	

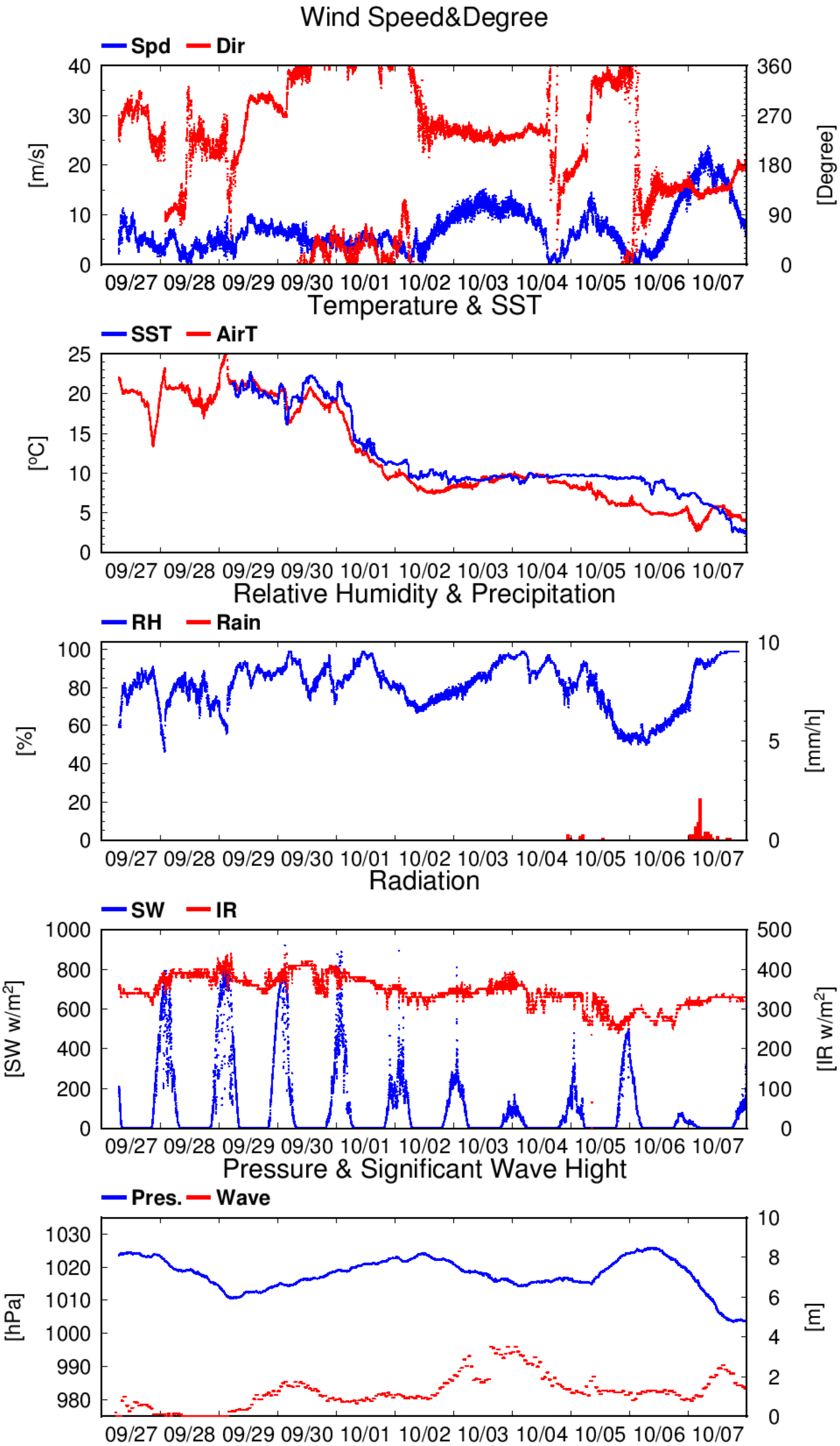

Figure 2.4-1: Time series of surface meteorological parameters during this cruise

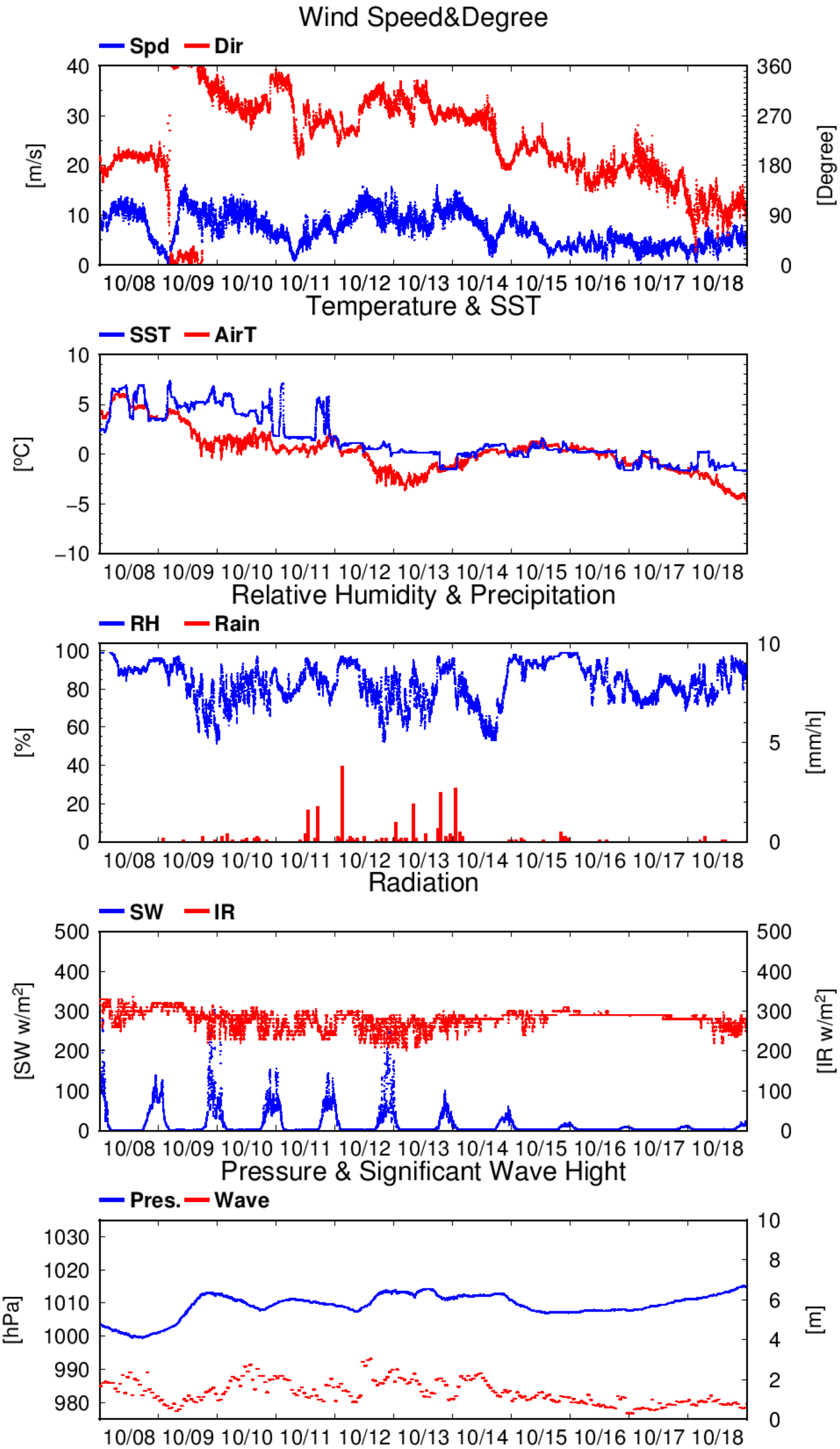

Figure 2.4-1: (Continued)

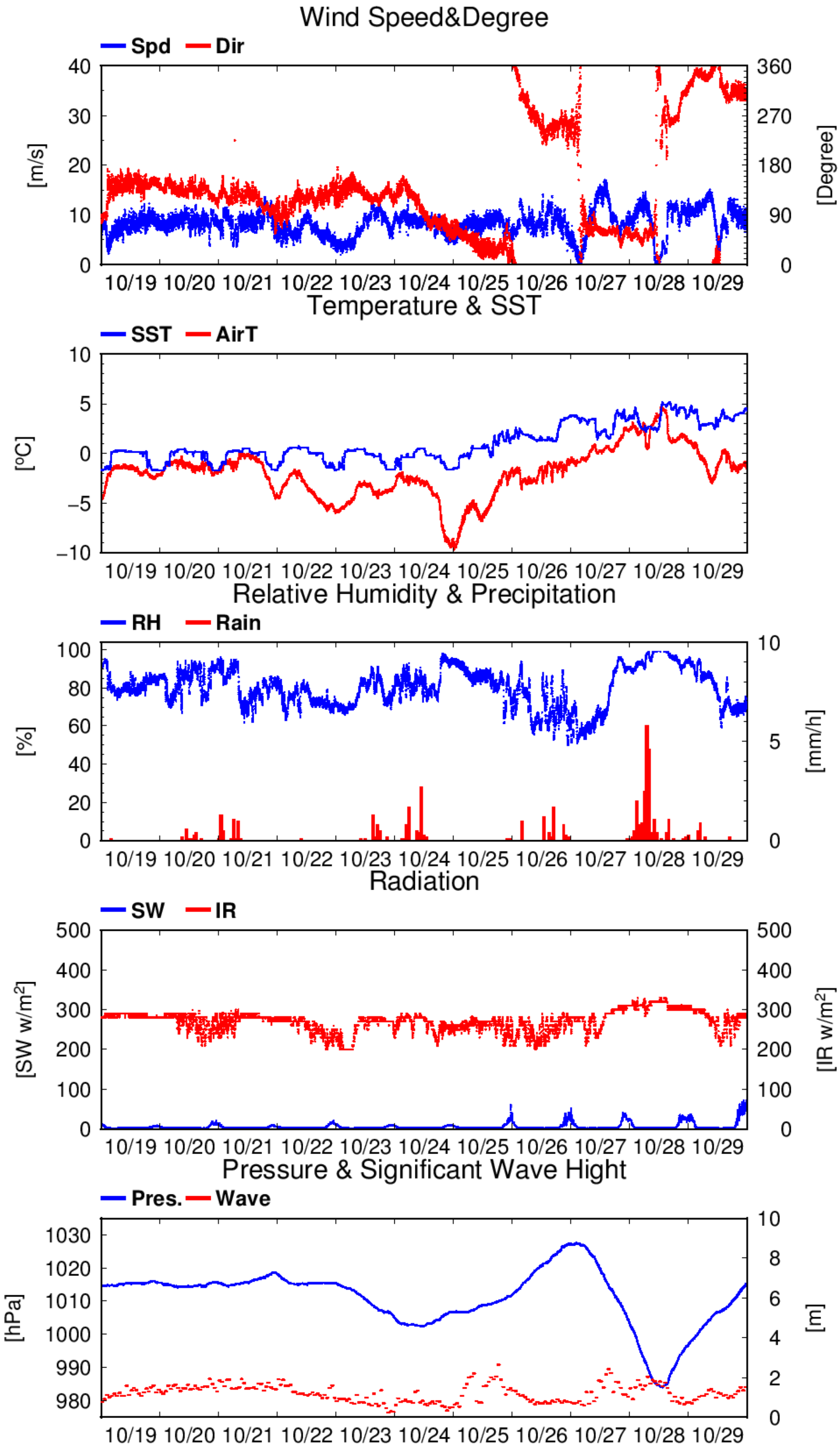

Figure 2.4-1: (Continued)

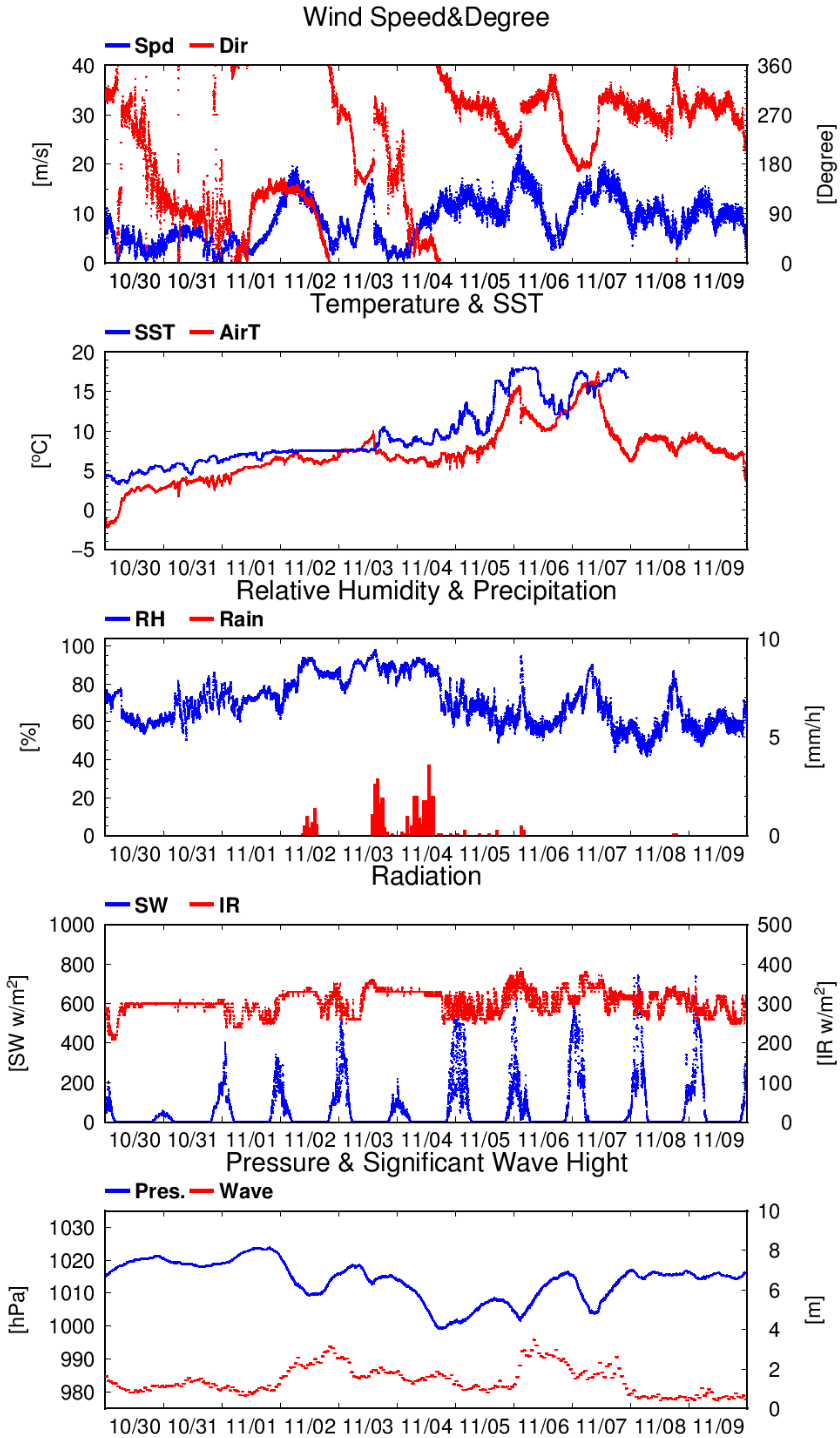

Figure 2.4-1: (Continued)

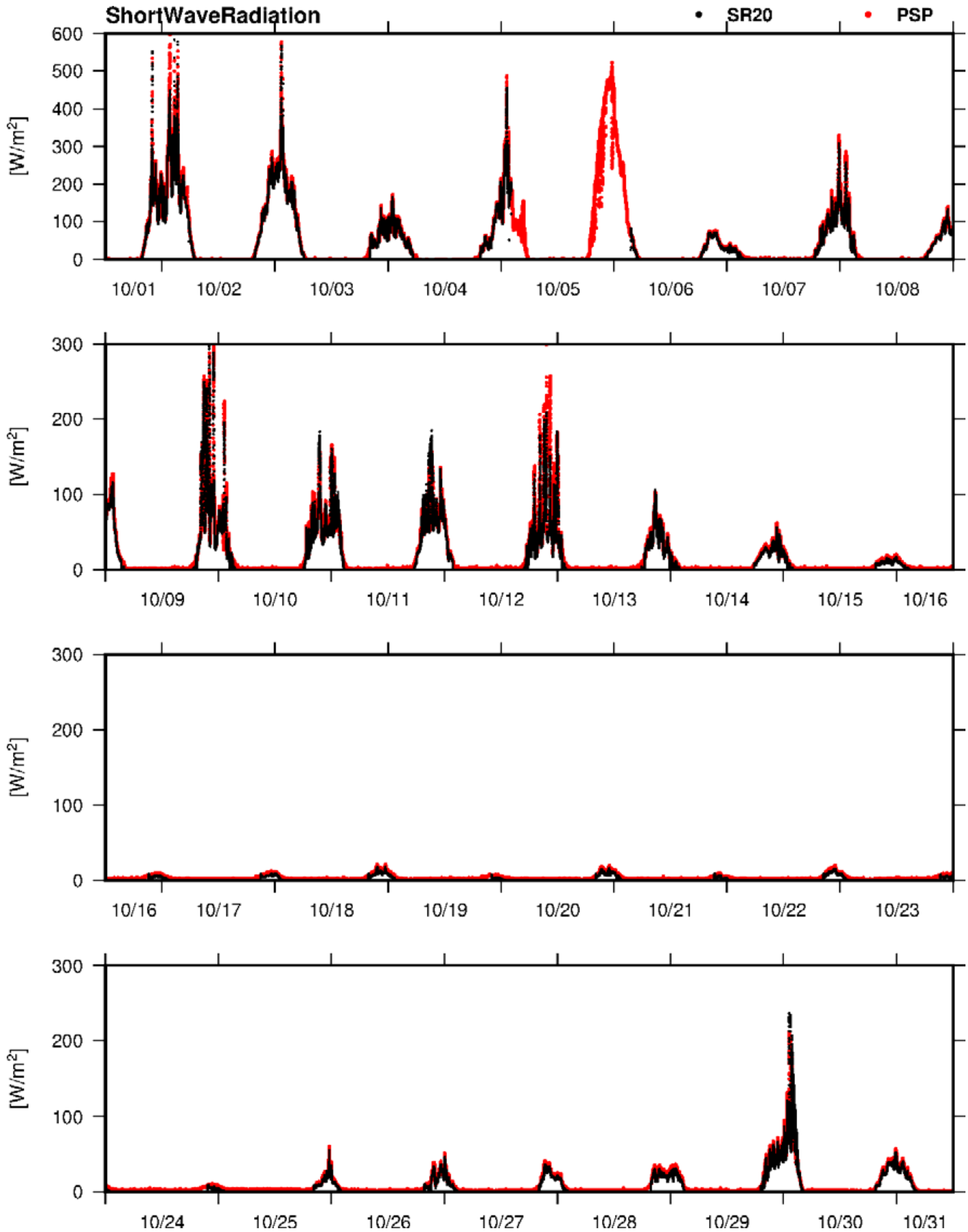

Figure 2.4-2: Time series of shortwave radiation amount of SR20(additional radiometer) and PSP in October 2019

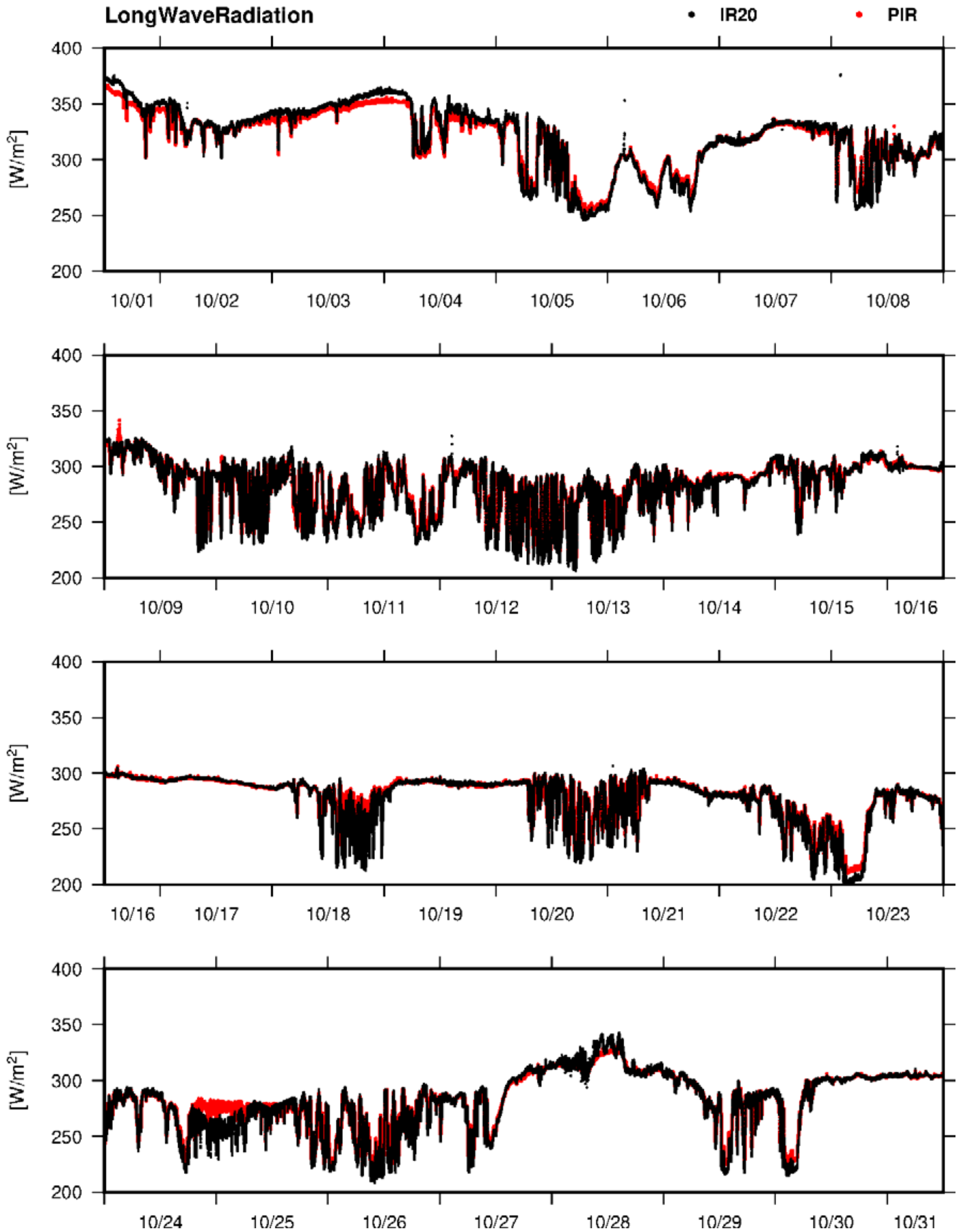

Figure 2.4-3: Time series of longwave radiation amount of IR20(additional radiometer) and PIR in October 2019

2.5 Ceilometer

(1) Personnel

Kazutoshi Sato	KIT	-PI
Ryo Oyama	NME	
Souichiro Sueyoshi	NME	
Shinya Okumura	NME	
Kazuho Yoshida	NME	
Yutaro Murakami	NME	
Takehito Hattori	MIRAI Crew	

(2) Objectives

The information of cloud base height and the liquid water amount around cloud base is important to understand the process on formation of the cloud. As one of the methods to measure them, the ceilometer observation was carried out.

(3) Parameters

1. Cloud base height [m].
2. Backscatter profile, sensitivity and range normalized at 10 m resolution.
3. Estimated cloud amount [oktas] and height [m]; Sky Condition Algorithm.

(4) Instruments and methods

We measured cloud base height and backscatter profile using ceilometer (CL51, VAISALA, Finland) throughout this cruise.

Major parameters for the measurement configuration are as follows;

Laser source:	Indium Gallium Arsenide (InGaAs) Diode Laser
Transmitting center wavelength:	910±10 nm at 25 degC
Transmitting average power:	19.5 mW
Repetition rate:	6.5 kHz
Detector:	Silicon avalanche photodiode (APD)
Measurement range:	0 ~ 15 km
	0 ~ 13 km (Cloud detection)
Resolution:	10 meter in full range
Sampling rate:	36 sec
Sky Condition	0, 1, 3, 5, 7, 8 oktas (9: Vertical Visibility)

(0: Sky Clear, 1: Few, 3: Scattered, 5-7: Broken, 8: Overcast)

On the archive dataset, cloud base height and backscatter profile are recorded with the resolution of 10 m.

(5) Observation log

27 Sep. 2019 - 10 Nov. 2019

(6) Preliminary results

Figure 2.5 shows the time series of cloud-base heights derived from the ceilometer during this cruise.

(7) Data archives

These data obtained in this cruise will be submitted to the Data Management Group of JAMSTEC, and will be opened to the public via “Data Research System for Whole Cruise Information in JAMSTEC

(DARWIN)” in JAMSTEC web site.
<http://www.godac.jamstec.go.jp/darwin/e>

(8) Remarks (Times in UTC)

1. Window cleaning
   01:07UTC 29 Sep. 2019
   05:43UTC 02 Oct. 2019
   01:52UTC 08 Oct. 2019
   02:40UTC 12 Oct. 2019
   23:52UTC 12 Oct. 2019
   19:25UTC 13 Oct. 2019
   02:16UTC 16 Oct. 2019
   00:10UTC 21 Oct. 2019
   01:05UTC 21 Oct. 2019
   01:03UTC 23 Oct. 2019
   00:47UTC 24 Oct. 2019
   19:29UTC 29 Oct. 2019
   04:44UTC 07 Nov. 2019

2. The blower with heater was stopped in this cruise, due to avoiding its poor insulation.

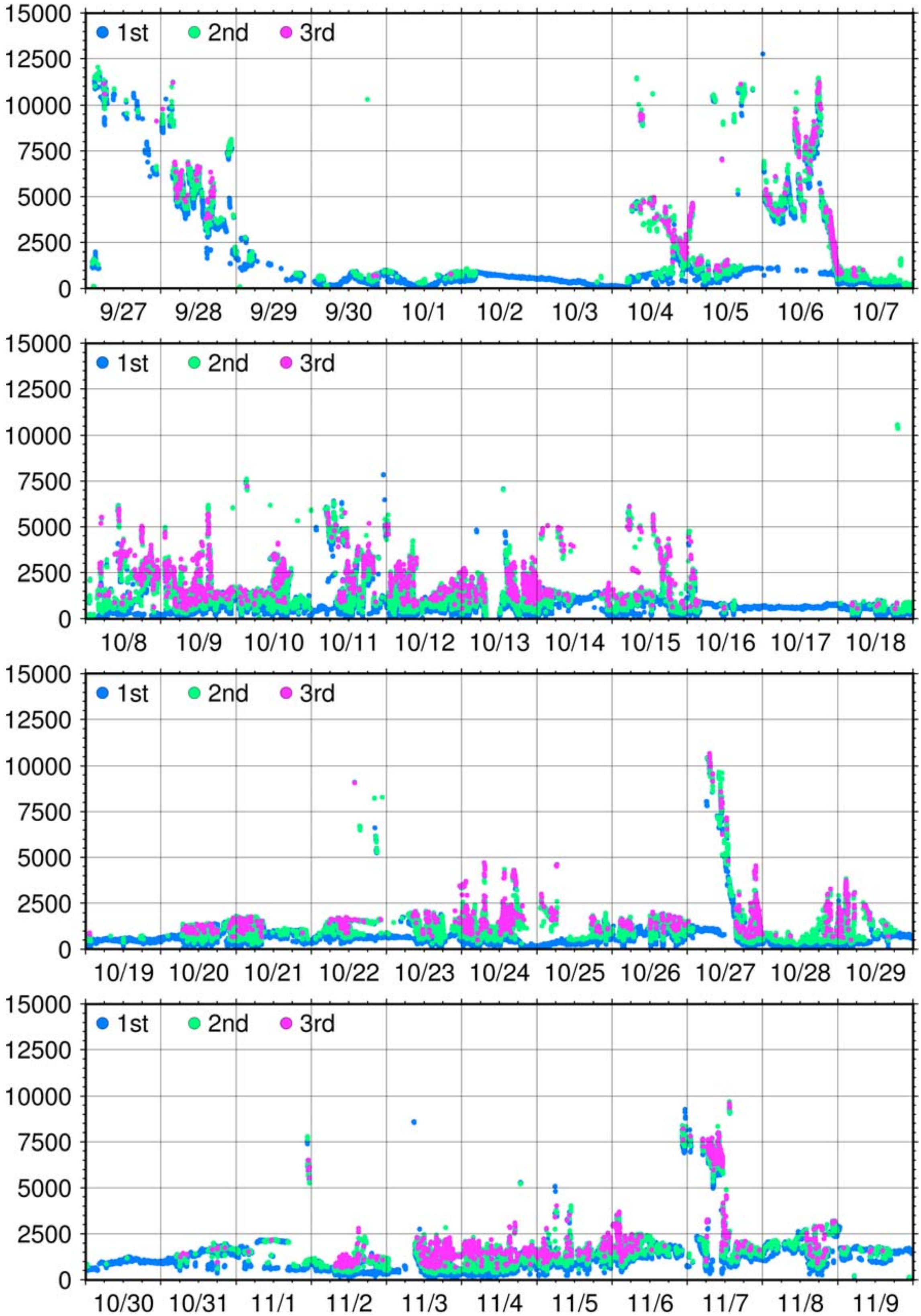

Figure 2.5: Time series of cloud base height during this cruise

2.6 Drones

(1) Personnel

Jun INOUE	NIPR	- PI
Kazutoshi SATO	KIT	
Tsubasa KODAIRA	The University of Tokyo	

(2) Objectives

The objective of this observation is to monitor the surface conditions of sea and sea ice.

(3) Instrumentations and Methods

Three types of DJI drones were used (Mavic Air, Mavic2 Enterprise Dual, and Phantom4 Pro+). Specification of each drone is shown in Table 2.6-1. All flights were made during daytime under calm wind condition. One or two assistants took a flight filed note (drawing the flight track, checking status of the drone) and watched a flying drone by their eyes (Figure 2.6-1).

Table 2.6-1

DJI Drones	 Mavic Air	 Mavic2 Enterprise Dual	 Phantom4 Pro+
Weight (g)	430	899	1388
Endurance (min)	21	31	30
Communication system	Wifi	OcuSync2.0	Lightbridge
Frequency	2.4GHz	2.4GHz	2.4GHz
Remarks	Intelligent flight mode	Self-heating batteries, a top-mount beacon, an infrared camera	

Figure 2.6-1: Pre-flight check with flight assistants on the deck.

Table 2.6-2: Flight summary

No.	mm/dd	Takeoff (SMT)	Landing (SMT)	Time (min)	Lat (˚N)	Lon (˚W)	Type of Drone	Purpose of flight Remarks (errors & other issues)
001	10/08	13:12	13:22	10	68.17	168.76	Mavic2	Test flight (GPS, gyrocompass, radio wave)
002	10/08	13:28	13:39	11	68.17	168.75	Mavic Air	Test flight (GPS, gyrocompass, radio wave, intelligent flight)
003	10/08	13:45	13:49	4	68.16	168.75	Phantom	Test flight (GPS, gyrocompass, radio wave)
		13:54	13:56	2				Errors (gyrocompass, GPS lost, gimbal)
004	10/15	14:52	15:12	20	77.10	164.62	Mavic2	Test flight (high altitude, RTH command, low battery)
005	10/16	11:54	12:09	15	78.08	164.93	Mavic2	Sea ice monitoring (sea ice distribution) Shipboard LIDAR beamed to the visible camera
006	10/17	10:01	10:02	1	78.01	165.02	Phantom	
		10:09	10:11	2				Errors (gyrocompass)
007	10/17	10:21	10:30	9	78.00	165.02	Mavic Air	Sea ice monitoring (sea ice distribution)
008	10/17	10:34	10:46	12	78.00	165.02	Mavic2	Sea ice monitoring (sea ice distribution)
009	10/18	11:25	11:42	17	78.07	165.17	Mavic2	Sea ice monitoring (surface temperature)
010	10/18	11:47	11:57	10	78.05	165.17	Phantom	Sea ice monitoring (sea ice distribution, waves) Errors (gyrocompass, unexpected flight App termination)
011	10/18	12:02	12:07	5	78/05	165.17	Mavic Air	Sea ice monitoring Errors (motor electric error), unexpected landing
012	10/24	10:52	11:09	17	77.81	163.52	Mavic2	Sea ice monitoring (surface temperature, waves) Errors (gyrocompass)
013	10/24	11:31	11:32	1	77.81	163.51	Phantom	Errors (gyrocompass, gimbal)
014	10/24	11:45	12:00	15	77.81	163.52	Mavic2	Sea ice monitoring (sea ice distribution, waves) Icing on propellers

(4) Preliminary Results

Table 2.6-2 shows the flight summary. The total number flights are 14 (1.5 hours). Flights #001-004 were test flights to check operation on the ship. Special conditions such as onboard operations under low temperature with heavy winter gears at high latitude were carefully assessed from the viewpoint of safety. In particular, the statuses of Global Navigation Satellite System (GPS & GLONASS), radio waves (2.4GHz), and a gyrocompass were fundamental for stable and safety operations. The latter flights focused on monitoring sea ice (its horizontal distribution, surface temperature, and wave attenuations into them). During the flight #005, there were a lot of small pan-cake ice floes near the ship (Figure 2.6-2). The surface temperature of sea ice was monitored by an infrared camera (Figure 2.6-3) and compered with a shipboard infrared radiometer.

(5) Data Archive

Data consists of photographs, movies, and additional information. All data obtained during this cruise will be submitted to the JAMSTEC Data Management Group (DMG).

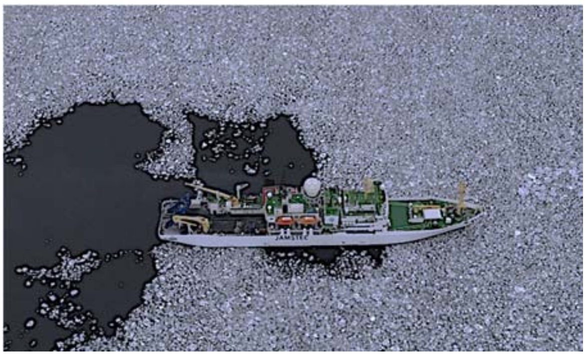

Figure 2.6-2: Sea-ice distribution around the ship (from flight #005).

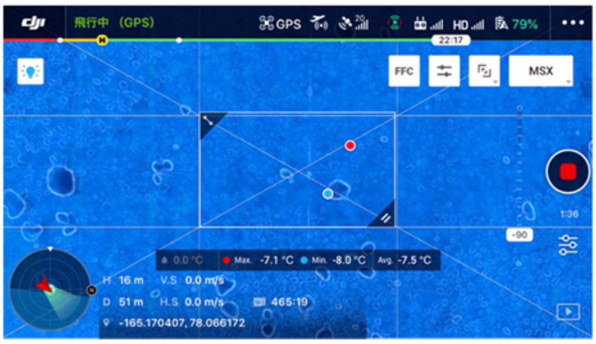

Figure 2.6-3: A screen shot of sea-ice surface temperature monitoring by an infrared camera (from flight #009).

(6) Remarks

The data from flights by Phantom (003 & 013) did not provide data because the drone did not fly correctly due to several mechanical errors. The time stamps of flights by Mavic Air (002, 007 & 011) are incorrect for some reasons. The flights by Mavic2 (001, 004, 005, 008, 009, 012 & 014) provided visible and infrared images, but digital values in infrared images are not available originally. RPReplay*.MP4 partly provides the values shown in the flight App on a flight monitor (iPad mini).

2.7 Infrared radiometer

(1) Personnel

Jun INOUE NIPR - PI

(2) Objectives

Surface temperature is a very important parameter for surface heat budget. The parameter is often used to calculate surface turbulent heat fluxes by bulk methods, upward longwave radiation, and conductive heat flux of sea ice. The objective of this observation is to monitor the skin temperature of sea and ice surface and to develop a method of quality control.

(3) Parameters

Surface temperature of water or sea-ice.

(4) Instrumentations and Methods

The infrared radiometer SI-431 model (Apogee Instruments, Inc.) has a spectral range between 8 to 14 µm with 14˚ half angle of field of view. The detectable range is from -40˚C to +70˚C. The sensor accuracy is 0.179˚C. The sensor was mounted on the starboard side of compass deck (about 20-m level above the sea surface) with 60˚ of mounting angle (Figure 2.7-1). Thus, the distance to the target (sea/ice surface) and target area is approximately 40m and 852m^2, in the along-ship direction ~20 m from the starboard of the ship (outside the ship's wake). The data is collected in every 10 minutes, and is recorded in a data logger (C-CR300). The raw dataset consists of time (yyyy-mm-dd hh:mm:ss), record number, target temperature, detector temperature, data logger temperature, and battery voltage.

Figure 2.7-1: IR sensor on the compass deck (a yellow arrow).

Daily maintenance was usually made after 08:30 SMT (19:30 UTC) with a cotton swab dipped in alcohol to remove frost, snow, dew, and sea spray (Table 2.7-1). It would be desired to exclude the period when rain and snowfall was observed. An optical rain gauge (see 2.10 Precipitation section) which also detects sea sprays is very useful to keep the data quality of the observed infrared temperature. Fog is not an appropriate condition for the surface measurement. In case of icing and snow accretion on the sensor, it does not observe sea/ice surface temperature but the temperature of the material on the sensor. To reduce these uncertainties in the dataset, the following quality control (QC) would be effective.

1. Exclude the period when relative humidity exceeds 99% to remove a fog situation
2. Exclude the period when ten-minute averaged intensity of precipitation (and/or sea spray) exceeding 0.01mm/h by using the Laser Precipitation Monitor (LPM2) (Adolf Thies GmbH & Co) (see section 2.10. Precipitation)
3. Exclude the period when the one-hour mean difference in temperature between a target and the detector is smaller than 0.2˚C to remove a situation of icing and snow accretion

In this QC-ed dataset "ir_data_lev01.txt", the suspected values have been replaced "-999.9".

In addition to this QC process, the data should be also corrected by atmospheric effect and emissivity. The radiation (E_o) observed by the instrument contains two components. One is the radiation directly emitted by the specific atmospheric layer (E_a) with an emissivity ε_a, and the other one is radiation from the surface (E_s). E_s can be divided by two components, one is the direct radiation from the target surface (E_t) with an emissivity ε_t, and the other one is the reflected radiation of background (E_b) with an emissivity ε_b. E_o is written by the following equation using the emissivity (ε) and reflectivity (1- ε) of the target surface:

$$E_o = \varepsilon_a E_a + (1-\varepsilon_a)E_s = \varepsilon_a E_a + (1-\varepsilon_a)[\varepsilon_t E_t + (1-\varepsilon_t)\varepsilon_b E_b] \qquad (1)$$

Eq. (1) can be written in terms of temperature using the Stefan-Boltzmann Law by the fourth power of its absolute temperature:

$$\sigma T_o^4 = \varepsilon_a \sigma T_a^4 + (1-\varepsilon_a)\sigma[\varepsilon_t T_t^4 + (1-\varepsilon_t)\,\varepsilon_b T_b^4] \qquad (2)$$

Here □ is the Stefan-Boltzmann constant (5.67×10^{-8} $Wm^{-2}K^{-4}$). The actual surface temperature (T_t) can be calculated by rearrangement of Eq. (2):

$$T_t = \sqrt[4]{\frac{T_o^4 - \varepsilon_a T_a^4 - (1-\varepsilon_a)(1-\varepsilon_t)\,\varepsilon_b T_b^4}{(1-\varepsilon_a)\varepsilon_t}} \qquad (3)$$

Here, T_a is the air temperature observed by the ship, and its emissivity ε_a is empirically estimated by using the effective water vapor (w*: mm) in the specific layer:

$$\varepsilon_a = 0.33\ln[1 + 3(w^*)^{0.45}] \qquad (4)$$

$$w^* = 0.2167\frac{e}{T_a}\Delta z \qquad (5)$$

Here, e is the water vapor pressure (hPa), and Δz (m) is the distance between the surface and the sensor. The corrected data (level 2 data: 'ir_data_lev02.txt') is a simple case of $\varepsilon_t = 1.00$ (i.e. without the reflection of background radiation).

In case of $\varepsilon_t < 1.00$ (i.e. reflection at the surface is considered), $\varepsilon_b T_b$ might be roughly estimated by downward longwave radiation ($LWD = \varepsilon_b \sigma T_b^4$) observed by an onboard infrared pygeometer with the 4~50µm spectral range (PIR Eppley labs, USA) at 31m height. This corrected data is archived as 'ir_data_lev03.txt'.

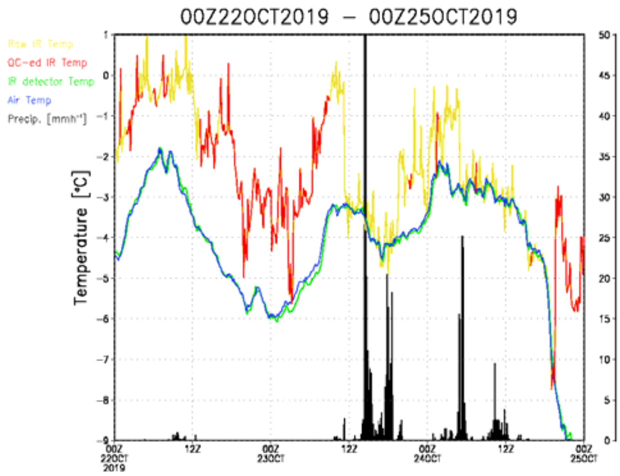

Figure 2.7-2: Preliminary result of surface temperature observed by an infrared radiometer. Raw data (yellow), quality-controlled surface temperature (red), and detector temperature (green). Precipitation intensity is indicated by black bars.

(5) Preliminary Results

Figure 2.7-2 shows time series of the raw infrared temperature (yellow), quality-controled temperature (red), and detector temperature (green) obtained by the instrument. As a reference, ten-minute averaged air temperature (blue: JamMet) and precipitation intensity (black bars: LPM2) are also shown. From 10:00 UTC to 12:00 UTC on 23 October, the value of raw infrared temperature dropped from 0˚C to -3.5˚C, and followed the values of detector and air temperatures, suggesting that the instrument observed snow temperature or the temperature of accreted snow on the sensor (heavy snowfall was observed in this day as shown in Figure 2.7-3). At the daily maintenance on 19:30 UTC 23 October, the snow accretion was found and cleaned. Although the raw temperature seems to be normal, the continuous snowfall on 24 October does not satisfy the requirement of QC-ed data (yellow line on 24 Oct). After daily maintenance on 19:30 UTC on 24 October, the temperature became normal. At this time, snow accretion and frost on the sensor was found as shown in Figure 2.7-4. After the maintenance, the surface temperature was well monitored under the cold environment (less than -7˚C) over the ice-covered area with grease ice on 24-25 October.

Figure 2.7-3: A snowfall event on 16:56 UTC 23 October. A yellow arrow shows the place of the IR sensor.

Figure 2.7-4: A situation of icing and snow accretion on 19:33UTC 24 October.

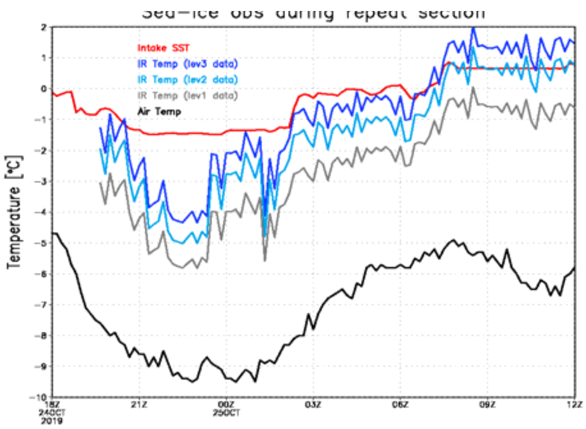

Figure 2.7-5: Surface temperature comparison among the QC-ed datasets during repeat section on 25 October.

Figure 2.7-6: Sea-ice condition at 22:00 UTC 24 October taken by a drone. The area overlaps the target surface of the IR sensor. A blue arrow in Figure 2.7-5 indicated the time of this image.

On 24 October, the ship entered the marginal ice zone at 20:31 UTC (based on the ice navigator's log). The intake SST kept -1.5˚C during a few hours, but the real sea-surface was covered by sea ice (Figure 2.7-6). The ice surface temperatures among three QC-ed datasets are compared here. The temperature is -5.5 ˚C (level 1), -4.6 ˚C (level 2), and -4.0 ˚C (level 3), respectively. Considering the sea surface temperature at 09:00 UTC 25 October, the level 1 dataset clearly underestimated the surface temperature. Level 2 & 3 datasets look better than the level 1 dataset.

Figure 2.7-7: Hard icing just before the daily maintenance on 19:36 UTC 29 October.

(6) Data Archive

The raw data obtained in this cruise and three QC-ed datasets will be submitted to the Data Management Group of JAMSTEC, and will be opened to the public via "Data Research System for Whole Cruise Information in JAMSTEC (DARWIN)" in JAMSTEC web site. http://www.godac.jamstec.go.jp/darwin/e

(7) Remarks

Note that the period of suspected data is from 05:00 UTC 24 October to 19:30 UTC 24 October as shown in Figure 2.7-2. Also, the data from 00:00 UTC 29 October to 19:30 UTC 29 October is influenced by hard icing (Figure 2.7-7, Table 2.7-1). A part of these periods still remains after the QC. A raw value during these periods has been replaced a value “-999.9” in the QC-ed files.

All QC-ed data would be a subject of modification because the data sources utilized in the QC processes (relative humidity, precipitation, etc) might be also changed after their QCs.

Table 2.7-1: Daily maintenance time

mm/dd	9/29	9/30	10/1	10/2	10/2	10/3	10/4	10/5	10/6	10/7	10/8
hh:mm (UTC)	03:00	23:31	0:05 22:22	21:23	21:23	21:31	23:37	20:27	19:31	19:36	1:31 19:34
remark	Start recording					fog				Sea spray	fog
mm/dd	10/9	10/10	10/11	10/12	10/13	10/14	10/15	10/16	10/17	10/18	10/19
hh:mm	19:35	19:32	19:34	19:32	19:34	19:35	19:34	19:41	21:52	19:32	19:36
remark				frost			drizzle			Sea spray	
mm/dd	10/20	10/21	10/22	10/23	10/24	10/25	10/26	10/27	10/28	10/26	10/27
hh:mm	19:33	19:35		0:13 19:34	19:32	19:33	19:32	19:35	19:42	19:32	19:35
remark		Sea spray		Snow accretion	Frost, snow accretion				Rain or sea spray		
mm/dd	10/28	10/29	10/30	10/31	11/1	11/2	11/3	11/4	11/5	11/6	11/7
hh:mm	19:42	19:36 19:42	19:35	20:32	20:32	20:32	21:31	21:31	22:31	22:31	22:30
remark	Heavy rain	Hard icing			Sea spray	Sea spray	Rain	Rain		Sea spray	End of recording

2.8 Sea spray

(1) Personal

Jun Inoue	NIPR	- PI
Toshihiro Ozeki	Hokkaido Univ. of Education	- not on board
Hajime Yamaguchi	University of Tokyo	- not on board
Ryo Kusakawa	University of Tokyo	

(2) Objectives

Marine disasters caused by ship icing occur frequently in cold regions. The typical growth mechanism of sea spray icing is as follows. First, sea spray is generated from the bow of the ship. Next, the spray drifts and impinges upon the superstructure, after which there is a wet growth of ice from the brine water flow. To address icing on the ship, we focus on the impinging seawater spray. We investigated the drop size of seawater spray on R/V Mirai.

(3) Parameters

Number of sea spray particles
Spray particle size distribution
Liquid water contents
The amount of spray impinging on ships

(4) Instruments and methods

The amount of seawater spray and the size distribution of seawater particles were measured by a spray particle counter (SPC) and a marine rain gauge type spray gauge (MRS).

(4-1) Spray particle counter (SPC)

The SPC, which was originally developed for the measurement of drifting snow, was improved to be a seawater spray particle counter. The flux distribution and the transport rate can be calculated as a function of particle size. The SPC (SPC-S7; Niigata Denki) consists of a sensor, data processor, and personal computer, and the measuring range is set from 100 to 1,000 μm in diameter. The sensing area is 25 mm wide, 3 mm high, and 0.5 mm deep, and SLD light is used as a parallel ray. The sensor measures light attenuation caused by particles that pass through the sensing area. The processor divides the particles into 32 classes depending on their diameters. The particles in each class are counted every second. The volume flux of the spray was calculated by ($4\pi r_c^3/3$) where r_c is class value of particle radius. The unit of the volume flux is millimeters [mm] per unit time, which is also the unit of precipitation.

(4-2) Marine rain gauge type spray gauge (MRS)

The marine rain gauge type spray gauge (MRS) consists of a marine rain gauge (CYG-50202, R M Young) and a cylindrical spray trap. The marine rain gauge was developed to measure rainfall on ships. It collects seawater spray or precipitation in a catchment funnel which has a cross sectional area of 100 cm^2. The inside diameter of the funnel is 112 mm. The cylindrical spray trap is attached above the marine rain gauge to capture the seawater spray from the horizontal direction instead of precipitation. The impinging spray particle is drained into the catchment funnel. The spray trap has a diameter of 76.3 mm, a height of 120 mm, and the projected area is 92 cm^2. The amount of seawater spray is measured every minute. The smallest measurable unit is 0.1 mm.

To reveal the positional relationship of the amount of seawater spray, observations were conducted from three different points on the deck. SPC were installed on center of the compass deck. The two MRSs were installed one on the port side and one on the starboard side of the bridge deck. They were set on the bulwark behind 42 m from the bow.

(5) Station list or Observation log

The data of SPCs, MRS were obtained continuously through the cruise from 27 Sep. 2019 to 7 Nov. 2019. Experimental cruise for generating sea spray is given at 06:20-08:20 on 13 Nov. 2019, 15:45-17:45 on 19 Nov. 2019, and 16:50-18:50 on 20 Nov. 2019 (UTC).

(6) Preliminary results

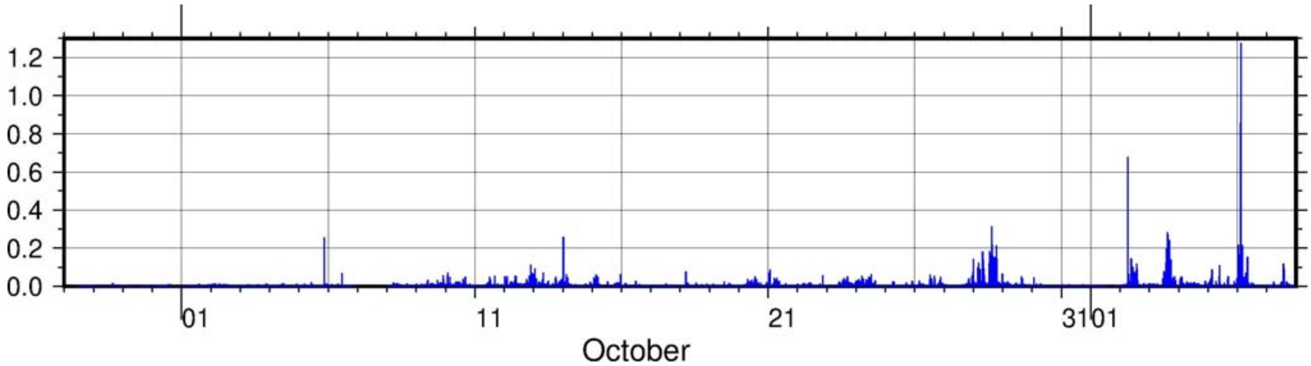

Figure 2.8-1: Spray and rainfall flux observed by SPC

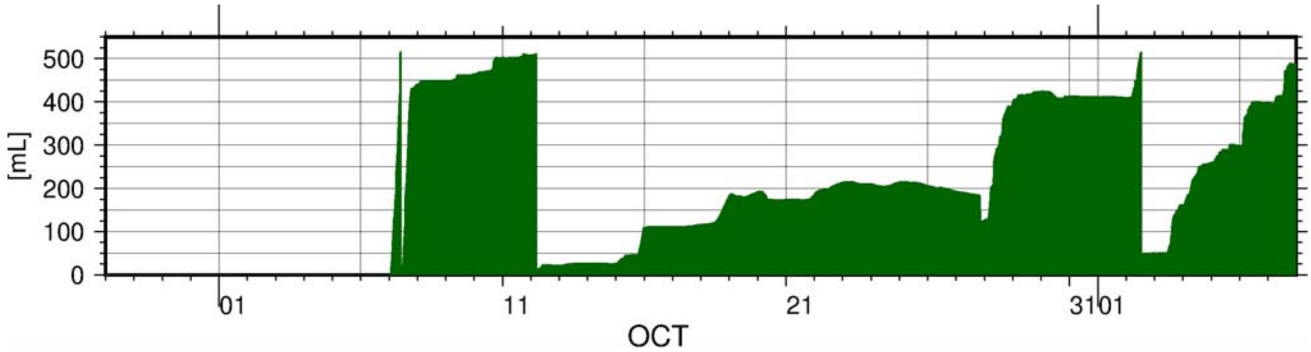

Figure 2.8-2: Spray and rainfall amount observed by the starboard side MRS

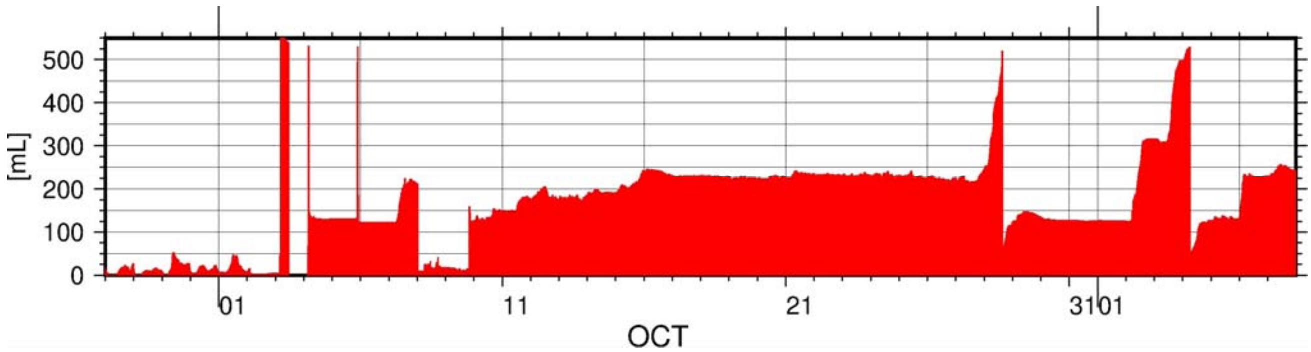

Figure 2.8-3: Spray and rainfall amount observed by the port side MRS

(6) Data archives

These data obtained in this cruise will be submitted to the Data Management Group of JAMSTEC, and will be opened to the public via “Data Research System for Whole Cruise Information in JAMSTEC (DARWIN)” in JAMSTEC web site.

2.9. Water vapor

2.9.1 Isotope observation

(1) Personnel

Hotaek Park JAMSTEC PI

(2) Background and objective

The Arctic sea-ice decline that results from global warming is progressing beyond the range of modeling projection. The results of the declining sea ice are identified as increased cyclone and clouds, further warming by ice-albedo feedbacks, especially significant in autumn and winter, and increased precipitation over the pan-Arctic. The ocean warming resulted from the warming air temperature enhances energy exchanges with atmosphere, particularly in autumn when sea ice initiates to recover. The resulting wetness of lower atmosphere boundary has likely the opportunity of water-vapor transports into the adjacent regions through atmospheric circulation. Indeed, the evidence of the transport has been observed as a result of increased snow depth in the autumn and early winter in the northern Arctic terrestrial regions, although there are still debates relating to the correlation between the increasing snow depth and declining sea ice. Snow is an import component in the fields of hydrological cycle, climate, and permafrost. The cumulated snow during winter season is rapidly melted in spring, distributing to soil moisture and river discharge. The observed discharges indicated significant increases in spring season, with advanced discharging timing as a result of earlier snow melt derived by the warming temperature. The snow insulates permafrost during the winter, enhancing the warming and thus likely discharging some of the melted water from permafrost to river. The linkage between the terrestrial hydrology and the Arctic sea ice suggests the potential impacts of the declining sea ice on the hydrological processes in the terrestrial regions.

Using numerical models are a useful way to identify the linkage of the declining sea ice and the terrestrial hydrology, while the modeling is requiring the validation of the simulated results against observations. Isotope is characterized by the strength to do backward tracing the source area of precipitated water. The combination of model simulation and isotope observation makes it possible to explore the relationship of the declining sea ice and the terrestrial water cycle. Therefore, a consecutive observation of the isotope of atmospheric water vapor was conducted during the MR19-03C Arctic cruise. The observed preliminary results are documented on here.

(3) Parameters

Isotope ratios of Oxygen and Hydrogen and water vapor concentration

(4) Instrument and method

The isotope of atmosphere water vapor was monitored by a Cavity Ringdown Spectrometer (L2130-i, Isotopic H_2O, Picarro, Figure 2.9.1-1), which simultaneously observes the isotope ratios of oxygen and hydrogen with 1–2 Hz frequency, including water vapor concentration. The observed data are archived on the storage of the spectrometer, operated by Windows system. Two standard liquids, for example with isotope values of -0.262 permil and -30.873 permil in oxygen, are individually injected for 15 minutes every 12-hour, in which the derived linear regression equation is used to calibrate the monitored

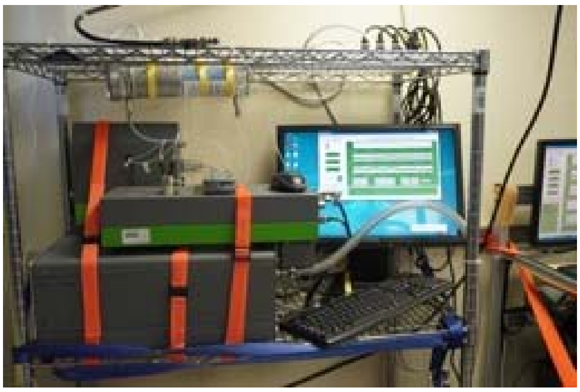

Figure 2.9.1-1: Isotope observing spectrometer system.

values by the spectrometer.

(5) Preliminary results

The observed isotope ratios were averaged to hourly time steps (Figure 2.9.1-2), which shows diurnal and inter-daily variability consistent with raw data. Figure 2.9.1-2 displays results observed in the Arctic Ocean during the period of October 10–27. The isotope ratios are generally decreasing with the elapse of dates, which represents influences of air temperature toward cooling phage. In reality, the isotope of oxygen significantly correlated with air temperature (Figure 2.9.1-3), as addressed by other observations. The isotopes show large diurnal and daily variability (Figure 2.9.1-2). Here discussed for the three days (i.e., October 13, 15, and 25) that recorded the lowest and highest isotope ratios. The isotope of oxygen indicated the minimum -29 permil on October 13 and -28.5 permil on October 25 when it recorded air temperature -9℃. The isotope has higher correlation with air temperature, as mentioned above. The air temperature of the date 13 was higher than one of the date 25. This deviation suggests impacts by other variables on the isotopes decoupled from air temperature. One of those is wind transporting warmer/colder water vapor. There was strong wind from north on the date 13. On the other hand, the date 15 was governed by strong southern wind, transported warmer and wetter water vapor. In this state, it is difficult to quantify the impact of wind on the changes in the isotope, which will be explored by the methods of model simulation and backward trajectory.

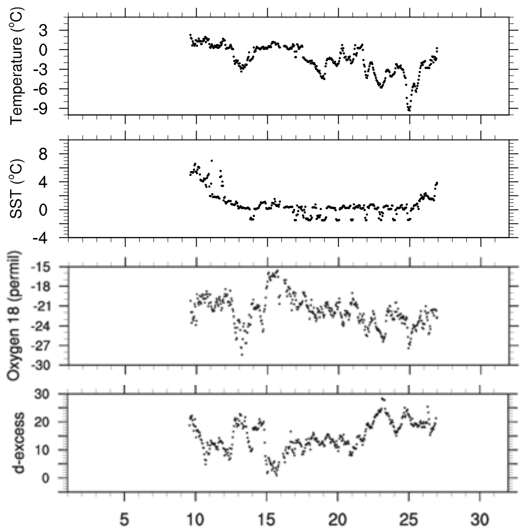

Figure 2.9.1-2: Variability of air temperature, sea surface temperature, and isotopes of oxygen and hydrogen during 10 and 27 October.

Both oxygen and hydrogen indicated significantly high correlation. Their relationship yielded a slope of 6.1, which is distributing within the ranges of 5 and 7 obtained at the Arctic regions.

(6) Data archive

The data obtained in this cruise will be submitted to the Data Management Group of JAMSTEC, and will be opened to the public via “Data Research System for Whole Cruise Information in JAMSTEC (DARWIN)” in JAMSTEC web site. http://www.godac.jamstec.go.jp/darwin/e.

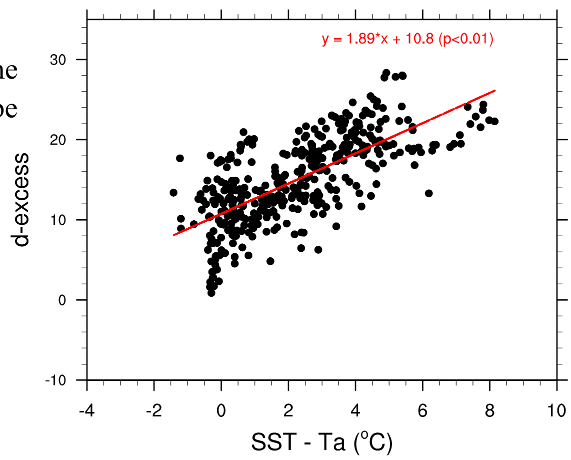

Figure 2.9.1-3: The relationship between d-excess and difference in temperature between sea surface and

2.9.2 GNSS precipitatble water

(1) Personnel

Fumikazu TAKETANI	JAMSTEC	- PI
Masaki KATSUMATA	JAMSTEC	- not on board
Mikiko FUJITA	JAMSTEC	- not on board
Kyoko TANIGUCHI	JAMSTEC	- not on board

(2) Objective

Getting the GNSS satellite data to estimate the total column integrated water vapor content of the atmosphere.

(3) Method

The GNSS satellite data was archived to the receiver (Trimble NetR9) with 5 sec interval. The GNSS antenna (Margrin) was set on the roof of aft wheel house. The observations were carried out all thru the cruise.

(4) Results

We will calculate the total column integrated water from observed GNSS satellite data after the cruise.

(5) Data archive

Raw data is recorded as T02 format and stream data every 5 seconds. These raw datasets are available from Mikiko Fujita of JAMSTEC. Corrected data will be submitted to JAMSTEC Marine-Earth Data and Information Department and will be archived there.

2.10 Tropospheric gas and particles observation in the Arctic Marine Atmosphere

2.10.1 Surface measurement

(1) Personnel

Fumikazu Taketani	JAMSTEC	- PI
Taro Maruo	JAMSTEC/Kobe Univ.	
Yugo Kanaya	JAMSTEC	- not on board
Takuma Miyakawa	JAMSTEC	- not on board
Kaori Kawana	JAMSTEC	- not on board
Hisahiro Takashima	JAMSTEC/Fukuoka Univ.	- not on board
Yutaka Tobo	NIPR	- not on board
Yoko Iwamoto	Hiroshima Univ.	- not on board
Masayuki Takigawa	JAMSTEC	- not on board
Masahiro Yamaguchi	JAMSTEC	- not on board
Zhu Chunmao	JAMSTEC	- not on board
Kazuyuki Miyazaki	JAMSTEC	- not on board
Kazuyo Yamaji	JAMSTEC/Kobe Univ.	- not on board

(2) Objectives

• To investigate roles of aerosols in the marine atmosphere in relation to climate change

• To investigate processes of biogeochemical cycles between the atmosphere and the ocean.

• To investigate contribution of suspended particles to the rain, and snow

(3) Parameters

• Black carbon(BC) and fluorescent particles

• Particle size distribution

• Particle number concentration

• Aerosol extinction coefficient (AEC)

• Composition of ambient particles

• Composition of snow and rain

• Surface ozone(O_3), and carbon monoxide(CO) mixing ratios

(4) Instruments and methods

(4-1) Online aerosol observations:

(4-1-1) Particle number concentration and size distribution

The number concentration of ament particles was measured by mixing condensation particle counter (MCPC) (Model 1720, Brechtel). The size distribution of particles was measured by a scanning mobility particle sizer (SMPS) (Nano Scan model 3910, TSI), and a handheld optical particle counter (OPC) (KR-12A, Rion). The number concentration of cloud condescended nuclei (CCN) in the ambient air were measured by a cloud condescended nuclei Counter (CCNC) (CCN-100, Droplet Measurement Technologies). The CCNC detected the activated particles using an optical particle counter under supersaturated water vapor condition made in a 50-cm-high column.

(4-1-2) Black carbon (BC)

Number and mass BC concentration were measured by an instrument based on laser-induced incandescence, single particle soot photometer (SP2) (model D, Droplet Measurement Technologies). The laser-induced incandescence technique based on intracavity Nd:YVO4 laser operating at 1064 nm were used for detection of single particles of BC.

(4-1-3) Fluorescent property

Fluorescent properties of aerosol particles were measured by a single particle fluorescence sensor, Waveband Integrated bioaerosol sensor (WIBS4) (WIBS-4A, Droplet Measurement Technologies). Two pulsed xenon lamps emitting UV light (280 nm and 370 nm) were used for excitation. Fluorescence emitted from a single particle within 310–400 nm and 420–650 nm wavelength windows was recorded.

(4-1-4) Aerosol extinction coefficient (AEC)

Multi-Axis Differential Optical Absorption Spectroscopy (MAX-DOAS), a passive remote sensing technique measuring spectra of scattered visible and ultraviolet (UV) solar radiation, was used for atmospheric aerosol and gas profile measurements. Our MAX-DOAS instrument consists of two main parts: an outdoor telescope unit and an indoor spectrometer (Acton SP-2358 with Princeton Instruments PIXIS-400B), connected to each other by a 14-m bundle optical fiber cable. The line of sight was in the directions of the portside of the vessel and the scanned elevation angles were 1.5, 3, 5, 10, 20, 30, 90 degrees in the 30-min cycle. The roll motion of the ship was measured to autonomously compensate additional motion of the prism, employed for scanning the elevation angle. For the selected spectra recorded with elevation angles with good accuracy, DOAS spectral fitting was performed to quantify the slant column density (SCD) of NO2 (and other gases) and O4 (O2-O2, collision complex of oxygen) for each elevation angle. Then, the O4 SCDs were converted to the aerosol optical depth (AOD) and the vertical profile of aerosol extinction coefficient (AEC) using an optimal estimation inversion method with a radiative transfer model. Using derived aerosol information, retrievals of the tropospheric vertical column/profile of NO2 and other gases were made.

For SP2, MCPC, SMPS, and CCNC instrument, the ambient air was commonly sampled from the compass deck by a 3-m-long conductive tube through the dryer to dry up the particles, and then introduced to each instrument installed at the environmental research room. WIBS4 and OPC instruments were installed at the compass deck. The ambient air was directory introduced to the instruments. MAXDOAS were installed at the deck above stabilizer of ship

(4-2) Ambient air sampling

Ambient air samplings were carried out by air samplers installed at compass deck. Ambient particles were collected on the quartz filter (ϕ=110 and ϕ=55), polycarbonate and nuclepore membrane filter (half-moon of 37mm and ϕ =47mm) along cruise track to analyze their composition and ice nuclei ability using a high-volume air sampler (HV-525PM, SIBATA), NANO sampler (model 3182, Kanomax), a handmade air sampler and MOUDI sampler (MOUDI-10, MSP) operated at flow rate of 500L/min, 40 L/min, 10L/min, and 1.8L/min respectively. Ambient aerosol sampling for bioaerosol analysis: Coarse-mode aerosol particles ($\geq$0.9 µm) were also sampled to a vial bottle using a cyclone (PM1,URG) with a flow rate of 20 L/min. For ambient bioaerosol analysis, Milli-Q water was added to the vial bottles and the solution was filtered by the membrane filter onto the gold-coated chip. The stained fluorescence measurements were also conducted with reagents of DAPI and Hoechst. Then, the abundance of bioaerosol particles (dead/alive) was counted using a Bioplorer (KB-VKH01, Koyo Sangyo Co., Ltd), based on the fluorescence measurements with UV and green light excitation.

To avoid collecting particles emitted from the funnel of the own vessel, the sampling period was controlled automatically by using a “wind-direction selection system”. These sampling logs are listed in Tables 2.10-1, 2.10-2, 2.10-3, 2.10-4, and 2.10-5. The samples are going to be analyzed in laboratory.

(4-4) CO and O_3

Ambient air was continuously sampled on the compass deck and drawn through ~20-m-long Teflon tubes connected to a gas filter correlation CO analyzer (Model 48C, Thermo Fisher Scientific) and a UV photometric ozone analyzer (2TB), located in the Research Information Center. The data will be used for characterizing air mass origins.

(5) Observation log

Table 2.10.1-1: Logs of ambient particles sampling on the quartz filter by HV sampler

On board ID	Date Collected					Latitude			Longitude		
	YYYY	MM	DD	hh:mm:ss	UTC/JST	Deg.	Min.	N/S	Deg.	Min.	E/W
MR1903C-HV-001	2019	9	29	07:11	UTC	40	22.65	N	142	28.29	E
MR1903C-HV-002	2019	10	1	01:19	UTC	42	13.80	N	152	47.16	E
MR1903C-HV-003	2019	10	2	22:31	UTC	48	43.12	N	163	46.54	E
MR1903C-HV-004	2019	10	4	21:14	UTC	55	01.43	N	173	38.17	E
MR1903C-HV-005	2019	10	6	20:59	UTC	60	56.43	N	176	56.95	W
MR1903C-HV-006	2019	10	8	20:23	UTC	67	33.49	N	168	45.04	W
MR1903C-HV-007	2019	10	10	20:09	UTC	72	59.92	N	160	01.04	W
MR1903C-HV-008	2019	10	12	20:04	UTC	72	20.40	N	144	59.75	W
MR1903C-HV-009	2019	10	14	20:48	UTC	74	46.45	N	150	30.51	W
MR1903C-HV-010	2019	10	16	20:13	UTC	77	39.86	N	165	00.08	W
MR1903C-HV-011	2019	10	18	20:13	UTC	78	02.11	N	164	58.68	W
MR1903C-HV-012	2019	10	20	20:18	UTC	77	45.00	N	165	00.11	W
MR1903C-HV-013	2019	10	23	00:44	UTC	77	46.78	N	164	03.13	W
MR1903C-HV-014	2019	10	24	20:04	UTC	77	46.15	N	164	32.57	W
MR1903C-HV-015	2019	10	26	20:34	UTC	72	00.01	N	168	45.01	W
MR1903C-HV-016	2019	10	28	20:08	UTC	66	02.61	N	168	44.96	W
MR1903C-HV-017	2019	10	30	19:58	UTC	58	56.86	N	179	21.09	E
MR1903C-HV-018	2019	11	1	21:20	UTC	51	18.65	N	168	19.35	E
MR1903C-HV-019	2019	11	3	22:20	UTC	47	49.53	N	162	11.19	E
MR1903C-HV-020	2019	11	5	23:10	UTC	41	36.35	N	151	44.69	E

Table 2.10.1-2: Logs of ambient particles sampling on the quartz filter by NANO sampler

On board ID	Date Collected					Latitude			Longitude		
	YYYY	MM	DD	hh:mm:ss	UTC/JST	Deg.	Min.	N/S	Deg.	Min.	E/W
MR1903C-NANO-001	2019	9	29	07:11	UTC	40	22.65	N	142	28.29	E
MR1903C-NANO-002	2019	10	1	01:19	UTC	42	13.80	N	152	47.16	E
MR1903C-NANO-003	2019	10	2	22:31	UTC	48	43.12	N	163	46.54	E
MR1903C-NANO-004	2019	10	5	20:52	UTC	58	06.54	N	168	23.17	W
MR1903C-NANO-005	2019	10	8	20:23	UTC	67	33.49	N	168	45.04	W
MR1903C-NANO-006	2019	10	11	20:08	UTC	72	05.53	N	153	21.91	W
MR1903C-NANO-007	2019	10	14	20:48	UTC	74	46.45	N	150	30.51	W
MR1903C-NANO-008	2019	10	18	02:24	UTC	77	42.91	N	165	00.29	W
MR1903C-NANO-009	2019	10	20	20:18	UTC	77	45.00	N	165	00.11	W
MR1903C-NANO-010	2019	10	23	20:29	UTC	77	45.36	N	163	53.40	W
MR1903C-NANO-011	2019	10	26	20:34	UTC	72	00.01	N	168	45.01	W
MR1903C-NANO-012	2019	10	29	20:30	UTC	62	29.98	N	174	41.13	W
MR1903C-NANO-013	2019	11	1	21:20	UTC	51	18.65	N	168	19.35	E
MR1903C-NANO-014	2019	11	3	22:20	UTC	47	49.53	N	162	11.19	E
MR1903C-NANO-015	2019	11	5	23:10	UTC	41	36.35	N	151	44.69	E

Table 2.10.1-3: Logs of ambient particles sampling on the nuclepore filter.

On board ID	Date Collected					Latitude			Longitude		
	YYYY	MM	DD	hh:mm:ss	UTC/JST	Deg.	Min.	N/S	Deg.	Min.	E/W
MR1903C-INP-001	2019	9	29	0.2993056	UTC	40	22.65	N	142	28.29	E
MR1903C-INP-002	2019	10	1	0.0548611	UTC	42	13.80	N	152	47.16	E
MR1903C-INP-003	2019	10	2	0.9381944	UTC	48	43.12	N	163	46.54	E
MR1903C-INP-004	2019	10	4	0.8847222	UTC	55	01.43	N	173	38.17	E
MR1903C-INP-005	2019	10	6	0.8743056	UTC	60	56.43	N	176	56.95	W
MR1903C-INP-006	2019	10	8	0.8493056	UTC	67	33.49	N	168	45.04	W
MR1903C-INP-007	2019	10	10	0.8395833	UTC	72	59.92	N	160	01.04	W
MR1903C-INP-008	2019	10	12	0.8361111	UTC	72	20.40	N	144	59.75	W
MR1903C-INP-009	2019	10	14	0.8666667	UTC	74	46.45	N	150	30.51	W
MR1903C-INP-010	2019	10	16	0.8423611	UTC	77	39.86	N	165	00.08	W
MR1903C-INP-011	2019	10	18	0.8423611	UTC	78	02.11	N	164	58.68	W
MR1903C-INP-012	2019	10	20	0.8458333	UTC	77	45.00	N	165	00.11	W
MR1903C-INP-013	2019	10	23	0.0305556	UTC	77	46.78	N	164	03.13	W
MR1903C-INP-014	2019	10	24	0.8361111	UTC	77	46.15	N	164	32.57	W
MR1903C-INP-015	2019	10	26	0.8569444	UTC	72	00.01	N	168	45.01	W
MR1903C-INP-016	2019	10	28	0.8388889	UTC	66	02.61	N	168	44.96	W
MR1903C-INP-017	2019	10	30	0.8319444	UTC	58	56.86	N	179	21.09	E
MR1903C-INP-018	2019	11	1	0.8888889	UTC	51	18.65	N	168	19.35	E
MR1903C-INP-019	2019	11	3	0.9305556	UTC	47	49.53	N	162	11.19	E
MR1903C-INP-020	2019	11	5	0.9652778	UTC	41	36.35	N	151	44.69	E

Table 2.10.1-4: Logs of ambient particles sampling on the polycarbonate filter by MOUDI.

On board ID	Date Collected					Latitude			Longitude		
	YYYY	MM	DD	hh:mm:ss	UTC/JST	Deg.	Min.	N/S	Deg.	Min.	E/W
MR1903C-MOUDI-001	2019	9	29	07:11	UTC	40	22.65	N	142	28.29	E
MR1903C-MOUDI-002	2019	10	6	20:59	UTC	60	56.43	N	176	56.95	W
MR1903C-MOUDI-003	2019	10	14	20:48	UTC	74	46.45	N	150	30.51	W
MR1903C-MOUDI-004	2019	10	21	22:53	UTC	78	01.36	N	164	58.01	W
MR1903C-MOUDI-005	2019	10	29	20:30	UTC	62	29.98	N	174	41.13	W

Table 2.10.1-5: Logs of ambient particles sampling by PM1 cyclone.

On board ID	Date Collected					Latitude			Longitude		
	YYYY	MM	DD	hh:mm:ss	UTC/JST	Deg.	Min.	N/S	Deg.	Min.	E/W
MR1903C-Cyclone-001	2019	10	8	01:36	UTC	64	50.60	N	169	30.20	W
MR1903C-Cyclone-002	2019	10	9	19:37	UTC	70	38.46	N	168	15.51	W
MR1903C-Cyclone-003	2019	10	11	20:08	UTC	72	05.12	N	153	12.82	W
MR1903C-Cyclone-004	2019	10	13	19:46	UTC	74	23.03	N	143	36.95	W
MR1903C-Cyclone-005	2019	10	15	19:38	UTC	76	34.41	N	162	15.18	W
MR1903C-Cyclone-006	2019	10	18	02:24	UTC	77	42.91	N	165	00.29	W
MR1903C-Cyclone-007	2019	10	19	19:55	UTC	77	47.07	N	164	59.84	W
MR1903C-Cyclone-008	2019	10	21	22:54	UTC	78	01.38	N	164	59.98	W
MR1903C-Cyclone-009	2019	10	24	01:37	UTC	77	29.01	N	164	08.35	W
MR1903C-Cyclone-010	2019	10	25	19:38	UTC	75	21.58	N	168	45.00	W
MR1903C-Cyclone-011	2019	10	27	19:43	UTC	68	30.05	N	168	45.10	W
MR1903C-Cyclone-012	2019	10	29	19:38	UTC	62	26.30	N	174	48.00	W
MR1903C-Cyclone-013	2019	10	31	20:30	UTC	55	08.37	N	173	38.31	E
MR1903C-Cyclone-014	2019	11	2	20:40	UTC	49	59.99	N	166	06.92	E
MR1903C-Cyclone-015	2019	11	4	21:32	UTC	44	47.12	N	156	57.12	E

(6) Data archives

These data obtained in this cruise will be submitted to the Data Management Group of JAMSTEC, and will be opened to the public via "Data Research System for Whole Cruise Information in JAMSTEC (DARWIN)" in JAMSTEC web site.
<http://www.godac.jamstec.go.jp/darwin/e>

2.10.2 Tethered balloon observation

(1) Personnel

Fumikazu Taketani	JAMSTEC	- PI
Taro Maruo	JAMSTEC/Kobe Univ.	
Yugo Kanaya	JAMSTEC	- not on board
Takuma Miyakawa	JAMSTEC	- not on board
Yoko Iwamoto	Hiroshima Univ.	- not on board
Masayuki Takigawa	JAMSTEC	- not on board
Kazuyo Yamaji	JAMSTEC/Kobe Univ.	- not on board
Ryo Oyama	NME	

(2) Objectives

• To investigate vertical profiles of aerosol number concentration and size distribution in the marine atmosphere

(3) Parameters

• Particle size distribution
• Particle number concentration
• Black carbon(BC) mass concentration
• Composition of ambient particles

(4) Instruments and methods

Tethered balloon observation were carried out by airship-shaped balloon (15m3, Kikyu-Seisakujo) connected to portable winch installed at upper deck (Figure 2.10.2-1) by the cable. The bag installed instruments and GPS sonde were connected below 5 m and 10 m from the balloon, respectively (Figure 2.10.2-2). Vertical profiles of particle number concentration, BC mass concentration, particle size distribution were measured by condensation particle counter (CPC) (Model 3007, TSI) and Black carbon (BC) monitor (AE51, Magii), optical particle counter (HHPC6+, Beckman coulter), respectively. Aerosol particles were also sampled by custom-made sampler at highest position in each observation. These samples will be analyzed in the laboratory after cruise. We carried out 7 times tethered balloon observation in this course. Date and location were listed in Table 2.10.2

(5) preliminary results

Figure 2.10.2-3 indicated the results of vertical profiles of number concentration, and size-selected number concentration, and relative humidity, measured by CPC, OPC, and GPS sonde.

(6) Data archives

These data obtained in this cruise will be submitted to the Data Management Group of JAMSTEC, and will be opened to the public via “Data Research System for Whole Cruise Information in JAMSTEC (DARWIN)” in JAMSTEC web site.
<http://www.godac.jamstec.go.jp/darwin/e>

Figure 2.10.2-1: tethered balloon observation

Figure 2.10.2-2: instruments employed in the tethered balloon observation

Table 2.10.2 Logs of tethered balloon observation

	date(UTC)	Lat(N)	Long(E)	Attained height(m)	location
1st	10/2 0:23	45.61	158.36	850	North Western Pacific
2nd	10/6 0:12	58.13	178.45	1200	Bering Sea
3rd	10/11 1:01	72.73	201.68	500	Arctic Ocean
4th	10/16 0:40	76.98	195.25	950	Arctic Ocean
5th	10/17 19:06	77.75	195.02	700	Arctic Ocean
6th	10/17 23:45	78.01	195.02	660	Arctic Ocean(MIZ)
7th	10/22 21:00	77.76	195.31	1050	Arctic Ocean

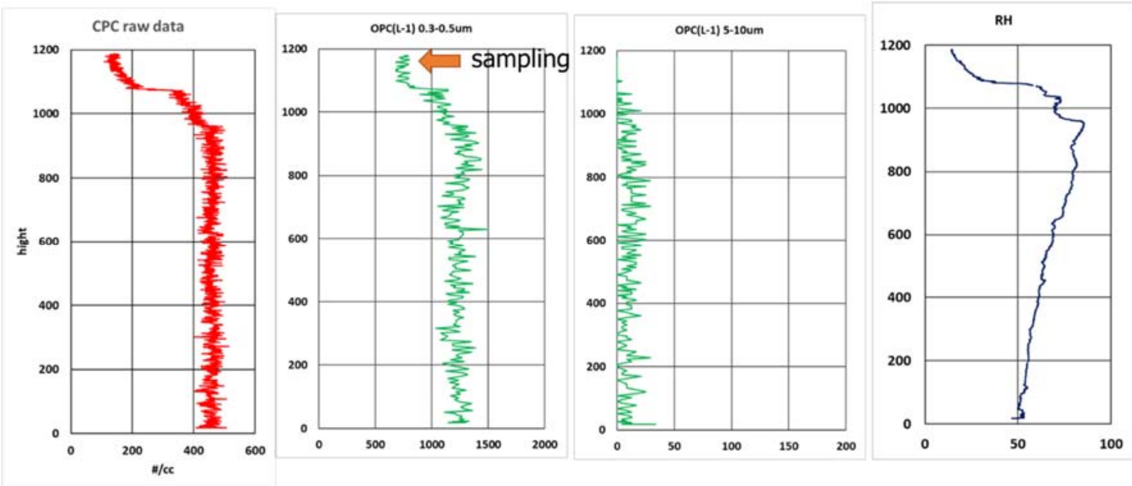

Figure 2.10.2-3: Vertical profiles of number concentration, and size-selected number concentration, and relative humidity

2.11 Precipitation

2.11.1 Disdrometer

(1) Personnel

Fumikazu TAKETANI	JAMSTEC	- PI
Masaki KATSUMATA	JAMSTEC	- not on board
Biao GENG	JAMSTEC	- not on board
Kyoko TANIGUCHI	JAMSTEC	- not on board

(2) Objectives

The disdrometer can continuously obtain size distribution of raindrops. The objective of this observation is (a) to reveal microphysical characteristics of the rainfall, depends on the type, temporal stage, etc. of the precipitating clouds, (b) to retrieve the coefficient to convert radar reflectivity (especially from C-band radar in Section 2.3) to the rainfall amount, and (c) to validate the algorithms and the products of the satellite-borne precipitation radars; TRMM/PR and GPM/DPR.

(3) Instrumentations and Methods

Two "Laser Precipitation Monitor (LPM)" (Adolf Thies GmbH & Co) are utilized. It is an optical disdrometer. The instrument consists of the transmitter unit which emit the infrared laser, and the receiver unit which detects the intensity of the laser come thru the certain path length in the air. When a precipitating particle fall thru the laser, the received intensity of the laser is reduced. The receiver unit detect the magnitude and the duration of the reduction and then convert them onto particle size and fall speed. The sampling volume, i.e. the size of the laser beam "sheet", is 20 mm (W) x 228 mm (D) x 0.75 mm (H).

The number of particles are categorized by the detected size and fall speed and counted every minutes. The categories are shown in Table 2.11.1.

The LPMs are installed on the top (roof) of the anti-rolling system, as shown in Figure 2.11.1-1. Both are installed at the corner at the bow side and the starboard side. One (in aft) equipped the "wind protection element" to reduce the effect of the wind on the measurement, and to estimate the effectiveness of the "element" by comparing data from two sensors.

(4) Preliminary Results

The data have been obtained all through the cruise, except non-permitted territorial waters and EEZs. An example of the obtained data is shown in Figure 2.11.1-2. The further analyses for the rainfall amount, drop-size-distribution parameters, etc., will be carried out after the cruise.

(5) Data Archive

All data obtained during this cruise will be submitted to the JAMSTEC Data Management Group (DMG).

(6) Acknowledgment

The operations are supported by Japan Aerospace Exploration Agency (JAXA) Precipitation Measurement Mission (PMM).

Figure 2.11.1-1: Onboard LPM sensors. (Left) The location of the sensors, as designated by the red broken circle. (Right) The sensors. Right one (aft one) equipped wind protection element to reduce the effect of the wind, while left one (fore one) did not.

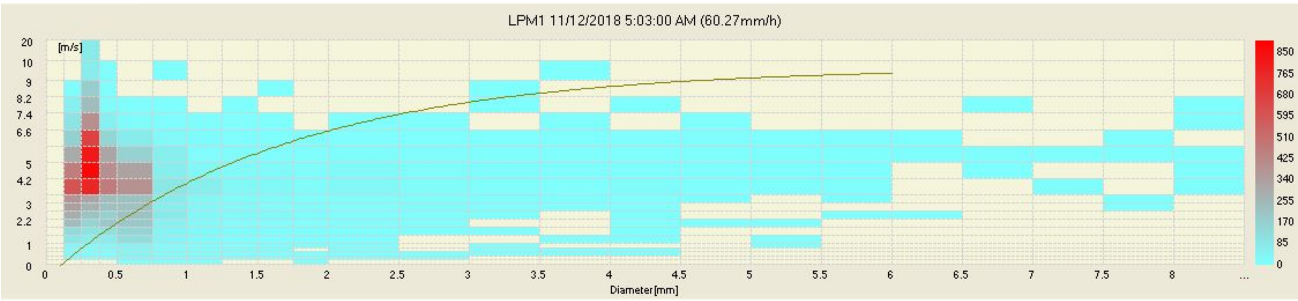

Figure 2.11.1-2: An example of 1-minute raw data, obtained by LPM at 0503UTC on Nov. 12, 2018. Data is shown by two-dimensional histogram to display numbers of observed raindrops categorized by diameter (x-axis) and fall speed (y-axis).

Table 2.11.1: Categories of the particle size and the fall speed.

Particle Size			Fall Speed		
Class	Diameter [mm]	Class width [mm]	Class	Speed [m/s]	Class width [m/s]
1	≥ 0.125	0.125	1	≥ 0.000	0.200
2	≥ 0.250	0.125	2	≥ 0.200	0.200
3	≥ 0.375	0.125	3	≥ 0.400	0.200
4	≥ 0.500	0.250	4	≥ 0.600	0.200
5	≥ 0.750	0.250	5	≥ 0.800	0.200
6	≥ 1.000	0.250	6	≥ 1.000	0.400
7	≥ 1.250	0.250	7	≥ 1.400	0.400
8	≥ 1.500	0.250	8	≥ 1.800	0.400
9	≥ 1.750	0.250	9	≥ 2.200	0.400
10	≥ 2.000	0.500	10	≥ 2.600	0.400
11	≥ 2.500	0.500	11	≥ 3.000	0.800
12	≥ 3.000	0.500	12	≥ 3.400	0.800
13	≥ 3.500	0.500	13	≥ 4.200	0.800
14	≥ 4.000	0.500	14	≥ 5.000	0.800
15	≥ 4.500	0.500	15	≥ 5.800	0.800
16	≥ 5.000	0.500	16	≥ 6.600	0.800
17	≥ 5.500	0.500	17	≥ 7.400	0.800
18	≥ 6.000	0.500	18	≥ 8.200	0.800
19	≥ 6.500	0.500	19	≥ 9.000	1.000
20	≥ 7.000	0.500	20	≥ 10.000	10.000
21	≥ 7.500	0.500			
22	≥ 8.000	unlimited			

2.11.2 Micro Rain Radar

(1) Personnel

Fumikazu TAKETANI	JAMSTEC	- PI
Masaki KATSUMATA	JAMSTEC	- not on board
Biao GENG	JAMSTEC	- not on board
Kyoko TANIGUCHI	JAMSTEC	- not on board

(2) Objectives

The micro rain radar (MRR) is a compact vertically-pointing Doppler radar, to detect vertical profiles of rain drop size distribution. The objective of this observation is to understand detailed vertical structure of the precipitating systems.

(3) Instruments and Methods

The MRR-2 (METEK GmbH) was utilized. The specifications are in Table 2.11.2. The antenna unit was installed at the starboard side of the anti-rolling systems (see Figure 2.11.2-1), and wired to the junction box and laptop PC inside the vessel.

The data was averaged and stored every one minute. The vertical profile of each parameter was obtained every 100 meters in range distance (i.e. height) up to 3100 meters. The recorded parameters were; Drop size distribution, radar reflectivity, path-integrated attenuation, rain rate, liquid water content and fall velocity..

Figure 2.11.2-1: Photo of the antenna unit of MRR

Table 2.11.2: Specifications of the MRR-2.

Transmitter power	50 mW
Operating mode	FM-CW
Frequency	24.230 GHz (modulation 1.5 to 15 MHz)
3dB beam width	1.5 degrees
Spurious emission	< -80 dBm / MHz
Antenna Diameter	600 mm
Gain	40.1 dBi

(4) Preliminary Results

The data have been obtained all through the cruise, except non-permitted territorial waters and EEZs. Figure 2.11.2-2 displays an example of the time-height cross section for one day. The temporal variation reasonably corresponds to the rainfall measured by the Mirai Surface Met sensors (see Section 2.4), C-band radar (see Section 2.3), etc. The further analyses will be after the cruise.

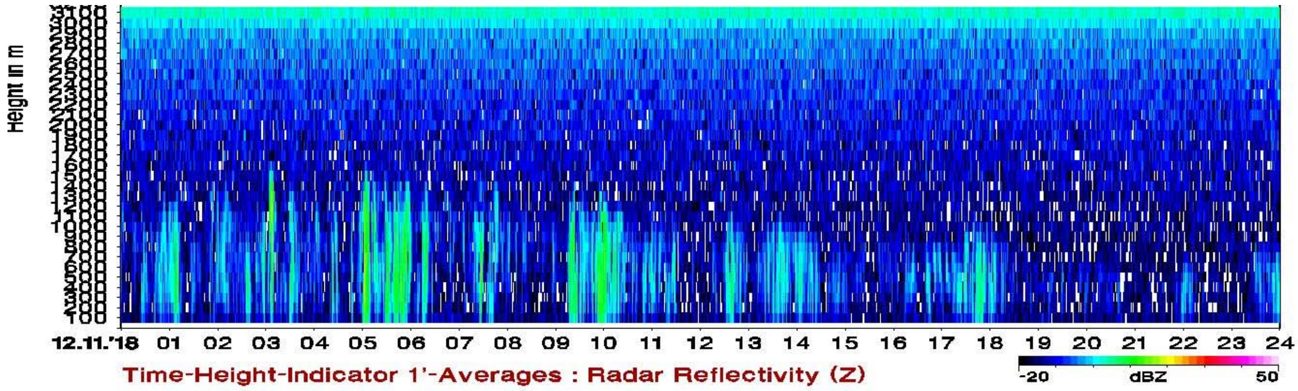

Figure 2.11.2-2: An example of the time-height cross section of the radar reflectivity, for 24 hours from 00UTC on November 12.

(5) Data Archive

All data obtained during this cruise will be submitted to the JAMSTEC Data Management Group (DMG).

(6) Acknowledgment

The operations are supported by Japan Aerospace Exploration Agency (JAXA) Precipitation Measurement Mission (PMM).

2.11.3 Precipitation sampling

(1) Personnel

Hotaek Park JAMSTEC

Fumikazu Taketani JAMSTEC

(2) Objectives

• To investigate contribution of suspended particles to the rain, and snow

• To investigate isotope ratio of Hydrogen and Oxygen in the rain and snow

(3) Parameters

• Chemical composition of snow and rain

• Isotope ratio of Oxygen in the rain and snow

(4) Instruments and methods

Snow and rain samples were corrected using hand-made rain/snow sampler. S. These sampling logs are listed in Table 2.11.3. To investigate the isotope ratio in the rain/snow and interaction from aerosols to rain/snow, these samples are going to be analyzed in laboratory.

(5) Observation log

Table 2.11.3: Logs of precipitation sampling

No.	Date (UTC)	latitude	longitude	type
1	10/4	56-12N	175-24E	rain
2	10/7	64-08N	171-28W	rain
3	10/9	71-18N	165-55W	rain
4	10/10	72-59N	160-00W	mixed
5	10/11	72-07N	153-38W	snow
6	10/11	72-00N	148-29W	snow
7	10/13	74-21N	143-38W	snow
8	10/14	74-46N	150-31W	mixed
9	10/15	76-34N	162-07W	mixed
10	10/15	76-46N	163-27W	mixed
11	10/16	77-30N	164-59W	snow
12	10/20	77-39N	164-59W	snow
13	10/21	77-39N	164-59W	snow
14	10/23	77-45N	164-49W	snow
15	10/24	77-46N	165-00W	snow
16	10/28	66-01N	168-45W	rain
17	10/29	62-38N	174-24W	rain
18	11/3	49-59N	166-06E	rain

19	11/4	47-54N	162-19E	rain
20	11/4	46-54N	160-33E	rain
21	11/5	44-45N	156-54E	rain
22	11/6	41-40N	151-52E	rain

(6) Data archives

These data obtained in this cruise will be submitted to the Data Management Group of JAMSTEC, and will be opened to the public via "Data Research System for Whole Cruise Information in JAMSTEC (DARWIN)" in JAMSTEC web site-
<http://www-godac-jamstec-go-jp/darwin/e>

2.12 Lidar Observation

(1) Personnel

Fumikazu TAKETANI	JAMSTEC	- PI
Masaki KATSUMATA	JAMSTEC	- not on board
Kyoko TANIGUCHI	JAMSTEC	- not on board
Ryo OYAMA	NME	
Souichiro SUEYOSHI	NME	
Shinya OKUMURA	NME	
Kazuho YOSHIDA	NME	
Yutaro MURAKAMI	NME	

(1) Objective

The objective of this observation is to capture the vertical distribution of clouds, aerosols, and water vapor in high spatio-temporal resolution.

(2) Instrumentations and Methods

The Mirai Lidar system transmits a 10-Hz pulse laser in three wavelengths: 1064nm, 532nm, 355nm. For cloud and aerosol observation, the system detects Mie scattering at these wavelengths. The separate detections of polarization components at 532 nm and 355 nm obtain additional characteristics of the targets. The system also detects Raman water vapor signals at 660 nm and 408nm, Raman nitrogen signals at 607 nm and 387nm at nighttime. Based on the signal ratio of Raman water vapor to Raman nitrogen, the system offers water vapor mixing ratio profiles.

(3) Preliminary Results

The lidar system observed the lower atmosphere throughout the cruise, except on EEZs and territorial waters without permission. All data will be reviewed after the cruise to maintain data quality.

(4)Data Archive

All data obtained during this cruise will be submitted to the JAMSTEC Data Management Group (DMG).

2.13 Greenhouse gasses observation

(1) Personnel

Yasunori Tohjima	NIES	-PI, not on board
Shigeyuki Ishidoya	AIST	-not on board
Fumikazu Taketani	JAMSTEC	
Taro Maruo	JAMSTEC	
Shinji Morimoto	Tohoku Univ.	-not on board
Shuji Aoki	Tohoku Univ.	-not on board
Ryo Fujita	Tohoku Univ.	-not on board
Hideki Nara	NIES	-not on board
Daisuke Goto	NIPR	-not on board
Prabir Patra	JAMSTEC	-not on board
Hiroshi Uchida	JAMSTEC	-not on board
Shohei Murayama	AIST	-not on board

(2) Objective

(2-1) Continuous observations of CO_2, CH_4 and CO mixing ratios

The Arctic region is considered to be vulnerable to the global warming, which would potentially enhance emissions of the greenhouse gases including CO_2 and CH_4 from the carbon pools in the Arctic regions into the atmosphere. The objective of this study is to detect the increases in the atmospheric greenhouse gas levels associated with the ongoing global warming in the Arctic region in the early stage. The continuous observations of the atmospheric CO_2 and CH_4 mixing ratios during this MR16-06 cruise would allow us to detect the enhanced mixing ratios associated with the regional emissions and to estimate the distribution of the regional emission sources. The atmospheric CO mixing ratios, which were also observed at the same time, can be used as an indicator of the anthropogenic emissions associated with the combustion processes.

(2-2) Discrete flask sampling

In order to clarify spatial variations and air-sea exchanges of the greenhouse gases at northern high latitude, whole air samples were corrected into 40 stainless-steel flasks on-board R/V MIRAI (MR19-03C). The collected air samples will be analyzed for the mixing ratios of CO_2, O_2, Ar, CH_4, CO, N_2O and SF_6 and the stable isotope ratios of CO_2 and CH_4.

(3) Parameters

(3-1) Continuous observations of CO_2, CH_4 and CO mixing ratios

Mixing ratios of atmospheric CO_2, CH_4, and CO.

(3-2) Discrete flask sampling

Mixing ratios of atmospheric CO_2, O_2 (O_2/N_2 ratio), Ar (Ar/N_2 ratio), CH_4, CO, N_2O and SF_6, □^{13}C and □^{18}O of CO_2, $\delta^{13}C$ and δD of CH_4.

(4) Instruments and Methods

(4-1) Continuous observations of CO_2, CH_4 and CO mixing ratios

Atmospheric CO_2, CH_4, and CO mixing ratios were measured by a wavelength-scanned cavity ring-down spectrometer (WS-CRDS, Picarro, G2401). An air intake, capped with an inverted stainless steel beaker covered with stainless steel mesh, was placed on the right-side of the upper deck. A diaphragm pump (GAST, MOA-P108) was used to draw in the outside air at a flow rate of ~8 L min^{-1}. Water vapor in the sample air was removed to a dew pint of about 2°C and about -35°C by passing it through a thermoelectric dehumidifier (KELK, DH-109) and a Nafion drier (PERMA PURE, PD-50T-24), respectively. Then, the dried sample air was introduced into the WS-CRDS at a flow rate of 100 ml min^{-1}. The WS-CRDS were automatically calibrated every 50 hour by introducing 3 standard airs with known CO_2, CH_4 and CO mixing ratios. The analytical precisions for CO_2, CH_4 and CO mixing ratios are about 0.02 ppm, 0.3 ppb and 3 ppb, respectively.

(4-2) Discrete flask sampling

The air sampling equipment consisted of an air intake, a piston pump (GAST LOA), a water trap, solenoid valves (CKD), an ethanol bath as refrigerant, a flow meter and an immersion cooler (EYELA ECS-80). Ambient air was pumped using a piston pump from an air intake, dried cryogenically and filled into a 1 L stainless-steel flask at a pressure of 0.55 MPa.

(5) Station list or Observation log

The continuous observations of CO_2, CH_4 and CO mixing ratios were conducted during the entire cruise. Sampling logs of the discrete flask sampling are listed in Table 2.13.

Table 2.13: List of logs of the discrete flask sampling

On board ID	Date Collected					Latitude			Longitude		
	YYYY	MM	DD	hh:mm:ss	UTC/JST	Deg.	Min.	N/S	Deg.	Min.	E/W
MR1903C-F001	2019	9	29	06:50	UTC	40	23.4	N	142	19.9	E
MR1903C-F002	2019	9	30	07:26	UTC	40	09.84	N	148	38.36	E
MR1903C-F003	2019	10	1	01:42	UTC	42	16.1	N	152	50.57	E
MR1903C-F004	2019	10	2	07:05	UTC	46	17.66	N	159	29.52	E
MR1903C-F005	2019	10	3	07:23	UTC	49	59.93	N	166	7.1	E
MR1903C-F006	2019	10	4	07:08	UTC	52	50.29	N	170	31.14	E
MR1903C-F007	2019	10	4	22:54	UTC	55	29.4	N	173	45.1	E
MR1903C-F008	2019	10	6	05:53	UTC	58	38.81	N	179	13.81	E
MR1903C-F009	2019	10	7	02:41	UTC	61	47.49	N	175	77.29	W
MR1903C-F010	2019	10	8	00:53	UTC	64	42.55	N	169	48.93	W
MR1903C-F011	2019	10	9	01:48	UTC	68	17.49	N	168	45.17	W
MR1903C-F012	2019	10	10	00:21	UTC	71	6.75	N	166	31.24	W
MR1903C-F013	2019	10	10	21:01	UTC	72	58.52	N	159	49.5	W
MR1903C-F014	2019	10	12	00:21	UTC	72	0.39	N	151	17.67	W
MR1903C-F015	2019	10	13	01:16	UTC	73	1.334	N	144	55.28	W
MR1903C-F016	2019	10	13	21:59	UTC	74	25.31	N	143	2.82	W
MR1903C-F017	2019	10	14	23:58	UTC	74	59.7	N	152	16.4	W
MR1903C-F018	2019	10	15	22:09	UTC	76	49.02	N	163	46.3	W
MR1903C-F019	2019	10	17	01:57	UTC	77	54.59	N	164	59.49	W
MR1903C-F020	2019	10	18	06:26	UTC	77	15.03	N	164	59.94	W
MR1903C-F021	2019	10	19	00:38	UTC	78	3.23	N	165	10.28	W
MR1903C-F022	2019	10	20	00:26	UTC	78	3.37	N	164	57.79	W
MR1903C-F023	2019	10	20	22:33	UTC	78	0.57	N	164	59.28	W
MR1903C-F024	2019	10	22	00:25	UTC	77	56.86	N	165	02.00	W
MR1903C-F025	2019	10	23	02:10	UTC	77	46.26	N	164	3.98	W
MR1903C-F026	2019	10	23	22:01	UTC	77	46.69	N	163	36.97	W
MR1903C-F027	2019	10	24	20:56	UTC	77	47.58	N	163	54.96	W
MR1903C-F028	2019	10	25	23:57	UTC	74	41.48	N	168	46.03	W
MR1903C-F029	2019	10	26	21:19	UTC	71	56.4	N	168	44.77	W
MR1903C-F030	2019	10	28	00:29	UTC	68	18.11	N	167	11.07	W
MR1903C-F031	2019	10	28	20:49	UTC	65	59.99	N	168	44.97	W
MR1903C-F032	2019	10	30	00:46	UTC	65	52.39	N	175	45.97	W
MR1903C-F033	2019	10	30	03:24	UTC	58	8.51	N	178	6.1	E
MR1903C-F034	2019	11	1	01:55	UTC	54	22.35	N	172	25.97	E
MR1903C-F035	2019	11	2	21:47	UTC	51	16.17	N	168	16.67	E
MR1903C-F036	2019	11	3	00:51	UTC	50	0.06	N	166	7.26	E
MR1903C-F037	2019	11	4	02:39	UTC	47	19.05	N	161	17.75	E
MR1903C-F038	2019	11	5	02:04	UTC	44	12.76	N	155	58.83	E
MR1903C-F039	2019	11	6	07:02	UTC	41	8.05	N	150	41.12	E
MR1903C-F040	2019	11	7	03:04	UTC	40	17.07	N	146	18.88	E

(6) Data archives

These data obtained in this cruise will be submitted to the Data Management Group (DMG) of JAMSTEC, and will opened to the public via “R/V Mirai Data Web Page” in JAMSTEC home page.

2.14 Sea ice radar

(1) Personnel

Kazutoshi Sato	KIT	-PI
Ryo Oyama	NME	
Souichiro Sueyoshi	NME	
Shinya Okumura	NME	
Kazuho Yoshida	NME	
Yutaro Murakami	NME	
Takehito Hattori	MIRAI Crew	

(2) Objectives

In the sea ice areas, Marine radar provides an important tool for the detection of sea ice and icebergs. It is importance to monitor the sea ice daily and produce ice forecasts to assist ship traffic and other marine operations. In order to select route optimally, ice condition prediction technology is necessary, and image information of ice-sea radar is used for constructing a route selection algorithm.

(3) Parameters

Capture format: JPEG

Capture interval: 60 seconds

Resolution: 1,280×1,024 pixel

Color tone: 256 gradation

(4) Instruments and methods

R/V MIRAI is equipped with an Ice Navigation Radar, “sigma S6 Ice Navigator (Rutter Inc.)”. The ice navigation radar, the analog signal from the x-band radar is converted by a modular radar interface and displayed as a digital video image (Figure 2.14). The sea ice radar is equipped with a screen capture function and saves at arbitrary time intervals.

(5) Observation Period

6 Oct. 2019 - 29 Oct. 2019

(6) Data archives

These data obtained in this cruise will be submitted to the Data Management Group of JAMSTEC, and will be opened to the public via “Data Research System for Whole Cruise Information in JAMSTEC (DARWIN)” in JAMSTEC web site.

<http://www.godac.jamstec.go.jp/darwin/e>

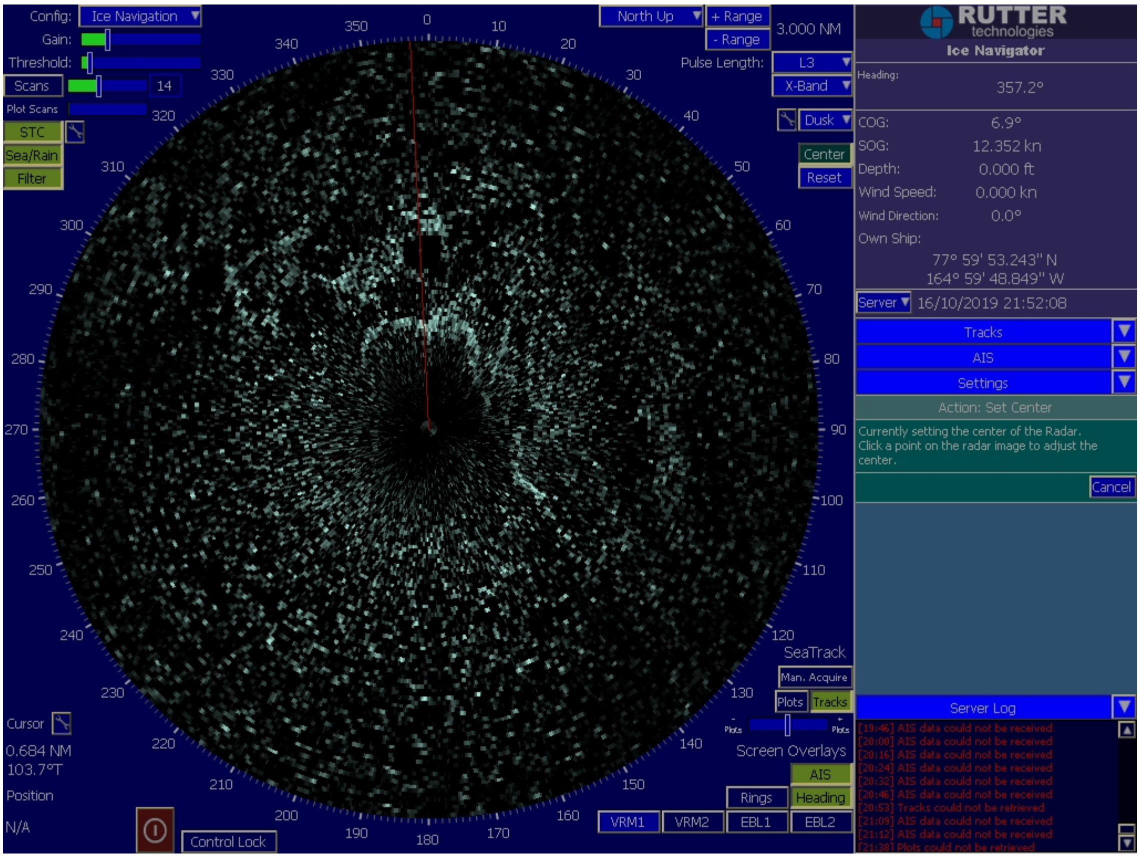

Figure 2.14: Image of sea ice from Sea ice radar

3. Physical Oceanography

3.1 CTD cast and water sampling

(1) Personnel

Yusuke KAWAGUCHI	The University of Tokyo	- not on board, PI
Shigeto NISHINO	JAMSTEC	- not on board, PI
Akihiko Murata	JAMSTEC	
Shinsuke TOYODA	MWJ	- Operation leader
Rio KOBAYASHI	MWJ	
Shungo OSHITANI	MWJ	
Tun Htet Aung	MWJ	

(2) Objective

Investigation of oceanic structure and water sampling.

(3) Parameters

Temperature (Primary and Secondary)
Salinity (Primary and Secondary)
Pressure
Dissolved Oxygen (Primary “RINKO III” and Secondary “SBE43”)
Fluorescence (Primary and Secondary)
Beam Transmission
Turbidity
Nitrate
Altimeter
Deep Ocean Standards Thermometer

(4) Instruments and Methods

CTD/Carousel Water Sampling System, which is a 36-position Carousel Water Sampler (CWS) with Sea-Bird Electronics, Inc. 12-liter sample Bottles were used for sampling seawater. The sensors attached on the CTD were temperature (primary and secondary), conductivity (primary and secondary), pressure, dissolved oxygen (primary: RINKO III, secondary: SBE43), fluorescence (primary and secondary), beam transmission, turbidity, nitrate, altimeter and Deep Ocean Standards Thermometer. Salinity was computed by measured values of pressure, conductivity and temperature. The CTD/CWS was deployed from starboard on working deck.

Specifications of the sensors are listed below.
CTD: SBE911plus CTD system
Under water unit:
SBE9plus (S/N: 09P21746-0575, Sea-Bird Electronics, Inc.)
Pressure sensor: Digiquartz pressure sensor (S/N: 79492)
Calibrated Date: 18 Apr. 2019

Carousel water sampler:
SBE32 (S/N: 3254451-0826, Sea-Bird Electronics, Inc.)

Temperature sensors:
Primary: SBE03-04/F (S/N: 031525, Sea-Bird Electronics, Inc.)
Calibrated Date: 01 Jun. 2019
Secondary: SBE03-04/F (S/N: 031464, Sea-Bird Electronics, Inc.)

Calibrated Date: 01 Jun. 2019

Conductivity sensors:

Primary: SBE04C (S/N: 042435, Sea-Bird Electronics, Inc.)

Calibrated Date: 25 Jun. 2019

Secondary: SBE04C (S/N: 043036, Sea-Bird Electronics, Inc.)

Calibrated Date: 25 Jun. 2019

Dissolved Oxygen sensor:

Primary: RINKOIII (S/N: 0287_163011BA, JFE Advantech Co., Ltd.)

Calibrated Date: 29 May. 2019

Secondary: SBE43 (S/N: 430575 Sea-Bird Electronics, Inc.)

Calibrated Date: 02 Jul. 2019

Fluorescence:

Primary:

Chlorophyll Fluorometer (S/N: 3618, Seapoint Sensors, Inc.)

Gain setting: 30X, 0-5 ug/l

Calibrated Date: None

Offset: 0.000

Secondary:

Chlorophyll Fluorometer (S/N: 3700, Seapoint Sensors, Inc.)

Gain setting: 3X, 0-50 ug/l

Calibrated Date: None

Offset: 0.000

Transmission meter:

C-Star (S/N CST-1726DR, WET Labs, Inc.)

Calibrated Date: 13 Jun. 2019

Casts used: 000M001-021M005

C-Star (S/N CST-1727DR, WET Labs, Inc.)

Calibrated Date: 03 Jun. 2015

Casts used:025M001-00M004

Nitrate:

Deep SUNA (S/N 895, Satlantic, Inc.)

Calibration Date: 19 Sep. 2019

Casts used: 000M001, 000M002, 001M001-014M001, 018M001

Turbidity:

Turbidity Meter (S/N: 14953)

Gain setting: 100X

Scale factor: 1.000

Calibrated Date: None

Altimeter:

Benthos PSA-916T (S/N: 1157, Teledyne Benthos, Inc.)

Submersible Pump:

Primary: SBE5T (S/N: 055816, Sea-Bird Electronics, Inc.)

Secondary: SBE5T (S/N: 054598, Sea-Bird Electronics, Inc.)

Bottom contact switch: (Sea-Bird Electronics, Inc.)

Deck unit: SBE11plus (S/N 11P54451-0872, Sea-Bird Electronics, Inc.)

Configuration file: MR1903C_A.xmlcon
000M001, 001M001 - 014M001, 018M001
MR1903C_B.xmlcon
000M002, 015M001 - 017M001, 019M001 - 021M004
MR1903C_C.xmlcon
024M001, 019M004, 020M006, 021M005
MR1903C_D.xmlcon
025M001 – 000M004,

The CTD raw data were acquired on real time using the Seasave-Win32 (ver.7.23.2) provided by Sea-Bird Electronics, Inc. and stored on the hard disk of the personal computer. Seawater was sampled during the up cast by sending fire commands from the personal computer.

For depths where vertical gradients of water properties were exchanged to be large, the bottle was exceptionally fired after waiting from the stop for 60 seconds to enhance exchanging the water between inside and outside of the bottle. 30 seconds below thermocline to stabilize then fire. 8 casts of CTD measurements were conducted (Table 3.1).

Data processing procedures and used utilities of SBE Data Processing-Win32 (ver.7.26.7.114) and SEASOFT were as follows:

(The process in order)

DATCNV: Convert the binary raw data to engineering unit data. DATCNV also extracts bottle information where scans were marked with the bottle confirm bit during acquisition. The duration was set to 4.4 seconds, and the offset was set to 0.0 seconds.

TCORP (original module): Corrected the pressure sensitivity of the temperature (SBE3) sensor.

S/N 031525: -1.714e-008 (degC/dbar)

S/N 031464: + 7.75293156e-009 (degC/dbar)

RINKOCOR (original module): Corrected the time dependent, pressure induced effect (hysteresis) of the RINKOIII profile data.

RINKOCORROS (original module): Corrected the time dependent, pressure induced effect (hysteresis) of the RINKOIII bottle information data by using the hysteresis corrected profile data.

BOTTLESUM: Create a summary of the bottle data. The data were averaged over 4.4 seconds.

ALIGNCTD: Convert the time-sequence of sensor outputs into the pressure sequence to ensure that all calculations were made using measurements from the same parcel of water. Dissolved oxygen data are systematically delayed with respect to depth mainly because of the long time constant of the dissolved oxygen sensor and of an additional delay from the transit time of water in the pumped pluming line. This delay was compensated by 5 seconds advancing dissolved oxygen sensor (SBE43) output (dissolved oxygen voltage) relative to the temperature data. RINKOIII voltage (User polynomial 0) was advanced 1 second and transmission data was advanced 2 seconds.

WILDEDIT: Mark extreme outliers in the data files. The first pass of WILDEDIT obtained the accurate estimate of the true standard deviation of the data. The data were read in blocks of 1000 scans. Data greater than 10 standard deviations were flagged. The second pass computed a standard deviation over the same 1000 scans excluding the flagged values. Values greater than 20 standard deviations were marked bad. This process was applied to pressure, depth, temperature (primary and secondary), conductivity (primary and secondary), dissolved oxygen voltage (SBE43).

CELLTM: Remove conductivity cell thermal mass effects from the measured conductivity. Typical values used were thermal anomaly amplitude alpha = 0.03 and the time constant 1/beta = 7.0.

FILTER: Perform a low pass filter on pressure and depth data with a time constant of 0.15 second. In order to produce zero phase lag (no time shift) the filter runs forward first then backward

WFILTER: Perform a median filter to remove spikes in the fluorescence data (primary and secondary), transmission data, transmission beam attenuation, transmission voltage, turbidity and nitrate. A median value was determined by 49 scans of the window.

SECTIONU (original module of SECTION): Select a time span of data based on scan number in order to reduce a file size. The minimum number was set to be the starting time when the CTD package was beneath the sea-surface after activation of the pump. The maximum number of was set to be the end time when the package came up from the surface.

LOOPEDIT: Mark scans where the CTD was moving less than the minimum velocity of 0.0 m/s (traveling backwards due to ship roll).

DESPIKE (original module): Remove spikes of the data. A median and mean absolute deviation was calculated in 1-dbar pressure bins for both down and up cast, excluding the flagged values. Values greater than 4 mean absolute deviations from the median were marked bad for each bin. This process was performed twice for temperature, conductivity and dissolved oxygen (RINKOIII and SBE43) voltage.

DERIVE: Compute dissolved oxygen (SBE43).

BINAVG: Average the data into 1 decibar bins.

BOTTOMCUT (original module): Deletes discontinuous scan bottom data, when it's created by BINAVG.

DERIVE: Compute salinity, potential temperature, and sigma-theta.

SPLIT: Separate the data from the input .cnv file into down cast and up cast files.

(5) Station list

During this cruise, 67casts of CTD observation were carried out. Date, time and locations of the CTD casts are listed in Table 3.1. In bottom attack of shallow casts, bottom contact switch was also used.

(6) Preliminary Results

During this cruise, we judged noise, spike or shift in the data of some casts. These were as follows.

000M001: Secondary Salinity

down 30 dbar : spike

Nitrate

down 55 dbar - down 501 dbar, up 500 dbar - up 37 dbar: overrange

000M002: Beam Transmission

down 2060 dbar - down 2266 dbar: noise

005M001: Secondary Salinity

down 45 dbar: spike

014M001: Nitrate

down 2 dbar - down 1644 dbar, up 1643 dbar - up 1 dbar: bad data

018M001 Primary Dissolved Oxygen (RINKO III)

down 1363 dbar - down 1368 dbar, down 1403 dbar - down 1409 dbar: spike, down 1702 dbar - down 1754 dbar: noise

Nitrate

down 3 dbar - down 1761 dbar, up 1760 dbar - up 1 dbar: bad data

021M001 Primary Salinity

down 10 dbar: spike

020M005 Secondary Temperature, Secondary Salinity down 28 dbar: spike

024M001 Secondary Temperature, Secondary Salinity
down 96 dbar: spike

019M004 Primary Temperature, Primary Salinity
down 205 dbar – down 208 dbar: spike

Secondary Temperature, Secondary Salinity
down 179 dbar, down 205 dbar – down 208 dbar: spike

026M001 Primary Temperature, Primary Salinity, Secondary Temperature, Secondary Salinity
down 203 dbar: spike

Beam Transmission
down 353 dbar – down 357 dbar: spike

019M006 Primary Temperature, Primary Salinity, Secondary Temperature, Secondary Salinity
down 204 dbar: spike

027M001 Primary Temperature, Primary Salinity, Secondary Temperature, Secondary Salinity
down 207 dbar: spike

019M007 Primary Temperature, Primary Salinity, Secondary Temperature, Secondary Salinity
down 204 dbar – down 208 dbar: spike

021M008 Beam Transmission
down 231 dbar - down 232 dbar: spike

035M001 Secondary Temperature, Secondary Salinity
down 32 dbar: spike

037M001 Primary Temperature
down 24 dbar, down 39 dbar: spike

Primary Salinity
down 24 dbar, down 28 dbar, down 39 dbar: spike

Secondary Dissolved Oxygen (SBE43)
down 39 dbar: spike

038M001 Primary Salinity
down 36 dbar: spike

015M001 sample bottle #13 was not closed
bottle flag 4

000M004 sample bottle #26 was not closed
bottle flag 4

(7) Data archive

These data obtained in this cruise will be submitted to the Data Management Group of JAMSTEC, and will be opened to the public via “Data Research System for Whole Cruise Information in JAMSTEC (DARWIN)” in JAMSTEC web site.
<http://www.godac.jamstec.go.jp/darwin/e>

Table 3.1: MR19-03C CTD cast table

Stnnbr	Castno	Date(UTC)	Time(UTC)		BottomPosition		Depth	Wire	HT Above	Max	Max	CTD	Remark
		(mmddyy)	Start	End	Latitude	Longitude	(m)	Out (m)	Bottom (m)	Depth	Pressure	Filename	
000	1	100319	07:06	07:58	49-59.92N	166-07.07E	5396.0	495.4	-	496.1	501.0	000M001	
000	2	100319	10:06	14:02	49-59.29N	166-07.87E	5395.0	5399.3	8.7	5374.2	5490.0	000M002	
001	1	100819	06:34	07:00	65-39.18N	168-27.77W	53.1	41.9	7.3	45.5	46.0	001M001	
002	1	100819	09:34	09:56	66-00.17N	168-44.72W	52.5	43.0	6.5	45.5	46.0	002M001	
003	1	100819	12:48	13:05	66-30.32N	168-45.09W	54.3	43.2	7.5	46.5	47.0	003M001	
004	1	100819	16:06	16:28	67-00.13N	168-44.26W	44.6	33.8	6.5	37.6	38.0	004M001	
005	1	100919	05:16	05:35	69-00.19N	168-45.18W	52.5	42.8	6.2	45.5	46.0	005M001	
006	1	100919	09:25	09:48	69-30.16N	168-45.21W	51.0	43.0	5.0	45.5	46.0	006M001	
007	1	100919	13:36	13:53	69-59.96N	168-45.03W	40.5	30.5	5.2	34.6	35.0	007M001	
008	1	100919	17:06	17:24	70-29.86N	168-45.38W	39.4	26.3	8.2	29.7	30.0	008M001	
009	1	101019	07:59	08:15	71-59.76N	163-29.99W	38.4	29.6	5.4	32.7	33.0	009M001	
010	1	101019	14:09	14:25	72-29.84N	161-44.78W	44.1	34.2	5.8	37.6	38.0	010M001	
011	1	101019	18:57	19:35	72-60.00N	160-00.20W	192.0	182.1	8.9	184.0	186.0	011M001	
012	1	101119	05:42	07:24	72-30.13N	156-16.69W	1607.0	1595.9	8.7	1589.3	1612.0	012M001	
013	1	101119	10:55	12:50	72-19.98N	155-00.52W	1957.0	1959.6	8.2	1956.3	1986.0	013M001	
014	1	101119	16:47	18:33	72-09.43N	153-47.41W	1637.0	1635.6	8.7	1620.8	1644.0	014M001	
015	1	101219	06:34	09:13	71-59.99N	147-29.98W	3515.0	3507.4	9.9	3500.0	3566.0	015M001	
016	1	101219	14:40	17:18	72-00.00N	145-00.05W	3316.0	3309.4	9.7	3303.3	3364.0	016M001	
017	1	101419	15:08	18:11	74-46.09N	150-30.13W	3834.0	3824.7	9.1	3819.5	3895.0	017M001	
018	1	101519	16:58	18:48	76-27.95N	161-38.51W	1750.0	1738.7	10.0	1735.3	1761.0	018M001	
019	1	101619	05:11	06:19	76-59.96N	164-59.94W	680.0	675.9	5.2	675.7	684.0	019M001	
020	1	101619	08:33	09:26	77-15.04N	164-59.71W	367.0	359.4	4.3	359.9	364.0	020M001	
020	2	101719	07:04	07:56	77-15.00N	164-59.93W	370.0	360.2	6.1	361.8	366.0	020M002	
021	1	101719	10:17	11:06	77-30.01N	165-00.01W	308.0	301.5	5.2	301.6	305.0	021M001	
022	1	101719	12:58	13:56	77-45.00N	165-00.01W	445.0	438.4	5.3	437.9	443.0	022M001	
020	3	101819	06:36	07:28	77-15.01N	164-59.99W	372.0	358.1	4.6	359.9	364.0	020M003	
021	2	101819	09:45	10:33	77-30.07N	165-00.19W	310.0	300.4	4.7	302.6	306.0	021M002	
022	2	101819	12:55	13:52	77-45.05N	165-00.19W	446.0	439.5	4.4	439.9	445.0	022M002	
023	1	101819	20:09	21:06	78-02.13N	164-58.49W	453.0	443.6	8.2	442.8	448.0	023M001	
019	2	101919	08:07	09:01	77-00.01N	164-59.96W	685.0	496.3	-	496.1	502.0	019M002	
020	4	101919	11:15	12:06	77-15.14N	164-59.89W	366.0	358.5	3.8	360.9	365.0	020M004	
021	3	101919	13:41	14:33	77-30.06N	164-59.93W	309.0	301.4	4.4	303.6	307.0	021M003	
019	3	102019	08:59	09:55	77-00.06N	164-59.94W	690.0	495.0	-	496.1	502.0	019M003	
020	5	102019	12:18	13:12	77-15.14N	164-59.65W	367.0	358.3	5.1	361.8	366.0	020M005	
021	4	102019	14:48	15:42	77-30.05N	164-59.99W	310.0	299.2	5.5	301.6	305.0	021M004	
024	1	102119	06:37	07:52	77-15.00N	165-59.97W	851.0	847.7	5.8	846.3	857.0	024M001	
019	4	102119	10:43	11:42	77-00.28N	164-59.75W	687.0	494.9	-	496.1	502.0	019M004	
020	6	102119	13:54	14:53	77-15.01N	165-00.05W	370.0	358.0	4.4	359.9	364.0	020M006	
021	5	102119	17:40	18:33	77-30.50N	164-59.67W	308.0	231.2	-	238.3	241.0	021M005	no sampling water
025	1	102219	07:04	08:15	77-00.37N	165-59.88W	711.0	708.7	5.7	708.3	717.0	025M001	
019	5	102219	10:27	11:28	77-00.10N	164-59.57W	685.0	495.0	-	496.1	502.0	019M005	
020	7	102219	13:43	14:43	77-15.00N	165-00.06W	371.0	359.8	3.7	360.9	365.0	020M007	
021	6	102219	17:32	17:48	77-30.30N	164-58.80W	306.0	299.5	3.9	301.6	305.0	021M006	no sampling water
026	1	102319	06:30	07:24	77-00.01N	164-00.01W	437.0	431.8	4.7	431.0	436.0	026M001	
019	6	102319	09:32	10:34	77-00.07N	164-59.32W	678.0	495.6	-	495.2	501.0	019M006	
020	8	102319	13:25	14:18	77-15.17N	164-59.94W	365.0	357.6	5.4	358.9	363.0	020M008	
021	7	102319	16:29	17:17	77-30.31N	164-58.79W	304.0	299.2	5.3	300.6	304.0	021M007	
027	1	102419	06:36	07:25	77-15.00N	164-00.01W	366.0	356.3	5.7	358.9	363.0	027M001	
019	7	102419	10:09	11:08	77-00.23N	165-00.16W	697.0	494.5	-	495.2	501.0	019M007	
020	9	102419	13:15	14:06	77-15.04N	165-00.14W	366.0	356.3	4.9	357.9	362.0	020M009	
021	8	102419	16:59	17:47	77-30.74N	165-00.21W	311.0	301.5	6.4	302.6	306.0	021M008	
028	1	102519	08:59	10:46	77-00.22N	168-46.13W	1896.0	1884.6	8.9	1882.4	1911.0	028M001	
029	1	102619	05:39	06:14	74-00.01N	168-44.83W	185.0	172.4	5.2	175.1	177.0	029M001	
030	1	102619	09:11	09:41	73-30.00N	168-45.00W	115.0	106.0	5.6	108.8	110.0	030M001	
031	1	102619	13:08	13:30	73-00.03N	168-45.04W	61.4	52.0	5.0	55.4	56.0	031M001	
032	1	102619	16:51	17:11	72-30.03N	168-44.61W	58.5	48.0	4.7	52.4	53.0	032M001	
033	1	102719	05:42	05:57	70-30.00N	168-44.92W	38.2	28.5	5.2	32.7	33.0	033M001	
034	1	102719	08:46	09:05	70-00.00N	168-45.04W	40.5	31.4	5.2	34.6	35.0	034M001	
035	1	102719	13:00	13:18	69-30.19N	168-45.23W	51.3	39.7	5.1	45.5	46.0	035M001	
036	1	102719	16:19	16:37	68-59.99N	168-45.29W	52.5	42.4	5.4	46.5	47.0	036M001	
037	1	102819	05:05	05:23	68-00.88N	167-52.05W	52.5	41.0	6.5	45.5	46.0	037M001	
038	1	102819	07:36	07:56	67-46.99N	168-36.29W	50.5	39.5	6.0	43.6	44.0	038M001	
039	1	102819	10:42	10:59	67-30.07N	168-45.11W	49.4	40.1	5.2	43.6	44.0	039M001	
040	1	102819	13:59	14:15	67-00.06N	168-44.71W	44.9	35.5	5.9	38.6	39.0	040M001	
041	1	102819	17:22	17:40	66-29.99N	168-45.02W	54.0	45.8	5.1	48.5	49.0	041M001	
000	3	110219	22:07	22:57	50-00.11N	166-07.40E	5397.0	494.1	-	497.1	502.0	000M003	
000	4	110319	00:06	04:04	49-59.95N	166-07.13E	5396.0	5389.4	7.9	5376.1	5492.0	000M004	

3.2 Salinity measurements

(1) Personnel

Shigeto NISHINO	JAMSTEC	- PI
Akihiko MURATA	JAMSTEC	
Shungo OSHITANI	MWJ	-Operation leader
Shinsuke TOYODA	MWJ	

(2) Objective

To measure bottle salinity obtained by CTD casts, bucket sampling, and the continuous sea surface water monitoring system (TSG).

(3) Method

a. Salinity Sample Collection

Seawater samples were collected with 12 liter water sampling bottles and TSG. The salinity sample bottle of the 250ml brown glass bottle with screw cap was used for collecting the sample water. Each bottle was rinsed 3 times with the sample water, and was filled with sample water to the bottle shoulder. The salinity sample bottles for TSG were sealed with a plastic cone and screw cap because we took into consideration the possibility of storage for about one month. The caps was rinsed 3 times with the sample seawater before its use. Each bottle was stored for more than 24 hours in the laboratory before the salinity measurement.

The kind and number of samples taken are shown as follows ;

Table 3.2: Kind and number of samples

Kind of Samples	Number of Samples
Samples for CTD and Bucket	586
Samples for TSG	34
Total	620

b. Instruments and Method

The salinity analysis was carried out on R/V MIRAI during the cruise of MR19-03C using the salinometer (Model 8400B “AUTOSAL” ; Guildline Instruments Ltd.: S/N 72874) with an additional peristaltic-type intake pump (Ocean Scientific International, Ltd.). A pair of precision digital thermometers (1502A; FLUKE: S/N B78466 and B81550) were used for monitoring the ambient temperature and the bath temperature of the salinometer.

The specifications of the AUTOSAL salinometer and thermometer are shown as follows ;

Salinometer (Model 8400B “AUTOSAL” ; Guildline Instruments Ltd.)

Measurement Range	: 0.005 to 42 (PSU)
Accuracy	: Better than ±0.002 (PSU) over 24 hours without re-standardization
Maximum Resolution	: Better than ±0.0002 (PSU) at 35 (PSU)

Thermometer (1502A: FLUKE)

Measurement Range	:	16 to 30 deg C (Full accuracy)
Resolution	:	0.001 deg C
Accuracy	:	0.006 deg C (@ 0 deg C)

The measurement system was almost the same as Aoyama *et al.* (2002). The salinometer was operated in the air-conditioned ship's laboratory at a bath temperature of 24 deg C. The ambient temperature varied from approximately 21 deg C to 23 deg C, while the bath temperature was very stable and varied within +/- 0.002 deg C on rare occasion. The measurement for each sample was done with a double conductivity ratio and defined as the median of 31 readings of the salinometer. Data collection was started 5 seconds after filling the cell with the sample and it took about 10 seconds to collect 31 readings by a personal computer. Data were taken for the sixth and seventh filling of the cell. In the case of the difference between the double conductivity ratio of these two fillings being smaller than 0.00002, the average value of the double conductivity ratio was used to calculate the bottle salinity with the algorithm for the practical salinity scale, 1978 (UNESCO, 1981). If the difference was greater than or equal to 0.00003, an eighth filling of the cell was done. In the case of the difference between the double conductivity ratio of these two fillings being smaller than 0.00002, the average value of the double conductivity ratio was used to calculate the bottle salinity. The measurement was conducted in about 8 hours per day and the cell was cleaned with soap after the measurement of the day.

(4) Results

a. Standard Seawater

Standardization control of the salinometer was set to 549 and all measurements were done at this setting. The value of STANDBY was 24+5996-6004 and that of ZERO was 0.0±0000-0004. The conductivity ratio of IAPSO Standard Seawater batch P162 was 0.99983 (double conductivity ratio was 1.99966) and was used as the standard for salinity. 33 bottles of P162 were measured.

Fig.3.2.-1 shows the time series of the double conductivity ratio of the Standard Seawater batch P162. The average of the double conductivity ratio was 1.99966 and the standard deviation was 0.00005 which is equivalent to 0.0009 in salinity.

Fig.3.2.-2 shows the time series of the double conductivity ratio of the Standard Seawater batch P162 after correction. The average of the double conductivity ratio after correction was 1.99966 and the standard deviation was 0.00001, which is equivalent to 0.0002 in salinity.

The specifications of SSW used in this cruise are shown as follows ;

Batch	:	P162
Conductivity ratio	:	0.99983
Salinity	:	34.993
Use by	:	16th April. 2021

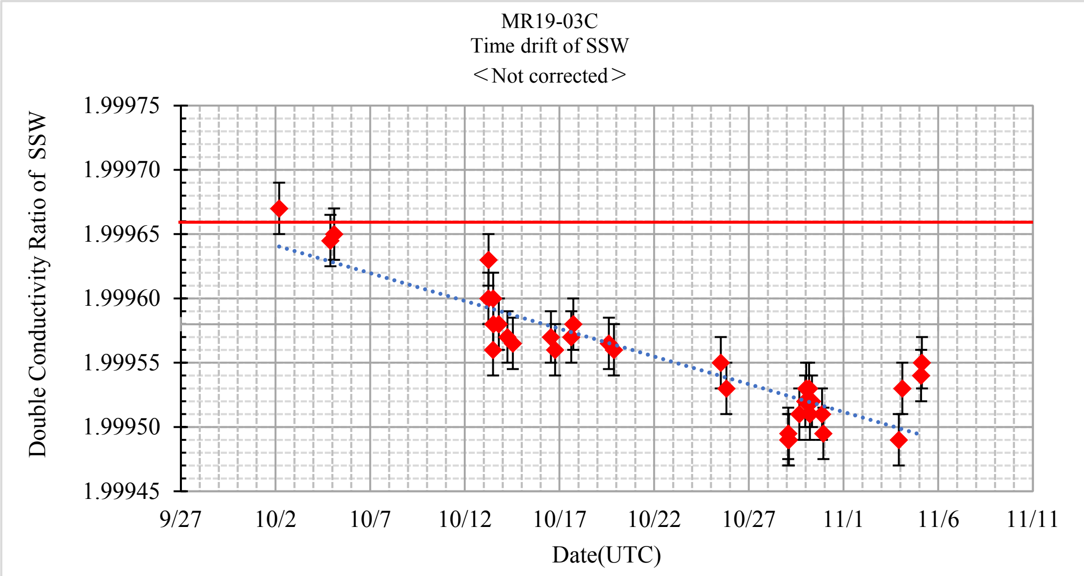

Figure 3.2-1: Time series of double conductivity ratio for the Standard Seawater batch P162 (before correction)

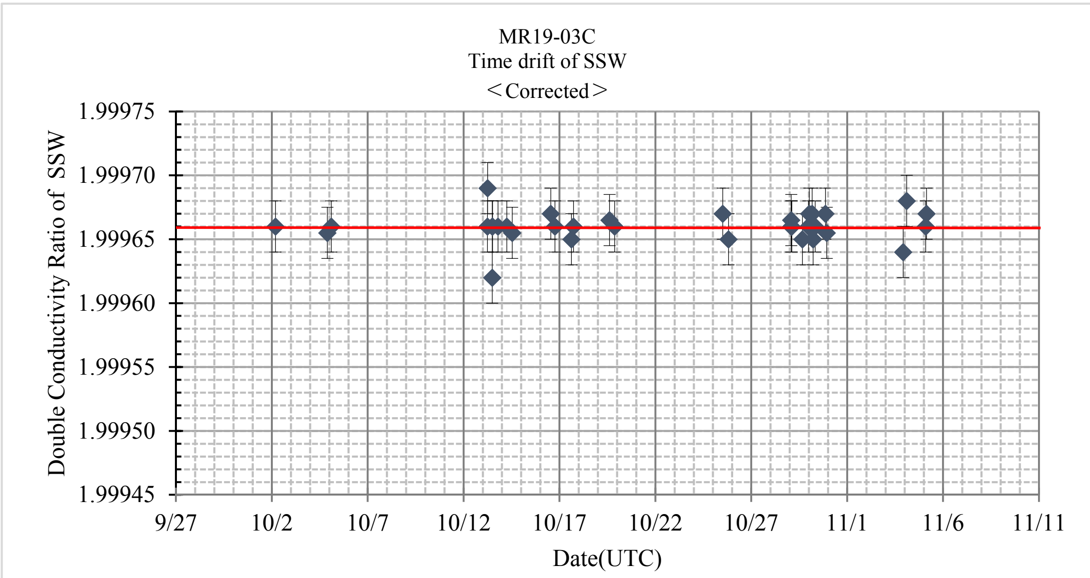

Figure 3.2-2: Time series of double conductivity ratio for the Standard Seawater batch P162 (after correction)

b. Sub-Standard Seawater

Sub-standard seawater was made from surface sea water filtered by a pore size of 0.2 micrometer and stored in a 20 liter container made of polyethylene and stirred for at least 24 hours before measuring. It was measured about every 6 samples in order to check for the possible sudden drifts of the salinometer.

c. Replicate Samples

We estimated the precision of this method using 108 pairs of replicate samples taken from the same water sampling bottle. Fig.3.2-3 shows the histogram of the absolute difference between each pair of the replicate samples. The average and the standard deviation of absolute difference among 108 pairs of replicate samples were 0.0006 and 0.0006 in salinity, respectively.

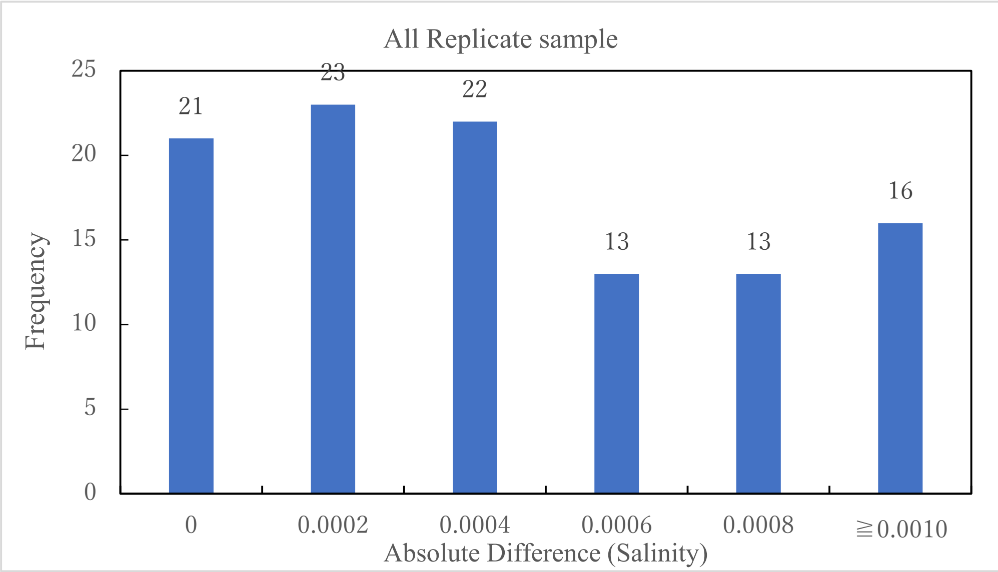

Figure 3.2-3: The histogram of the double conductivity ratio for the absolute difference of all replicate samples

33 pairs of replicate samples were to estimate the precision of shallow (<200dbar) samples. Fig.3.2-4 shows the histogram of the absolute difference between each pair of shallow (<200dbar) replicate samples. The average and the standard deviation of absolute difference among 33 pairs were 0.0006 and 0.0007 in salinity, respectively.

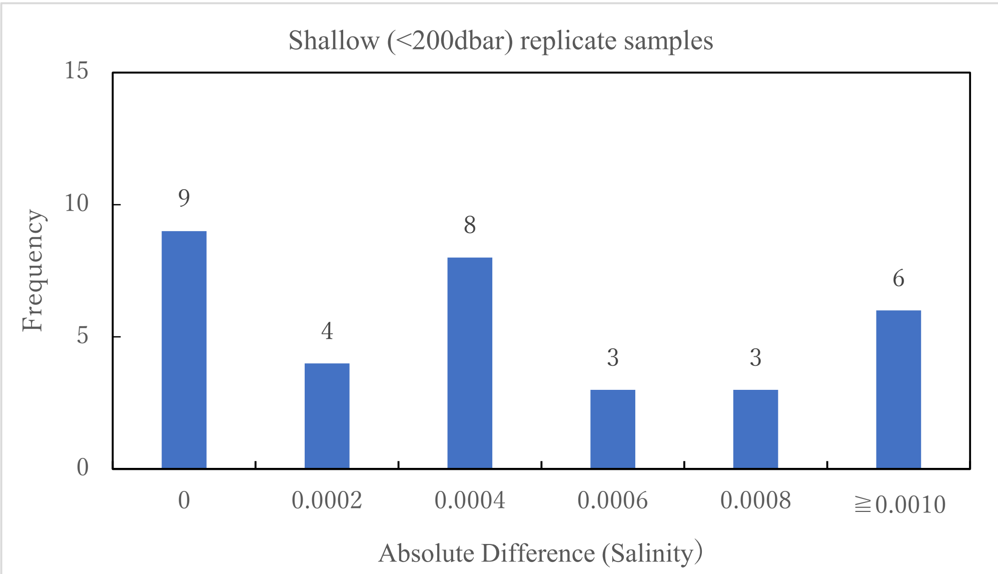

Figure 3.2-4: The histogram of the absolute difference between Shallow (<200dbar) replicate samples

75 pairs of replicate samples were to estimate the precision of deep (>=200dbar) samples. Fig.3.2-5 shows the histogram of the absolute difference between each pair of deep (>=200dbar) replicate samples. The average and the standard deviation of absolute difference among 75 pairs were 0.0006 and 0.0005 in salinity, respectively.

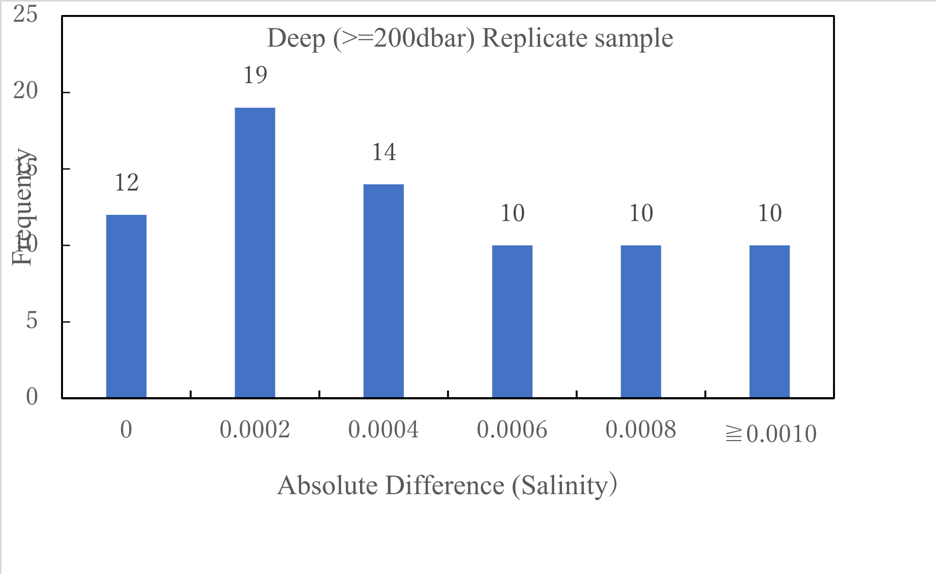

Figure 3.2-5: The histogram of the absolute difference between Deep (>=200dbar) replicate samples

(5) Data archive

These raw datasets will be submitted to JAMSTEC Data Management Group (DMG).

(6) Reference

・Aoyama, M., T. Joyce, T. Kawano and Y. Takatsuki : Standard seawater comparison up to P129. Deep-Sea Research, I, Vol. 49, 1103～1114, 2002

・ UNESCO : Tenth report of the Joint Panel on Oceanographic Tables and Standards. UNESCO Tech. Papers in Mar. Sci., 36, 25 pp., 1981

3.3 XCTD

(1) Personnel

Jun Inoue	NIPR	-PI
Takuji Waseda	The University of Tokyo	- not on board
Tsubasa Kodaira	The University of Tokyo	
Yusuke Kawaguchi	The University of Tokyo	- not on board
Eun Yae Son	The University of Tokyo	
Ryo Oyama	NME	
Shinya Okumura	NME	
Kazuho Yoshida	NME	
Yutaro Murakami	NME	
Soichiro Sueyoshi	NME	

(2) Objective

To obtain vertical profiles of sea water temperature and salinity (calculated by the function of temperature, pressure (depth), and conductivity).

(3) Parameters

The range and accuracy of parameters measured by the XCTD (eXpendable Conductivity, Temperature & Depth profiler) are as follows;

Parameter	Range	Accuracy
Conductivity	0 ~ 60 [mS/cm]	+/- 0.03 [mS/cm]
Temperature	-2 ~ 35 [deg-C]	+/- 0.02 [deg-C]
Depth	0 ~ 1000 [m]	5 [m] or 2 [%] (either of them is major)

(4) Instruments and Methods

We observed the vertical profiles of the sea water temperature and conductivity measured by XCTD-1 manufactured by Tsurumi-Seiki Co. (TSK). The signal was converted by MK-150N(TSK) and was recorded by AL-12B software (Ver.1.1.4, TSK). We launched 26 probes by using the automatic launcher. The summary of XCTD observation log is shown in Table 3.3.

Table 3.3: XCTD observation log

No.	Date [YYYY/MM/DD]	Time [hh:mm]	Latitude [degN]	Longitude [degW]	Depth [m]	SST [deg-C]	SSS [PSU]	Probe S/N	Probe Type
1	2019/10/08	20:06	67-29.9969	168-44.9535	48	3.503	32.195	17110515	XCTD-1
2	2019/10/08	22:32	68-00.0631	168-45.1056	58	3.610	31.971	17110517	XCTD-1
3	2019/10/09	02:38	68-30.0533	168-45.0005	53	3.583	32.311	17110516	XCTD-1
4	2019/10/09	22:29	71-00.0009	166-59.9931	45	6.831	31.605	17110518	XCTD-1
5	2019/10/10	03:41	71-29.9875	165-15.0715	43	6.099	30.987	17110519	XCTD-1
6	2019/10/12	06:47	71-59.9908	147-29.9095	3512	1.255	26.497	17110520	XCTD-1
7	2019/10/13	05:36	73-45.3341	145-06.3694	3710	0.200	26.647	19040333	XCTD-1
8	2019/10/13	19:13	74-18.0722	143-49.5586	3711	−1.378	26.333	19040334	XCTD-1
9	2019/10/13	21:40	74-25.4099	143-00.2768	3705	−1.391	26.323	19040335	XCTD-1
10	2019/10/14	00:00	74-17.1291	143-31.0744	3710	−1.399	26.374	19040337	XCTD-1
11	2019/10/14	01:04	74-17.1291	143-46.4098	3709	−1.392	26.272	17110522	XCTD-1
12	2019/10/14	01:28	74-15.0270	144-00.0245	3710	−1.366	26.313	17110523	XCTD-1
13	2019/10/14	01:44	74-13.4356	144-08.2456	3711	−0.963	26.452	17110524	XCTD-1
14	2019/10/14	01:50	74-12.8899	144-11.0899	3711	−0.274	26.591	17110525	XCTD-1
15	2019/10/14	02:27	74-11.9213	144-14.0936	3709	0.154	26.723	17110526	XCTD-1
16	2019/10/14	03:24	74-09.2035	144-28.7344	3712	0.121	26.714	19040399	XCTD-1
17	2019/10/14	03:55	74-06.7290	144-43.5529	3723	−0.026	26.724	19040338	XCTD-1
18	2019/10/14	04:42	74-03.9046	144-58.0717	3719	−0.055	26.719	19040332	XCTD-1
19	2019/10/16	22:36	78-05.0731	164-55.3744	488	−1.496	28.479	19040340	XCTD-1
20	2019/10/20	19:32	77-38.0633	165-00.0179	316	−0.806	28.851	19040342	XCTD-1
21	2019/10/20	20:52	77-49.9459	164-59.8765	405	−0.935	28.812	19040344	XCTD-1
22	2019/10/20	21:17	77-55.0005	164-59.9874	391	−1.254	28.722	19040343	XCTD-1
23	2019/10/21	01:49	77-40.0096	165-27.7923	497	−0.739	28.883	19040341	XCTD-1
24	2019/10/21	02:57	77-27.8973	165-43.1546	731	−0.104	29.060	19040345	XCTD-1
25	2019/10/25	16:34	75-59.9980	168-45.1069	601	1.598	29.738	18086022	XCTD-1
26	2019/11/03	00:18	50-00.0733	166-07.3278	5400	7.707	32.788	18086.23	XCTD-1

SST: Sea Surface Temperature [deg-C] measured by TSG (Thermo Salino Graph).

SSS: Sea Surface Salinity [PSU] measured by TSG.

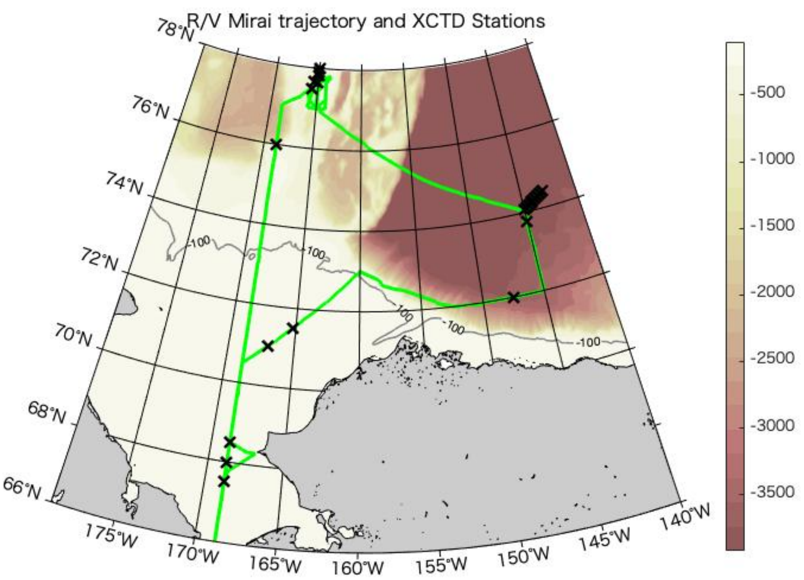

Figure 3.3-1: Trajectory of R/V Mirai (green line) and XCTD measurement locations (x). The color shows the bathymetry.

(5) Preliminary results

An intensive XCTD measurements were conducted 13-14 October 2019 near the Marginal Ice Zone. The measurements were linked to the ocean turbulence measurements and deployments of surface drifting buoys, some of which measured surface waves, and the others measured upper ocean currents and temperature. The XCTD results indicate the clear hydrographic conditions under the sea-ice formation and also the subsurface oceanic eddy under the sea-ice covered area (see, Figure 3.3-2). Most of the other probes are used to map the hydrographic conditions near the ridge and also the Chukchi Shelf.

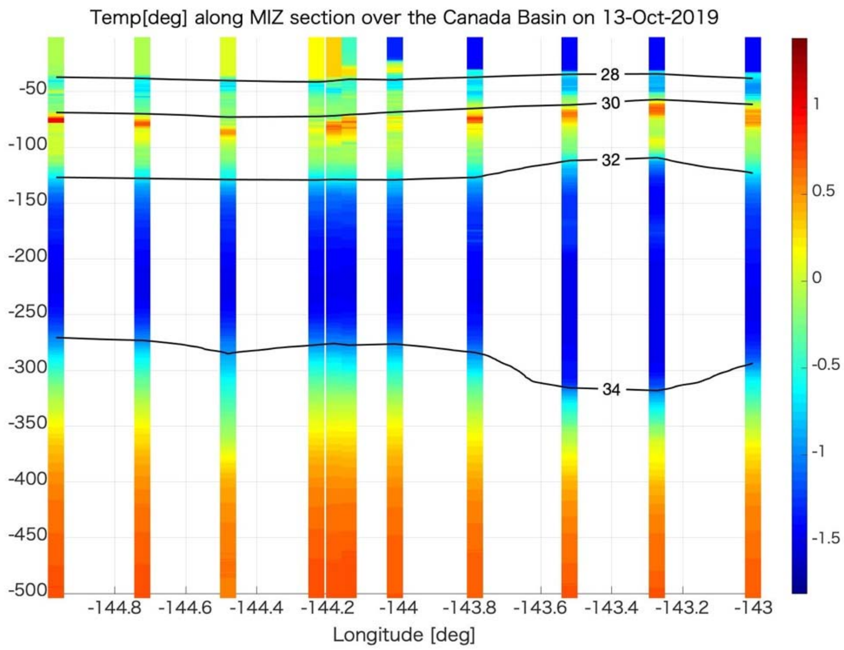

Figure 3.3-2: XCTD measurement results along the section between the open ocean and the ice-covered area. The color shows the temperature [degree] and the black lines show salinity [psu].

(6) Data archives

These data obtained in this cruise will be submitted to the Data Management Group of JAMSTEC and will be opened to the public via "Data Research System for Whole Cruise Information in JAMSTEC (DARWIN)" in JAMSTEC web site. <http://www.godac.jamstec.go.jp/darwin/e>

3.4 Shipboard ADCP

(1) Personnel

Kazutoshi Sato	KIT	-PI
Ryo Oyama	NME	
Sueyoshi Souichiro	NME	
Shinya Okumura	NME	
Kazuho Yoshida	NME	
Yutaro Murakami	NME	
Takehito Hattori	MIRAI Crew	

(2) Objectives

To obtain continuous measurement data of the current profile along the ship's track.

(3) Parameters

Major parameters for the measurement, Direct Command, are shown in Table 3.4.

Table 3.4: Major parameters

Bottom-Track Commands	
BP = 001	Pings per Ensemble (almost less than 1,200m depth)
Environmental Sensor Commands	
EA = 04500	Heading Alignment (1/100 deg)
ED = 00065	Transducer Depth (0 - 65535 dm)
EF = +001	Pitch/Roll Divisor/Multiplier (pos/neg) [1/99 - 99]
EH = 00000	Heading (1/100 deg)
ES = 35	Salinity (0-40 pp thousand)
EX = 00000	Coordinate Transform (Xform:Type; Tilts; 3Bm; Map)
EZ = 10200010	Sensor Source (C; D; H; P; R; S; T; U)
	C (1): Sound velocity calculates using ED, ES, ET (temp.)
	D (0): Manual ED
	H (2): External synchro
	P (0), R (0): Manual EP, ER (0 degree)
	S (0): Manual ES
	T (1): Internal transducer sensor
	U (0): Manual EU
EV = 0	Heading Bias (1/100 deg)
Timing Commands	
TE = 00:00:02.00	Time per Ensemble (hrs:min:sec.sec/100)
TP = 00:02.00	Time per Ping (min:sec.sec/100)
Water-Track Commands	
WA = 255	False Target Threshold (Max) (0-255 count)

WC = 120	Low Correlation Threshold (0-255)
WD = 111 100 000	Data Out (V; C; A; PG; St; Vsum; Vsum^2; #G; P0)
WE = 1000	Error Velocity Threshold (0-5000 mm/s)
WF = 0800	Blank After Transmit (cm)
WN = 100	Number of depth cells (1-128)
WP = 00001	Pings per Ensemble (0-16384)
WS = 800	Depth Cell Size (cm)
WV = 0390	Radial Ambiguity Velocity (cm/s)

(4) Instruments and methods

Upper ocean current measurements were made in this cruise, using the hull-mounted Acoustic Doppler Current Profiler (ADCP) system. For most of its operation, the instrument was configured for water-tracking mode. Bottom-tracking mode, interleaved bottom-ping with water-ping, was made to get the calibration data for evaluating transducer misalignment angle in the shallow water. The system consists of following components;

1. R/V MIRAI has installed the Ocean Surveyor for vessel-mount ADCP (frequency 76.8 kHz; Teledyne RD Instruments, USA). It has a phased-array transducer with single ceramic assembly and creates 4 acoustic beams electronically. We mounted the transducer head rotated to a ship-relative angle of 45 degrees azimuth from the keel.
2. For heading source, we use ship's gyro compass (Tokyo Keiki, Japan), continuously providing heading to the ADCP system directory. Additionally, we have Inertial Navigation Unit (Phins, Ixblue, France) which provide high-precision heading, attitude information, pitch and roll. They are stored in ".N2R" data files with a time stamp.
3. Differential GNSS system (Star Pack-D, Fugro, Netherlands) providing precise ship's position.
4. We used VmDas software version 1.49 (TRDI) for data acquisition.
5. To synchronize time stamp of ping with Computer time, the clock of the logging computer is adjusted to GPS time server every 10 minutes.
6. Fresh water is charged in the sea chest to prevent bio fouling at transducer face.
7. The sound speed at the transducer does affect the vertical bin mapping and vertical velocity measurement, and that is calculated from temperature, salinity (constant value; 35.0 PSU) and depth (6.5 m; transducer depth) by equation in Medwin (1975).

Data were recorded every ping as raw ensemble data (.ENR). Additionally, 15 seconds averaged data were recorded as short-term average (.STA). 300 seconds averaged data were long-term average (.LTA), respectively. The blanking distance (command : WF) was basically set "8m". However, in the shallow water (Depth < 100m) and Arctic Ocean, the blanking distance was changed to "2m". With this, center depth of first layer was changed from about 23m to 17m below the sea surface.

(5) Preliminary results

Figure 3.4 shows the time series plot of the current velocity during the stay in the repeat section (round-trip from Sta.039 to Marginal Ice Zone).

(6) Observation Log

27 Sep. 2019 to 10 Nov. 2019

(7) Data archives

These data obtained in this cruise will be submitted to the Data Management Group of JAMSTEC and will be opened to the public via “Data Research System for Whole Cruise Information in JAMSTEC (DARWIN)” in JAMSTEC web site.

<http://www.godac.jamstec.go.jp/darwin/e>

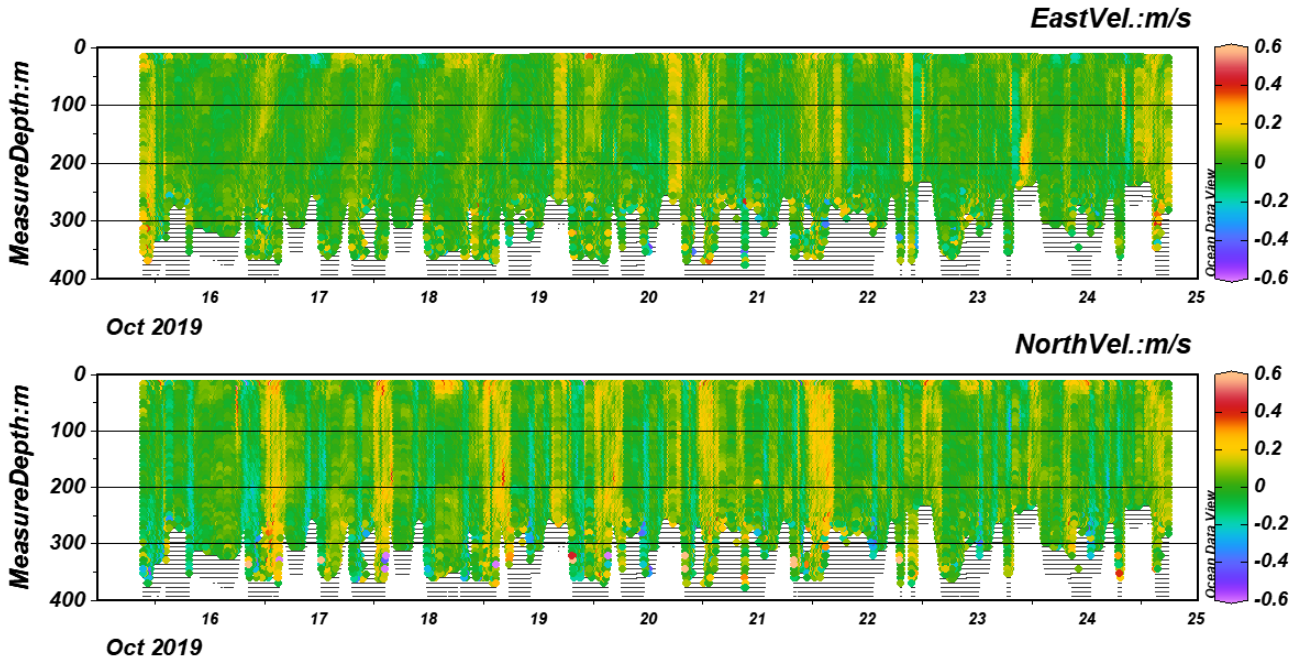

Figure 3.4: The time series plot of the current velocity

3. 5 RINKO Profiler

(1) Personnel

Jun Inoue	NIPR	-PI
Koji Shimada	Tokyo University of Marine Science and Technology	-not on board
Junpei Yamamoto	Tokyo University of Marine Science and Technology	
Rio Maya	Tokyo University of Marine Science and Technology	
Eri Yoshizawa	Korea Polar Research Institute	
Tsubasa Kodaira	University of Tokyo	

(2) Objectives

Thermohaline property of oceanic surface mixed layer is a key for forecasting a timing of freeze-up in the Arctic Ocean. To investigate its variation in freeze-up season, vertical profiles of temperature and salinity were observed by a hand-operated CTD profiler. Daily observations were conducted just after launching GPS radiosondes between 7 and 28 October 2019. In addition to these routine observations, there were some casts performed among stations of other hydrographic observations to complement mapping of hydrography. The obtained data will be used to assess oceanic impacts on freeze-up and to validate forecasts.

(3) Parameters

Temperature, conductivity, depth, turbidity, chlorophyll and dissolved oxygen.

(4) Instruments and methods

RINKO-Profiler (model: ASTD102, S/N: 0563) manufactured by the JFE Advantech Co. was used for all casts. The profiler installs multiple sensors to measure physical and bio-optical parameters. According to the manufacture's nominal specification, measurement type, range and accuracy of parameters are listed below:

Parameter	Type	Range	Accuracy
Temperature	Platinum wire thermistor	-3-45 deg-C	±0.01 deg-C
Conductivity	Inductive cell	0.5-70 mS/cm	±0.01 mS/cm
Depth	Semiconductor stain gauge	0-600 m	±0.3 %
Turbidity	Backscatter	0-1000 FTU	±0.3 FTU
Chlorophyll	Fluorescence	0-400 ppb	±1 %
Dissolved Oxygen	Phosphorescence	0-200% or 0-20 mg/l	±2 %

We deployed the profiler by hand from starboard on working deck and collected data at 0.1-s intervals. After recoveries of the profiler, raw data recorded as binary format was converted to CSV format using the RINKO-Profiler software (ver. 1. 09).

To test performances of temperature and conductivity measurements, comparisons with SBE9plus data were conducted. The profiler was deployed together with the SBE9puls sensor in test casts at 50-00 N, 166-07 E conducted on 3 October and 2 November 2019. During up casts, data for comparisons was collected at the following depths: 170, 250, 300, 400 and 500 m. Standard deviations of differences between the two data were negligibly small at each depth for both temperature and salinity.

(5) Station list

Observations were performed at stations listed in Table 3.5.

Table 3.5: Station list of RINKO-Profiler observation.

St. No	Cast. No	Date (UTC) [yyyy/mm/dd]	Time (UTC) [hh:mm]	Lat. [deg-min]	Lon. [deg-min]	Observation depth [m]	Bottom depth [m]
0	1	2019/10/3	7:03	50-00.001 N	166-07.143 E	497	5398
1	1	2019/10/7	23:51	64-40.137 N	169-55.153 W	32	47
2	1	2019/10/8	23:32	68-09.910 N	168-45.382 W	31	58
3	1	2019/10/9	23:32	71-06.540 N	166-30.656 W	30	45
4	1	2019/10/10	23:37	72-46.903 N	158-22.495 W	33	299
5	1	2019/10/11	23:32	72-00.620 N	151-17.739 W	35	2588
6	1	2019/10/12	23:35	72-58.535 N	144-55.523 W	36	3547
7	1	2019/10/13	23:29	74-20.085 N	143-30.897 W	37	3712
8	1	2019/10/14	23:33	74-59.965 N	152-16.159 W	39	3844
9	1	2019/10/15	23:31	76-57.802 N	164-45.190 W	36	396
10	1	2019/10/16	18:00	77-15.108 N	164-59.484 W	39	367
11	1	2019/10/16	23:33	78-03.941 N	164-56.893 W	37	490
12	1	2019/10/17	2:00	77-53.380 N	164-59.984 W	40	411
13	1	2019/10/17	23:23	78-00.287 N	164-59.055 W	35	461
14	1	2019/10/18	2:00	77-45.129 N	165-00.094 W	36	445
15	1	2019/10/18	23:34	78-03.878 N	165-10.126 W	36	478
16	1	2019/10/19	2:17	77-45.217 N	164-59.798 W	41	443
17	1	2019/10/19	23:33	78-03.066 N	164-59.602 W	40	457
18	1	2019/10/20	2:40	77-45.168 N	165-00.328 W	50	443
19	1	2019/10/20	20:11	77-44.981 N	164-59.959 W	55	442
20	1	2019/10/20	23:33	78-00.916 N	164-58.441 W	42	452
21	1	2019/10/21	19:59	77-44.872 N	164-59.985 W	40	446

22	1	2019/10/21	23:33	78-01.559 N	164-57.640 W	38	475
23	1	2019/10/22	19:13	77-44.961 N	165-00.199 W	41	456
24	1	2019/10/22	23:33	77-46.149 N	164-05.429 W	38	276
25	1	2019/10/23	18:45	77-44.985 N	165-00.319 W	41	444
26	1	2019/10/23	23:24	77-47.021 N	163-35.816 W	41	284
27	1	2019/10/24	19:08	77-44.999 N	165-00.324 W	41	444
28	1	2019/10/24	23:33	77-47.621 N	163-40.605 W	44	282
29	1	2019/10/25	23:33	74-41.305 N	168-45.668 W	41	183
30	1	2019/10/26	20:12	72-00.073 N	168-45.013 W	44	50
30	2	2019/10/26	20:35	72-00.073 N	168-45.013 W	50	50
31	1	2019/10/26	23:29	71-30.190 N	168-44.615 W	48	48
32	1	2019/10/27	2:30	71-00.027 N	168-44.826 W	44	44
33	1	2019/10/27	19:46	68-30.125 N	168-45.190 W	51	53
34	1	2019/10/27	23:49	68-18.125 N	167-23.016 W	44	46
35	1	2019/10/28	20:28	66-00.033 N	168-44.923 W	53	54
36	1	2019/10/28	23:33	65-36.852 N	168-28.797 W	53	52
37	1	2019/11/02	21:57	50-00.020 N	166-07.300 E	497	5396

(6) Preliminary results

During the repeat observation of the north-south section along 168-00 W, temporal variations of the surface mixed layer were monitored at 77-45 N from 19 to 24 October 2019. This site was located in open water areas near marginal ice zones. The clear surface mixed layer was captured throughout the observational period. The surface mixed layer depth defined by the buoyancy frequency maximum was almost unchanged (~30.5 m) with the vertically homogeneous salinity (~29.0), as shown in Figure 3.5-1a. In this layer, temperature was highly variable in a vertical direction and showed the local maxima of up to 0.5 deg-C at the base of the layer (Fig. 3.5b). The temperature was 0.5-2.0 deg-C warmer than the local freezing temperature in the entire surface mixed layer, suggesting oceanic conditions slowing a timing of freeze-up.

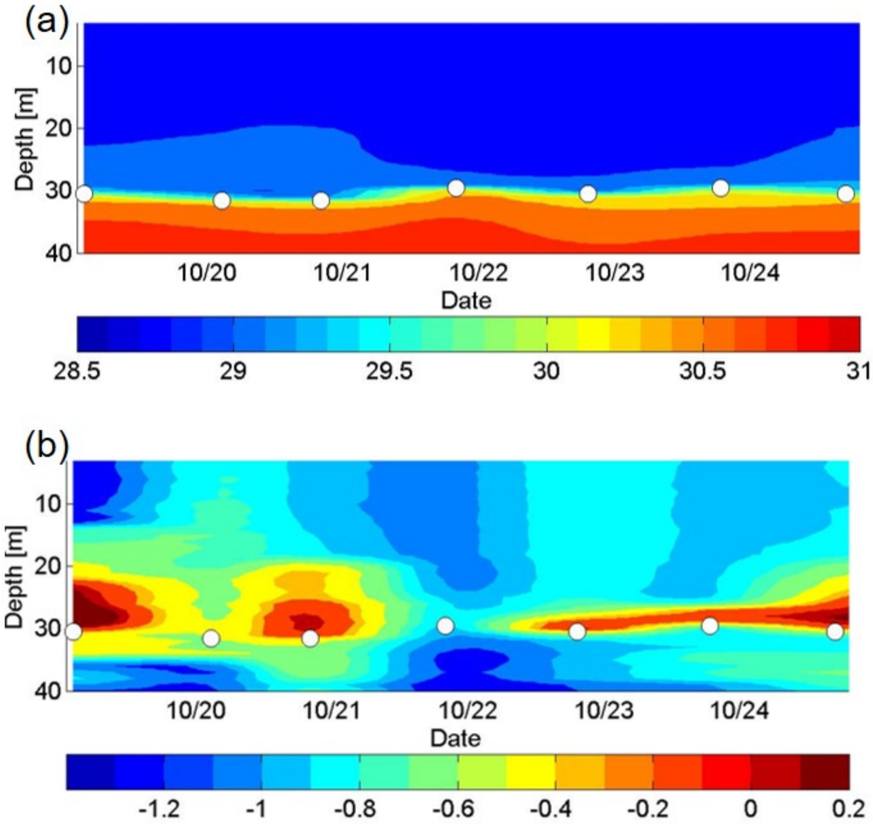

Figure 3.5: Time-depth cross section of (a) salinity and (b) in situ temperature at the site of 77-45 N, 168-00 W from 18 to 24 October 2019. The surface mixed layer depth defined by the buoyancy frequency maximum is denoted by white dots.

(7) Data archive

The raw data obtained in this cruise will be submitted to the Data Management Group (DMG) of JAMSTEC.

(8) Remarks

Station 0: Test cast was performed. Conductivity data collected at depths deeper than 400 m in down cast was bad, because of contaminations of inductive cell.

Station 30: Cast 2 was performed to obtain near bottom data that was not collected in cast 1.

Station 37: Test cast was performed.

3.6 Microstructure measurement

(1) Personnel

Yusuke Kawaguchi	University of Tokyo	- not on board, PI
ShigetoNishino	JAMSTEC	-not on board
Eun Yae Son	University of Tokyo	
Tsubasa Kodaira	University of Tokyo	
Yoshizawa Eri	KOPRI	
Ryo Oyama	NME	-Operation leader
Shinya Okumura	NME	
Kazuho Yoshida	NME	
Yutaro Murakami	NME	
Soichiro Sueyoshi	NME	
Takehito Hattori	NME	

(2) Objectives

1. Investigate on turbulent mixing at the surface front in the marginal ice zone and under newly formed sea ice during MR19-03C.
2. Collect examples for verification of proper fine-scale parameterization in the Arctic Basin.

(3) Parameter

According to the manufacture's nominal specifications, the range, accuracy and sampling rates of acquisition parameters are shown in Table 3.6-1.

Table 3.6-1:

Parameter	Sensor type	Measurable range	Accuracy	Sampling rate
$\partial u/\partial z$ (primary)	Shear probe	0~10 /s	5%	512Hz
$T+\partial T/\partial z$	FPO-7 thermistor	±0.01°C	±0.01°C	512Hz
T	Platinum wire	−5~45°C	±0.01°C	64 Hz
Conductivity	Inductive Cell	0~70 mS	±0.01 mS	64 Hz
Depth	Semiconductor strain	0~1000 m	±0.2%	64Hz
x- acceleration	Solid-state fixed mass	±2 G	±1%	256 Hz
y- acceleration	Solid-state fixed mass	±2 G	±1%	256 Hz
z- acceleration	Solid-state fixed mass	±2 G	±1%	64Hz
Chlorophyll	Solid-state fixed mass	0~100 µg/Lm	0.5 µg/L or ±1%	256 Hz
Turbidity	Backscatter	0~100 ppm	1ppm or ±2%	256 Hz
$\partial u/\partial z$ (Secondary)	$\partial u/\partial z$ Shear	0~10 s^{-1}	5%	512 Hz

(4) Instruments and methodology

Turbulence Ocean Microstructure Acquisition Profiler (TurboMAP-L, manufactured by JFE Alec Co Ltd.) was used to measure turbulence-scale temperature and shear. TurboMap is a quasi-free-falling instrument that obtains turbulent mixing parameters ($\partial u/\partial z$ and $\partial T/\partial z$), bio-optical parameters (in vivo fluorescence and back scatter) and hydrographic parameters (conductivity, temperature, and pressure). The TurboMAP is a loosely tethered free-fall profiler that carries two airfoil shear probes, a fast-response thermistor (FP07), a light-emitting diode fluorescence/turbidity probe, and a CTD package (Wolk et al. 2002). The TurboMAP collects vertical profiles of microscale velocity shear, high- and low-resolution temperature, conductivity, and pressure, as the underwater device descends from the surface to maximum depth. The free-falling speed of the instrument is roughly at 0.5–0.6 m s−1. Operation of the ship's side thrusters is halted under operation of micro-data acquisition so that they may not create any artificial noise corruption or disturbance in the micro-scale data. The microscale data within 5 m depth are not recommended for the use in analysis as they may include potential noise due to the instrument's initial adjustment to free-falling. TurboMAP observation log is shown in Table. 3.6-2.

Table 3.6-2: Station lists

Stn.	Date [Y/M/D]	Lat. [deg-min]	Lon. [deg-min]	Time (UTC)		Dep. [m]	Obs. Dep. [m]	Sensor S/N		
				Start	End			FP07	Sh1	Sh2
01	2019/10/03	49-59.8521N	166-06.9197E	8:06	8:25	5398	567	144	1232	1233
02	2019/10/03	49-59.7338N	166-07.0970E	8:59	9:17	5401	596	144	1232	1234
03	2019/10/08	65-39.8021N	168-27.6861W	7:23	7:28	52	48	144	1232	1234
04	2019/10/08	65-39.9191N	168-27.6569W	7:29	7:30	52	45	144	1232	1234
05	2019/10/08	65-40.0093N	168-27.6242W	7:31	7:33	52	42	144	1232	1234
06	2019/10/08	66-30.6988N	168-45.261W	13:19	13:21	54	44	144	1232	1234
07	2019/10/08	66-30.7587N	168-45.2213W	13:22	13:23	54	45	144	1232	1234
08	2019/10/08	66-30.8066N	168-45.1858W	13:24	13:25	54	43	144	1232	1234
09	2019/10/08	67-00.4760N	168-43.2958W	16:40	16:43	45	41	144	1232	1234
10	2019/10/08	67-00.5035N	168-43.1616W	16:44	16:45	45	42	144	1232	1234
11	2019/10/08	67-00.5306N	168-43.0656W	16:46	16:47	45	39	144	1232	1234
12	2019/10/08	68-09.9216N	168-45.3434W	23:41	23:43	58	50	144	1232	1234
13	2019/10/08	68-09.9351N	168-45.3301W	23:44	23:47	58	52	144	1232	1234
14	2019/10/08	68-09.9532N	168-45.3045W	23:47	23:49	58	50	144	1232	1234
15	2019/10/09	69-00.4770N	168-45.3655W	5:45	5:47	52	49	144	1232	1234
16	2019/10/09	69-00.5034N	168-45.4092W	5:49	5:49	52	48	144	1232	1234

17	2019/10/09	69-00.5374N	168-45.4578W	5:52	5:52	52	45	144	1232	1234
18	2019/10/09	69-30.3513N	168-45.9433W	9:59	10:02	51	44	144	1233	1234
19	2019/10/09	69-30.3581N	168-45.0331W	10:03	10:05	51	44	144	1233	1234
20	2019/10/09	69-30.3597N	168-45.1039W	10:05	10:07	51	43	144	1233	1234
21	2019/10/09	70-29.8375N	168-45.7190W	17:38	17:39	38	28	144	1233	1234
22	2019/10/09	70-29.8366N	168-45.7784W	17:40	17:41	38	32	144	1233	1234
23	2019/10/09	70-29.8357N	168-45.8826W	17:42	17:43	38	33	144	1233	1234
24	2019/10/10	71-09.2483N	166-25.1891W	0:44	0:46	44	30	144	1233	1234
25	2019/10/10	71-09.2483N	166-25.1891W	0:47	0:49	44	32	144	1233	1234
26	2019/10/10	71-09.2483N	166-25.1891W	0:49	0:51	44	37	144	1233	1234
27	2019/10/10	71-59.3997N	163-30.7643W	8:33	8:35	38	33	144	1233	1234
28	2019/10/10	71-59.3748N	163-30.8411W	8:37	8:37	38	35	144	1233	1234
29	2019/10/10	71-59.3461N	163-30.9131W	8:38	8:38	38	33	144	1233	1234
30	2019/10/10	71-29.7207N	161-44.9374W	14:37	14:38	44	42	144	1233	1234
31	2019/10/10	71-29.7002N	161-44.9267W	14:40	14:41	44	39	144	1233	1234
32	2019/10/10	71-29.6716N	161-44.8961W	14:43	14:43	44	36	144	1233	1234
33	2019/10/10	72-59.9234N	160-01.0259W	20:06	20:11	189	172	144	1233	1234
34	2019/10/10	72-59.9244N	160-01.1010W	20;14	20:19	189	150	144	1233	1234
35	2019/10/10	72-46.9092N	158-22.9159W	23:45	23:54	300	265	144	1233	1234
36	2019/10/10	72-46.9417N	158-23.7892W	23:58	0:07	305	278	144	1233	1234
37	2019/10/11	72-30.1502N	156-18.7587W	7:35	7:51	1619	579	144	1233	1234
38	2019/10/11	72-19.9306N	155-00.7130W	13:20	13:38	1955	680	144	1233	1234
39	2019/10/11	72-08.8840N	153-48.3499W	18:40	-	1705	565	144	1233	1234
40	2019/10/11	72-00.6442N	151-18.0845	23:42	23:59	2669	580	144	1233	1234
41	2019/10/12	71-59.9922N	147-29.9673W	9:41	9:43	3514	600	144	1233	1234
42	2019/10/12	71-59.7477N	144-59.9952W	17:32	17:58	3321	600	144	1233	1234
43	2019/10/12	72-58.5125N	144-55.5249W	23:46	0:00	3555	570	144	1233	1234
44	2019/10/13	72-58.3191N	144-55.8316W	0:11	0:26	3554	566	144	1233	1234
45	2019/10/13	74-25.6864N	142-58.3406W	21:13	21:18	3702	115	144	1233	1234
46	2019/10/13	74-25.5952N	142-58.5283W	21:20	21:24	3707	117	144	1233	1234
47	2019/10/13	74-23.1989N	143-16.1473W	22:26	22:30	3709	117	144	1233	1234
48	2019/10/13	74-23.1594N	143-16.1506W	22:33	22:36	3710	117	144	1233	1234
49	2019/10/13	74-20.3644N	143-30.8557W	23:39	23:44	3712	120	144	1233	1234
50	2019/10/13	74-20.3193N	143-30.8302W	23:47:0	23:51	3710	127	144	1233	1234

				0						
51	2019/10/14	74-17.7599N	143-45.1738W	0:35	0:40	3709	-	144	1233	1234
52	2019/10/14	74-17.6544N	143-44.8224W	0:44	0:52	3711	132	144	1233	1234
53	2019/10/14	74-12.2673N	144-13.7462W	2:01	2:06	3710	112	144	1233	1234
54	2019/10/14	74-12.2052N	144-13.7180W	2:08	2:11	3711	122	144	1233	1234
55	2019/10/14	74-09.4681N	144-28.5057W	3:03	3:07	3712	108	144	1233	1234
56	2019/10/14	74-09.3755N	144-28.4901W	3:10	3:14	3712	115	144	1233	1234
57	2019/10/14	74-03.9934N	144-57.8202W	4:27	4:31	3719	116	144	1233	1234
58	2019/10/14	74-46.4150N	150-31.1201W	20:23	20:40	3835	563	144	1233	1234
59	2019/10/14	74-59.7055N	152-16.4074W	23:46	0:04	3848	587	144	1233	1234
60	2019/10/15	74-59.6590N	152-16.1599W	0:14	0:30	3846	572	144	1233	1234
61	2019/10/16	76-57.7674N	164-45.3915W	23:51	23:55	396	392	144	1233	1234
62	2019/10/16	76-57.7642N	166-44.9311W	0:00	0:08	396	392	144	1233	1234
63	2019/10/16	77-15.0015N	164-59.8112W	7:54	8:02	370	230	144	1233	1234
64	2019/10/16	77-15.0454N	164-59.5942W	8:06	8:13	370	233	144	1233	1234
65	2019/10/16	77-03.9297N	164-56.3229W	23:42	23:49	471	219	144	1233	1234
66	2019/10/16	77-03.9478N	164-55.5717W	23:54	23:59	471	320	144	1233	1234
67	2019/10/17	77-14.9617N	164-59.9329W	5:47	5:55	367	235	144	1233	1234
68	2019/10/17	77-14.9679N	164-59.7267W	6:00	6:07	371	239	144	1233	1234
69	2019/10/17	77-30.0435N	165-00.1776W	9:36	9:43	308	232	144	1233	1234
70	2019/10/17	77-30.0675N	165-00.0837W	9:47	9:54	310	240	144	1233	1234
71	2019/10/17	78-00.2441N	165-00.7489W	21:59	21:07	454	244	144	1233	505
72	2019/10/17	78-00.2612N	165-00.1502W	22:12	22:19	454	229	144	1233	505
73	2019/10/18	77-15.0006N	164-59.9585W	4:56	5:04	370	227	144	1233	505
74	2019/10/18	77-15.0571N	164-59.8944W	5:07	5:14	366	230	144	1233	505
75	2019/10/18	77-30.0269N	165-00.2550W	9:03	9:11	308	245	144	1233	505
76	2019/10/18	77-30.0603N	165-00.2145W	9:16	9:23	309	234	144	1233	505
77	2019/10/18	77-45.0392N	164-59.8296W	14:31	14:38	348	215	144	1233	505
78	2019/10/18	77-45.1693N	164-59.9306W	14:42	14:49	348	238	144	1233	505
79	2019/10/18	77-45.5226N	164-59.4505W	17:59	18:07	439	222	144	1233	505
80	2019/10/18	77-45.6783N	164-59.0496W	18:11	18:17	439	219	144	1233	505
81	2019/10/19	78-04.0251N	165-10.3834W	23:48	23:55	473	222	144	1233	505
82	2019/10/19	78-04.1496N	165-10.3560W	23:59	0:05	473	216	144	1233	505
83	2019/10/19	77-00.0231N	164-59.8730W	6:47	6:54	669	230	144	1233	505

84	2019/10/19	77-00.0550N	164-59.7756W	6:59	7:05	671	236	144	1233	505
85	2019/10/19	77-15.1084N	165-00.1615W	10:35	10:42	362	236	144	1233	505
86	2019/10/19	77-15.1605N	165-00.0141W	10:46	10:53	364	226	144	1233	505
87	2019/10/19	77-30.0184N	164-59.9647W	15:01	15:07	309	188	144	1233	505
88	2019/10/19	77-30.0613N	164-59.7102W	15:16	15:18	309	198	144	1233	505
89	2019/10/19	77-30.1162N	164-59.5181W	15:21	15:26	309	177	144	1233	505
90	2019/10/19	78-03.1133N	164-59.1429W	23:45	23:50	460	173	144	1233	505
91	2019/10/19	78-03.1731N	164-58.6471W	23:54	23:59	460	168	144	1233	505
92	2019/10/20	78-03.2298N	164-58.2186W	0:02	0:06	460	163	144	1233	505
93	2019/10/20	77-00.0290N	164-59.8200W	7:27	7:33	672	171	144	1233	505
94	2019/10/20	77-00.0676N	164-59.7295W	7:35	7:40	663	170	144	1233	505
95	2019/10/20	77-00.1151N	164-59.6577W	7:43	7:48	662	167	144	1233	505
96	2019/10/20	77-15.0168N	164-59.9991W	11:35	11:41	365	167	144	1233	505
97	2019/10/20	77-15.0742N	164-59.7690W	11:44	11:49	365	167	144	1233	505
98	2019/10/20	77-15.1499N	164-59.5407W	11:52	11:57	362	165	144	1233	505
99	2019/10/20	77-30.1018N	164-59.1995W	16:09	16:15	308	165	144	1233	505
100	2019/10/20	77-30.1588N	164-58.8220W	16:18	16:22	308	164	144	1233	505
101	2019/10/20	77-30.2305N	164-58.4328W	16:26	16:30	308	163	144	1233	505
102	2019/10/20	78-00.3450N	165-00.4578W	21:57	22:03	455	172	144	1233	505
103	2019/10/20	78-00.4221N	165-00.1065W	22:06	22:11	455	163	144	1233	505
104	2019/10/20	78-00.4893N	164-59.6686W	22:14	22:18	455	167	144	1233	505
105	2019/10/21	77-15.0072N	165-59.9773W	4:17	4:23	852	178	144	1233	505
106	2019/10/21	77-15.0470N	165-59.9454W	4:27	4:32	852	180	144	1233	505
107	2019/10/21	77-15.0948N	165-59.8892W	4:35	4:36	852	20	144	1233	505
108	2019/10/21	77-15.1001N	165-59.8671W	4:36	4:41	852	168	144	1233	505
109	2019/10/21	77-00.0690N	164-59.9934W	10:02	10:08	708	168	144	1233	505
110	2019/10/21	77-00.1433N	164-59.8591W	10:12	10:17	708	178	144	1233	505
111	2019/10/21	77-00.1973N	164-59.7176W	10:20	10:25	708	176	144	1233	505
112	2019/10/21	77-15.0228N	164-59.9817W	15:02	15:08	372	180	144	1233	505
113	2019/10/21	77-15.0846N	164-59.8435W	15:11	15:16	372	178	144	1233	505
114	2019/10/21	77-15.1262N	164-59.7434W	15:19	15:24	372	173	144	1233	505
115	2019/10/21	77-30.0902N	165-00.0872W	16:58	17:04	306	172	144	1233	505
116	2019/10/21	77-30.1491N	164-59.9966W	17:07	17:11	306	167	144	1233	505
117	2019/10/21	77-30.1932N	164-59.7542W	17:15	17:20	306	171	144	1233	505

118	2019/10/21	78-00.5449N	164-59.9344W	21:57	22:03	463	157	144	1233	505
119	2019/10/21	78-00.7032N	164-59.6497W	22:07	22:12	463	158	144	1233	505
120	2019/10/21	78-00.8762N	164-59.3135W	22:16	22:21	463	164	144	1233	505
121	2019/10/22	77-00.1451N	166-00.1091W	5:35	5:41	603	169	144	1233	505
122	2019/10/22	77-00.2049N	166-00.0938W	5:44	4:49	603	186	144	1233	505
123	2019/10/22	77-00.2541N	166-00.0728W	5:53	5:58	603	173	144	1233	505
124	2019/10/22	76-59.9157N	165-00.0425W	9:40	9:45	737	164	144	1233	505
125	2019/10/22	76-59.9833N	164-59.8779W	9:49	9:54	737	184	144	1233	505
126	2019/10/22	77-00.0394N	164-59.7181W	9:57	10:02	737	164	144	1233	505
127	2019/10/22	77-15.0187N	164-59.9712W	14:54	15:00	371	174	144	1233	505
128	2019/10/22	77-15.0650N	164-59.8826W	15:02	15:07	371	173	144	1233	505
129	2019/10/22	77-15.1104N	169-59.8076W	15:10	15:14	371	175	144	1233	505
130	2019/10/22	77-30.0320N	164-59.6690W	16:47	16:52	309	178	144	1233	505
131	2019/10/22	77-30.1032N	164-59.4797W	16:55	16:59	309	169	144	1233	505
132	2019/10/22	77-30.1599N	164-59.2379W	17:02	17:07	309	164	144	1233	505
133	2019/10/22	77-46.2299N	164-04.7955W	23:52	23:53	275	180	144	1233	505
134	2019/10/22	77-46.2981N	164-04.5649W	23:56	0:01	275	171	144	1233	505
135	2019/10/23	77-46.3559N	164-04.3546W	0:04	0:09	275	168	144	1233	505
136	2019/10/23	76-59.9702N	163-59.7083W	5:06	5:12	437	171	144	1233	505
137	2019/10/23	77-00.0281N	163-59.8135W	5:15	5:20	437	168	144	1233	505
138	2019/10/23	77-00.0839N	164-00.0240W	5:23	5:28	437	166	144	1233	505
139	2019/10/23	76-59.9250N	164-59.7254W	8:49	8:55	670	167	144	1233	505
140	2019/10/23	77-00.0136N	164-59.5948W	8:58	9:03	670	173	144	1233	505
141	2019/10/23	77-00.0548N	164-59.3884W	9:07	9:12	670	175	144	1233	505
142	2019/10/23	77-14.9759N	165-00.3586W	12:43	12:49	365	165	144	1233	505
143	2019/10/23	77-15.0343N	165-00.1760W	12:52	12:59	365	163	144	1233	505
144	2019/10/23	77-15.1011N	164-59.9652W	13:00	13:04	365	168	144	1233	505
145	2019/10/23	77-29.9561N	165-00.2722W	15:47	15:52	309	161	144	1233	505
146	2019/10/23	77-30.0408N	165-00.0219W	15:50	16:01	309	163	144	1233	505
147	2019/10/23	77-30.1203N	164-59.6431W	16:04	16:09	309	171	144	1233	505
148	2019/10/23	77-46.7549N	163-36.4233W	22:00	22:06	289	172	144	1233	505
149	2019/10/23	77-46.8118N	163-36.2003W	22:09	22:14	289	174	144	1233	505
150	2019/10/23	77-46.8951N	163-35.9086W	22:18	22:23	289	167	144	1233	505
151	2019/10/24	77-15.0406N	164-00.2612W	2:53	2:58	365	174	144	1233	505

152	2019/10/24	77-15.0632N	164-00.0346W	3:01	3:06	365	182	144	1233	505
153	2019/10/24	77-15.0751N	163-59.7522W	3:10	3:15	365	173	144	1233	505
154	2019/10/24	77-00.0379N	165-00.3718W	9:24	9:29	682	180	144	1233	505
155	2019/10/24	77-00.0882N	165-00.3285W	9:33	9:38	682	167	144	1233	505
156	2019/10/24	77-00.1615N	165-00.1762W	9:42	9:47	682	171	144	1233	505
157	2019/10/24	77-15.0317N	164-59.9736W	14:28	14:33	370	164	144	1233	505
158	2019/10/24	77-15.1114N	165-00.0154W	14:36	14:41	370	160	144	1233	505
159	2019/10/24	77-15.2027N	165-00.2230W	14:44	14:48	370	160	144	1233	505
160	2019/10/24	77-30.0955N	164-59.9872W	16:19	16:25	307	162	144	1233	505
161	2019/10/24	77-30.2165N	164-59.9896W	16:28	16:33	307	153	144	1233	505
162	2019/10/24	77-30.3441N	165-00.1151W	16:35	16:40	307	160	144	1233	505
163	2019/10/25	77-48.1967N	163-46.2576W	0:03	0:08	237	163	144	1233	505
164	2019/10/25	77-48.3194N	163-46.7506W	0:13	0:17	237	169	144	1233	505
165	2019/10/25	77-48.4510N	163-47.2585W	0:21	0:26	237	165	144	1233	505
166	2019/10/25	76-59.9434N	168-44.6127W	8:10	8:14	1885	102	144	1233	505
167	2019/10/25	76-59.9892N	168-45.0471W	8:17	8:29	1885	439	144	1233	505
168	2019/10/25	74-41.5100N	168-46.0646W	23:45	23:51	184	167	144	1233	505
169	2019/10/25	74-41.5528N	168-46.1547W	23:53	23:58	184	164	144	1233	505
170	2019/10/25	74-41.6773N	168-46.4730W	0:01	0:05	184	170	144	1233	505
171	2019/10/26	74-00.1065N	168-44.2929W	4:21	4:26	186	166	144	1233	505
172	2019/10/26	74-00.0775N	168-44.3735W	4:29	4:34	186	166	144	1233	505
173	2019/10/26	74-00.0730N	168-44.3841W	4:37	4:41	186	166	144	1233	505
174	2019/10/26	73-00.0892N	168-45.2488W	12:45	12:46	61	46	144	1233	505
175	2019/10/26	73-00.0795N	168-45.2376W	12:48	12:49	61	41	144	1233	505
176	2019/10/26	73-00.0705N	168-45.2071W	12:51	12:50	61	46	144	1233	505
177	2019/11/02	50-00.2626N	166-07.3557E	23:08	23:24	5398	536	144	1233	1234

(4) Remarks

TurboMAP is designed to be used stand-alone without additional CTD observation. However, it is recommended to check incoming CTD data's quality by comparing SBE9plus (Sea Bird Electronics). We conducted several TurboMAP observation down to 500 m in the Canada Basin where CTD observation is accompanied. Since, TurboMAP is not able to attach CTD frame, TurboMAP cast was accomplished right after or before the CTD cast. Sensor's validity is judged by temperature, salinity and pressure below the pycnocline where no significant variation within short period (Figure.3.6-1).

Since the observation was conducted under cold air temperature (< 0°C), slow temperature sensor showed delayed response to the real-upper ocean temperature. It is recommended to use data acquired from second or third cast for the CTD, shear, and FP07 data. In the area where bottom depth was between 200–300 m, 4 seconds regular noises was detected in both shear sensors. Those noises were revealed by multi-beam sonar, which measures bottom depth from the acoustic signal. The multi-beam sonar was turned off after cast No. 79.

TurboMAP consists 2 shear probes for checking shear data validity. It is able to be utilized with only one shear probe, however, a pair of shear sensor is recommended. Figure 3.6-2 is turbulence dissipation rate that obtained by each shear sensors. During MR19-03C, we changed shear probe twice (St.18: shear1 to S/N 1233; St.71: shear2 to S/N 505). After escaped from the Arctic Ocean, we made another test cast for checking CTD and shear probe (S/N 1234) status. Shear S/N 1234 was changed by repeated noise, however, it revealed that the noise was acoustic signal of Multi-Beam Sonar (Figure 3.6-3).

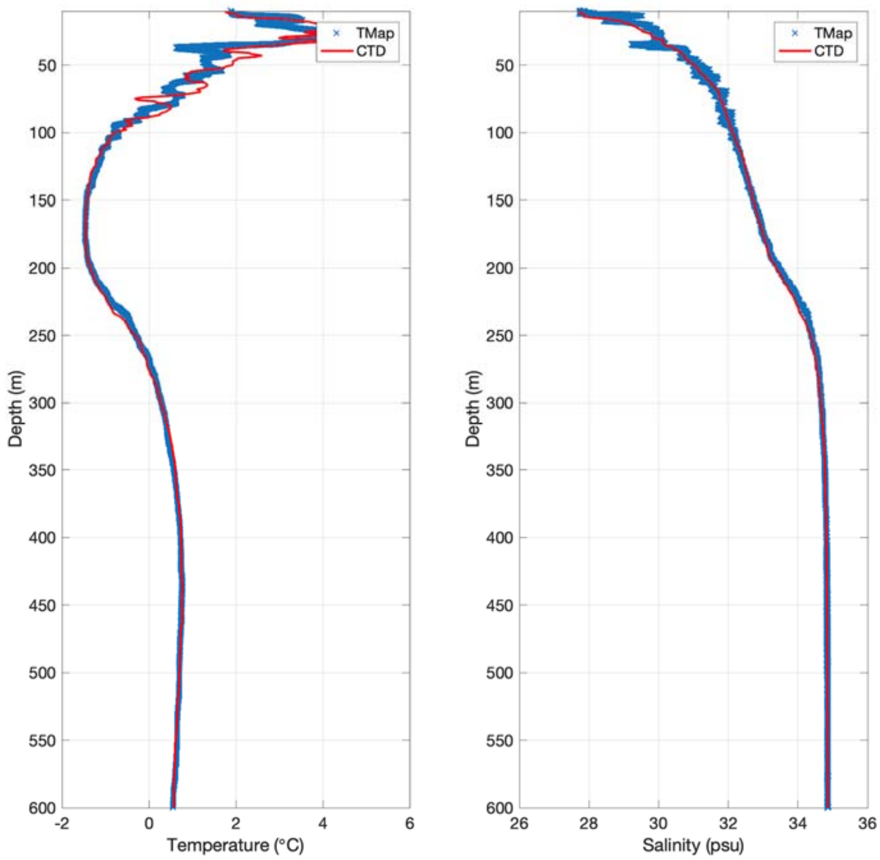

Figure 3.6-1: Comparison of temperature and salinity acquired by SBE9plus and TurboMAP.

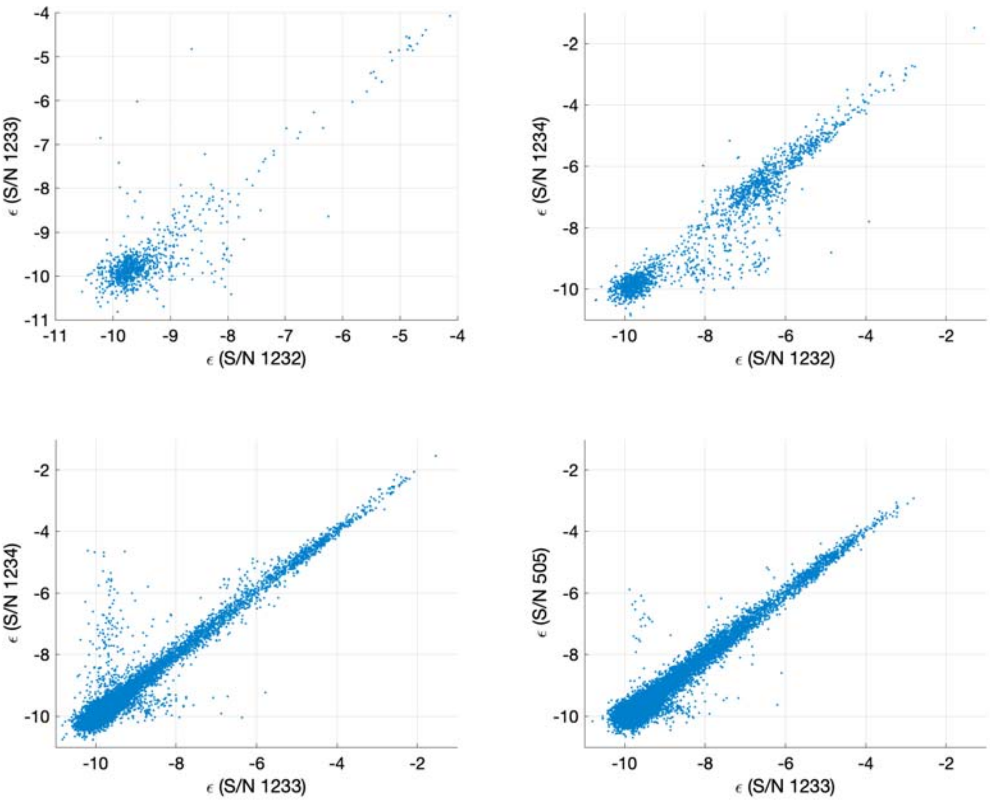

Figure 3.6-2: Correlation between the two shear sensors that used for MR19-03C.

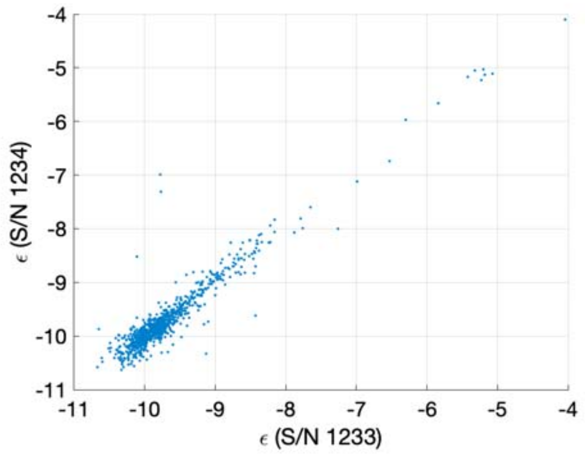

Figure 3.6-3: Correlation between the two shear probes of S/N 1234 and 1233 from test cast

(5) Data archive

The raw data obtained in this cruise will be submitted to the Data Management Group (DMG) of JAMSTEC.

3.7 Subsurface ocean current and heat observation with drifting buoy

(1) Personnel

Yusuke Kawaguchi	University of Tokyo	- not on board, PI
Shigeto Nishino	JAMSTEC	- not on board
Eun Yae Son	University of Tokyo	

(2) Objectives

To examine the upper ocean bulk-heat variation in the western Arctic during sea ice freezing season and explore the upper ocean current at the surface front between dense-warm water and fresh-cold water in the marginal ice zone.

(3) Parameter

Surface Velocity Profiler (SVP)

GPS positions of drifting buoy

IceBTC60/40

GPS positions and air pressure of drifting buoy

Water temperature and hydrostatic pressure at certain depth

(4) Instruments and methodology

We deployed two types of drifting buoys for investigating upper ocean current and heat variability in the marginal ice area. We deployed two SVP buoys with the drogue at depths of 40 and 15 m, respectively, in horizontal front where surface temperature changes rapidly (MIZ5). IceBTC60/40 is designed for utilization in the sea ice covered area which has a 60 m-long thermistor chain with the pressure sensors. It measures upper ocean temperature with the accuracy of +/-0.1°C (resolution of 0.04°C) and air pressure with the accuracy of +/-1 hPa (resolution of 0.1 hPa). IceBTC40/60 has thermistors at depths of 0, 2.5, 5, 7.5, 10, 12.5, 15, 17.5, 20, 25, 30, 35, 40, 45, 50, 55, and 60 m and especially, it consists hydrostatic pressure sensor at depths of 20, 40, and 60 m. We deployed IceBTC40/60 in the marginal ice zone where covered with the grease ice (MIZ2) to explore the upper ocean bulk-heat flux during the sea ice forming season.

Table 3.7: Deployment information

Type	S/N	Deploy time (UTC)	Deploy location [deg-min]	Data interval	Drogue depth	denotes
SVP	35924	02:20 Oct 14, 2019	74-12.2052N, 144-13.718W	hourly	40 m	Deployed in surface front
SVP	145580	02:26 Oct 14, 2019	74-12.2052N, 144-13.718W	hourly	15 m	Deployed in surface front
IceBTC40/60	11800	23:43 Oct 13, 2019	74-23.15N, 143-16.151W	hourly	-	Deployed in the grease ice zone

(5) Data archive

The raw data obtained in this cruise will be submitted to the Data Management Group (DMG) of JAMSTEC.

3.8 Surface wave measurement

(1) Personnel

Jun Inoue	NIPR	-PI
Takuji Waseda	The University of Tokyo	- not on board
Tsubasa Kodaira	The University of Tokyo	
Takehiko Nose	The University of Tokyo	- not on board

(2) Objective

Recent research has recognized surface ocean waves as one of the key physical processes in sea ice freeze up and break up. We aimed to study generation, propagation, and attenuation of surface ocean waves under the sea ice based on the in-situ observation over the western Arctic Ocean. Drifting type wave buoys and stereo-camera system on board were used to measure surface wave characteristics.

(3) Parameters

Drifting wave buoys: Significant wave height (Hm0), Peak period (Tp), Peak direction, Peak directional spread, Mean period (Tm01), Mean direction, Mean directional spread, and Power Spectral Density (PSD), time and GPS coordinates.

Stereo camera system: Monochrome images (4064×4064 pixels), Acceleration (3-axis), gyro (3-axis), geomagnetism (3-axis)

(4) Instruments and methods

Drifting wave buoys: The drifting type wave buoy is Spotter device manufactured by Sofar Ocean Technologies (Figure 3.8-1). The device is fully solar powered, and has two-way communication function via Iridium satellite communication. One of the three wave buoys was deployed at the north of Pt. Barrow to measure the waves for relatively long time. The other two wave buoys are deployed near the sea-ice, one in the pancake-ice covered area and the other in the open ocean, with the distance of about 40km.

Stereo camera system: Two cameras are mounted on the portside of R/V Mirai to capture the images of surface ocean waves, being synchronized for the stereo reconstruction. The cameras installed to the camera housing, and they are connected by USB-cables to a laptop computer installed in the water tight black plastic box(see, Figure 3.8-1). A 5-bay HDD storage and wireless rooter were also installed in the box. A 9-axis inertial moment unit (ZMP-IMUZ) was also installed in the box to measure the motion of the cameras.

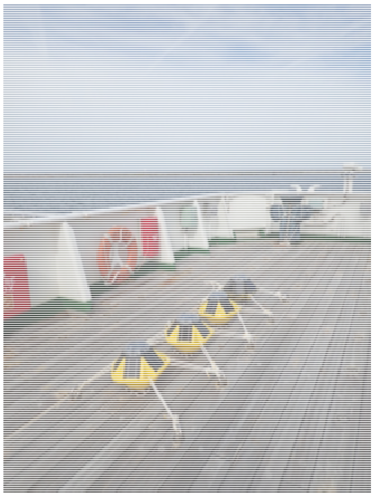

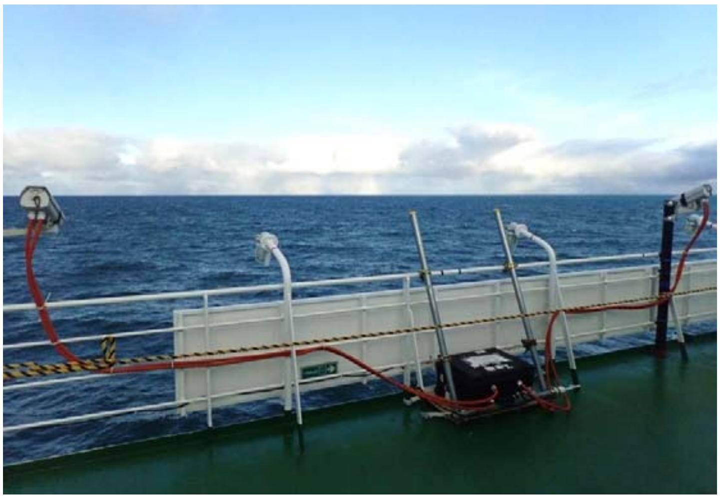

Figure 3.8-1: Drifting wave buoys (left) and the stereo camera system on board (right).

(5) Observation log

Drifting wave buoys: One of the wave buoys SPOT-0339 was deployed in open water at 10:35 UTC on the 11th October at 72.3407 N, 155.0548 W (see Figure 3.8-2). The wave buoy stopped sending data at 20:50 on 21st October, 2019 because the battery was not sufficiently charged by solar power due to the limited solar radiation at the high latitude in October.

The other two wave buoys SPOT-0257 and SPOT-0258 were deployed near the sea-ice edge to compare the waves under the sea-ice and in the open ocean. The deployment of SPOT-0257 was in pancake-ice-covered water at 21:40 on the 13th October 2019 at 74.4235N, 143.0032W. The subsequent deployment of SPOT-0258 was in open ocean at the thermal front at 2:20 on the 13th October 2019 at 74.2012N, 144.2273W (see Figure 3.8-2). The wave buoys SPOT-0257 and SPOT-0258 stopped the transmission at 05:01 on 21st October 2019 and at 17:01 on 19th October 2019, respectively.

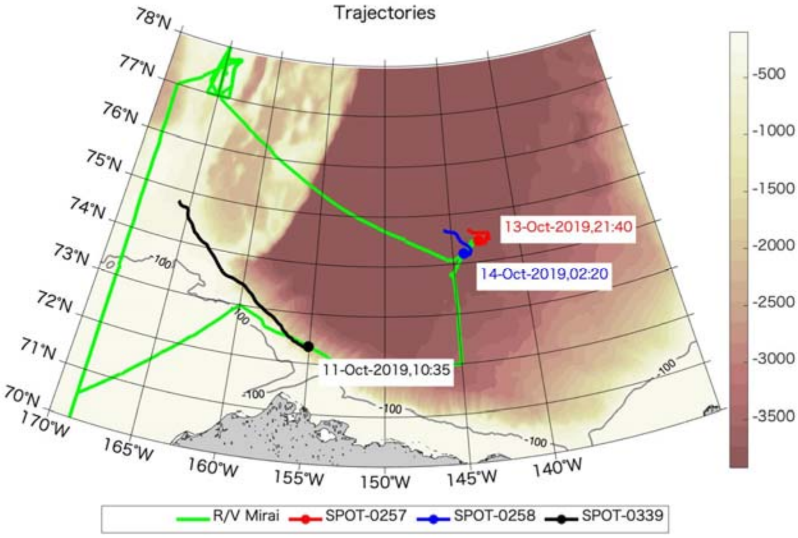

Figure 3.8-2: Trajectories of R/V Mirai and drifting wave buoys. The circle indicates the deployment location for each buoy. The text near the circle shows the date and time [UTC] of the deployment. The color shows the bathymetry.

Stereo camera system: The stereo camera system was used every hour and sometiimes every half an hour when R/V Mirai cruise near the sea ice covered area.

(6) Preliminary Results

Drifting wave buoys: Figure 3.8-3 shows the wave statistics recorded by the drifting wave buoys. SPOT-0339 measured the maximum significant wave height of 3.38m with the peak period of 9.31s at 06:50 on 12-Oct-2019. The wave height changed with time as the wind speed changed. The concurrent measurements of surface waves under the sea-ice by SPOT-0257 and the waves in the open ocean by SPOT-0258 exhibit the transformation of the waves by the sea-ice. The waves under the sea-ice were at first similar height compared to the open ocean, but gradually became smaller. The results indicate that the waves attenuate or scattered as they propagate over the sea-ice. In addition, the mean wave period of the waves under the sea-ice was consistently smaller than those in the open ocean, while the peak period shows similar values. The results imply that shorter waves are more easily attenuated.

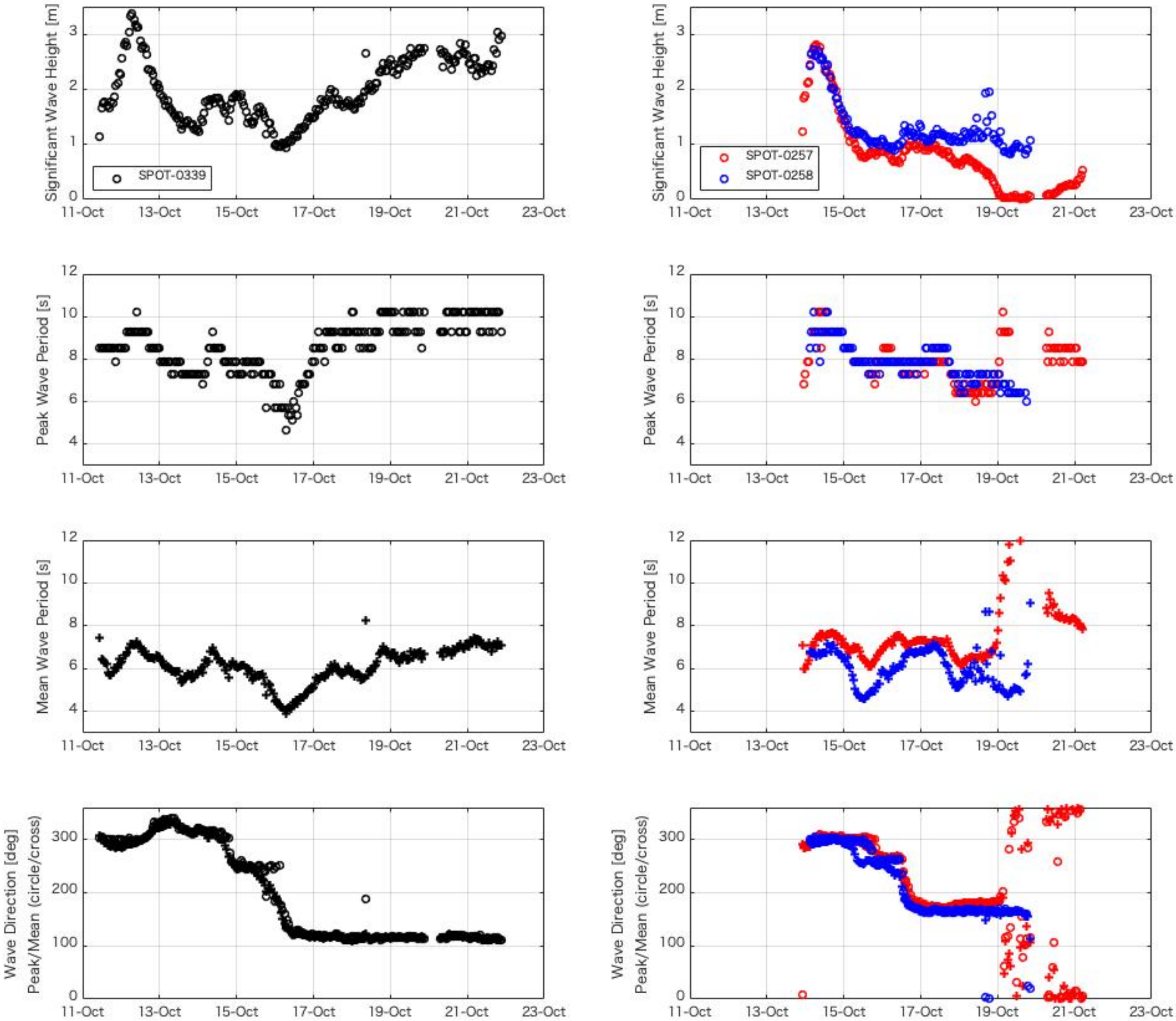

Figure 3.8-3: Significant wave heights (top), periods (middle), and direction measurements (bottom). The left column for SPOT-339 and the right column for SPOT-0257 and SPOT-0258, respectively.

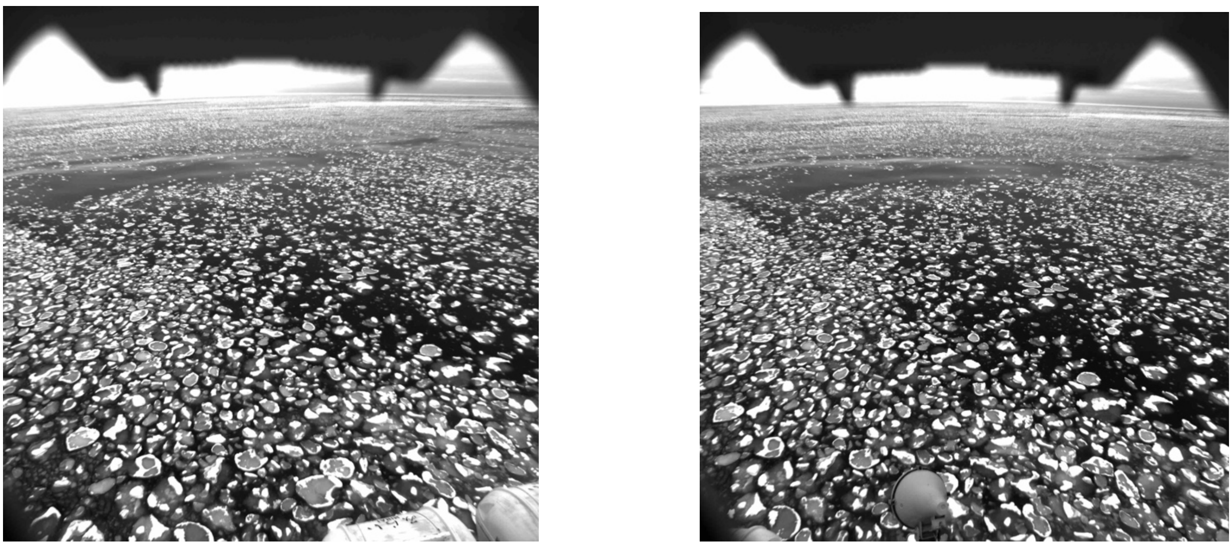

Figure 3.8-4: Sample images of the stereo camera system.

(7) Data archives

These data obtained in this cruise will be submitted to the Data Management Group of JAMSTEC and will be opened to the public via “Data Research System for Whole Cruise Information in JAMSTEC (DARWIN)” in JAMSTEC web site. <http://www.godac.jamstec.go.jp/darwin/e>

3.9 LADCP

(1) Personnel

Yusuke Kawaguchi	University of Tokyo	- not on board, PI
Shigeto Nishino	JAMSTEC	- not on board
Eun Yae Son	University of Tokyo	
Shinsuke Toyoda	MWJ	- Operation leader
Rio Kobayashi	MWJ	
Tun Htet Aung	MWJ	

(2) Objectives and methodology

The lowered ADCP (LADCP), Workhorse Monitor WHM300 (Teledyne RD Instrument, San Diego, California, USA) was utilized at the every CTD point in MR19-03C to get a shear data at the same time. LADCP system consist of two ADCP of upward-and downward looking transducer and a 45V battery package. The LADCP system were set for recording before the CTD cast and its data were recovered right after CTD cast. Velocity conversion from the two transducers were done by LDEO LADCP software (version 10; Visbeck 2002). For the data conversion, navigation data and CTD data were applied for the improvement of data quality.

Every LADCP data is separated by independent folder, which has same name with the CTD station name. Detailed configuration is below:

Bin size: 8.0 m

Number of bins: 25

Pings per ensemble: 1

Ping interval: 1.0 sec

(3) Data archive

The raw data obtained in this cruise will be submitted to the Data Management Group (DMG) of JAMSTEC.

Reference

Visbeck, M. (2002): Deep velocity profiling using Acoustic Doppler Current Profilers: Bottom track and inverse solutions, J. Atmos. Oceanic Technol., 19, 794–807.

4. Chemical and Biological Oceanography

4.1 Dissolved Oxygen

(1) Personnel

Akihiko Murata	JAMSTEC	- PI
Erii Irie	MWJ	- Operation Leader
Yuko Miyoshi	MWJ	
Kanako Yoshida	MWJ	

(2) Objective

Determination of dissolved oxygen in seawater by Winkler titration.

(3) Parameters

Dissolved Oxygen

(4) Instruments and Methods

Following procedure is based on winkler method (Dickson, 1996; Culberson, 1991).

a. Instruments

Burette for sodium thiosulfate and potassium iodate;

Automatic piston burette (APB-510 / APB-610 / APB-620) manufactured by Kyoto Electronics Manufacturing Co., Ltd. / 10 cm^3 of titration vessel

Detector;

Automatic photometric titrator (DOT-15X) manufactured by Kimoto Electric Co., Ltd.

Software;

DOT_Terminal Ver. 1.3.1

b. Reagents

Pickling Reagent I: Manganese(II) chloride solution (3 mol dm^{-3})

Pickling Reagent II:

Sodium hydroxide (8 mol dm^{-3}) / Sodium iodide solution (4 mol dm^{-3})

Sulfuric acid solution (5 mol dm^{-3})

Sodium thiosulfate (0.025 mol dm^{-3})

Potassium iodate (0.001667 mol dm^{-3})

c. Sampling

Seawater samples were collected with Niskin bottle attached to the CTD/Carousel Water Sampling System (CTD system). Seawater for oxygen measurement was transferred from the bottle to a volume calibrated flask (ca. 100 cm^3), and three times volume of the flask was overflowed. Temperature was simultaneously measured by digital thermometer during the overflowing. After transferring the sample, two reagent solutions (Reagent I and II) of 1 cm^3 each were added immediately and the stopper was inserted carefully into the flask. The sample flask was then shaken vigorously to mix the contents and to disperse the precipitate finely throughout. After the precipitate has settled at least halfway down the flask, the flask was shaken again vigorously to disperse the precipitate. The sample flasks containing pickled samples were stored in a laboratory until they were titrated.

d. Sample measurement

For over two hours after the re-shaking, the pickled samples were measured on board. Sulfuric acid solution with its volume of 1 cm^3 and a magnetic stirrer bar were put into the sample flask and the sample was stirred. The samples were titrated by sodium thiosulfate solution whose morality was determined by potassium iodate solution. Temperature of sodium thiosulfate during titration was recorded by a digital thermometer. Dissolved oxygen concentration ($\mu mol\ kg^{-1}$) was calculated by sample temperature during seawater sampling, salinity of the sensor on CTD system, flask volume, and titrated volume of sodium thiosulfate solution without the blank. During this cruise, 2 sets of the titration apparatus were used.

e. Standardization and determination of the blank

Concentration of sodium thiosulfate titrant was determined by potassium iodate solution. Pure potassium iodate was dried in an oven at 130 ºC, and 1.7835 g of it was dissolved in deionized water and diluted to final weight of 5 kg in a flask. After 10 cm^3 of the standard potassium iodate solution was added to another flask using a volume-calibrated dispenser, 90 cm^3 of deionized water, 1 cm^3 of sulfuric acid solution, and 1 cm^3 of pickling reagent solution II and I were added in order. Amount of titrated volume of sodium thiosulfate for this diluted standard potassium iodate solution (usually 5 times measurements average) gave the morality of sodium thiosulfate titrant.

The oxygen in the pickling reagents I (1 cm^3) and II (1 cm^3) was assumed to be 7.6×10^{-8} mol (Murray et al., 1968). The blank due to other than oxygen was determined as follows. First, 1 and 2 cm^3 of the standard potassium iodate solution were added to each flask using a calibrated dispenser. Then 100 cm^3 of deionized water, 1 cm^3 of sulfuric acid solution, 1 cm^3 of pickling II reagent solution, and same volume of pickling I reagent solution were added into the flask in order. The blank was determined by difference between the first (1 cm^3 of potassium iodate) titrated volume of the sodium thiosulfate and the second (2 cm^3 of potassium iodate) one. The titrations were conducted for 3 times and their average was used as the blank value.

(5) Observation log

a. Standardization and determination of the blank

Table 4.1-1 shows results of the standardization and the blank determination during this cruise.

Table 4.1-1: Results of the standardization and the blank determinations during cruise

Date (yyyy/mm/dd)	Potassium iodate ID	Sodium thiosulfate ID	DOT-01X (No.9)		DOT-01X (No.10)		Instrumental Error (%)	Stations
			E.P. (cm^3)	Blank (cm^3)	E.P. (cm^3)	Blank (cm^3)		
2019/10/2	K19C04	T-19G	3.954	0.001	3.964	0.001	-0.21	Stn.000 Cast001, Stn.000 Cast002
2019/10/5	K19C06	T-19G	3.955	-0.002	3.965	0.001	-0.18	Stn.001 Cast001, Stn.004 Cast001, Stn.006 Cast001, Stn.008 Cast001, Stn.009 Cast001
			3.959	0.000	3.966	0.002	-0.12	Stn.002 Cast001, Stn.003 Cast001, Stn.005 Cast001, Stn.007 Cast001 Stn.008 Cast001, Stn.009 Cast001
2019/10/10	K19C05	T-19I	3.955	0.002	3.965	0.006	-0.16	Stn.010 Cast001, Stn.011 Cast001, Stn.012 Cast001, Stn.013 Cast001, Stn.014 Cast001, Stn.015 Cast001, Stn.016 Cast001

2019/10/14	K19C08	T-19I	3.956	0.000	3.965	0.004	-0.14	Stn.017 Cast001, Stn.018 Cast001, Stn.019 Cast001, Stn.020 Cast001
2019/10/16	K19C10	T-19K	3.965	-0.001	3.967	0.003	0.07	Stn.019 Cast002, Stn.020 Cast002- 004, Stn.021 Cast001-003, Stn.022 Cast001-002, Stn.023 Cast001
2019/10/20	K19D01	T-19K	3.963	-0.003	3.966	0.001	0.03	Stn.019 Cast003-004, Stn.020 Cast005- 006, Stn.021 Cast004-005, Stn.024 Cast001

2019/10/22	K19D02	T-19J	3.965	-0.004	3.966	0.000	0.08	Stn.019 Cast005-007, Stn.020 Cast007- 009, Stn.021 Cast007-008, Stn.025 Cast001, Stn.026 Cast001, Stn.027 Cast001, Stn.028 Cast001
2019/10/26	K19D03	T-19J	3.967	-0.001	3.969	0.001	0.02	Stn.029 Cast001, Stn.030 Cast001 Stn.031 Cast001, Stn.032 Cast001, Stn.033 Cast001, Stn.034 Cast001, Stn.035 Cast001, Stn.036 Cast001 Stn.037 Cast001, Stn.038 Cast001, Stn.039 Cast001, Stn.040 Cast001, Stn.041 Cast001,

2019/11/4	K19D05	T-19M	3.972	0.005	3.970	0.006	0.09	Stn.000 Cast003 - 004

b. Repeatability of sample measurement

Replicate samples were taken at every CTD casts. The standard deviation of the replicate measurement (Dickson et al., 2007) was 0.13 μmol kg^{-1} (n=174). Results of replicate samples were shown in Table 4.1-2 and this diagram shown in Figure 4.1. These data use the preliminary data. The standard deviation (s) is given by the expression

$$s = \sqrt{\frac{\sum_{i=1} {d_i}^2}{2k}}$$

where d and k are the difference of replicate measurements and the number of replicate samples respectively.

Table 4.1-2: Results of the replicate sample measurements

Layer	Number of replicate sample pairs	Oxygen concentration (μmol kg^{-1}) Standard Deviation
200m>	86	0.14
>=200m	88	0.11
All	174	0.13

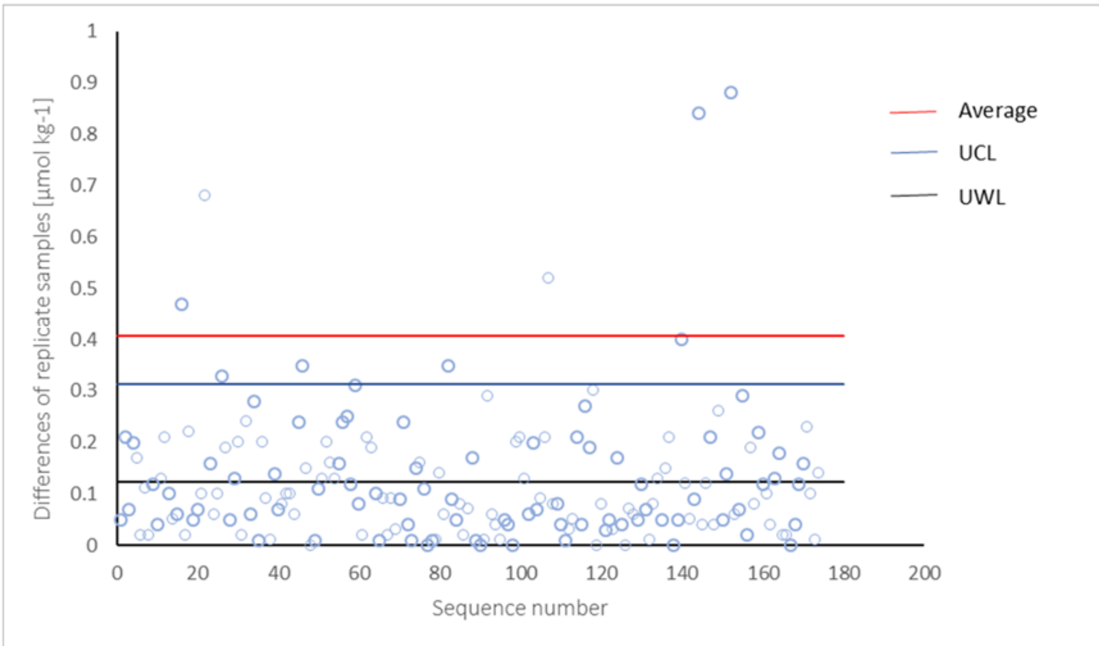

Figure 4.1: Difference of replicate samples against sequence number

(6) Data archives

These data obtained in this cruise will be submitted to the Data Management Group (DMG) of JAMSTEC, and will opened to the public via “Data Research System for Whole Cruise Information in JAMSTEC (DARWIN)” in JAMSTEC web site.
<http://www.godac.jamstec.go.jp/darwin/e>

(7) References

Culberson, C. H. (1991). *Dissolved Oxygen.* WHPO Publication 91-1.

Dickson, A. G. (1996). Determination of dissolved oxygen in sea water by Winkler titration. In *WOCE Operations Manual*, Part 3.1.3 Operations & Methods, WHP Office Report WHPO 91-1.

Dickson, A. G., Sabine, C. L., & Christian, J. R.(Eds.), (2007). *Guide to best practices for ocean CO_2 measurements, PICES Special Publication 3*: North Pacific Marine Science Organization.

Murray, C. N., Riley, J. P., & Wilson, T. R. S. (1968). The solubility of oxygen in Winklerreagents used for the determination of dissolved oxygen. *Deep Sea Res.*, 15, 237-238.

4.2. Nutrients

(1) Personnel

Michio AOYAMA	JAMSTEC/Tsukuba Univ.	-PI
Akihiko MURATA	JAMSTEC	
Mikio KITADA	MWJ	- Operation Leader
Shinichiro YOKOGAWA	MWJ	
Keitaro MATSUMOTO	MWJ	
Tomomi SONE	MWJ	

(2) Objectives

The objectives of nutrients analyses during the R/V Mirai MR19-03C cruise in the Arctic Ocean, of which EXPOCODE is 49NZ20190927, is as follows:

- Describe the present status of nutrients concentration with excellent comparability using certified reference material of nutrient in seawater.

(3) Parameters

The determinants are nitrate, nitrite, silicate, phosphate and ammonia in the Arctic Ocean.

(4) Instruments and methods

(4.1) Analytical detail using QuAAtro 2-HR systems (BL TEC K.K.)

Nitrate + nitrite and nitrite are analyzed following a modification of the method of Grasshoff (1976). The sample nitrate is reduced to nitrite in a cadmium tube the inside of which is coated with metallic copper. The sample stream after reduction is treated with an acidic, sulfanilamide reagent to produce a diazonium ion. N-1-Naphthylethylenediamine Dihydrochloride added to the sample stream to produce a red azo dye. With reduction of the nitrate to nitrite, both nitrate and nitrite react and are measured; without reduction, only nitrite reacts. Thus, for the nitrite analysis, no reduction is performed and the alkaline buffer is not necessary. Nitrate is computed by difference.

The silicate method is analogous to that described for phosphate. The method used is essentially that of Grasshoff et al. (1999). Silicomolybdic acid is first formed from the silicate in the sample and molybdic acid. The silicomolybdic acid is reduced to silicomolybdous acid, or "molybdenum blue," using ascorbic acid.

The phosphate analysis is a modification of the procedure of Murphy and Riley (1962). Molybdic acid is added to the seawater sample to form phosphomolybdic acid which is in turn reduced to phosphomolybdous acid using L-ascorbic acid as the reductant.

The ammonia in seawater is mixed with an alkaline containing EDTA, ammonia as gas state is formed from seawater. The ammonia (gas) is absorbed in sulfuric acid by way of 0.5 μm pore size membrane filter (ADVANTEC PTFE) at the dialyzer attached to analytical system. The ammonia absorbed in sulfuric acid is determined by coupling with phenol and hypochlorite to form indophenols blue. Wavelength using ammonia analysis is 630 nm, which is absorbance of indophenols blue.

The details of modification of analytical methods for four parameters, Nitrate, Nitrite, Silicate and Phosphate, used in this cruise are also compatible with the methods described in nutrients section in new GO-SHIP repeat hydrography nutrients manual (Becker et al., 2019) which is revised version of the GO-SHIP repeat hydrography nutrients manual (Hydes et al., 2019), while an analytical method of ammonium is compatible with Determination of ammonia in seawater using a vaporization membrane permeability method (Kimura, 2000). The flow diagrams and reagents for each parameter are shown in Figures 4.2-1 to 4.2-5.

(4.2) Nitrate + Nitrite Reagents

50 % Triton solution

50 mL Triton^{TM} X-100 provided by Sigma-Ardrich Japan G. K. (CAS No. 9002-93-1), were mixed with 50 mL Ethanol (99.5 %).

Imidazole (buffer), 0.06 M (0.4 % w/v)

Dissolve 4 g Imidazole (CAS No. 288-32-4), in 1000 mL Ultra-pure water, add 2 mL Hydrogen chloride (CAS No. 7647-01-0). After mixing, 1 mL 50 % Triton solution is added.

Sulfanilamide, 0.06 M (1 % w/v) in 1.2 M HCl

Dissolve 10 g 4-Aminobenzenesulfonamide (CAS No. 63-74-1), in 900 mL of Ultra-pure water, add 100 mL Hydrogen chloride (CAS No. 7647-01-0). After mixing, 2 mL 50 % Triton solution is added.

NED, 0.004 M (0.1 % w/v)

Dissolve 1 g N-(1-Naphthalenyl)-1,2-ethanediamine, dihydrochloride (CAS No. 1465-25-4), in 1000 mL of Ultra-pure water and add 10 mL Hydrogen chloride (CAS No. 7647-01-0). After mixing, 1 mL 50 % Triton solution is added. This reagent was stored in a dark bottle.

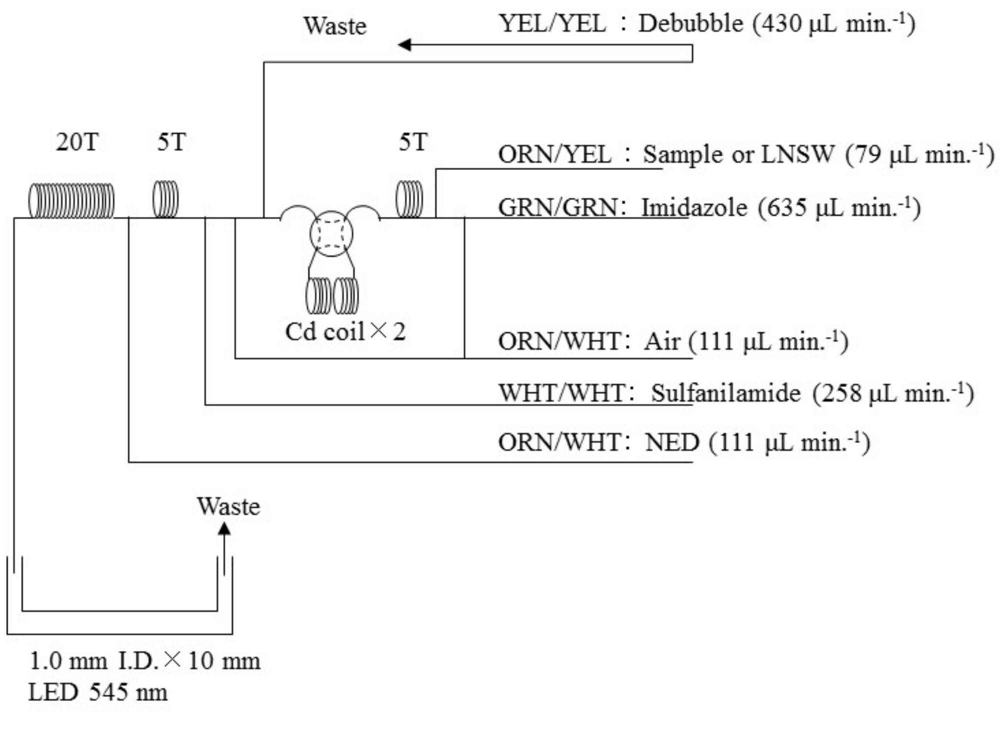

Figure 4.2-1: NO_3+NO_2 (1ch.) Flow diagram.

(4.3) Nitrite Reagents

50 % Triton solution

50 mL Triton™ X-100 provided by Sigma-Ardrich Japan G. K. (CAS No. 9002-93-1), were mixed with 50 mL Ethanol (99.5 %).

Sulfanilamide, 0.06 M (1 % w/v) in 1.2 M HCl

Dissolve 10 g 4-Aminobenzenesulfonamide (CAS No. 63-74-1), in 900 mL of Ultra-pure water, add 100 mL Hydrogen chloride (CAS No. 7647-01-0). After mixing, 2 mL 50 % Triton solution is added.

NED, 0.004 M (0.1 % w/v)

Dissolve 1 g N-(1-Naphthalenyl)-1,2-ethanediamine, dihydrochloride (CAS No. 1465-25-4), in 1000 mL of Ultra-pure water and add 10 mL Hydrogen chloride (CAS No. 7647-01-0). After mixing, 1 mL 50 % Triton solution is added. This reagent was stored in a dark bottle.

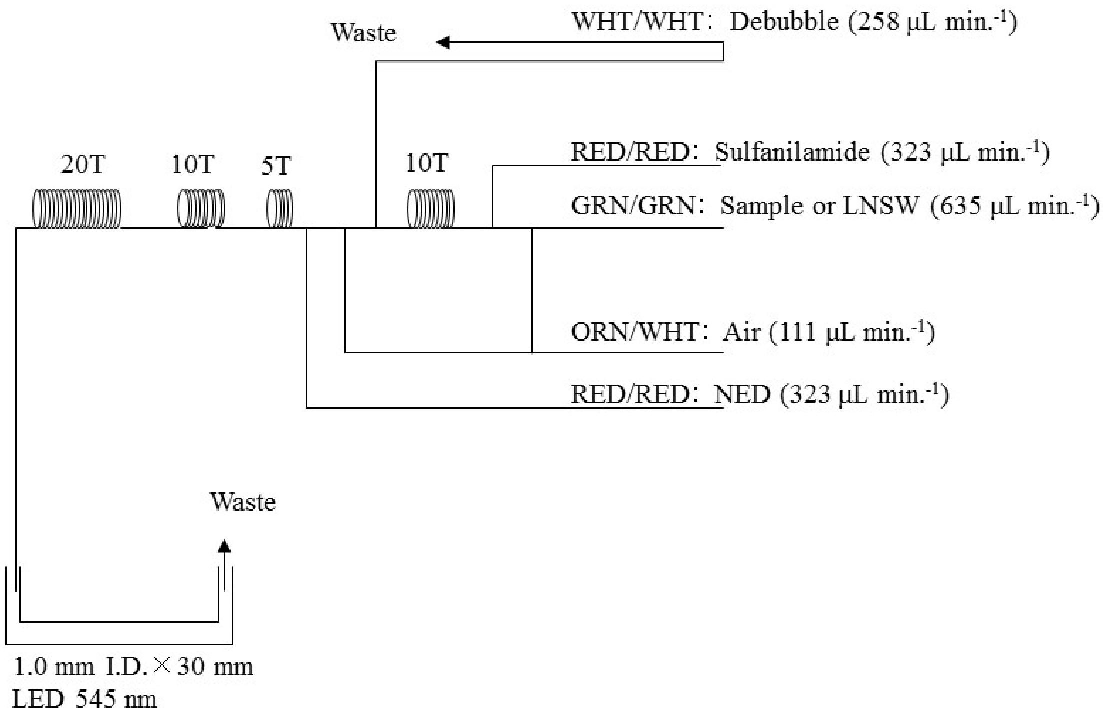

Figure 4.2-2: NO_2 (2ch.) Flow diagram.

(4.4) Silicate Reagents

15 % Sodium dodecyl sulfate solution

75 g Sodium dodecyl sulfate (CAS No. 151-21-3) were mixed with 425 mL Ultra-pure water.

Molybdic acid, 0.03 M (1 % w/v)

Dissolve 7.5 g Sodium molybdate dihydrate (CAS No. 10102-40-6), in 980 mL Ultra-pure water, add 12 mL 4.5M Sulfuric acid. After mixing, 20 mL 15 % Sodium dodecyl sulfate solution is added. Note: the amount of Sulfuric acid is reduced from previous report because we readjusted to Grasshoff et al. (1999).

Oxalic acid, 0.6 M (5 % w/v)

Dissolve 50 g Oxalic acid (CAS No. 144-62-7), in 950 mL of Ultra-pure water.

Ascorbic acid, 0.01 M (3 % w/v)

Dissolve 2.5 g L-Ascorbic acid (CAS No. 50-81-7), in 100 mL of Ultra-pure water. This reagent was freshly prepared at every day.

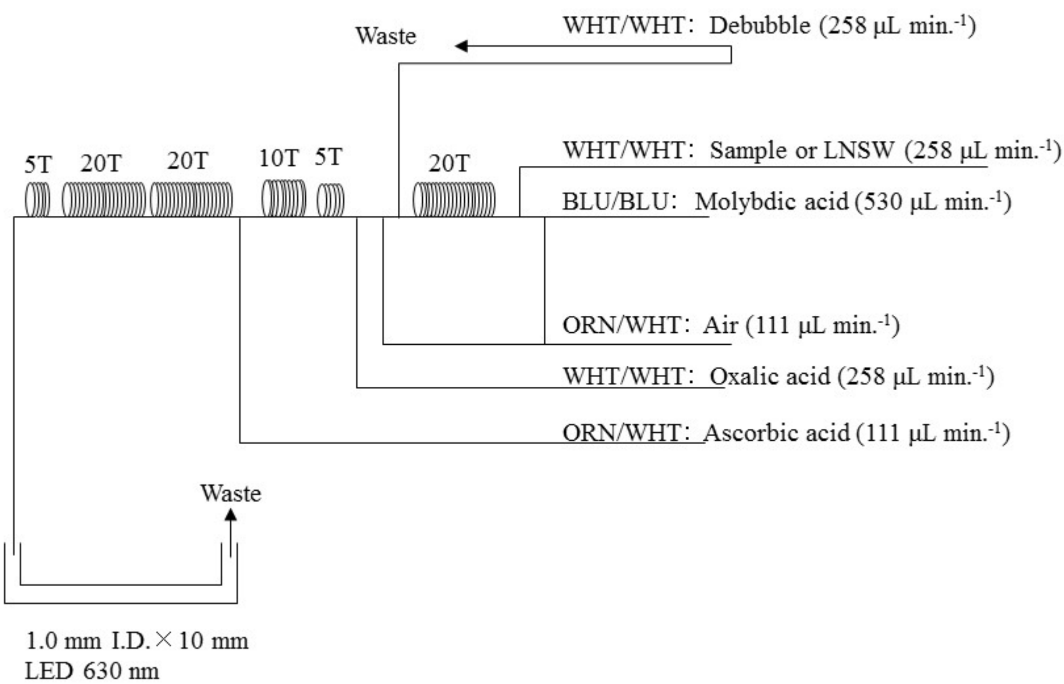

Figure 4.2-3: SiO_2 (3ch.) Flow diagram.

(4.5) Phosphate Reagents

15 % Sodium dodecyl sulfate solution

75 g Sodium dodecyl sulfate (CAS No. 151-21-3) were mixed with 425 mL Ultra-pure water.

Stock molybdate solution, 0.03 M (0.8 % w/v)

Dissolve 8 g Sodium molybdate dihydrate (CAS No. 10102-40-6), and 0.17 g Antimony potassium tartrate trihydrate (CAS No. 28300-74-5), in 950 mL of Ultra-pure water and added 50 mL Sulfuric acid (CAS No. 7664-93-9).

PO_4 color reagent

Dissolve 1.2 g L-Ascorbic acid (CAS No. 50-81-7), in 150 mL of stock molybdate solution. After mixing, 3 mL 15 % Sodium dodecyl sulfate solution is added. This reagent was freshly prepared before every measurement.

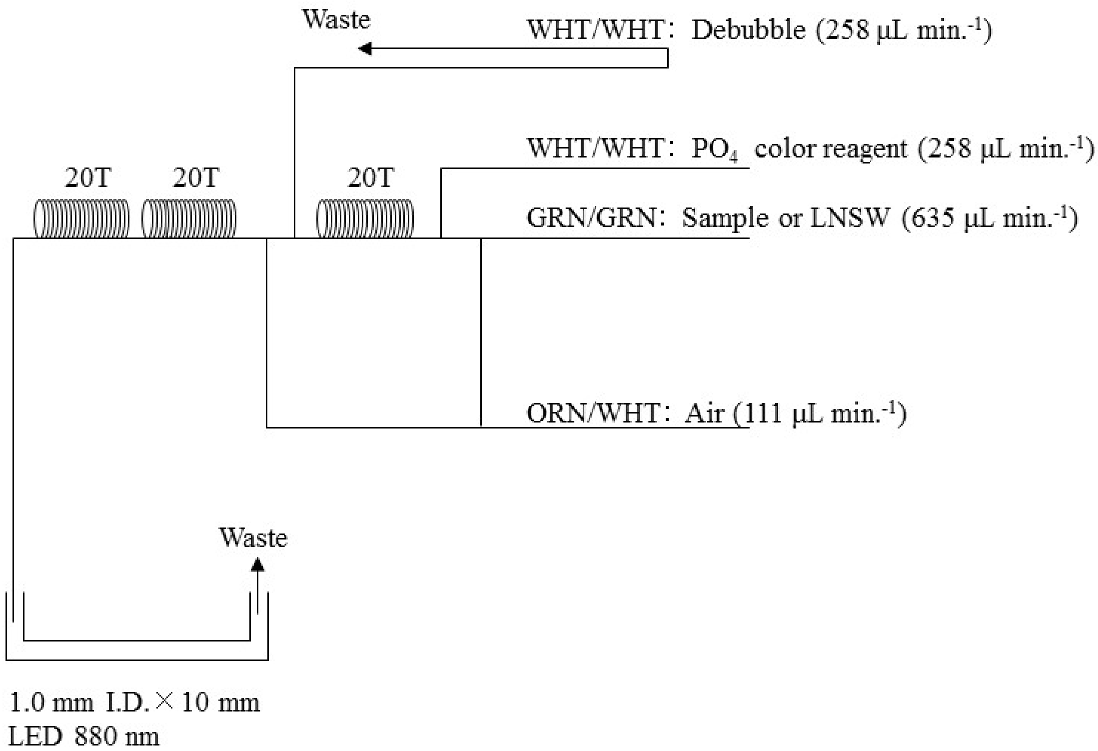

Figure 4.2-4: PO_4 (4ch.) Flow diagram.

(4.6) Ammonia Reagents

30 % Triton solution

30 mL Triton™ X-100 provided by Sigma-Ardrich Japan G. K. (CAS No. 9002-93-1), were mixed with 70 mL Ultra-pure water.

EDTA

Dissolve 41 g tetrasodium;2-[2-[bis(carboxylatomethyl)amino]ethyl-(carboxylateme-thyl)amino]acetate;tetrahydrate (CAS No. 13235-36-4), and 2 g Boric acid (CAS No. 10043-35-3), in 200 mL of Ultra-pure water. After mixing, 1 mL 30 % Triton solution is added. This reagent is prepared at a week about.

NaOH liquid

Dissolve 1.5 g Sodium hydroxide (CAS No. 1310-73-2), and 16 g tetrasodium;2-[2-[bis(carboxylatomethyl)amino]ethyl-(carboxylatomethyl)amino]acetate;tetrahydrate (CAS No. 13235-36-4) in 100 mL of Ultra-pure water. This reagent is prepared at a week about. Note: We reduced amount of Sodium hydroxide from 5 g to 1.5 g because pH of C standard solutions lowered 1 due to change of recipe of B standards solution.

Stock nitroprusside

Dissolve 0.25 g Sodium nitroferricyanide dihydrate (CAS No. 13755-38-9) in 100 mL of Ultra-pure water and add 0.2 mL 1M Sulfuric acid. Stored in a dark bottle and prepared at a month about.

Nitroprusside solution

Mix 4 mL stock nitroprusside and 5 mL 1M Sulfuric acid in 500 mL of Ultra-pure water. After mixing, 2 mL 30 % Triton solution is added. This reagent is stored in a dark bottle and prepared at every 2 or 3 days.

Alkaline phenol

Dissolve 10 g Phenol (CAS No. 108-95-2), 5 g Sodium hydroxide (CAS No. 1310-73-2) and 2 g Sodium citrate dihydrate (CAS No. 6132-04-3), in 200 mL Ultra-pure water. Stored in a dark bottle and prepared at a week about.

NaClO solution

Mix 5 mL Sodium hypochlorite (CAS No. 7681-52-9) in 45 mL Ultra-pure water. Stored in a dark bottle and fleshly prepared before every measurement. This reagent is prepared 0.3 % available chlorine.

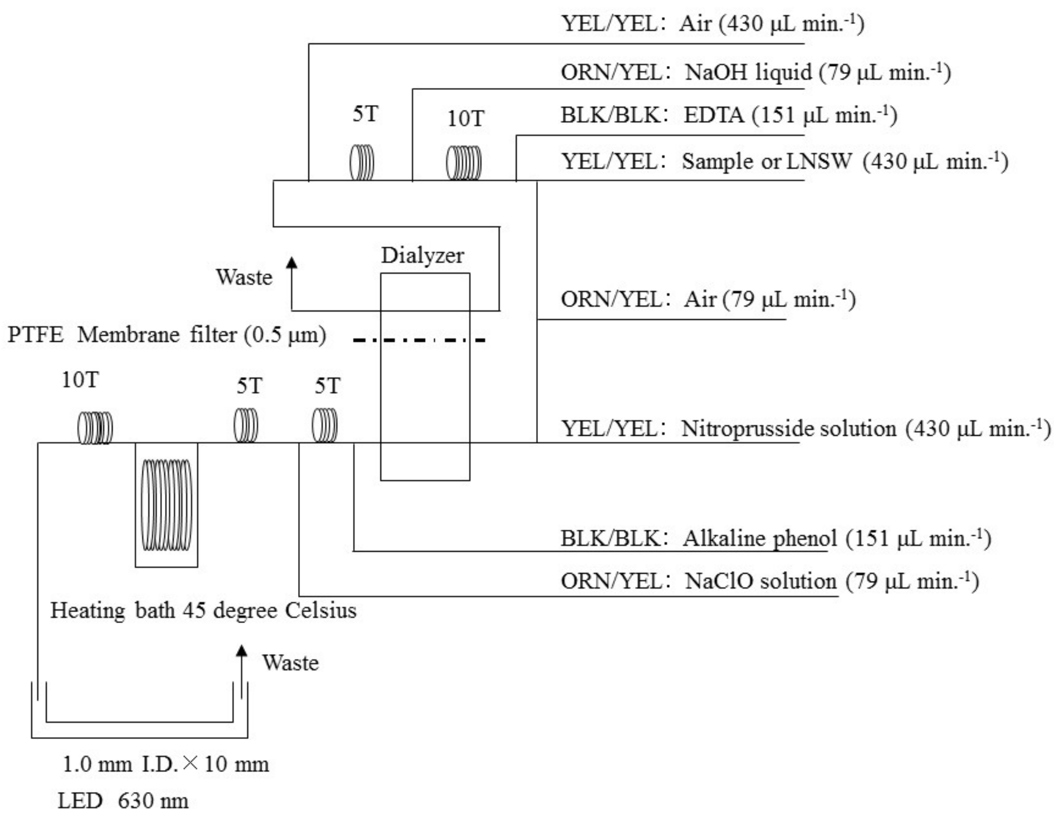

Figure 4.2-5: NH_4 (5ch.) Flow diagram.

(4.7) Sampling procedures

Sampling of nutrients followed that oxygen, salinity and trace gases. Samples were drawn into a virgin 10 mL polyacrylates vials without sample drawing tubes. These were rinsed three times before filling and vials were capped immediately after the drawing. The vials are put into water bath adjusted to ambient temperature, 21.1 ± 1.0 degree Celsius, in about 30 minutes before use to stabilize the temperature of samples. When we found the value of Xmiss of the sample was less than 95 % or doubtful for the particles in the sample, we carried out centrifuging for the samples by using the centrifuge (type: CN-820, Hsiang Tai). The conditions of centrifuging were set about 3400 rpm for 2.5 minute. We also put coolant in the centrifuge to suppress temperature increase of samples during centrifugation.

No transfer was made and the vials were set an auto sampler tray directly. Samples were analyzed after collection within 24 hours.

(4.8) Data processing

Raw data from QuAAtro 2-HR were treated as follows:

- Check baseline shift.
- Check the shape of each peak and positions of peak values taken, and then change the positions of peak values taken if necessary.
- Carry-over correction and baseline drift correction were applied to peak heights of each samples followed by sensitivity correction.
- Baseline correction and sensitivity correction were done basically using liner regression.
- Load pressure and salinity from uncalibrate CTD data to calculate density of seawater tentatively. To calculate the final nutrients concentration we used salinity obtained from bottle samples for 62 samples and salinity from uncalibrate CTD data for 896 samples.
- Calibration curves to get nutrients concentration were assumed second order equations.

(4.9) Summary of nutrients analysis

We made 34 QuAAtro runs for the water columns sample collected by 62 casts at 41 stations as shown in Table 4.2-1 during MR19-03C. The total amount of layers of the seawater sample reached to 958. We also measured 5 samples from test cast conducted before start of observation. We made basically duplicate measurement. The station locations for nutrients measurement is shown in Figure 4.2-6.

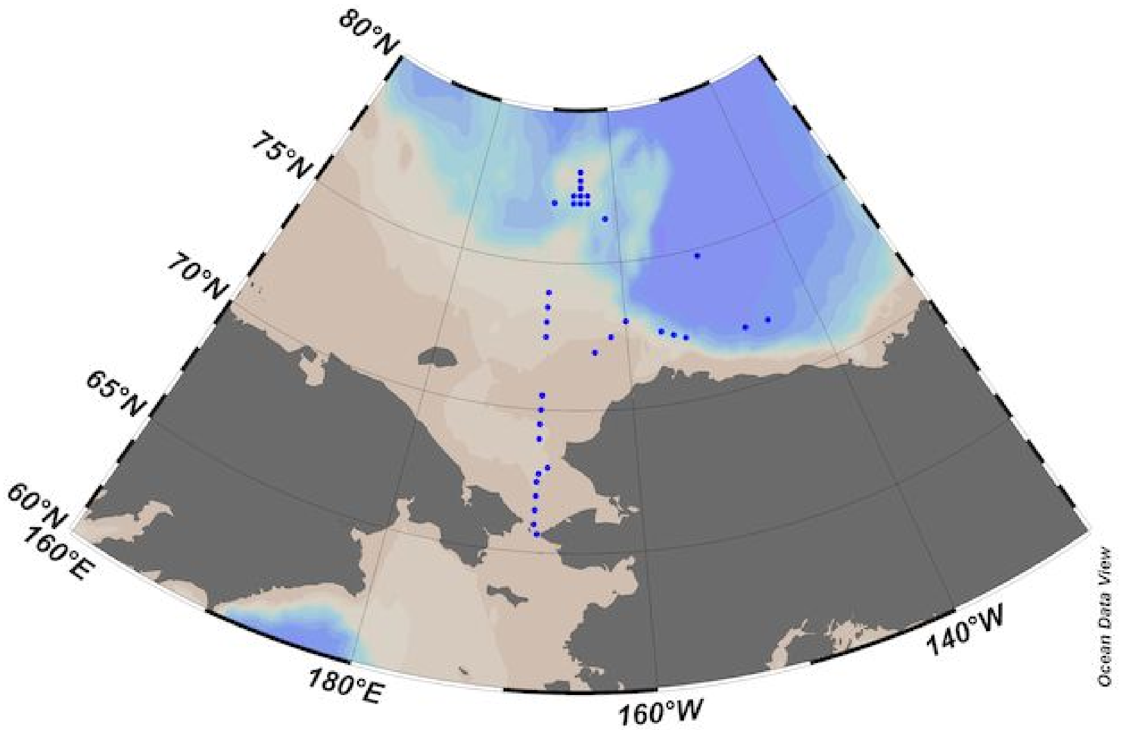

Figure 4.2-6: Sampling positions of nutrients sample.

(5) Station list

The sampling station list for nutrients is shown in Table 4.2-1.

Table 4.2-1: List of stations

Station	Cast	Date (UTC) (mmddyy)	Position* Latitude	Longitude	Depth (m)
001	1	100819	65-39.18N	169-32.23W	53
002	1	100819	66-00.17N	169-15.28W	53
003	1	100819	66-30.32N	169-14.90W	54
004	1	100819	67-00.13N	169-15.74W	45
005	1	100919	69-00.19N	169-14.82W	53
006	1	100919	69-30.16N	169-14.79W	51
007	1	100919	69-59.96N	169-14.97W	41
008	1	100919	70-29.86N	169-14.62W	39
009	1	101019	71-59.77N	164-30.01W	38
010	1	101019	72-29.84N	162-15.22W	44
011	1	101019	72-59.99N	161-59.80W	192
012	1	101119	72-30.13N	157-43.31W	1607
013	1	101119	72-19.98N	156-59.48W	1957
014	1	101119	72-09.43N	154-12.59W	1637
015	1	101219	71-59.99N	148-30.02W	3515
016	1	101219	72-00.01N	146-59.95W	3316
017	1	101419	74-46.10N	151-29.87W	3834
018	1	101519	76-27.95N	162-21.49W	1750
019	1	101619	76-59.96N	165-00.06W	680
020	1	101619	77-15.04N	165-00.29W	367
020	2	101719	77-14.99N	165-00.07W	370
021	1	101719	77-30.01N	166-59.99W	308
022	1	101719	77-45.00N	166-59.99W	445
020	3	101819	77-15.01N	165-00.01W	372
021	2	101819	77-30.07N	166-59.81W	310
022	2	101819	77-45.05N	166-59.81W	446
023	1	101819	78-02.13N	165-01.52W	453
019	2	101919	77-00.01N	165-00.04W	685
020	4	101919	77-15.14N	165-00.11W	366
021	3	101919	77-30.06N	165-00.07W	309
019	3	102019	77-00.06N	165-00.06W	690
020	5	102019	77-15.14N	165-00.35W	367

021	4	102019	77-30.05N	165-00.01W	310
024	1	102119	77-15.00N	166-00.04W	851
019	4	102119	77-00.28N	165-00.25W	687
020	6	102119	77-15.01N	166-59.95W	370
021	5	102119	77-30.50N	165-00.34W	308
025	1	102219	77-00.37N	166-00.12W	711
019	5	102219	77-00.10N	165-00.43W	685
020	7	102219	77-15.01N	166-59.94W	371
026	1	102319	77-00.01N	165-59.99W	437
019	6	102319	77-00.07N	165-00.68W	678
020	8	102319	77-15.17N	165-00.07W	365
021	7	102319	77-30.31N	165-01.21W	304
027	1	102419	77-15.00N	165-59.99W	366
019	7	102419	77-00.23N	166-59.84W	697
020	9	102419	77-15.04N	166-59.86W	366
021	8	102419	77-30.74N	166-59.79W	311
028	1	102519	77-00.22N	169-13.87W	1896
029	1	102619	74-00.01N	169-15.17W	185
030	1	102619	73-30.00N	169-15.00W	115
031	1	102619	73-00.03N	169-14.96W	61
032	1	102619	72-30.03N	169-15.39W	59
033	1	102719	70-30.01N	169-15.08W	38
034	1	102719	70-00.01N	169-14.96W	41
035	1	102719	69-30.19N	169-14.77W	51
036	1	102719	68-59.99N	169-14.71W	53
037	1	102819	68-00.88N	168-07.96W	53
038	1	102819	67-46.99N	169-23.71W	51
039	1	102819	67-30.07N	169-14.89W	49
040	1	102819	67-00.06N	169-15.29W	45
041	1	102819	66-29.99N	169-14.98W	54

*: Position indicates latitude and longitude where CTD reached maximum depth at the cast.

(6) Certified Reference Material of nutrients in seawater

KANSO CRMs (Lot: CE, CJ, CG) were used to ensure the comparability and traceability of nutrient measurements during this cruise. The details of CRMs are shown below.

<u>Production</u>

KANSO CRMs are certified reference material (CRM) for inorganic nutrients in seawater. These were produced by KANSO Co.,Ltd. This certified reference material has been produced using autoclaved natural seawater on the basis of quality control system under ISO Guide 34 (JIS Q 0034).

KANSO Co.,Ltd. has been accredited under the Accreditation System of National Institute of Technology and Evaluation (ASNITE) as a CRM producer since 2011. (Accreditation No.: ASNITE 0052 R)

Property value assignment

The certified values are arithmetic means of the results of 30 bottles from each batch (measured in duplicates) analysed by KANSO Co.,Ltd. and Japan Agency for Marine-Earth Science and Technology (JAMSTEC) using the colorimetric method (continuous flow analysis, CFA, method). The salinity of calibration solutions were adjusted to the salinity of this CRM ± 0.5.

Metrological Traceability

Each certified value of nitrate, nitrite, and phosphate of KANSO CRMs were calibrated versus one of Japan Calibration Service System (JCSS) standard solutions for each nitrate ions, nitrite ions, and phosphate ions. JCSS standard solutions are calibrated versus the secondary solution of JCSS for each of these ions. The secondary solution of JCSS is calibrated versus the specified primary solution produced by Chemicals Evaluation and Research Institute (CERI), Japan. CERI specified primary solutionsare calibrated versus the National Metrology Institute of Japan (NMIJ) primary standards solution of nitrate ions, nitrite ions and phosphate ions, respectively.

For a certified value of silicate of KANSO CRM was determined by one of Merck KGaA silicon standard solution 1000 mg L^{-1} Si traceable to National Institute of Standards and Technology (NIST) SRM of silicon standard solution (SRM 3150).

The certified values of nitrate, nitrite, and phosphate of KASNO CRM are thus traceable to the International System of Units (SI) through an unbroken chain of calibrations, JCSS, CERI and NMIJ solutions as stated above, each having stated uncertainties. The certified values of silicate of KANSO CRM are traceable to the International System of Units (SI) through an unbroken chain of calibrations, Merck KGaA and NIST SRM 3150 solutions, each having stated uncertainties.

As stated in the certificate of NMIJ CRMs each certified value of dissolved silica, nitrate ions, and nitrite ions was determined by more than one method using one of NIST (National Institute of Standards and Technology) SRM of silicon standard solution and NMIJ primary standards solution of nitrate ions and nitrite ions. The concentration of phosphate ions as stated information value in the certificate was determined NMIJ primary standards solution of phosphate ions. Those values in the certificate of NMIJ CRMs are traceable to the International System of Units (SI).

One of analytical methods used for certification of NMIJ CRM for nitrate ions, nitrite ions, phosphate ions and dissolved silica was colorimetric method (continuous mode and batch one). The colorimetric method is same as the analytical method (continuous mode only) used for certification of KANSO CRM. For certification of dissolved silica, exclusion chromatography/isotope dilution-inductively coupled plasma mass spectrometry and Ion exclusion chromatography with post-column detection were used. For certification of nitrate ions, Ion chromatography by direct analysis and Ion chromatography after halogen-ion separation were used. For certification of nitrite ions, Ion chromatography by direct analysis was used.

NMIJ CRMs were analysed at the time of certification process for CRM and the results were confirmed within expanded uncertainty stated in the certificate of NMIJ CRMs.

(6.1) CRM for this cruise

CRM lots CE, CJ and CG, which almost cover range of nutrients concentrations in the Arctic Ocean are prepared 21 sets.

These CRM assignments were completely done based on random number. The CRM bottles were stored at a room in the ship, BIOCHEMICAL LABORATORY, where the temperature was maintained around 17.8 degree Celsius - 22.6 degree Celsius.

(6.2) CRM concentration

We used nutrients concentrations for CRM lots CE CJ and CG as shown in - 4.2-2.

Table 4.2-2 Certified concentration and uncertainty (k=2) of CRMs.

unit: $\mu mol\ kg^{-1}$

Lot	Nitrate	Nitrite	Silicate	Phosphate	Ammonia*
CE	0.01 ± 0.03	0.02 ± 0.01	0.06 ± 0.09	0.012 ± 0.006	0.69
CJ	16.20 ± 0.20	0.03 ± 0.01	38.50 ± 0.40	1.190 ± 0.020	0.77
CG	23.70 ± 0.20	0.06 ± 0.03	56.40 ± 0.50	1.700 ± 0.020	0.61

*For ammonia values are references

Note for Nitrite concentration: We observed systematic increase of nitrite concentration in the CRMs at a rate about 0.02 $\mu mol\ kg^{-1}\ year^{-1}$. Therefore, as shown in Figure 4.2-13, the observed concentration of nitrite for CRM lot CG were high compared with certified concentration.

(7) Nutrients standards

(7.1) Volumetric laboratory ware of in-house standards

All volumetric glass ware and polymethylpentene (PMP) ware used were gravimetrically calibrated. Plastic volumetric flasks were gravimetrically calibrated at the temperature of use within 4 K.

(7.1.1) Volumetric flasks

Volumetric flasks of Class quality (Class A) are used because their nominal tolerances are 0.05 % or less over the size ranges likely to be used in this work. Class A flasks are made of borosilicate glass, and the standard solutions were transferred to plastic bottles as quickly as possible after they are made up to volume and well mixed in order to prevent excessive dissolution of silicate from the glass. PMP volumetric flasks were gravimetrically calibrated and used only within 4 K of the calibration temperature.

The computation of volume contained by glass flasks at various temperatures other than the calibration temperatures were done by using the coefficient of linear expansion of borosilicate crown glass.

Because of their larger temperature coefficients of cubical expansion and lack of tables constructed for these materials, the plastic volumetric flasks were gravimetrically calibrated over the temperature range of intended use and used at the temperature of calibration within 4 K. The weights obtained in the calibration weightings were corrected for the density of water and air buoyancy.

(7.1.2) Pipettes

All pipettes have nominal calibration tolerances of 0.1 % or better. These were gravimetrically calibrated in order to verify and improve upon this nominal tolerance.

(7.2) Reagents, general considerations

(7.2.1) Specifications

For nitrate standard, “potassium nitrate 99.995 suprapur®” provided by Merck, Batch B1452165, CAS No. 7757-79-1, was used.

For nitrite standard solution, we used “nitrite ion standard solution (NO_2^- 1000) provided by Wako, Lot APJ6212, Code. No. 140-06451.” This standard solution was certified by Wako using Ion chromatograph method. Calibration result is 1003 mg L^{-1} at 20 degree Celsius. Expanded uncertainty of calibration (k=2) is 0.8 % for the calibration result.

For the silicate standard, we changed from “Silicon standard solution SiO_2 in NaOH 0.5 M CertiPUR®” provided by Merck, to JAMSTEC-KANSO in-house Si standard solution exp64 which was produced by alkali fusion technique from 5N SiO_2 powder. The mass fraction of Si in exp64 solution was calibrated based on NMIJ CRM 3645-a02 Si standard solution.

For phosphate standard, “potassium dihydrogen phosphate anhydrous 99.995 suprapur®” provided by Merck, Batch B1642608, CAS No.: 7778-77-0, was used.

For ammonia standard, “Ammonium Chloride” provided by NMIJ, CAS No. 12125-02-9. We used NMIJ CRM 3011-a. The purity of this standard was greater than 99.9 %. Expanded uncertainty of calibration (k=2) is 0.053 %.

(7.2.2) Ultra-pure water

Ultra-pure water (Milli-Q water) freshly drawn was used for preparation of reagent, standard solutions and for measurement of reagent and system blanks.

(7.2.3) Low nutrients seawater (LNSW)

Surface water having low nutrient concentration was taken and filtered using 0.20 μm pore capsule cartridge filter at MR18-04 cruise on August, 2018. This water is stored in 20 L cubitainer with cardboard box.

LNSW concentrations were assigned to February, 2019.

(7.2.4) Concentrations of nutrients for A, D, B and C standards

Concentrations of nutrients for A, D, B and C standards are set as shown in Table 4.2-3.

We changed from Merck silicon standards solution to JAMSTEC-KANSO in-house Si standard solution for A standard of silicate. We also developed new receipt to prepare B standard without adding hydrochloric acid which was added to neutralize alkali Merck silicon standard solution previously. Pure water was used to prepare B standard and to adjust salinity and density, we add sodium chloride powder as appropriately.

The C standard is prepared according recipes as shown in Table 4.2-4. All volumetric laboratory tools were calibrated prior the cruise as stated in chapter (6.1) Then the actual concentration of nutrients in each fresh standard was calculated based on the ambient, solution temperature and determined factors of volumetric laboratory wares.

The calibration curves for each run were obtained using 4 levels, C-1, C-2, C-3 and C-4.

Table 4.2-3: Nominal concentrations of nutrients for A, D, B and C standards.

Unit: µmol kg^{-1}

	A	D	B	C-1	C-2	C-3	C-4
NO_3	22500	900	675	LNSW	13	27	40
NO_2	21800	870	26	LNSW	0.5	1.0	1.6
SiO_2	35600		1430	LNSW	29	58	86
PO_4	6000		60	LNSW	1.2	2.4	3.6
NH_4	4000		160	LNSW	3.2	6.4	9.6

Table 4.2-4: Working calibration standard recipes.

C Std.	B Std.
C-2	10 mL
C-3	20 mL
C-4	30 mL

(7.2.5) Renewal of in-house standard solutions

In-house standard solutions as stated in paragraph (6.2) were renewed as shown in Table 4.2-5(a) to (c).

Table 4.2-5(a): Timing of renewal of in-house standards.

NO_3, NO_2, SiO_2, PO_4, NH_4	Renewal
A-1 Std. (NO_3)	maximum a month
A-2 Std. (NO_2)	commercial prepared solution
A-3 Std. (SiO_2)	JAMSTEC-KANSO in-house Si standard solution
A-4 Std. (PO_4)	maximum a month
A-5 Std. (NH_4)	maximum a month
D-1 Std.	maximum 8 days
D-2 Std.	maximum 8 days
B Std. (mixture of A-1, D-2, A-3, A-4 and A-5 std.)	maximum 8 days

Table 4.2-5(b): Timing of renewal of working calibration standards.

Working standards	Renewal
C Std. (dilute B Std.)	every 24 hours

Table 4.2-5(c): Timing of renewal of in-house standards for reduction estimation.

Reduction estimation	Renewal
36 µM NO_3 (dilute D-1 Std.)	when C Std. renewed
35 µM NO_2 (dilute D-2 Std.)	when C Std. renewed

(8) Quality control

(8.1) Precision of nutrients analyses during the cruise

Precision of nutrients analyses during this cruise was evaluated based on the 6 to 10 measurements, which are measured every 7 to 14 samples, during a run at the concentration of C-4 std. Summary of precisions are shown as shown in Table 4.2-6 and Figures 4.2-7 to 4.2-11. The precisions for each parameter are generally good considering the analytical precisions during the R/V Mirai cruses conducted in 2009 - 2018. During in this cruise, analytical precisions were 0.15 % for nitrate, 0.17 % for nitrite, 0.12 % for silicate, 0.11 % for phosphate and 0.26 % for ammonia in terms of median of precision, respectively. Then we can conclude that the analytical precisions for nitrate, nitrite, silicate, phosphate and ammonia were maintained throughout this cruise.

Table 4.2-6: Summary of precision based on the replicate analyses.

	Nitrate CV %	Nitrite CV %	Silicate CV %	Phosphate CV %	Ammonia CV %
Median	0.15	0.17	0.12	0.11	0.26
Mean	0.14	0.17	0.11	0.11	0.27
Maximum	0.20	0.41	0.18	0.18	0.54
Minimum	0.06	0.05	0.05	0.05	0.07
N	34	34	34	34	34

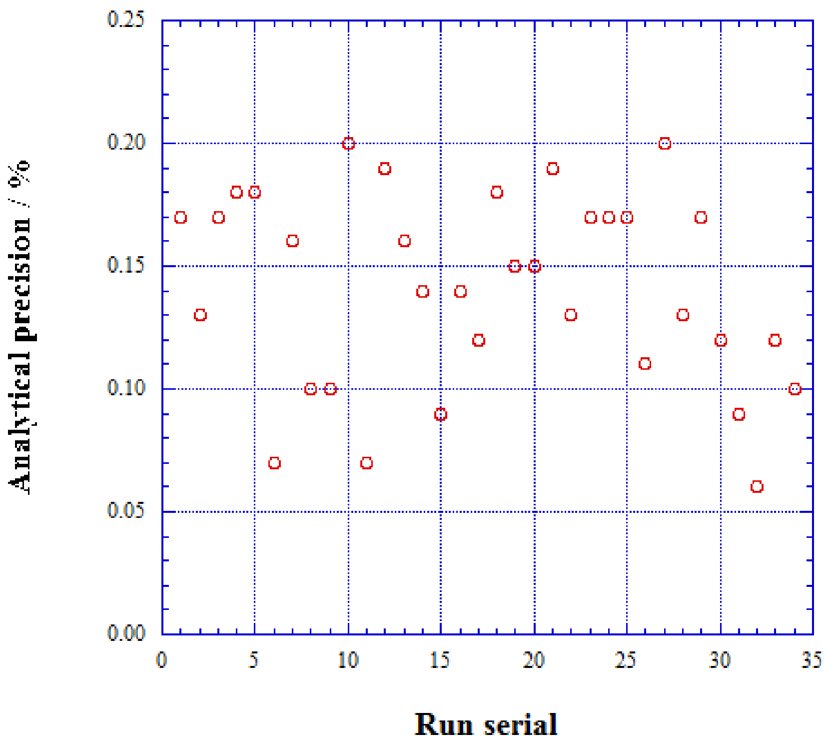

Figure 4.2-7: Time series of precision of nitrate in MR19-03C

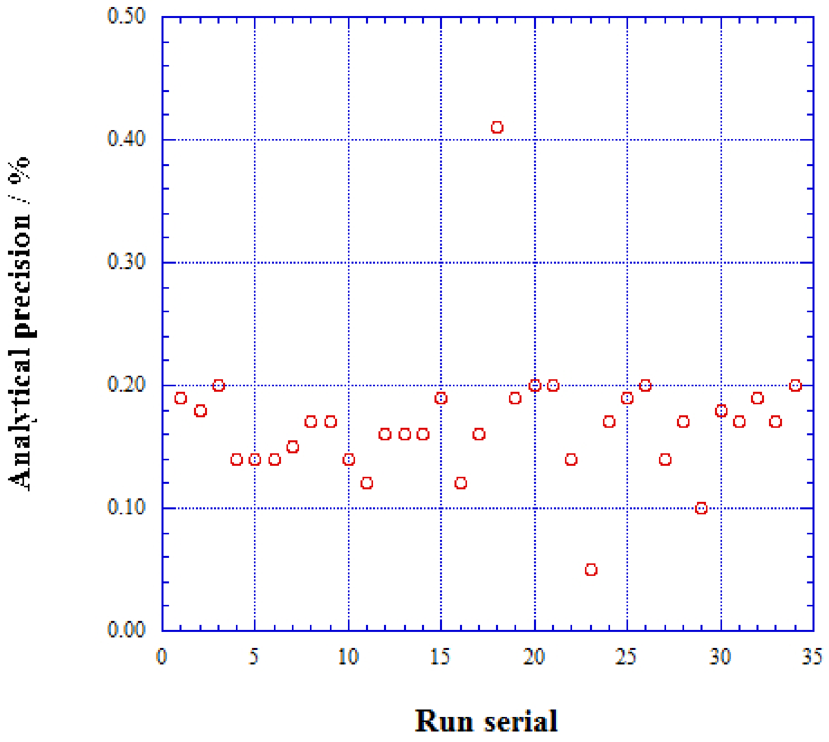

Figure 4.2-8: Time series of precision of nitrite in MR19-03C.

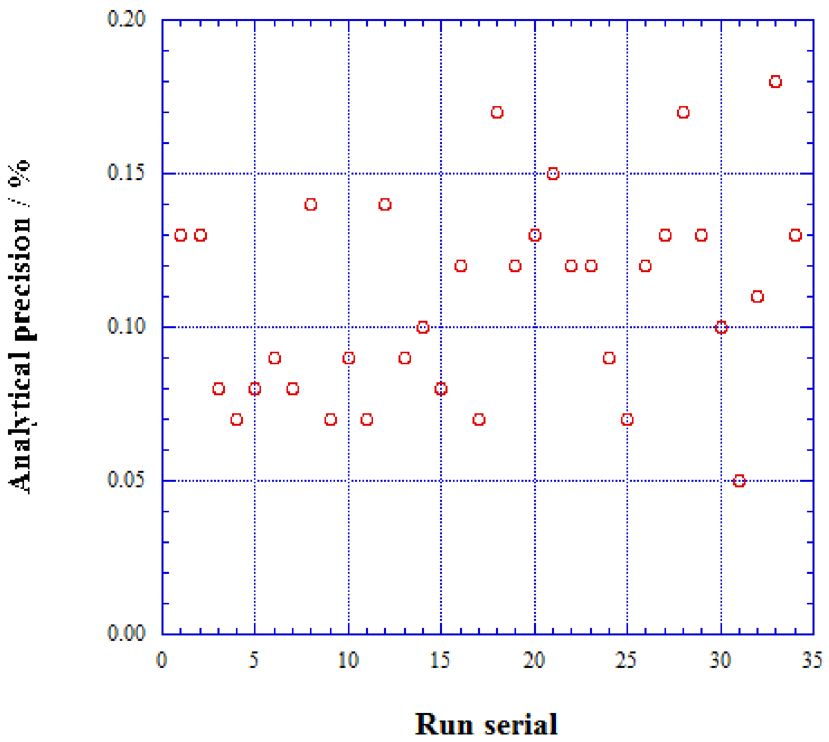

Figure 4.2-9: Time series of precision of silicate in MR19-03C.

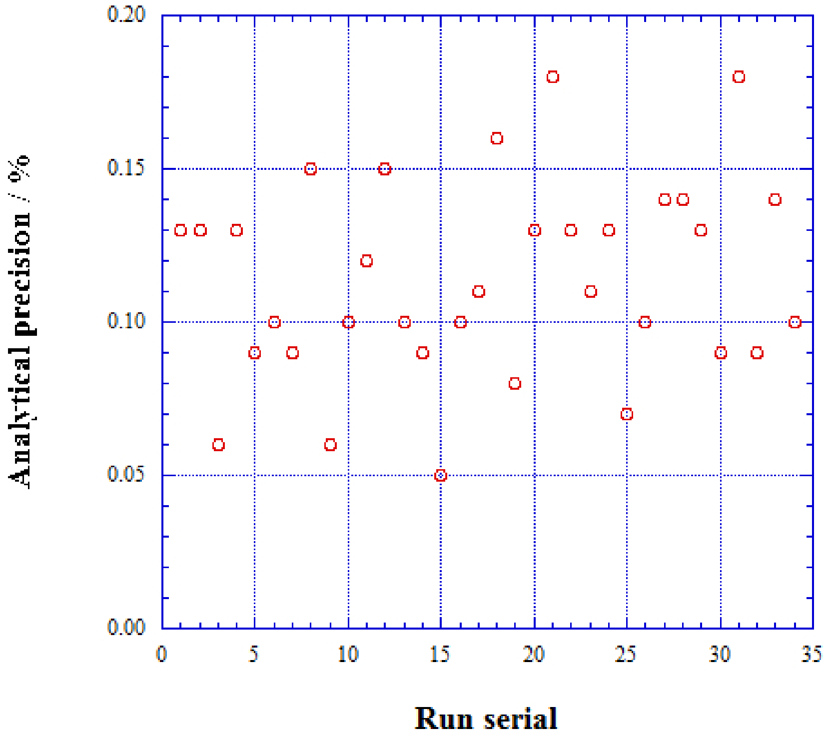

Figure 4.2-10: Time series of precision of phosphate in MR19-03C.

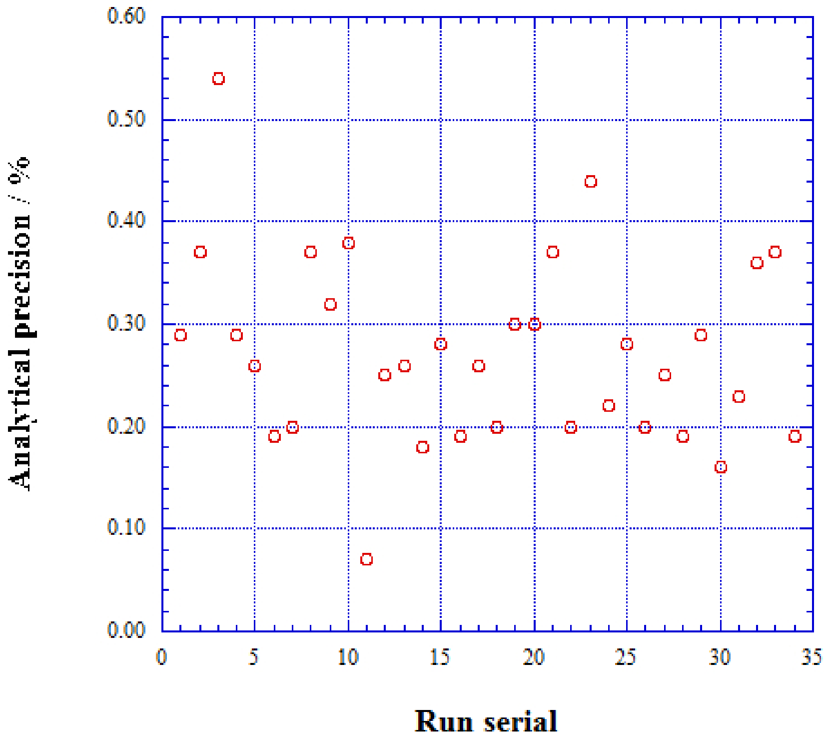

Figure 4.2-11: Time series of precision of ammonia in MR19-03C.

(8.2) CRM lot. CG measurement during this cruise

CRM lot. CG was measured every run to keep the comparability. The results of lot. CG during this cruise are shown as Figures 4.2-12 to 4.2-16.

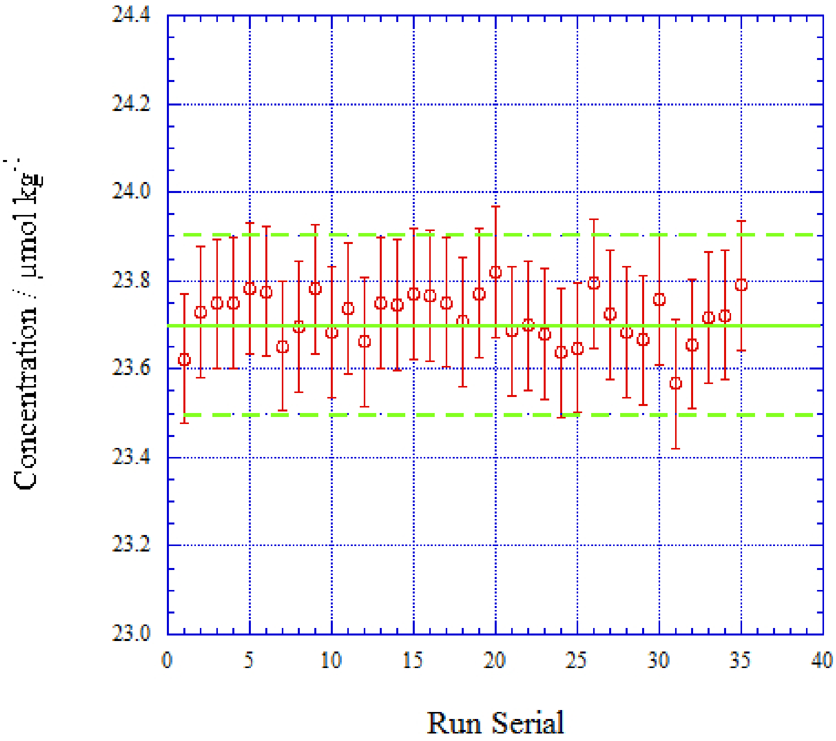

Figure 4.2-12: Time series of CRM-CG of nitrate in MR19-03C. Green line is certified nitrate concentration of CRM.

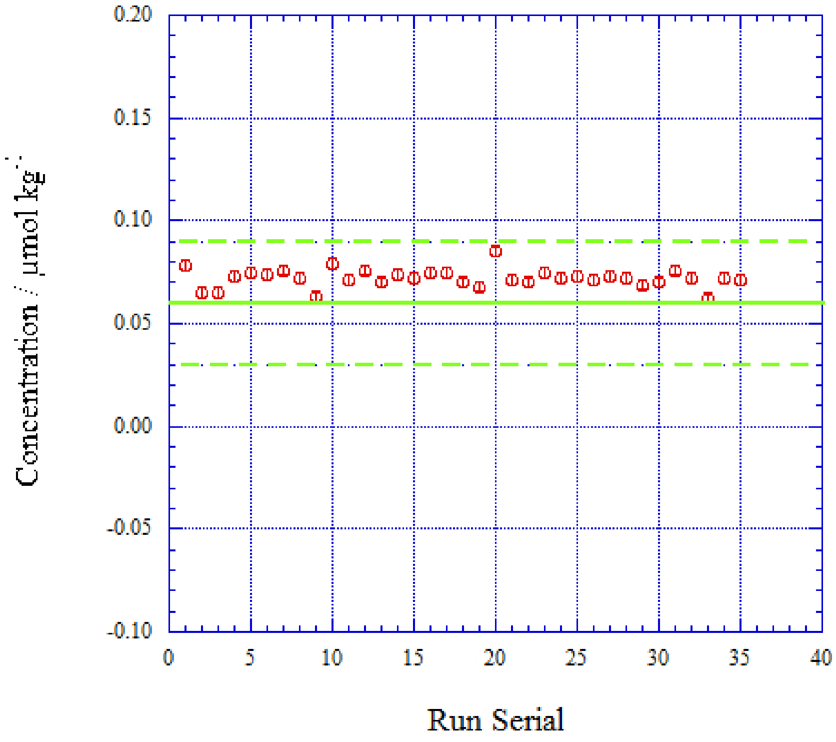

Figure 4.2-13: Time series of CRM-CG of nitrite in MR19-03C. Green line is certified nitrite concentration of CRM.

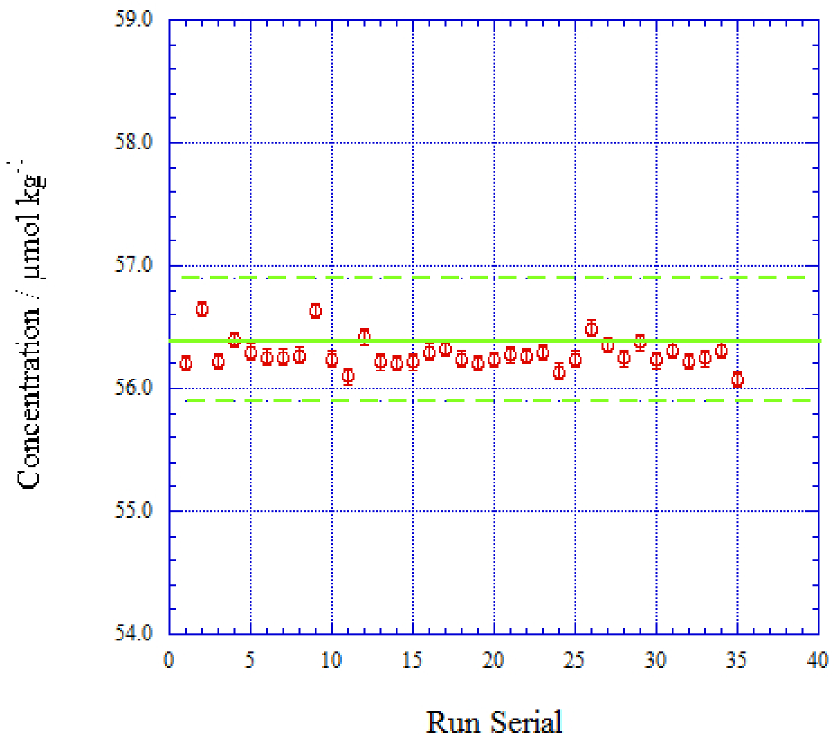

Figure 4.2-14: Time series of CRM-CG of silicate in MR19-03C. Green line is certified silicate concentration of

CRM.

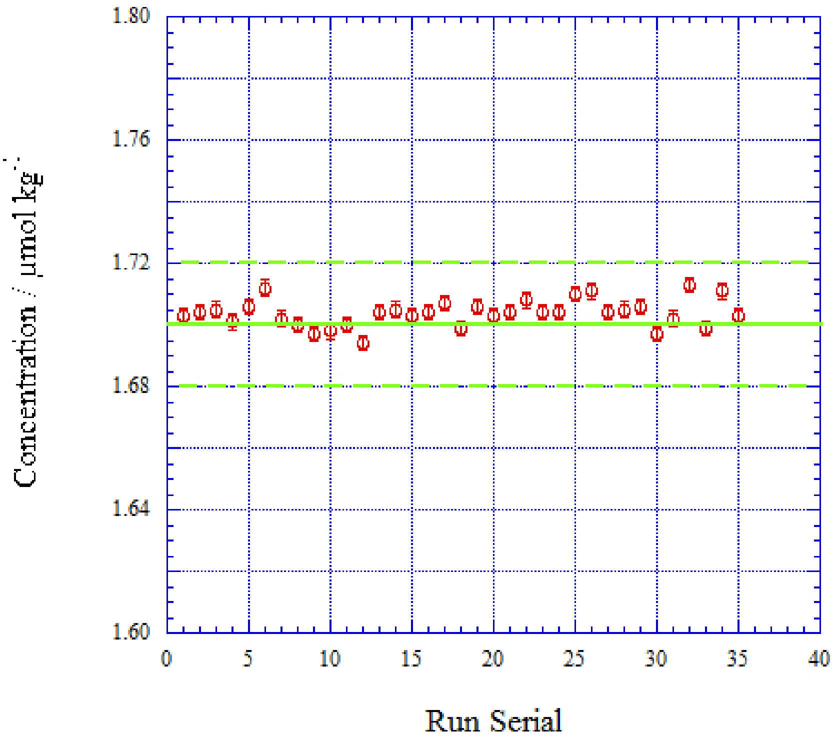

Figure 4.2-15: Time series of CRM-CG of phosphate in MR19-03C. Green line is certified phosphate concentration of CRM.

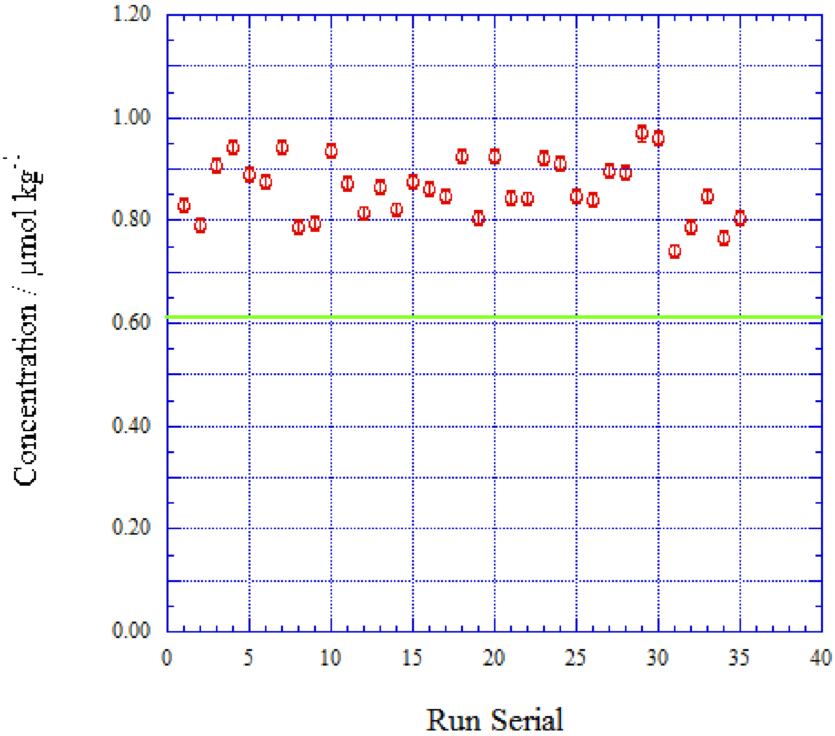

Figure 4.2-16: Time series of CRM-CG of ammonia in MR19-03C. Green line is reference value for ammonia concentration of CRM.

(8.3) Carry over

We can also summarize the magnitudes of carry over throughout the cruise. These are small enough within acceptable levels as shown in Table 4.2-7 and Figure 4.2-17 to 4.2-21.

Table 4.2-7: Summary of carry over throughout MR19-03C.

	Nitrate %	Nitrite %	Silicate %	Phosphate %	Ammonia %
Median	0.18	0.04	0.09	0.10	0.37
Mean	0.18	0.05	0.10	0.10	0.38
Maximum	0.34	0.28	0.19	0.22	0.71
Minimum	0.04	0.00	0.03	0.00	0.21
N	34	34	34	34	34

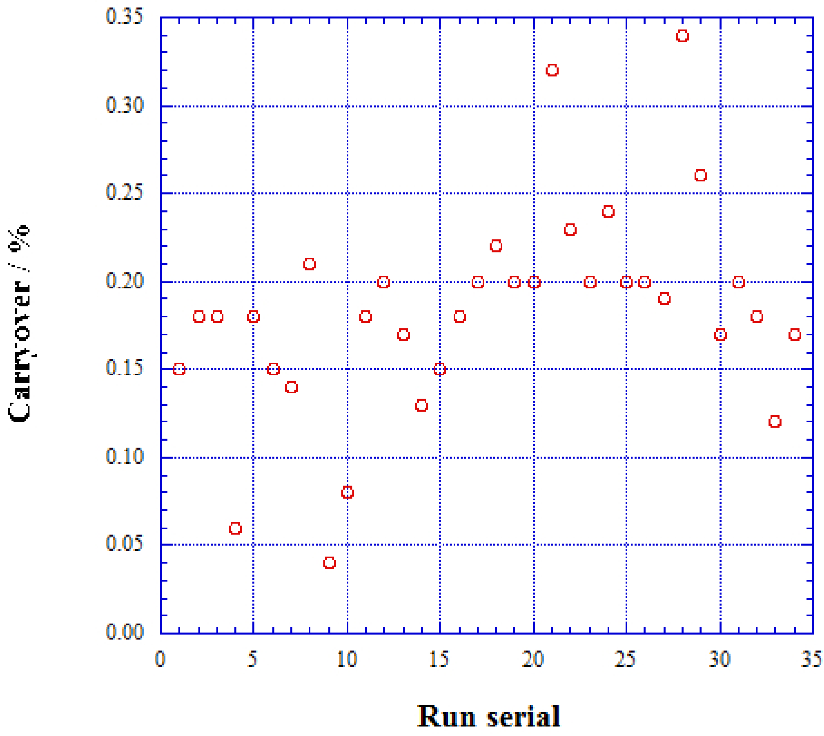

Figure 4.2-17: Time series of carry over of nitrate in MR19-03C.

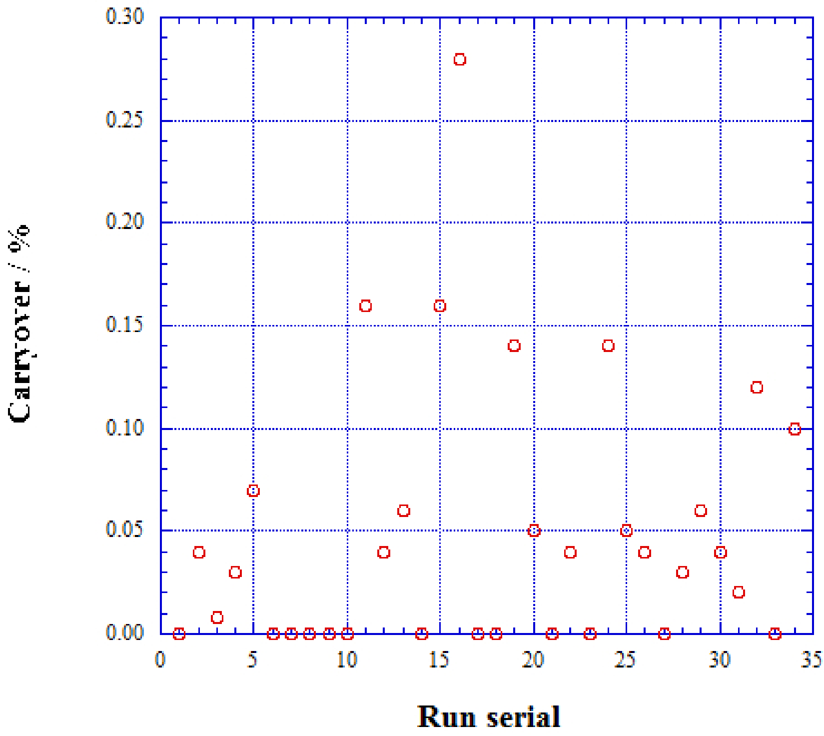

Figure 4.2-18: Time series of carry over of nitrite in MR19-03C.

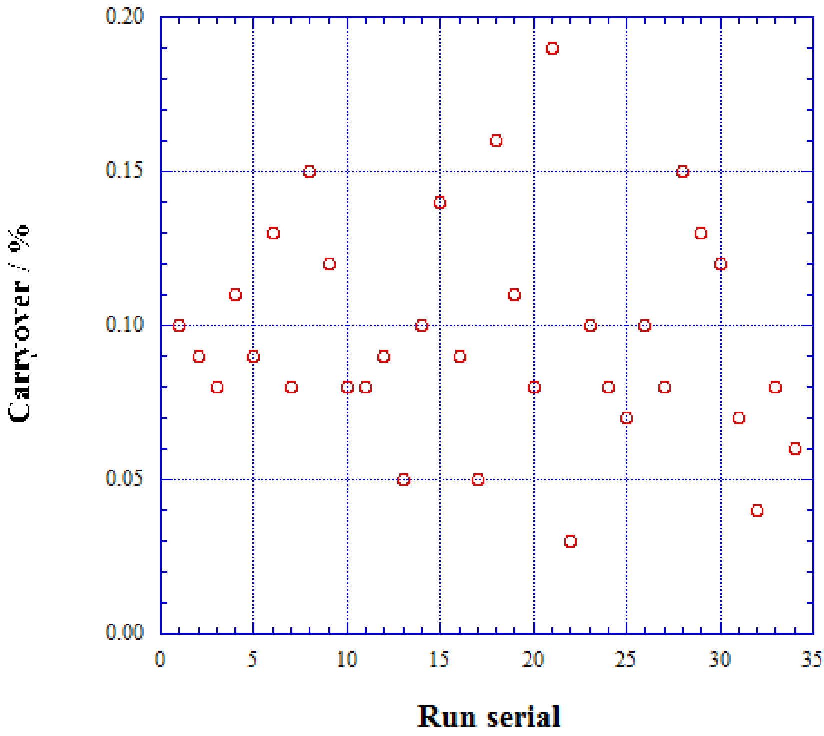

Figure 4.2-19: Time series of carry over of silicate in MR19-03C.

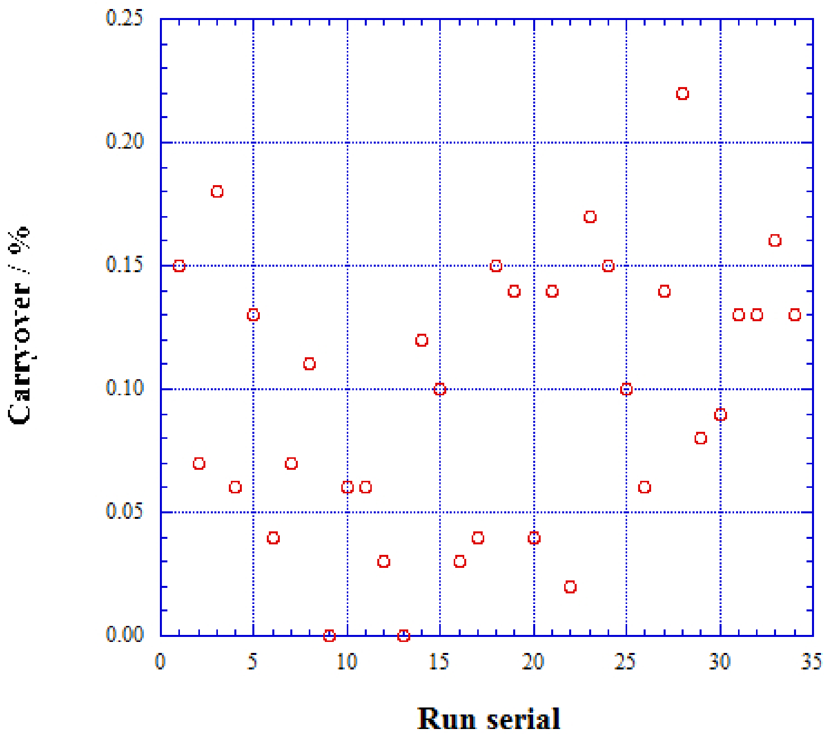

Figure 4.2-20: Time series of carry over of phosphate in MR19-03C.

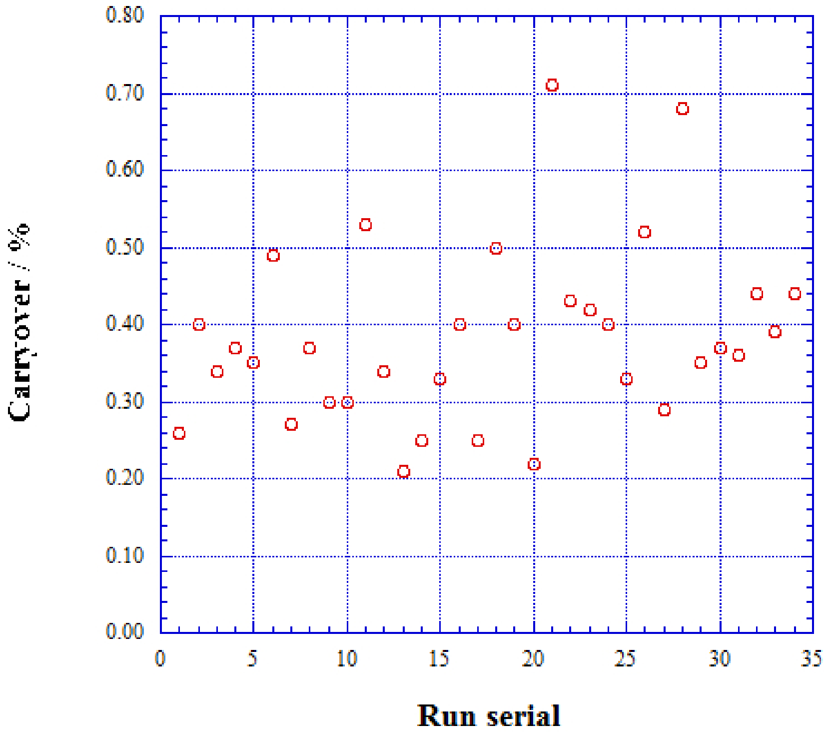

Figure 4.2-21: Time series of carry over of ammonia in MR19-03C.

(8.4) Estimation of uncertainty of nitrate, silicate, phosphate, nitrite and ammonia concentrations

Empirical equations, eq. (1), (2), (3), (4) and (5) to estimate uncertainty of measurement of nitrate, nitrite, silicate, phosphate and ammonia are estimated based on differences of 958 pairs of duplicate measurement and drift samples during each run. These empirical equations are as follows, respectively.

Nitrate Concentration C_{NO3} in μmol kg^{-1}:
Uncertainty of measurement of nitrate (%) =
$0.51165 + 2.5869 * (1 / C_{NO3})$ --- (1)
where C_{NO3} is nitrate concentration of sample.

Nitrate Concentration C_{NO2} in μmol kg^{-1}:
Uncertainty of measurement of nitrite (%) =
$0.51152 + 0.2095 * (1 / C_{NO2}) – 0.000048789 * (1 / C_{NO2}) * (1 / C_{NO2})$ --- (2)
where C_{NO2} is nitrite concentration of sample.

Silicate Concentration C_{SiO2} in μmol kg^{-1}:
Uncertainty of measurement of silicate (%) =
$0.078148 + 1.9825 * (1/ C_{SiO2})$ --- (3)

where C_{SiO2} is silicate concentration of sample.

Phosphate Concentration C_{PO4} in µmol kg^{-1}:
Uncertainty of measurement of phosphate (%) =
$0.11934 + -0.017782 * (1/ C_{PO4}) – 0.10545 * (1 / C_{PO4}) * (1 / C_{PO4})$ --- (4)
where C_{PO4} is phosphate concentration of sample.

Ammonia Concentration C_{NH4} in µmol kg^{-1}:
Uncertainty of measurement of ammonia (%) =
$0.30581 + 1.1441 * (1 / C_{NH4}) – 0.01213 * (1 / C_{NH4}) * (1 / C_{NH4})$ --- (5)
where C_{NH4} is ammonia concentration of sample.

(9) Problems / improvements occurred and solutions.

When we changed LNSW from box#62 to box#12 at RUN#20, we observed systematic decrease of phosphate concentration of CRM lot CE from 0.015 to 0.007 µmol kg^{-1}. We had assumed that phosphate concentration of LNSW in boxes 62 and 12 were same, but it was not. We made direct comparison of LNSW once and the results of comparison showed that phoshate concentration of LNSW in box#62 was 0.044 µmol kg^{-1} while that in box#12 was 0.053 µmol kg^{-1}. Therefore we recalcurated phosphte cocentration using 0.053 µmol kg^{-1} as LNSW concentration from box#12 after run#20. As a results of recalculation, phosphate concentration of CRM lot CE became back to around 0.015 µmol kg^{-1} and impact of recalculation for samples was less than 0.005 µmol kg^{-1} for phosphate concentration range from 0.5 to 1.8 µmol kg^{-1} .

(10) List of reagent

List of reagent is shown in Table 4.2-8.

Table 4.2-8: List of reagent in MR19-03C.

IUPAC name	CAS Number	Formula	Compound Name	Manufacture	Grade
4-Aminobenzenesulfonamide	63-74-1	C6H8N2O2S	Sulfanilamide	Wako Pure Chemical Industries, Ltd.	JIS Special Grade
Ammonium sulfate	7783-20-2	(NH4)2SO4	Ammonium Sulfate	National Metrology Institute of Japan	Certified Reference Material
Antimony potassium tartrate trihydrate	28300-74-5	K2(SbC4H2O6)2·3H2O	Bis[(+)-tartrato]diantimonate(III) Dipotassium Trihydrate	Wako Pure Chemical Industries, Ltd.	JIS Special Grade
Boric acid	10043-35-3	H3BO3	Boric Acid	Wako Pure Chemical Industries, Ltd.	JIS Special Grade
Hydrogen chloride	7647-01-0	HCl	Hydrochloric Acid	Wako Pure Chemical Industries, Ltd.	JIS Special Grade
Imidazole	288-32-4	C3H4N2	Imidazole	Wako Pure Chemical Industries, Ltd.	JIS Special Grade
L-Ascorbic acid	50-81-7	C6H8O6	L-Ascorbic Acid	Wako Pure Chemical Industries, Ltd.	JIS Special Grade
N-(1-Naphthalenyl)-1,2-ethanediamine, dihydrochloride	1465-25-4	C12H16Cl2N2	N-1-Naphthylethylenediamine Dihydrochloride	Wako Pure Chemical Industries, Ltd.	for Nitrogen Oxides Analysis
Oxalic acid	144-62-7	C2H2O4	Oxalic Acid	Wako Pure Chemical Industries, Ltd.	Wako Special Grade
Phenol	108-95-2	C6H6O	Phenol	Wako Pure Chemical Industries, Ltd.	JIS Special Grade
Potassium nitrate	7757-79-1	KNO3	Potassium Nitrate	Merck KGaA	Suprapur®
Potassium dihydrogen phosphate	7778-77-0	KH2PO4	Potassium dihydrogen phosphate anhydrous	Merck KGaA	Suprapur®
Sodium citrate dihydrate	6132-04-3	Na3C6H5O7·2H2O	Trisodium Citrate Dihydrate	Wako Pure Chemical Industries, Ltd.	JIS Special Grade
Sodium dodecyl sulfate	151-21-3	C12H25NaO4S	Sodium Dodecyl Sulfate	Wako Pure Chemical Industries, Ltd.	for Biochemistry
Sodium hydroxide	1310-73-2	NaOH	Sodium Hydroxide for Nitrogen Compounds Analysis	Wako Pure Chemical Industries, Ltd.	for Nitrogen Analysis
Sodium hypochlorite	7681-52-9	NaClO	Sodium Hypochlorite Solution	Kanto Chemical co., Inc.	Extra pure
Sodium molybdate dihydrate	10102-40-6	Na2MoO4·2H2O	Disodium Molybdate(VI) Dihydrate	Wako Pure Chemical Industries, Ltd.	JIS Special Grade
Sodium nitroferricyanide dihydrate	13755-38-9	Na2[Fe(CN)5NO]·2H2O	Sodium Pentacyanonitrosylferrate(III) Dihydrate	Wako Pure Chemical Industries, Ltd.	JIS Special Grade
Sulfuric acid	7664-93-9	H2SO4	Sulfuric Acid	Wako Pure Chemical Industries, Ltd.	JIS Special Grade
tetrasodium;2-[2-[bis(carboxylatomethyl)amino]ethyl-(carboxylatomethyl)amino]acetate;tetrahydrate	13235-36-4	C10H12N2Na4O8·4H2O	Ethylenediamine-N,N,N',N'-tetraacetic Acid Tetrasodium Salt Tetrahydrate (4NA)	Dojindo Molecular Technologies, Inc.	-
Synonyms: t-Octylphenoxypolyethoxyethanol 4-(1,1,3,3-Tetramethylbutyl)phenyl-polyethylene glycol Polyethylene glycol tert-octylphenyl ether	9002-93-1	(C2H4O)nC14H22O	Triton™ X-100	Sigma-Aldrich Japan G.K.	-

(11) Data archives

These data obtained in this cruise will be submitted to the Data Management Group of JAMSTEC, and will be opened to the public via "Data Research System for Whole Cruise Information in JAMSTEC (DARWIN)" in JAMSTEC web site (http://www.godac.jamstec.go.jp/darwin/e).

(12) References

Susan Becker, Michio Aoyama E. Malcolm S. Woodward, Karel Bakker, Stephen Coverly, Claire Mahaffey, Toste Tanhua, (2019) The precise and accurate determination of dissolved inorganic nutrients in seawater, using Continuous Flow Analysis methods, n: The GO-SHIP Repeat Hydrography Manual: A Collection of Expert Reports and Guidelines. Available online at: http://www.go-ship.org/HydroMan.html. DOI: http://dx.doi.org/10.25607/OBP-555

Grasshoff, K. 1976. Automated chemical analysis (Chapter 13) in Methods of Seawater Analysis. With contribution by Almgreen T., Dawson R., Ehrhardt M., Fonselius S. H., Josefsson B., Koroleff F., Kremling K. Weinheim, New York: Verlag Chemie.

Grasshoff, K., Kremling K., Ehrhardt, M. et al. 1999. Methods of Seawater Analysis. Third, Completely Revised and Extended Edition. WILEY-VCH Verlag GmbH, D-69469 Weinheim (Federal Republic of Germany).

Hydes, D.J., Aoyama, M., Aminot, A., Bakker, K., Becker, S., Coverly, S., Daniel, A., Dickson, A.G., Grosso, O., Kerouel, R., Ooijen, J. van, Sato, K., Tanhua, T., Woodward, E.M.S., Zhang, J.Z., 2010. Determination of Dissolved Nutrients (N, P, Si) in Seawater with High Precision and Inter-Comparability Using Gas-Segmented Continuous Flow Analysers, In: GO-SHIP Repeat Hydrography Manual: A Collection of Expert Reports and Guidelines. IOCCP Report No. 14, ICPO Publication Series No 134.

Kimura, 2000. Determination of ammonia in seawater using a vaporization membrane permeability method. 7th auto analyzer Study Group, 39-41.

Murphy, J., and Riley, J.P. 1962. Analytica chimica Acta 27, 31-36.

4.3 DIC and TA

(1) Personnel

Akihiko Murata	JAMSTEC	-PI
Minoru Hamana	JAMSTEC	
Masahiro Orui	MWJ	
Hiroshi Hoshino	MWJ	
Atsushi Ono	MWJ	

(2) Objectives

Concentrations of CO_2 in the atmosphere are now increasing at a rate of 1.9 ppmv y^{-1} owing to human activities such as burning of fossil fuels, deforestation, and cement production. It is an urgent task to estimate as accurately as possible the absorption capacity of the oceans against the increased atmospheric CO_2, and to clarify the mechanism of the CO_2 absorption, because the magnitude of the anticipated global warming depends on the levels of CO_2 in the atmosphere, and because the ocean currently absorbs 1/3 of the 6 Gt of carbon emitted into the atmosphere each year by human activities.

In this cruise, we were aimed at quantifying how much anthropogenic CO_2 absorbed in the ocean are transported and redistributed in the Arctic Ocean. For the purpose, we measured CO_2-system parameters such as dissolved inorganic carbon (DIC) and total alkalinity (TA).

(3) Apparatus

Measurements of DIC and TA were made with a DIC-TA measuring system (Nippon ANS, Inc., Japan), which can analyze DIC and TA simultaneously. The system comprises of DIC and TA units. The DIC unit comprises of a seawater dispensing system, a CO_2 extraction system and a coulometer. The seawater dispensing system had an auto-sampler (6 ports), which took seawater in a 250 ml borosilicate glass bottle ((DURAN® glass bottle, 250 ml) and dispensed the seawater to a pipette of nominal 15 ml volume by PC control. The pipette is kept at 25°C by a water jacket, in which water from a water bath set at 25°C is circulated. CO_2 dissolved in a seawater sample is extracted in a stripping chamber of the CO_2 extraction system by adding phosphoric acid (10 % v/v). The stripping chamber is made approx. 25 cm long and had a fine frit at the bottom. The acid is added to the stripping chamber from the bottom of the chamber by pressurizing an acid bottle for a given time to push out the right amount of acid. The pressurizing is made with nitrogen gas (99.9999 %). After the acid is transferred to the stripping chamber, a seawater sample kept in a pipette is introduced to the stripping chamber by the same method as in adding an acid. The seawater reacts with phosphoric acid was stripped of CO_2 by bubbling the nitrogen gas through a fine frit at the bottom of the stripping chamber. The CO_2 stripped in the chamber is carried by the nitrogen gas (flow rates is 130 ml min^{-1}) to the coulometer through a dehydrating module.

The TA unit comprises of a water dispensing system, an auto-syringe (Hamilton) for hydrochloric acid, a spectrophotometer (TM-UV/VIS C10082CAH, Hamamatsu Photonics, Japan), and a light source (Mikropack, Germany), which are automatically controlled by a PC. The water dispensing system has a water-jacketed pipette and a titration cell, which is controlled at 25°C.

A seawater of approx. 42 ml is transferred from a sample bottle (DURAN® glass bottle, 250 ml) into the pipette by pressurizing the sample bottle (nitrogen gas), and is introduced into the titration cell. The seawater is used to rinse the titration cell. Then, Milli-Q water is introduced into the titration cell, also for rinse. A seawater of approx. 42 ml is weighted again by the pipette, and is transferred into the titration cell. Then, for seawater blank, absorbances are measured at three wavelengths (730, 616 and 444 nm). After the measurement, an acid titrant, which is a mixture of approx. 0.05 M HCl at 25°C in 0.65 M NaCl and 38 μM bromocresol green (BCG) is added into the titration cell. The volume of the acid titrant is changed between 1.780 mL and 2.100 mL according to estimated values of TA. The seawater + acid titrant solution is stirred for over 9 minutes with bubbling by nitrogen gas in the titration cell. Then, absorbances at the three wavelengths are measured.

Calculation of TA is made by the following equation:

$$\mathrm{TA} = (-[\mathrm{H}^+]_\mathrm{T} \mathrm{V}_\mathrm{SA} + \mathrm{M}_\mathrm{A} \mathrm{V}_\mathrm{A})/\mathrm{V}_\mathrm{S},$$

where M_A is the molarity of the acid titrant added to the seawater sample, $[H^+]_T$ is the total excess hydrogen ion concentration in the seawater, and V_S, V_A and V_{SA} are the initial seawater volume, the added acid titrant volume, and the combined seawater plus acid titrant volume, respectively. $[H^+]_T$ is calculated from the measured absorbances based on the following equation (Yao and Byrne, 1998):

$$\begin{aligned}\mathrm{pH_T} = -\log[\mathrm{H}^+]_\mathrm{T} &= 4.2699 + 0.002578(35-\mathrm{S}) + \log((\mathrm{R}-0.00131)/(2.3148-0.1299\mathrm{R})) \\ &\quad -\log(1-0.001005\mathrm{S}),\end{aligned}$$

where S is the sample salinity, and R is the absorbance ratio calculated as:

$$\mathrm{R} = (\mathrm{A}_{616} - \mathrm{A}_{730})/(\mathrm{A}_{444} - \mathrm{A}_{730}),$$

where A_i is the absorbance at wavelength i nm.

The measurement sequence such as system blank (phosphoric acid blank), 1.5 % CO_2 gas in a nitrogen base, sea water samples (6) was programmed to repeat. The measurement of 1.5 % CO_2 gas was made to monitor response of coulometer solutions (from UIC, Inc.) or laboratory-made.

(4) Performances

Replicate analysis was made approximately on every about 5th seawater sample. The repeatability for DIC and TA were estimated to be 0.20 ± 2.49 (n = 108) and 0.63 ± 3.05 (n = 108) μmol kg^{-1}, respectively. They are based on not QCed data.

(5) Results

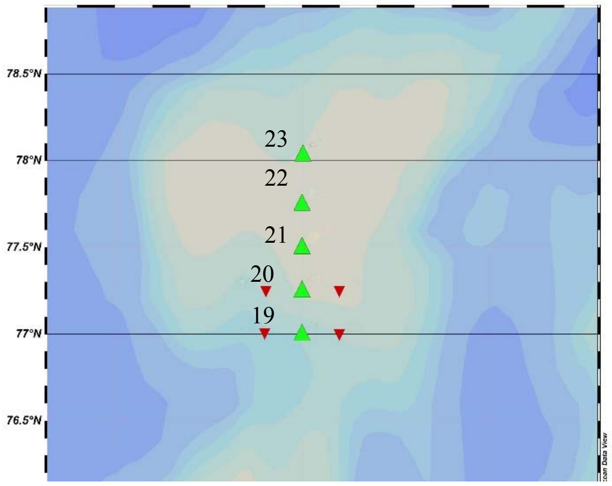

Figure 4.3-1: Positions of repeat line stations (triangles).

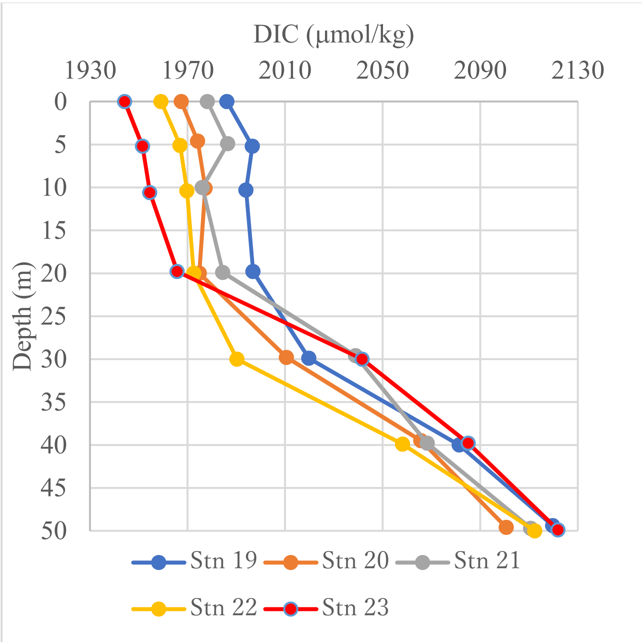

Figure 4.3-2: Vertical distributions of DIC in upper 100 m at repeat line stations.

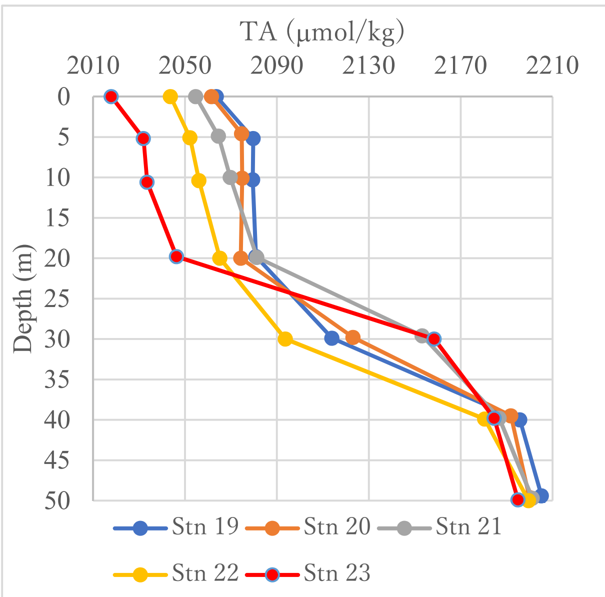

Figure 4.3-3: Vertical distributions of TA in upper 100 m at repeat line stations.

References

Yao W. and R. H. Byrne (1998) Simplified seawater alkalinity analysis: Use of linear array spectrometers. Deep-Sea Research I 45, 1383-1392.

4.4 CH_4

(1) Personnel

Akihiko Murata	JAMSTEC	- PI
Sohiko Kameyama	Hokkaido Univ.	- not on board

(2) Objectives

Methane (CH_4) is one of strong greenhouse gases, whose concentrations in the atmosphere have increased over the past decades. In spite of the importance for global CH_4 budget, marine contributions to the global budget of CH_4 reveal substantial uncertainty, because CH_4 observations in the ocean have been limited. For the Arctic Ocean, it is known that the surface waters are usually super-saturated with respect to atmospheric CH_4, implying that the ocean acts as a source for atmospheric CH_4. However, the magnitude of CH_4 emission varies considerably over both time and space. This large variability reflects complicated biogeochemical dynamics in the Arctic Ocean. Our water column observations of CH_4 were made to understand processes, which control large spatial and temporal variability of CH_4 distributions in the Arctic Ocean.

(3) Parameters

Dissolved CH_4 concentration

Carbon isotopic composition of CH_4

(4) Instruments and methods

(4-1) Discrete bottle sampling

Discrete water samples for each station (Table 4.4) were collected at multiple depths using 12L Niskin bottles mounted on a CTD system. An aliquot of 100 ml seawater was transferred from Niskin bottles to amber vials (100 ml). The vial was filled with seawater smoothly from the bottom using a drawing tube which extends from the Niskin drain to the bottom of the vial. The seawater was overflowed by about a full and half a vial volume. After sampling, saturated mercuric chloride of 0.5 ml was added to each sample to poison the sample. Then vials were crimp sealed with butyl-rubber stoppers and aluminum caps.

(4-2) Sample storage

The samples were stored at 4°C in the dark on board the *Mirai*, and transported chilled to laboratories on land for analysis when the *Mirai* returned to Japan.

(4-3) Sample measurement

The samples will be measured by a gas chromatography-isotope ratio mass spectrometry (GC-IRMS) coupling with a purge and trap extraction system in Nagoya University.

(5) Station list or Observation log

Water sampling stations for CH_4 are shown in Table 4.4.

Table 4.4: List of sampling stations for water column CH_4.

Stn.	Sampling date (UTC)	Latitude (N)	Longitude (W)
002	08 Oct.	66°-00.17”	168°-44.72”
004	08 Oct.	67°-00.13”	168°-44.26”
005	09 Oct.	69°-00.19”	168°-45.18”
007	09 Oct.	69°-59.96”	168°-45.03”
009	10 Oct.	71°-59.76”	163°-29.99”
011	10 Oct.	72°-60.00”	160°-00.20”
013	11 Oct.	72°-19.98”	155°-00.52”
015	12 Oct.	71°-59.99”	147°-29.98”
019-1	16 Oct.	76°-59.96”	164°-59.94”
020-1	16 Oct.	77°-15.04”	164°-59.71”
021-1	17 Oct.	77°-30.01”	165°-00.01”
022-1	17 Oct.	77°-45.00”	165°-00.01”
023	18 Oct.	78°-02.13”	164°-58.49”

(6) Data archives

These data obtained in this cruise will be submitted to the Data Management Group of JAMSTEC, and will be opened to the public via “Data Research System for Whole Cruise Information in JAMSTEC (DARWIN)” in JAMSTEC web site.

<http://www.godac.jamstec.go.jp/darwin/e>

4.5 Radiocesium (^{134}Cs and ^{137}Cs), radioradium (^{226}Ra and ^{228}Ra) and PAHs

(1) Personnel

Yuichiro Kumamoto JAMSTEC - not on board, PI

(2) Objective

Determination of activity concentrations of radiocesium (^{134}Cs and ^{137}Cs), radioradium (^{226}Ra and ^{228}Ra), and polycyclic aromatic hydrocarbons (PAHs) in the Arctic Ocean, Bering Sea, and northern North Pacific Ocean.

(3) Parameters

^{134}Cs, ^{137}Cs, ^{226}Ra, ^{228}Ra, and PAHs

(4) Instruments and Methods

a. Sampling

Surface seawater samples were collected from continuous pumped-up water from about 4-m depth. The sample volumes for radiocesium, radioradium, and PAHs are 40 L (two 20-L plastic containers), 20 L (a 20-L plastic container), and 10 L (a 10-L stainless container), respectively.

b. Preparation and analysis

The seawater sample for radiocesium measurement was not filtered and was acidified by adding nitric acid. Radiocesium in the seawater sample is concentrated using ammonium phosphomolybdate (AMP) that forms an insoluble compound with cesium. The radiocesium (^{134}Cs and ^{137}Cs) in the compound is measured using Ge gamma-ray spectrometers.

The seawater sample for radioradium measurement was not filtered. Least Ra-contaminated Barium carrier and SO_4^{2-} are added to 20 L seawater sample to coprecipitate radium with $BaSO_4$. After evaporating to dryness, the $BaSO_4$ fractions are compressed to disc as a mixture of $Fe(OH)_3$ and NaCl for gamma-ray spectrometry using Ge-detectors.

Particulate and dissolved phases of 10 L seawater sample are separated by filtration through 0.5 μm glass-fiber filters. Dissolved organic compounds, including PAHs, are concentrated using C18 solid-phase extraction disks. Particulate and dissolved PAHs are respectively extracted from the glass-fiber filters using an ultrasonic method and eluted from the C18 disks with dichloromethane. Dimethyl sulfoxide is added to both extracted solutions, the dichloromethane is evaporated to dryness, and the residue of dimethyl sulfoxide is dissolved in acetonitrile. PAHs in the samples were quantified using the HPLC system with a fluorescence detector.

(5) Sample list

We collected 9 seawaters for the radiocesium, radioradium, and PAHs measurements in the Arctic Ocean, Bering Sea, and northern North Pacific Ocean during this cruise (Table 4.5).

(6) Data archives

These data obtained in this cruise will be submitted to the Data Management Group of JAMSTEC and will be opened to the public via “Data Research System for Whole Cruise Information in JAMSTEC (DARWIN)” in JAMSTEC web site.

Table 4.5: Seawater samples collected for the radiocesium, radioradium, and PAHs measurements.

No.	Station	Depth (m)	Method	Latitude (N)	Longitude (E)	Date (UTC)
1	surface-1	4	pump	46.76	160.30	2019/10/2
2	surface-2	4	pump	52.47	170.02	2019/10/4
3	surface-3	4	pump	59.16	180.05	2019/10/6
4	surface-4	4	pump	64.67	190.08	2019/10/8
5	surface-5	4	pump	69.89	191.27	2019/10/9
6	surface-6	4	pump	72.97	200.18	2019/10/10
7	surface-7	4	pump	73.79	214.75	2019/10/13
8	surface-8	4	pump	75.52	204.26	2019/10/15
9	surface-9	4	pump	78.07	194.83	2019/10/18

4.6 ^{129}I

(1) Personnel

Yuichiro Kumamoto JAMSTEC - not on board, PI

(2) Objective

Determination of activity concentrations of ^{129}I in the Arctic Ocean, Bering Sea, and northern North Pacific Ocean.

(3) Parameters

^{129}I

(4) Instruments and Methods

a. Sampling

Seawater samples for ^{129}I were collected using 12-liter Niskin-X bottles. Surface seawater was collected using a bucket or from continuous pumped-up water at about 4-m depth. The seawater sample was collected into a 1-L plastic bottle after two-time rinsing.

b. Preparation and analysis

Iodine in the seawater samples is extracted by the solvent extraction technique. Extracted iodine is then precipitated as silver iodide by the addition of the silver nitrate. Iodine isotopic ratios ($^{129}I/^{127}I$) of the silver iodide are measured by the Accelerator Mass Spectrometry (AMS). To evaluate the ^{129}I concentration in the seawater samples, iodine concentration (^{127}I) will be measured by the inductively coupled plasma mass spectrometry (ICP-MS) and/or the voltammetry.

(5) Sample list

We collected 74 seawater samples for ^{129}I measurements in the Arctic Ocean, Bering Sea, and northern North Pacific Ocean during this cruise (Table 4.6).

(6) Data archives

These data obtained in this cruise will be submitted to the Data Management Group of JAMSTEC and will be opened to the public via “Data Research System for Whole Cruise Information in JAMSTEC (DARWIN)” in JAMSTEC web site.

Table 4.6: Seawater samples collected for the ^{129}I measurement.

No.	Station	Depth (m)	Method	Latitude (N)	Longitude (E)	Date (UTC)
1	Stn.13	0	bucket	72.33	204.99	2019/10/11
2	Stn.13	20	niskin	72.33	204.99	2019/10/11
3	Stn.13	50	niskin	72.33	204.99	2019/10/11
4	Stn.13	100	niskin	72.33	204.99	2019/10/11
5	Stn.13	150	niskin	72.33	204.99	2019/10/11
6	Stn.13	200	niskin	72.33	204.99	2019/10/11
7	Stn.13	250	niskin	72.33	204.99	2019/10/11
8	Stn.13	300	niskin	72.33	204.99	2019/10/11
9	Stn.13	400	niskin	72.33	204.99	2019/10/11
10	Stn.13	600	niskin	72.33	204.99	2019/10/11
11	Stn.13	800	niskin	72.33	204.99	2019/10/11
12	Stn.13	1000	niskin	72.33	204.99	2019/10/11
13	Stn.13	1500	niskin	72.33	204.99	2019/10/11
14	Stn.13	1952	niskin	72.33	204.99	2019/10/11
15	Stn.15	0	bucket	71.20	212.50	2019/10/12
16	Stn.15	20	niskin	71.20	212.50	2019/10/12
17	Stn.15	50	niskin	71.20	212.50	2019/10/12
18	Stn.15	100	niskin	71.20	212.50	2019/10/12
19	Stn.15	150	niskin	71.20	212.50	2019/10/12
20	Stn.15	200	niskin	71.20	212.50	2019/10/12
21	Stn.15	250	niskin	71.20	212.50	2019/10/12
22	Stn.15	300	niskin	71.20	212.50	2019/10/12
23	Stn.15	400	niskin	71.20	212.50	2019/10/12
24	Stn.15	600	niskin	71.20	212.50	2019/10/12
25	Stn.15	800	niskin	71.20	212.50	2019/10/12
26	Stn.15	1000	niskin	71.20	212.50	2019/10/12
27	Stn.15	1500	niskin	71.20	212.50	2019/10/12
28	Stn.15	2000	niskin	71.20	212.50	2019/10/12
29	Stn.15	2500	niskin	71.20	212.50	2019/10/12
30	Stn.15	3000	niskin	71.20	212.50	2019/10/12
31	Stn.15	3505	niskin	71.20	212.50	2019/10/12
32	Stn.16	0	bucket	72.00	215.00	2019/10/12
33	Stn.16	20	niskin	72.00	215.00	2019/10/12
34	Stn.16	50	niskin	72.00	215.00	2019/10/12
35	Stn.16	100	niskin	72.00	215.00	2019/10/12
36	Stn.16	150	niskin	72.00	215.00	2019/10/12

Table 4.6: continued.

No.	Station	Depth (m)	Method	Latitude (N)	Longitude (E)	Date (UTC)
37	Stn.16	200	niskin	72.00	215.00	2019/10/12
38	Stn.16	250	niskin	72.00	215.00	2019/10/12
39	Stn.16	300	niskin	72.00	215.00	2019/10/12
40	Stn.16	400	niskin	72.00	215.00	2019/10/12
41	Stn.16	600	niskin	72.00	215.00	2019/10/12
42	Stn.16	800	niskin	72.00	215.00	2019/10/12
43	Stn.16	1000	niskin	72.00	215.00	2019/10/12
44	Stn.16	1500	niskin	72.00	215.00	2019/10/12
45	Stn.16	2000	niskin	72.00	215.00	2019/10/12
46	Stn.16	2500	niskin	72.00	215.00	2019/10/12
47	Stn.16	3000	niskin	72.00	215.00	2019/10/12
48	Stn.16	3306	niskin	72.00	215.00	2019/10/12
49	Stn.17	0	bucket	74.77	209.50	2019/10/14
50	Stn.17	20	niskin	74.77	209.50	2019/10/14
51	Stn.17	50	niskin	74.77	209.50	2019/10/14
52	Stn.17	100	niskin	74.77	209.50	2019/10/14
53	Stn.17	150	niskin	74.77	209.50	2019/10/14
54	Stn.17	200	niskin	74.77	209.50	2019/10/14
55	Stn.17	250	niskin	74.77	209.50	2019/10/14
56	Stn.17	300	niskin	74.77	209.50	2019/10/14
57	Stn.17	400	niskin	74.77	209.50	2019/10/14
58	Stn.17	600	niskin	74.77	209.50	2019/10/14
59	Stn.17	800	niskin	74.77	209.50	2019/10/14
60	Stn.17	1000	niskin	74.77	209.50	2019/10/14
61	Stn.17	1500	niskin	74.77	209.50	2019/10/14
62	Stn.17	2000	niskin	74.77	209.50	2019/10/14
63	Stn.17	2500	niskin	74.77	209.50	2019/10/14
64	Stn.17	3000	niskin	74.77	209.50	2019/10/14
65	Stn.17	3824	niskin	74.77	209.50	2019/10/14
66	surface-1	4	pump	46.76	160.30	2019/10/2
67	surface-2	4	pump	52.47	170.02	2019/10/4
68	surface-3	4	pump	59.16	180.05	2019/10/6
69	surface-4	4	pump	64.67	190.08	2019/10/8
70	surface-5	4	pump	69.89	191.27	2019/10/9
71	surface-6	4	pump	72.97	200.18	2019/10/10
72	surface-7	4	pump	73.79	214.75	2019/10/13

Table 4.6: continued.

No.	Station	Depth (m)	Method	Latitude (N)	Longitude (E)	Date (UTC)
73	surface-8	4	pump	75.52	204.26	2019/10/15
74	surface-9	4	pump	78.07	194.83	2019/10/18

4.7 DOC and FDOM

(1) Personnel

Masahito Shigemitsu	JAMSTEC	- not on board, PI
Akihiko Murata	JAMSTEC	

(2) Objectives

The Arctic Ocean receives about 10 % of global river runoff. The rivers draining into the Arctic Ocean have high concentrations of dissolved organic carbon (DOC) and supply a large amount of DOC there. The supply rates of DOC must spatially and temporally change, which should affect the quantity and composition of dissolved organic matter (DOM) in the Arctic Ocean. The change in the quantity and composition of DOM plays an important role in the growth of microbes, and ultimately the fate of supplied DOM in the Arctic Ocean. In order to better understand the quantity and composition of DOM in the Arctic Ocean, the samples in the surface waters for measuring DOC concentration and excitation-emission matrix (EEM) of fluorescent dissolved organic matter (FDOM) were collected.

(3) Parameters

DOC concentration
EEM of FDOM

(4) Instruments and methods

(4-1) Bottle sampling

Discrete water samples for each station (Table 4.7) were collected in the surface waters using 12L Niskin bottles mounted on a CTD system. Each sample was filtered using a pre-combusted glass fiber filter (GF/F, Whatman). The filtration was carried out by connecting a spigot of Niskin bottle through silicone tube to an inline plastic filter holder. Filtrates for DOC concentration and EEM of FDOM were collected in acid-washed 60 mL High Density Polyethylene (HDPE) bottles and pre-combusted glass vials with acid-washed teflon-lined caps after triple rinsing, respectively.

(4-2) Sample storage

The samples were stored frozen in the dark on board the *Mirai* until analysis.

(4-3) Sample measurement

The samples for DOC concentration and EEM of FDOM will be measured by a Shimadzu TOC-L system coupled with a Shimadzu Total N analyzer in JAMSTEC, and by a Horiba Aqualog in JAMSTEC, respectively.

(5) Station list

Water sampling stations for DOC concentration and EEM of FDOM are shown in Table 4.7.

Table 4.7: List of sampling stations for DOC concentration and EEM of FDOM.

CTD Stn.	Latitude	Longitude
002	66-00.17N	168-44.72W
004	67-00.13N	168-44.26W
005	69-00.19N	168-45.18W
007	69-59.96N	168-45.03W
009	71-59.76N	163-29.99W
011	72-60.00N	160-00.20W
013	72-19.98N	155-00.52W
014	72-09.43N	153-47.41W
015	71-59.99N	147-29.98W
016	72-00.00N	145-00.05W
017	74-46.09N	150-30.13W
018	76-27.95N	161-38.51W
019	76-59.96N	164-59.94W
020	77-15.04N	164-59.71W
021	77-30.01N	165-00.01W
022	77-45.00N	165-00.01W
023	78-02.13N	164-58.49W
024	77-15.00N	165-59.97W
025	77-00.37N	165-59.88W
026	77-00.01N	164-00.01W
027	77-15.00N	164-00.01W
028	77-00.22N	168-46.13W
029	74-00.01N	168-44.83W
030	73-30.00N	168-45.00W
031	73-00.03N	168-45.04W
032	72-30.03N	168-44.61W
033	70-30.00N	168-44.92W
034	70-00.00N	168-45.04W
035	69-30.19N	168-45.23W
036	68-59.99N	168-45.29W
037	68-00.88N	167-52.05W
038	67-46.99N	168-36.29W
039	67-30.07N	168-45.11W
040	67-00.06N	168-44.71W
041	66-29.99N	168-45.02W

(6) Data archives

These data obtained in this cruise will be submitted to the Data Management Group of JAMSTEC, and will be open to the public via “Data Research System for Whole Cruise Information in JAMSTEC (DARWIN)” in JAMSTEC web site.

<http://www.godac.jamstec.go.jp/darwin/e>

4.8 Underway surface water monitoring

(1) Personnel

Akihiko Murata	JAMSTEC	- PI
Erii Irie	MWJ	- Operation leader
Yuko Miyoshi	MWJ	
Kanako Yoshida	MWJ	

(2) Objective

Our purpose is to obtain temperature, salinity, dissolved oxygen, and fluorescence data continuously in near-sea surface water, and to reveal their spatial and temporal variations.

(3) Parameters

Temperature
Salinity
Dissolved oxygen
Fluorescence
Turbidity

(4) Instruments and Methods

The Continuous Sea Surface Water Monitoring System (Marine Works Japan Co. Ltd.) has four sensors and automatically measures temperature, salinity, dissolved oxygen, fluorescence, and turbidity in near-sea surface water every one minute. This system is located in the "sea surface monitoring laboratory" and connected to shipboard LAN-system. Measured data, time, and location of the ship were stored in a data management PC. Sea water was continuously pumped up to the laboratory from an intake placed at the approximately 4.5 m below the sea surface and flowed into the system through a vinyl-chloride pipe. The flow rate of the surface seawater was adjusted to 10 dm^3 min^{-1}.

a. Instruments

Software

Seamoni Ver.1.2.0.0

Sensors

Specifications of each sensor in this system are listed below:

Temperature and Conductivity sensor

Model:	SBE-45, SEA-BIRD ELECTRONICS, INC.
Serial number:	4557820-0319
Measurement range:	Temperature -5 °C - +35 °C
	Conductivity 0 S m^{-1} - 7 S m^{-1}
Initial accuracy:	Temperature 0.002 °C
	Conductivity 0.0003 S m^{-1}

Typical stability (per month):	Temperature 0.0002 ^{o}C
	Conductivity 0.0003 S m^{-1}
Resolution:	Temperature 0.0001 ^{o}C
	Conductivity 0.00001 S m^{-1}

Bottom of ship thermometer

Model:	SBE 38, SEA-BIRD ELECTRONICS, INC.
Serial number:	3852788-0457
Measurement range:	-5 ^{o}C - +35 ^{o}C
Initial accuracy:	±0.001 ^{o}C
Typical stability (per 6 month):	0.001 ^{o}C
Resolution:	0.00025 ^{o}C

Dissolved oxygen sensor

Model:	RINKO II, JFE ADVANTECH CO. LTD.
Serial number:	0013
Measuring range:	0 mg L^{-1} - 20 mg L^{-1}
Resolution:	0.001 mg L^{-1} - 0.004 mg L^{-1} (25 ^{o}C)
Accuracy:	Saturation ± 2 % F.S. (non-linear) (1 atm, 25 ^{o}C)

Fluorescence & Turbidity sensor

Model:	C3, TURNER DESIGNS
Serial number:	2300384
Measuring range:	Chlorophyll in vivo 0 μg L^{-1} – 500 μg L^{-1}
Minimum Detection Limit:	Chlorophyll in vivo 0.03 μg L^{-1}
Measuring range:	Turbidity 0 NTU - 1500 NTU
Minimum Detection Limit:	Turbidity 0.05 NTU

(5) Observation log

Spatial distributions of each property are shown in Fig. 4.8-1. We took the surface water samples from this system once a day to compare sensor data with bottle data of salinity, dissolved oxygen, and chlorophyll a. The results are shown in Figure 4.8-2. All the salinity samples were analyzed by the Model 8400B “AUTOSAL” manufactured by Guildline Instruments Ltd. (see Chapter 3.2), and dissolve oxygen samples were analyzed by Winkler method (see Chapter 4.1), chlorophyll a were analyzed by 10-AU manufactured by Turner Designs. (see Chapter 4.11).

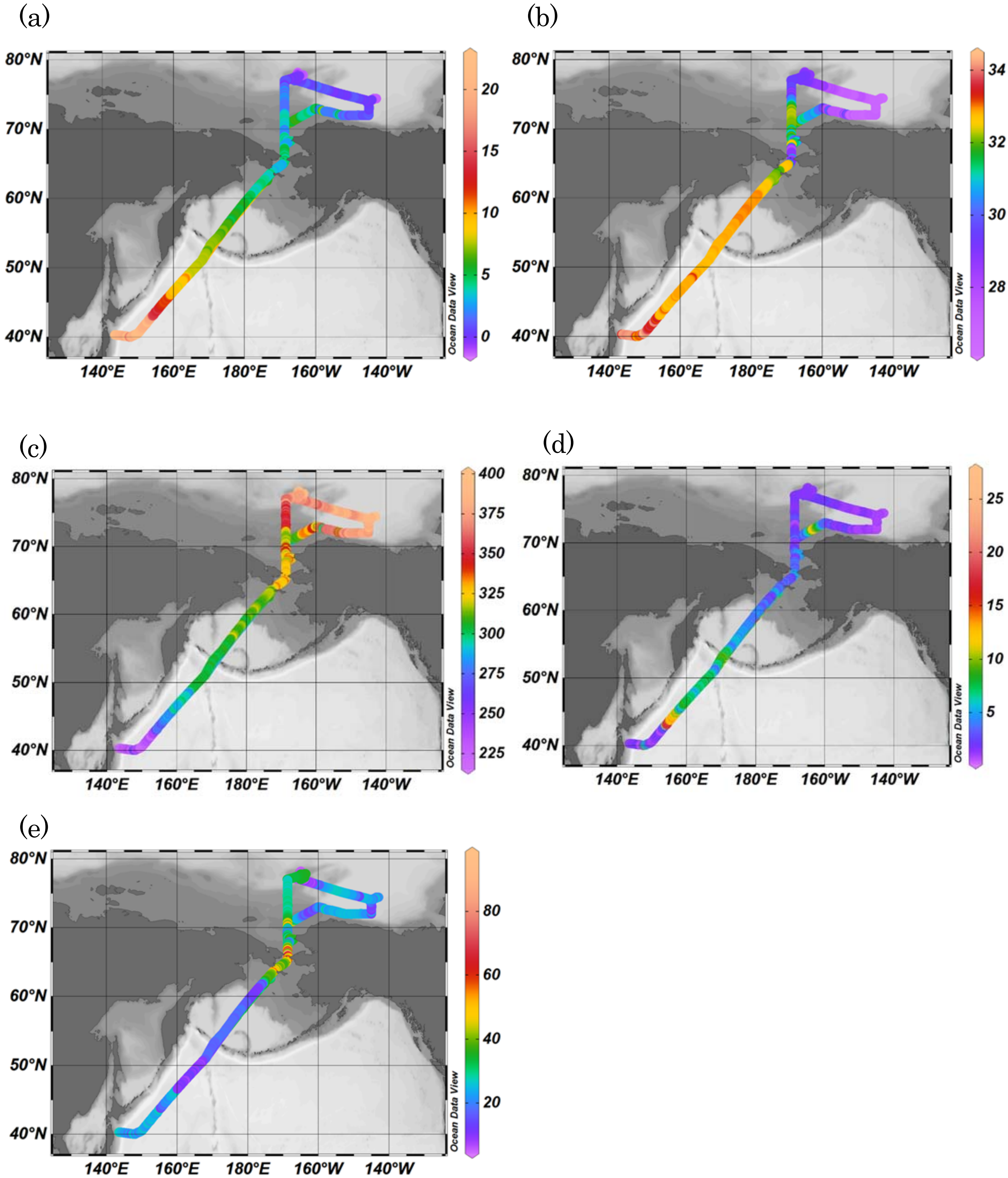

Figure 4.8-1: Spatial and temporal distribution of (a) temperature, (b) salinity, (c) dissolved oxygen, (d) fluorescence, and (e) turbidity in MR19-03C cruise.

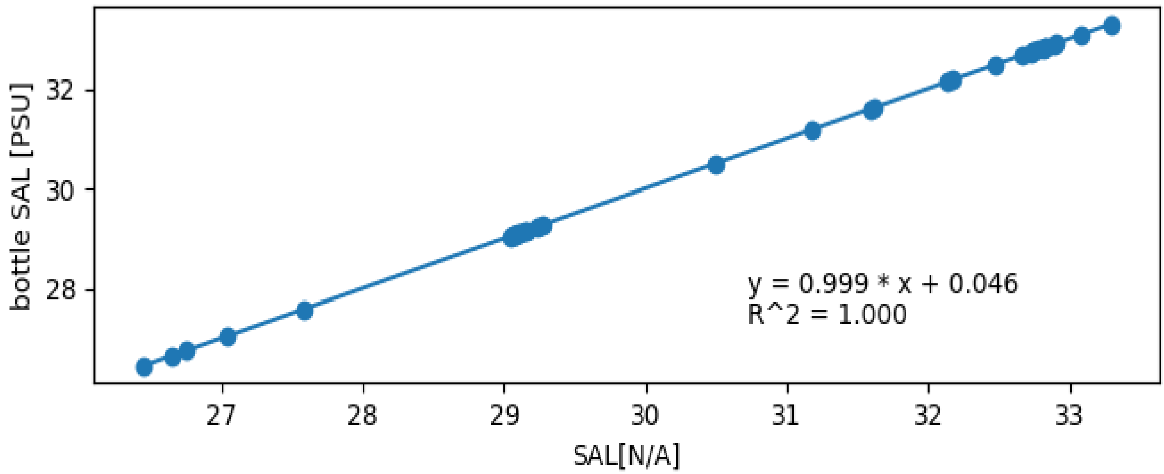

Figure 4.8-2: Correlation of salinity between sensor data and bottle data.

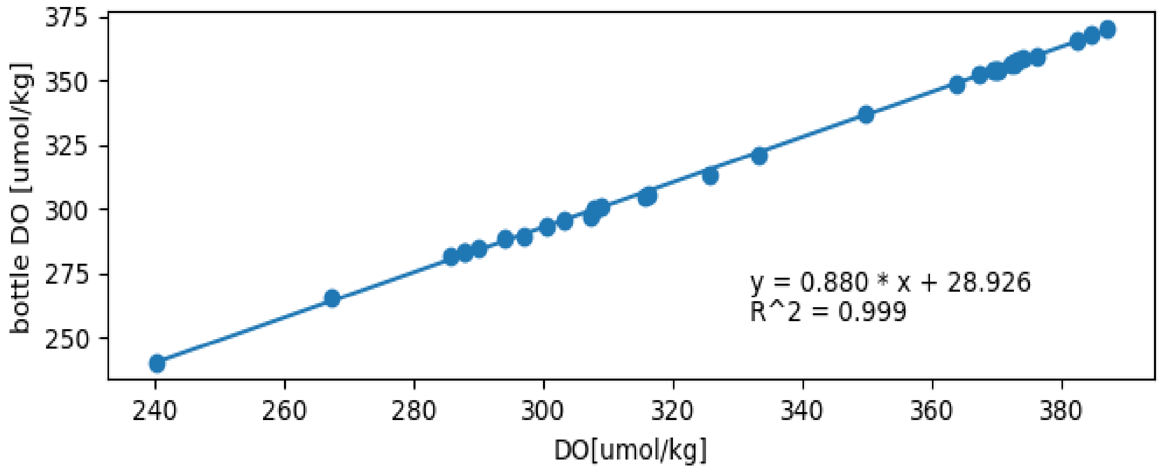

Figure 4.8-3: Correlation of dissolved oxygen between sensor data and bottle data.

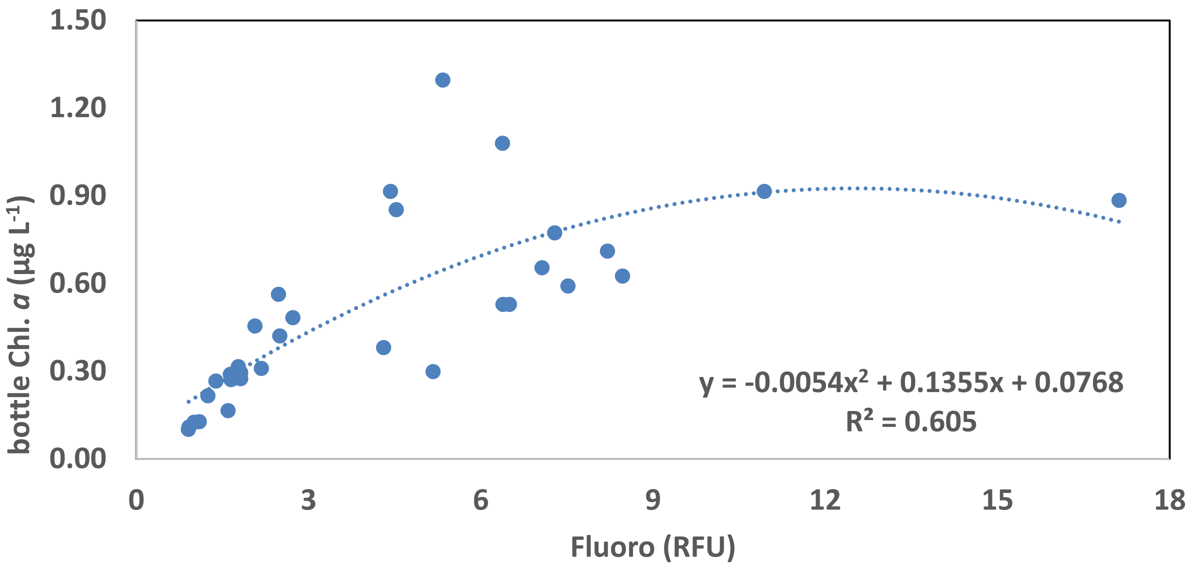

Figure 4.8-4: Correlation of fluorescence between sensor data and bottle data.

(6) Data archives

These data obtained in this cruise will be submitted to the Data Management Group (DMG) of JAMSTEC, and will opened to the public via “Data Research System for Whole Cruise Information in JAMSTEC (DARWIN)” in JAMSTEC web site.
<http://www.godac.jamstec.go.jp/darwin/e>

4.9 Continuous measurement of CO_2 and CH_4

(1) Personnel

Akihiko Murata	JAMSTEC	- PI
Atsushi Ono	MWJ	
Masahiro Orui	MWJ	
Hiroshi Hoshino	MWJ	
Sohiko Kameyama	Hokkaido University	

(2) Objective

Our purpose is in-situ measurement of concentrations of carbon dioxide (CO_2) and methane (CH_4) in near-sea surface water.

(3) Methods, Apparatus and Performance

CO_2 and CH_4 standard gases (Table 4.9-1), atmospheric air, the both CO_2 and CH_4 equilibrated air with sea surface water were analyzed using an automated system equipped with both a non-dispersive infrared gas analyzer (NDIR; LI-7000, Li-Cor) and Off-Axis Integrated-Cavity output Spectroscopy gas analyzer (Off-Axis ICOS; 911-0011, Los Gatos Research) developed on the basis of Cavity Ring-Down.Spectroscopy. Standard gases and atmospheric air taken from the bow of the ship (approx.13 m above the sea level) were measured every about two hours. Seawater was taken from an intake placed at the approximately 4.5 m below the sea surface and introduced into the equilibrator at the flow rate of (4 - 5) L min-1 by a pump. The equilibrated air was circulated in a closed loop by a pump at flow rate of (0.6 - 0.7) L min^{-1} through two electric cooling units, a starling cooler, the NDIR and the Off-Axis ICOS.

We also conducted discrete water sampling for surface seawater CH_4 in order to check underway CH_4 measurements (Table 4.9-2)

(4) Preliminary result

Temporal variations of CO_2 and CH_4 concentrations were shown in Figures 4.9-1 and 4.9-2, respectively.

Table 4.9-1: Concentrations of CO_2 and CH_4 standard gases

	CO_2 (ppmv)	CH_4 (ppmv)
STD 1	249	-
STD 2	319	-
STD 3	390	-
STD 4	461	-
STD 5	241	1.62
STD 6	380	1.91
STD 7	-	2.13

Table 4.9-2: Sampling points of seawater CH_4 samples used for check of contamination

CTD Stn.	Sampling date (UTC)	Latitude (N)	Longitude (W)
002	08 Oct.	66°-00.17”	168°-44.72”
004	08 Oct.	67°-00.13”	168°-44.26”
005	09 Oct.	69°-00.19”	168°-45.18”
007	09 Oct.	69°-59.96”	168°-45.03”
009	10 Oct.	71°-59.76”	163°-29.99”
011	10 Oct.	72°-60.00”	160°-00.20”
013	11 Oct.	72°-19.98”	155°-00.52”
015	12 Oct.	71°-59.99”	147°-29.98”
019-1	16 Oct.	76°-59.96”	164°-59.94”
020-1	16 Oct.	77°-15.04”	164°-59.71”
021-1	17 Oct.	77°-30.01”	165°-00.01”
022-1	17 Oct.	77°-45.00”	165°-00.01”

(5) Data archive

Data obtained in this cruise will be submitted to the Data Management Group (DMG) of JAMSTEC, and will opened to the public via “Data Research System for Whole Cruise Information in JAMSTEC (DARWIN)” in JAMSTEC web site. <http://www.godac.jamstec.go.jp/darwin/e>

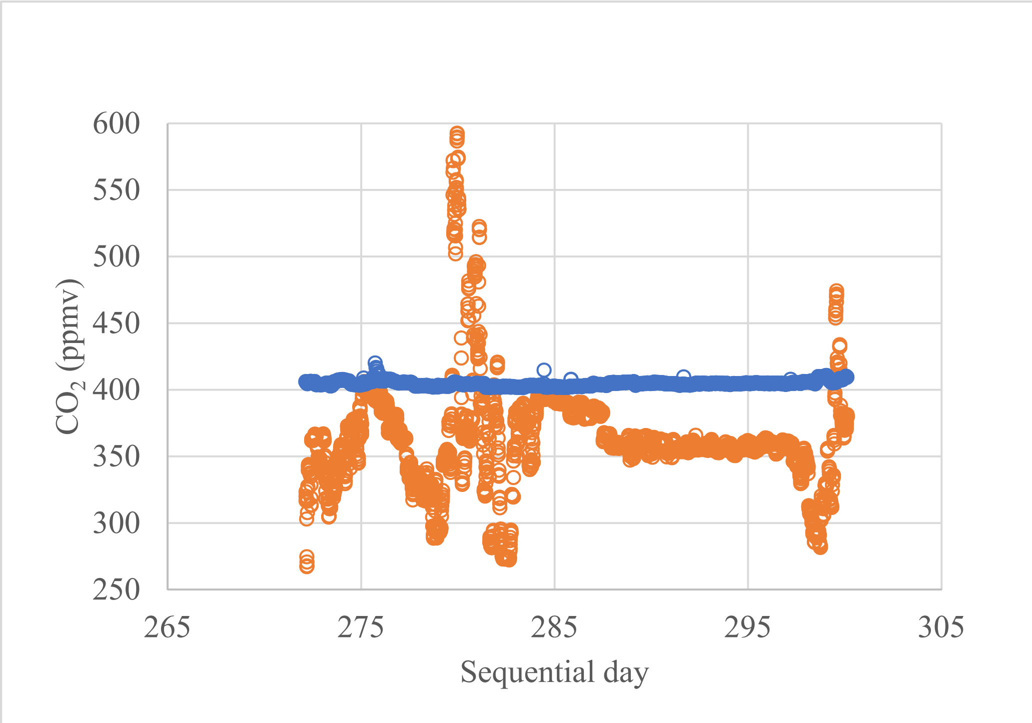

Figure 4.9-1: Temporal variations of atmospheric and surface seawater CO_2. Blue and orange colors show atmospheric and surface seawater CO_2 concentrations, respectively. The x-axis shows sequential day starting from Jan. 1, 2019

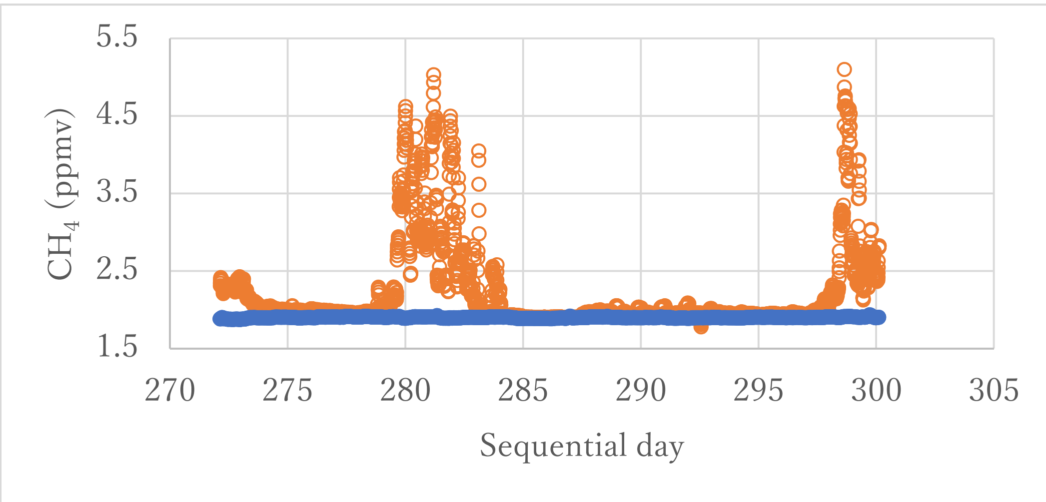

Figure 4.9-2: Temporal variations of atmospheric and surface seawater CH_4. Blue and orange colors show atmospheric and surface seawater CH_4 concentrations, respectively. The x-axis shows sequential day starting from Jan. 1, 2019

4.10 Underway DIC

(1) Personnel

Akihiko Murata	JAMSTEC	- PI
Hiroshi Hoshino	MWJ	
Masahiro Orui	MWJ	
Atsushi Ono	MWJ	

(2) Objective

Our purpose is to measure total dissolved inorganic carbon (DIC) concentration in surface seawater and reveal its spatial and temporal variations.

(3) Parameter

DIC

(4) Instruments and Methods

Continuous underway measurements of surface seawater C_T were made with the C_T measuring system (Nihon ANS, Inc.) installed in the R/V *Mirai* of JAMSTEC.

The underway water sampling device collects surface seawater in a ~300 ml borosilicate glass bottle automatically after overflow of the 3 times volume. Before measurement, water samples are kept at 20°C. The seawater is then transferred into a pipette (~15 ml), which is kept at 20°C by a water jacket, in which water from a water bath set at 20°C is circulated. CO_2 dissolved in a seawater sample is extracted in a stripping chamber of the CO_2 extraction system by adding phosphoric acid (~10 % v/v) of about 2 ml. The stripping chamber is approx. 25 cm long and has a fine frit at the bottom. The acid is added to the stripping chamber from the bottom of the chamber by pressurizing an acid bottle for a given time to push out the right amount of acid. The pressurizing is made with nitrogen gas (99.9999 %). After the acid is transferred to the stripping chamber, a seawater sample kept in a pipette is introduced to the stripping chamber by the same method as in adding an acid. The seawater reacted with phosphoric acid is stripped of CO_2 by bubbling the nitrogen gas through a fine frit at the bottom of the stripping chamber. The CO_2 stripped in the chamber is carried by the nitrogen gas (flow rates is 140 ml min^{-1}) to the coulometer through a dehydrating module. The module consists of two electric dehumidifiers (kept at ~2°C) and a chemical desiccant ($Mg(ClO_4)_2$).

(5) Observation log

Cruise track during underway DIC observation is shown in Figure 4.10-1.

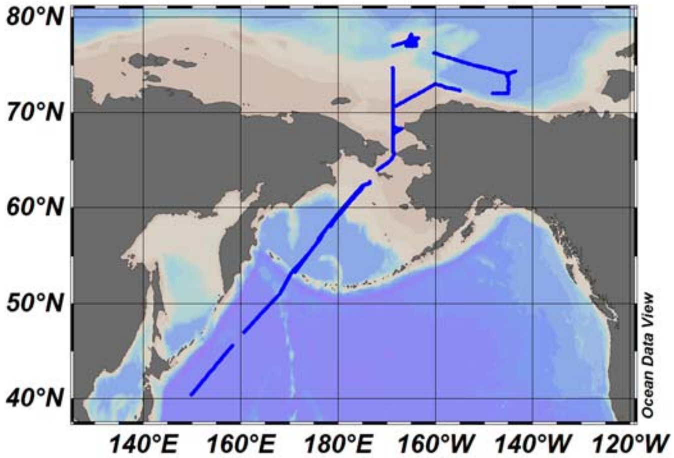

Figure 4.10-1: Cruise track for underway DIC

(6) Results

Temporal variations of surface seawater DIC and salinity-normalized DIC are shown in Figure 4.10-2.

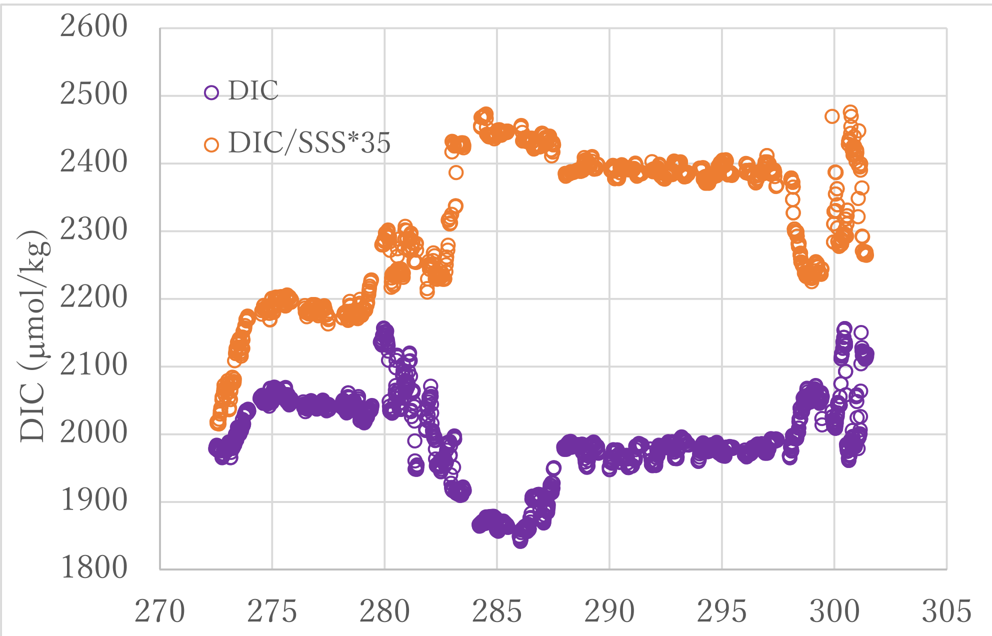

Figure 4.10-2: Temporal variations of surface seawater DIC and DIC normalized by a salinity of 35.

(7) Date archives

These data obtained in this cruise will be submitted to the Data Management Group (DMG) of JAMSTEC, and will open to the public via "Data Research System for Whole Cruise Information in JAMSTEC (DARWIN)" in JAMSTEC web site.

<http://www.godac.jamstec.go.jp/darwin/e>

4.11 Marine bioaerosol particles

(1) Personnel

Kaori Kawana	JAMSTEC	- not on board
Fumikazu Taketani	JAMSTEC	
Kazuhiko Matsumoto	JAMSTEC	- not on board
Yugo Kanaya	JAMSTEC	- not on board

(9) Objectives

Marine bioaerosol particles ejected from the sea surface affect the climate change via cloud processes by acting as cloud condensation nuclei and ice nucleating particles. Marine bioaerosol is produced directly at the sea surface due to the interaction between wind and waves. Organic matter becomes enriched in the surface microlayer with the organic gels. Transparent exopolymer particles (TEP), i.e., polysaccharide-rich microgels that are produced primarily by the abiotic coagulation of phytoplankton exudates, and Coomassie stainable particles (CSP) containing proteinaceous polymers released during cell lysis and decomposition are identifying as organic gels in the ocean interior. To investigate the air-sea interaction of biological particles, the abundance of biological particles in seawater is measured at the stations.

(10) Methods

i. Sampling and filtration for marine gel particles

Seawater samples were collected using a bucket and Niskin bottles or from laboratory water outlet (Table 4.11). To estimate the CSP concentrations, triplicate water samples of 200 mL were filtered onto 0.4-μm polycarbonate filters, and the filters were stained with 1 mL Coomassie brilliant blue solution and rinsed five times with 1 mL of Milli-Q water. Stained filter samples were stored in freezer until analysis. Water samples for the TEP were preserved through addition of formalin to a final concentration of 1% in refrigerator (4°C). Preserved samples will be filtered in the same way as CSP sample at the laboratory on land, and the filters will be stained with 1 mL alcian blue solution and rinsed thrice with 1 mL of Milli-Q water.

ii. Colorimetric measurement for marine gel particles

For the colorimetric analysis of TEP, the stained filter samples will be soaked for 2 - 5 h in 6 mL of 80% sulfuric acid (H_2SO_4) to elute the dye and then the absorbance of the solution is measured at 787 nm in a 1 cm cuvette. For the colorimetric analysis of CSP, the stained filter samples will be soaked for 2 h in 4 mL of 3% sodium dodecyl sulfate (SDS) in 50% isopropyl alcohol with sonication to elute the dye and then the absorbance of the solution is measured at 615 nm in a 1 cm cuvette. All samples are going to be analyzed in laboratory by above method.

iii. measurements for marine bioaerosols

For marine bioaerosol analysis, seawater samples were filtered by the membrane filter onto the gold-coated chip, and the abundance of bioaerosol particles (dead/alive) was counted using a Bioplorer (KB-VKH01, Koyo Sangyo Co., Ltd), based on the fluorescence measurements with UV and green light excitation. The stained fluorescence measurements were also conducted with reagents of DAPI and Hoechst.

(11) Data archive

The data obtained during this cruise will be submitted to the JAMSTEC Data Management Group (DMG).

Table 4.11: Sampling locations

On board ID	Date Collected					Latitude			Longitude		
	YYYY	MM	DD	hh:mm:ss	UTC/JST	Deg.	Min.	N/S	Deg.	Min.	E/W
MR1903C-TEP-001	2019	10	05	2:20	UTC	55	48.49	N	174	47.96	E
MR1903C-TEP-002	2019	10	08	6:45	UTC	65	39.66	N	168	27.73	W
MR1903C-TEP-003	2019	10	09	5:10	UTC	69	00.00	N	168	45	W
MR1903C-TEP-004	2019	10	10	7:55	UTC	71	59.51	N	163	30.51	W
MR1903C-TEP-005	2019	10	11	6:55	UTC	72	30.00	N	156	17.79	W
MR1903C-TEP-006	2019	10	12	8:45	UTC	71	59.99	N	147	29.98	W
MR1903C-TEP-007	2019	10	15	16:48	UTC	76	27.95	N	161	38.51	W
MR1903C-TEP-008	2019	10	16	5:15	UTC	77	00.00	N	165	00.00	W
MR1903C-TEP-009	2019	10	18	6:35	UTC	77	15.00	N	165	00.03	W
MR1903C-TEP-010	2019	10	21	6:37	UTC	77	15.00	N	165	59.97	W
MR1903C-TEP-011	2019	10	21	6:37	UTC	77	15.00	N	165	59.97	W
MR1903C-TEP-012	2019	10	21	6:37	UTC	77	15.00	N	165	59.97	W
MR1903C-TEP-013	2019	10	21	6:37	UTC	77	15.00	N	165	59.97	W
MR1903C-TEP-014	2019	10	22	7:04	UTC	77	00.37	N	165	59.88	W
MR1903C-TEP-015	2019	10	23	6:30	UTC	77	00.01	N	164	00.01	W
MR1903C-TEP-016	2019	10	25	8:59	UTC	77	00.22	N	168	46.13	W
MR1903C-TEP-017	2019	10	26	5:39	UTC	74	00.01	N	168	44.83	W
MR1903C-TEP-018	2019	10	26	13:08	UTC	73	00.03	N	168	45.04	W
MR1903C-TEP-019	2019	10	26	16:51	UTC	72	30.00	N	168	44.61	W
MR1903C-TEP-020	2019	10	27	5:42	UTC	70	00.00	N	168	44.92	W
MR1903C-TEP-021	2019	10	27	13:00	UTC	69	30.19	N	168	45.23	W
MR1903C-TEP-022	2019	10	28	5:05	UTC	68	00.88	N	168	52.05	W
MR1903C-TEP-023	2019	10	28	10:42	UTC	67	30.07	N	168	45.11	W
MR1903C-TEP-024	2019	10	28	17:22	UTC	66	29.99	N	168	45.02	W
MR1903C-TEP-025	2019	11	03	0:10	UTC	50	00.00	N	166	08.00	E
MR1903C-TEP-026	2019	11	03	0:00	UTC	50	00.00	N	166	08.00	E
MR1903C-TEP-027	2019	11	03	0:00	UTC	50	00.00	N	166	08.00	E

4.12. Phytoplankton

(1) Personnel

Kohei Matsuno	Hokkaido University	- PI
Atsushi Yamaguchi	Hokkaido University	
Yoshiyuki Abe	Tokyo University	
Koki Tokuhiro	Hokkaido University	
Yuri Fukai	Hokkaido University	
Fumihiko Kimura	Hokkaido University	
Nao Sato	Hokkaido University	

(2) Objective

The goals of this study are following:

1) Clarify the horizontal distribution of phytoplankton community analyzed by a multi-spectral excitation/emission fluorometer (MFL), a high-performance liquid chromatography (HPLC) and chlorophyll *a* in surface water
2) Clarify the spatial distribution of microprotist community analyzed by MFL, HPLC, chlorophyll *a* and microscopy

(3) Sampling and treatment

(3-1) Surface monitoring

A multi-spectral excitation/emission fluorometer (MFL) was set in a calibration black bucket. The surface water from a branch line of underway monitoring system was continuously flowing into the bucket from 30 September to 11 November. We took the surface water samples from underway system once a day for measure chlorophyll *a* and HPLC. Seawater samples (0.25 L) for total chlorophyll *a* were vacuum-filtrated (< 0.013 MPa) through Whatman GF/F filter (25 mm-in diameter). Phytoplankton pigments retained on the filters were immediately extracted in a cuvette tube immersed with 6 ml of *N,N*-dimethylformamide, stored and extracted for >24 hours. After extract the pigment, these samples were measured fluorescence with a Turner model 10-005-R Filter Fluorometer. To estimate the chlorophyll *a* concentrations, we applied to the fluorometric “Acidification method” (Holm-Hansen et al., 1965). The correlation of fluorescence between sensor data and bottle data was shown (Fig. 4.12-1). For HPLC sample, seawater (2 L) were vacuum-filtrated (< 0.013 MPa) through Whatman GF/F filter (25 mm-in diameter). The filters were preserved in –80°C.

(3-2) Spatial distribution by Niskin sampler and bucket

Sea water samples (1 L) were collected from 0, 10, 20, 30, 40, 50 m and chlorophyll *a* maximum layer by bucket and Niskin water sampler at 44 stations (Fig. 4.12-2, Table 4.12). The water samples were fixed by acid lugol (1% final concentration). In the land laboratory, the samples will be concentrated to 20 mL with a syphon, and microprotists will be enumerated and identified under an inverted microscopy. Additionally, seawater samples (0.25 L) for total chlorophyll *a* were also vacuum-filtrated (< 0.013 MPa) through Whatman GF/F filter (25 mm-in diameter). After the filtering, the chlorophyll *a* was measured as mentioned above (see 3-1). A multi-spectral excitation/emission fluorometer (Multi-Exciter, JFE-Advantech Co. Ltd.) was attached on the CTD frame to measure the vertical profile of chl. *a* fluorescence.

(4) Station list

Table 4.12: Data on water samples collected by niskin sampler and bucket. Circle indicate MFL was attached on the CTD frame. Chlorophyll *a* was measured at same depth to lugol samples for microscopy.

St.	Date	Latitude (N)		Longitude			Sampling depth (m)	MFL
St. 011 (CTD001)	2019/10/7	65	38.27	168	27.79	W	0,10,20,30,40	○
St. 013 (CTD003)	2019/10/8	66	30.03	168	45.12	W	0,10,20,30,40	○
St. 014 (CTD004)	2019/10/8	67	0.72	168	42.61	W	0,10,20,30,25	○
St. 018 (CTD005)	2019/10/8	69	0.62	168	45.63	W	0,10,20,30,40,5	○
St. 019 (CTD006)	2019/10/8	69	29.91	168	45.04	W	0,10,20,30,40,15	○
St. 021 (CTD008)	2019/10/9	70	29.81	168	46.26	W	0,10,20,30,15	○
St. 024 (CTD009)	2019/10/9	71	59.23	163	30.98	W	0,10,20,30	○
St. 025 (CTD010)	2019/10/10	72	29.94	161	44.83	W	0,10,20,30,13	○
St. 026 (CTD011)	2019/10/10	72	59.93	160	0.76	W	0,10,20,30,40,50,12	○
St. 029 (CTD012)	2019/10/10	72	30.01	156	15.16	W	0,10,20,30,40,50,27	
St. 030 (CTD013)	2019/10/11	72	19.94	155	0.4	W	0,10,20,30,40,50,18	
St. 031 (CTD014)	2019/10/11	72	9.84	153	45.51	W	0,10,20,30,40,50,13	
St. 034 (CTD015)	2019/10/11	72	0	147	30	W	0,10,20,30,40,50,33	
St. 035 (CTD016)	2019/10/12	71	59.94	144	59.79	W	0,10,20,30,40,50,45	
St. FP2 (CTD017)	2019/10/14	74	46.17	150	30.68	W	0,10,20,30,40,50,34	
St. FP3 (CTD018)	2019/10/15	76	28.18	161	37.53	W	0,10,20,30,40,50,5	
St. 39-01 (CTD019-01)	2019/10/15	76	59.98	164	59.99	W	0,10,20,30,40,50,43	
St. 40-02 (CTD020-02)	2019/10/16	77	14.95	164	59.57	W	0,10,20,30,40,50,38	○
St. 42-01 (CTD022-01)	2019/10/17	77	45.03	165	0	W	0,10,20,30,40,50,45	○
St. 40-03 (CTD020-03)	2019/10/17	77	15.14	164	59.8	W	0,10,20,30,40,50,15	○
St. 42-02 (CTD022-02)	2019/10/18	77	45.01	165	0.35	W	0,10,20,30,40,50,45	○
St. MIZ-03 (CTD023)	2019/10/18	78	2.63	164	57.41	W	0,10,20,30,40,50,25	○
St. 39-02 (CTD019-02)	2019/10/18	77	0.11	164	59.79	W	0,10,20,30,40,50,15	○
St. 41-03 (CTD021-03)	2019/10/19	77	30	165	0.04	W	0,10,20,30,40,50,12	○
St. 39-03 (CTD019-03)	2019/10/19	77	0.18	164	59.78	W	0,10,20,30,40,50,27	○
St. 41-04 (CTD021-04)	2019/10/20	77	30	164	59.99	W	0,10,20,30,40,50,15	○
St. 43 (CTD024)	2019/10/20	77	15.14	166	0.01	W	0,10,20,30,40,50,15	
St. 39-04 (CTD019-04)	2019/10/21	77	0.19	164	59.74	W	0,10,20,30,40,50,42	○
St. 44 (CTD025)	2019/10/21	77	0.32	166	0.09	W	0,10,20,30,40,50,34	
St. 39-05 (CTD019-05)	2019/10/22	77	0.08	164	59.78	W	0,10,20,30,40,50,36	○
St. 45 (CTD026)	2019/10/22	77	0.13	164	0.16	W	0,10,20,30,40,50,15	

St.	Date	Latitude (N)		Longitude			Sampling depth (m)	MFL
St. 39-06 (CTD019-06)	2019/10/22	77	0.02	164	59.75	W	0,10,20,30,40,50,15	○
St. 46 (CTD027)	2019/10/23	77	15.15	163	59.29	W	0,10,20,30,40,50,15	
St. 39-07 (CTD019-07)	2019/10/24	77	0.29	164	59.71	W	0,10,20,30,40,50,17	○
St. 49 (CTD028)	2019/10/24	77	0.13	168	45.56	W	0,10,20,30,40,50,15	
St. 52 (CTD029)	2019/10/25	74	0.02	168	44.46	W	0,10,20,30,40,50,15	○
St. 54 (CTD031)	2019/10/26	73	0	168	44.99	W	0,10,20,30,40,50,17	○
St. 60 (CTD034)	2019/10/26	70	0	168	44.98	W	0,10,20,30,40,50,15	
St. 61 (CTD035)	2019/10/27	69	30.04	168	45.26	W	0,10,20,30,40,50,15	
St. 62 (CTD036)	2019/10/27	69	0.09	168	41.27	W	0,10,20,30,40,50,12	
St. 68 (CTD037)	2019/10/27	68	0.83	167	52.23	W	0,10,20,30,40,50,15	
St. 70 (CTD038)	2019/10/27	67	47.02	168	36.15	W	0,10,20,30,40,50,15	
St. 71 (CTD039)	2019/10/27	67	30.03	168	45.08	W	0,10,20,30,40,50,12	
St. 72 (CTD040)	2019/10/28	67	0.03	168	44.69	W	0,10,20,30,40,50,12	

(5) Preliminary results

As a preliminary results, we present following items.

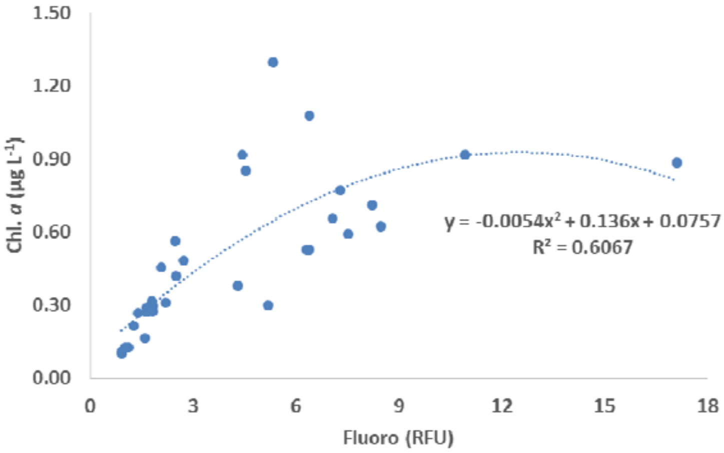

Figure 4.12-1: Correlation of fluorescence between sensor data and bottle data.

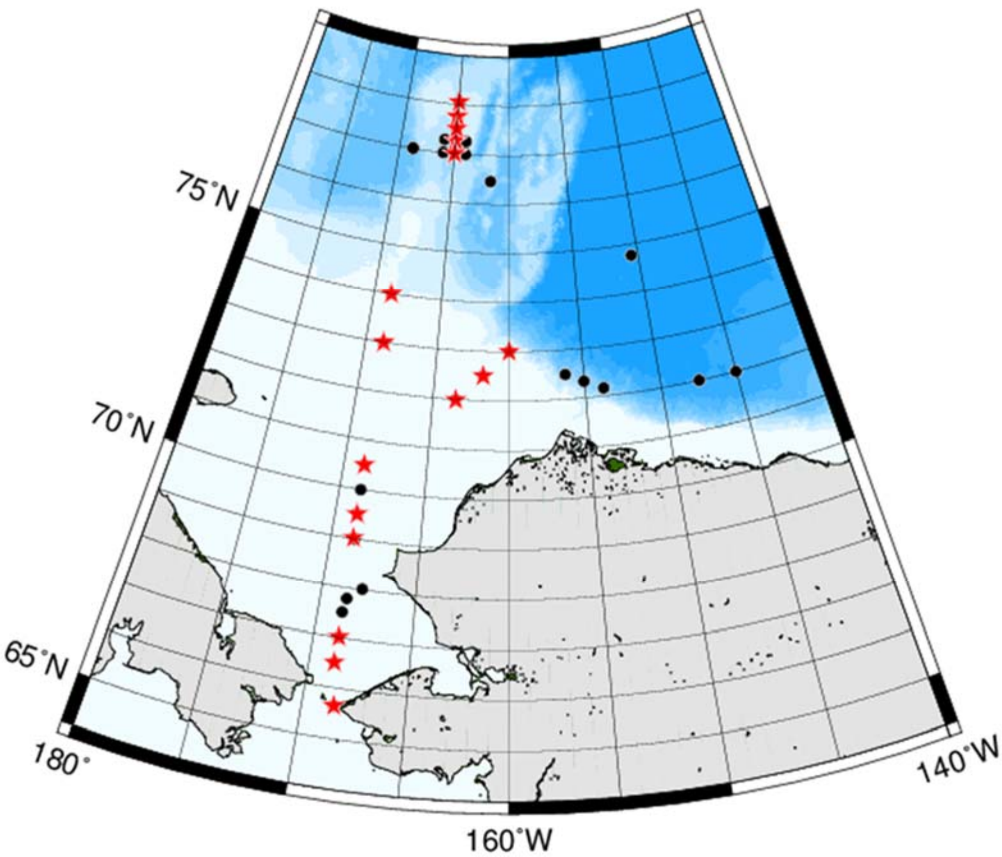

Figure 4.12-2: Location of the water sampling and MFL stations in the Pacific sector of Arctic Ocean (circles: CTD+bucket, stars: CTD+bucket+MFL).

4.13 Zooplankton net samplings

(1) Personnel

Kohei Matsuno	Hokkaido University	-PI
Atsushi Yamaguchi	Hokkaido University	
Yoshiyuki Abe	Tokyo University	
Koki Tokuhiro	Hokkaido University	
Yuri Fukai	Hokkaido University	
Fumihiko Kimura	Hokkaido University	
Nao Sato	Hokkaido University	

(2) Objective

The goals of this study are following:

1) Clarify the temporal changes of plankton community in pre- ice covered season
2) Evaluate physical conditions (gut pigments, DNA of fecal pellets, stable isotope and lipid composition) of the Pacific and Arctic copepods in the Arctic Ocean
3) Estimate the amount of the transported Pacific copepods into the Arctic Ocean
4) Clarify the grazing impact of the arctic copepods in pre- ice covered season

(3) Sampling

Zooplankton samples were collected by vertical haul of Quad-NORPAC nets at 58 stations in the pacific sector of Arctic Ocean. Quad-NORPAC net (mesh sizes: 335, 150 and two 63 µm [one is for fixed sample and the other has large size cod-end to collected fresh samples for incubation], mouth diameter: 45 cm) was towed between surface and 150 m depth or bottom -10 m (stations where the bottom shallower than 150 m) at all stations (Figure 4.13 and Table 4.13-1). Zooplankton samples collected by the NORPAC net with 335, 150 and 63 µm mesh were immediately fixed with 5% buffered formalin for zooplankton structure analysis. Samples collected with 63 µm mesh were used for picking up pterapods and evaluation of the copepod physiological activity (i.e., gut pigments, DNA of fecal pellets, stable isotope and lipid composition). After the sorting, the remaining sub-samples were fixed with 99.5% ethanol for analysis on radiolaria (investigator: Dr. Yasuhide Nakamura [JSPS PD]). The volume of water filtered through the net was estimated from the reading of a flow-meter mounted in the mouth ring.

80 cm ring net (mesh: 335 µm, mouth diameter: 80 cm) was towed between surface and 300 m depth or bottom -10 m at 32 stations (Figure 4.13 and Table 4.13-2),fresh samples were used for picking up pterapods and evaluation of the copepod physiological activity (i.e., gut pigments, DNA of fecal pellets, stable isotope and lipid composition).

Closing PCP net (mesh size: 63 µm, mouth diameter: 45 cm) was towed at shallow 3 stations from 2 layers (0-20, 20-bottom-10 m) and deep one station from 5 layers (0−50, 50–100, 100–250, 250–500, 500–1000 m). The volume of water filtered through the net was estimated from the reading of a flow-meter mounted in the mouth ring. Zooplankton samples collected by closing PCP net were immediately fixed with 5% buffered formalin for zooplankton structure analysis (Figure 4.13 and Table 4.13-3).

(4) On-board treatment

[gut pigments, DNA of fecal pellets, stable isotope and lipid composition]

Fresh zooplankton samples collected with Bucket net or ring net were roughly divided. One aliquot was immediately added with 10% soda water (CO_2 water) used for gut pigment and lipid composition analyses. We sorted with late copepodid stages of the Pacific copepods (*Neocalanus cristatus, N. plumchrus, N. flemingeri, Eucalanus bungii, Metridia pacifica*), the Arctic copepods (*Calanus glacialis, C. hyperboreus, M. longa*). Some specimens were rinsed with Milli-Q water, transferred into a small plastic case (3 mL) and stored in –20°C for lipid analysis. Other specimens transferred into a cuvette tube immersed with 6 ml dimethylformamide, stored and extracted for >24 hours. After extract the pigment, these samples were measured fluorescence with a Turner model 10-005-R Filter Fluorometer. The other aliquot without soda water were used for DNA of fecal pellets and stable isotope analyses. The identified species were targeted as much as possible (copepods, krills, chaetognaths, appendicularians, ostracods etc.). The sorted animals were incubated in DNA-free sea water collected from chl. *a* maximum layer with niskin bottle. After several hours, the evacuated fecal pellets were picked up and preserved in -20°C. And, the remaining animals were rinsed with Milli-Q water, transferred into a microplate and stored in –20°C for stable isotope analysis. Additionally, seawater (1-4 L) collected by niskin sampler from chlorophyll *a* maximum layer were filtered through 100, 10 and 0.8 μm filters for *in-situ* DNA, and 100 μm and GF/F filters for *in-situ* stable isotope. All of the filters were preserved in –20°C.

(5) Station list

Table 4.13–1: Data on plankton samples collected by vertical hauls with Quad- NORPAC net. GG54: 335 μm mesh.

Table 4.13–2: Data on plankton samples collected by vertical hauls with ring net (mesh size 335 μm).

Table 4.13–3: Data on plankton samples collected by vertical hauls with closing net (mesh size 63 μm).

Table 4.13-1. Data on plankton samples collected by vertical hauls with Quad-NORPAC net.
GG54: 0.335 mm mesh.

Station no.	Position Lat. (N)		Lon.		S.M.T. Date	Hour	Length of wire (m)	Angle of wire (°)	Depth estimated by wire angle (m)	Kind of cloth	Flowmeter No.	Reading	Estimated volume of water filtered (m^3)	Remark
FP1	64	40.11	169	55.12 W	7 Oct	13:02	37	18	35	GG54	3994	408	5.68	no CTD cast
RINKO 001										150 µm	3993	449	6.81	UTC-11h
										63 µm	3998	378	5.20	
										63 µm				for experiment, remaining ethanol
St. 011	65	38.27	168	27.79 W	7 Oct	19:08	38	10	37	GG54	3994	403	5.61	
CTD001										150 µm	3993	370	5.61	
										63 µm	3998	289	3.98	1)
										63 µm				for experiment, remaining ethanol
St. 013	66	30.03	168	45.12 W	8 Oct	1:25	39	3	39	GG54	3994	362	5.04	
CTD003										150 µm	3993	311	4.72	
										63 µm	3998	134	1.84	1)
										63 µm				for experiment, remaining ethanol
St. 014	67	0.72	168	42.61 W	8 Oct	6:01	34	5	34	GG54	3994	400	5.57	
CTD004										150 µm	3993	328	4.97	
										63 µm	3998	275	3.79	1)
										63 µm				for experiment, remaining ethanol
St. 018	69	0.62	168	45.63 W	8 Oct	19:03	42	8	42	GG54	3994	444	6.18	2)
CTD005										150 µm	3993	376	5.70	2)
										63 µm	3998	295	4.06	2)
										63 µm				for experiment, remaining ethanol
St. 019	69	29.91	168	45.04 W	8 Oct	22:03	42	8	42	GG54	3994	350	4.87	
CTD006										150 µm	3993	281	4.26	
										63 µm	3998	230	3.17	
										63 µm				for experiment, remaining ethanol
St. 021	70	29.81	168	46.26 W	9 Oct	6:55	28	1	28	GG54	3994	375	5.22	
CTD008										150 µm	3993	300	4.55	
										63 µm	3998	235	3.24	
										63 µm				for experiment, remaining ethanol
St. 024	71	59.23	163	30.98 W	9 Oct	21:54	28	7	28	GG54	3994	435	6.06	
CTD009										150 µm	3993	399	6.05	
										63 µm	3998	389	5.36	
										63 µm				for experiment, remaining ethanol
St. 025	72	29.94	161	44.83 W	10 Oct	2:48	35	5	35	GG54	3994	609	8.48	
CTD010										150 µm	3993	499	7.57	
										63 µm	3998	435	5.99	
										63 µm				for experiment, remaining ethanol
St. 026	72	59.93	160	0.76 W	10 Oct	8:49	151	8	150	GG54	3994	1502	20.92	
CTD011										150 µm	3993	1263	19.15	
										63 µm	3998	941	12.96	
										63 µm				for experiment, remaining ethanol
St. 029	72	30.01	156	15.16 W	10 Oct	18:07	150	1	150	GG54	3994	1522	21.20	
CTD012										150 µm	3993	1318	19.99	
										63 µm	3998	939	12.93	
										63 µm				for experiment, remaining ethanol
St. 030	72	19.94	155	0.4 W	11 Oct	2:05	150	4	150	GG54	3994	1450	20.19	
CTD013										150 µm	3993	1271	19.27	
										63 µm	3998	897	12.35	
										63 µm				for experiment, remaining ethanol
St. 031	72	9.84	153	45.51 W	11 Oct	5:17	151	7	150	GG54	3994	1514	21.08	
CTD014										150 µm	3993	1323	20.06	
										63 µm	3998	1122	15.45	
										63 µm				for experiment, remaining ethanol
St. 034	72	0	147	30 W	11 Oct	22:26	150	4	150	GG54	3994	1408	19.61	
CTD015										150 µm	3993	1153	17.48	
										63 µm	3998	842	11.59	
										63 µm				for experiment, remaining ethanol
St. 035	71	59.94	144	59.79 W	12 Oct	3:15	154	13	150	GG54	3994	1541	21.46	
CTD016										150 µm	3993	1298	19.68	
										63 µm	3998	951	13.09	
										63 µm				for experiment, remaining ethanol
St. FP2	74	46.17	150	30.68 W	14 Oct	7:22	151	8	150	GG54	3994	1870	26.04	
CTD017										150 µm	3993	1573	23.85	
										63 µm	3998	1390	19.14	
										63 µm				for experiment, remaining ethanol
St. FP3	76	28.18	161	37.53 W	15 Oct	4:45	151	7	150	GG54	3994	1377	19.18	
CTD018										150 µm	3993	1185	17.97	
										63 µm	3998	910	12.53	
										63 µm				for experiment, remaining ethanol
St. 39-01	76	59.98	164	59.99 W	15 Oct	17:30	150	4	150	GG54	3994	1302	18.13	line observation start
CTD019										150 µm	3993	1174	17.80	
										63 µm	3998	916	12.61	
										63 µm				for experiment, remaining ethanol

S.M.T. is UTC-11h
1) phytoplankton abundant
2) clione&limacina abundant

Table 4.13-1. (Continued.)

Station no.	Position Lat. (N)		Position Lon.		S.M.T. Date	S.M.T. Hour	Length of wire (m)	Angle of wire (°)	Depth estimated by wire angle (m)	Kind of cloth	Flowmeter No.	Flowmeter Reading	Estimated volume of water filtered (m^3)	Remark
St. MIZ-01	78	3.95	164	53.66 W	16 Oct	13:20	160	20	150	GG54	3994	1496	20.83	
RINKO 011										150 µm	3993	1254	19.01	
										63 µm	3998	1050	14.46	
										63 µm				for experiment, remaining ethanol
St. 040-02	77	14.95	164	59.57 W	16 Oct	19:22	150	0	150	GG54	3994	1345	18.73	
CTD020-02										150 µm	3993	1167	17.70	
										63 µm	3998	818	11.26	
										63 µm				for experiment, remaining ethanol
St. 042-01	77	45.03	165	0 W	17 Oct	3:08	150	2	150	GG54	3994	1362	18.97	
CTD022										150 µm	3993	1173	17.79	
										63 µm	3998	878	12.09	
										63 µm				for experiment, remaining ethanol
St. MIZ-02	78	0.26	164	59.61 W	17 Oct	11:35	153	12	150	GG54	3994	1315	18.31	
RINKO 013										150 µm	3993	1157	17.54	
										63 µm	3998	836	11.51	
										63 µm				for experiment, remaining ethanol
St. 040-03	77	15.14	164	59.8 W	17 Oct	18:34	151	6	150	GG54	3994	1383	19.26	
CTD020-03										150 µm	3993	1179	17.88	
										63 µm	3998	870	11.98	
										63 µm				for experiment, remaining ethanol
St. 042-02	77	45.01	165	0.35 W	18 Oct	1:35	155	14	150	GG54	3994	1430	19.91	
CTD022-02										150 µm	3993	1256	19.05	
										63 µm	3998	868	11.95	
										63 µm				for experiment, remaining ethanol
St. MIZ-03	78	2.63	164	57.41 W	18 Oct	10:21	154	13	150	GG54	3994	1585	22.07	
CTD023										150 µm	3993	1317	19.97	
										63 µm	3998	966	13.30	
										63 µm				for experiment, remaining ethanol
St. 39-02	77	0.11	164	59.79 W	18 Oct	20:24	150	0	150	GG54	3994	1320	18.38	
CTD019-02										150 µm	3993	1131	17.15	
										63 µm	3998	834	11.48	
										63 µm				for experiment, remaining ethanol
St. 41-03	77	30	165	0.04 W	19 Oct	3:44	150	1	150	GG54	3994	1358	18.91	
CTD021-03										150 µm	3993	1147	17.39	
										63 µm	3998	870	11.98	
										63 µm				for experiment, remaining ethanol
St. MIZ-04	78	3.40	164	57.68 W	19 Oct	13:23	155	14	150	GG54	3994	1485	20.68	
RINKO 017										150 µm	3993	1250	18.95	
										63 µm	3998	1019	14.03	
										63 µm				for experiment, remaining ethanol
St. 39-03	77	0.18	164	59.78 W	19 Oct	21:03	151	8	150	GG54	3994	1430	19.91	
CTD019-03										150 µm	3993	1175	17.82	
										63 µm	3998	951	13.09	
										63 µm				for experiment, remaining ethanol
St. 41-04	77	30	164	59.99 W	20 Oct	4:52	152	9	150	GG54	3994	1547	21.54	
CTD021-04										150 µm	3993	1322	20.05	
										63 µm	3998	1055	14.53	
										63 µm				for experiment, remaining ethanol
St. MIZ-05	78	0.64	164	59.14 W	20 Oct	11:35	162	22	150	GG54	3994	1785	24.86	
RINKO 020										150 µm	3993	1455	22.06	
										63 µm	3998	1310	18.04	
										63 µm				for experiment, remaining ethanol
St. 43	77	15.14	166	0.01 W	20 Oct	17:58	151	6	150	GG54	3994	1546	21.53	
CTD024										150 µm	3993	1302	19.74	
										63 µm	3998	1071	14.75	
										63 µm				for experiment, remaining ethanol
St. 39-04	77	0.19	164	59.74 W	21 Oct	0:53	150	3	150	GG54	3994	1361	18.95	
CTD019-04										150 µm	3993	1173	17.79	
										63 µm	3998	888	12.23	
										63 µm				for experiment, remaining ethanol
St. MIZ-06	78	1.17	164	58.78 W	21 Oct	11:40	164	24	150	GG54	3994	1694	23.59	
RINKO 022										150 µm	3993	1419	21.52	
										63 µm	3998	1383	19.04	
										63 µm				for experiment, remaining ethanol
St. 44	77	0.32	166	0.09 W	21 Oct	19:10	150	0	150	GG54	3994	1525	21.24	
CTD025										150 µm	3993	1247	18.91	
										63 µm	3998	1052	14.48	
										63 µm				for experiment, remaining ethanol
St. 39-05	77	0.08	164	59.78 W	22 Oct	0:39	153	12	150	GG54	3994	1493	20.79	
CTD019-05										150 µm	3993	1247	18.91	
										63 µm	3998	1020	14.04	
										63 µm				for experiment, remaining ethanol

S.M.T. is UTC-11h
1) phytoplankton abundant
2) clione&limacina abundant

Table 4.13-1. (Continued.)

Station no.	Position Lat. (N)		Lon.		S.M.T. Date	Hour	Length of wire (m)	Angle of wire (°)	Depth estimated by wire angle (m)	Kind of cloth	Flowmeter No.	Reading	Estimated volume of water filtered (m^3)	Remark
St. MIZ-07	77	46.6	164	4.28 W	22 Oct	13:26	153	12	150	GG54	3994	1518	21.14	
RINKO 024										150 µm	3993	1292	19.59	
										63 µm	3998	1004	13.82	
										63 µm				for experiment, remaining ethanol
St. 45	77	0.13	164	0.16 W	22 Oct	18:42	150	3	150	GG54	3994	1336	18.61	
CTD026										150 µm	3993	1115	16.91	
										63 µm	3998	852	11.73	
										63 µm				for experiment, remaining ethanol
St. 39-06	77	0.02	164	59.75 W	22 Oct	23:44	152	9	150	GG54	3994	1363	18.98	
CTD019-06										150 µm	3993	1169	17.73	
										63 µm	3998	862	11.87	
										63 µm				for experiment, remaining ethanol
St. MIZ-08	77	47.02	163	35.49 W	23 Oct	11:38	160	20	150	GG54	3994	1598	22.25	
RINKO 026										150 µm	3993	1295	19.64	
										63 µm	3998	1119	15.41	
										63 µm				for experiment, remaining ethanol
St. 46	77	15.15	163	59.29 W	23 Oct	16:28	153	12	150	GG54	3994	1530	21.31	
CTD027										150 µm	3993	1263	19.15	
										63 µm	3998	1047	14.42	
										63 µm				for experiment, remaining ethanol
St. 39-07	77	0.29	164	59.71 W	24 Oct	0:19	151	6	150	GG54	3994	1412	19.66	
CTD019-07										150 µm	3993	1196	18.14	
										63 µm	3998	938	12.91	
										63 µm				for experiment, remaining ethanol
St. MIZ-09	77	50	163	0 W	24 Oct	13:44	153	12	150	GG54	3994	1445	20.12	line observation end
RINKO 028										150 µm	3993	1464	22.20	
										63 µm	3998	1088	14.98	
										63 µm				for experiment, remaining ethanol
St. 49	77	0.13	168	45.56 W	24 Oct	23:57	151	6	150	GG54	3994	1381	19.23	
CTD028										150 µm	3993	1227	18.61	
										63 µm	3998	850	11.70	
										63 µm				for experiment, remaining ethanol
St. FT18	74	41.77	168	46.67 W	25 Oct	13:24	150	0	150	GG54	3994	1500	20.89	
RINKO 029										150 µm	3993	1282	19.44	
										63 µm	3998	1032	14.21	
										63 µm				for experiment, remaining ethanol
St. 52	74	0.02	168	44.46 W	25 Oct	17:52	151	6	150	GG54	3994	1417	19.73	
CTD029										150 µm	3993	1165	17.67	
										63 µm	3998	884	12.17	
										63 µm				for experiment, remaining ethanol
St. 54	73	0	168	44.99 W	26 Oct	2:41	51	10	50	GG54	3994	565	7.87	
CTD031										150 µm	3993	462	7.01	
										63 µm	3998	376	5.18	
										63 µm				for experiment, remaining ethanol
St. 56	72	0.01	168	44.95 W	26 Oct	9:27	40	14	39	GG54	3994	392	5.46	
RINKO 030										150 µm	3993	308	4.67	
										63 µm	3998	239	3.29	
										63 µm				for experiment, remaining ethanol
St. 58	70	59.99	168	45.03 W	26 Oct	15:44	34	3	34	GG54	3994	398	5.54	
RINKO 032										150 µm	3993	349	5.29	
										63 µm	3998	294	4.05	
										63 µm				for experiment, remaining ethanol
St. 60	70	0	168	44.98 W	26 Oct	22:22	30	12	29	GG54	3994	304	4.23	
CTD034										150 µm	3993	237	3.59	
										63 µm	3998	181	2.49	
										63 µm				for experiment, remaining ethanol
St. 61	69	30.04	168	45.26 W	27 Oct	1:35	41	0	41	GG54	3994	571	7.95	
CTD035										150 µm	3993	459	6.96	
										63 µm	3998	413	5.69	
										63 µm				for experiment, remaining ethanol
St. 62	69	0.09	168	41.27 W	27 Oct	5:48	42	13	41	GG54	3994	541	7.53	2)
CTD036										150 µm	3993	446	6.76	2)
										63 µm	3998	425	5.85	2)
										63 µm				for experiment, remaining ethanol
St. 63	68	30.15	168	45.17 W	27 Oct	9:02	43	7	43	GG54	3994	669	9.32	
RINKO 033										150 µm	3993	522	7.92	
										63 µm	3998	540	7.44	
										63 µm				for experiment, remaining ethanol
St. 64	68	17.97	166	56.32 W	27 Oct	14:02	24	13	23	GG54	3994	357	4.97	
RINKO 034										150 µm	3993	284	4.31	
										63 µm	3998	307	4.23	
										63 µm				for experiment, remaining ethanol

S.M.T. is UTC-11h

1) phytoplankton abundant

2) clione&limacina abundant

Table 4.13-1. (Continued.)

Station no.	Position Lat. (N)		Lon.		S.M.T. Date	Hour	Length of wire (m)	Angle of wire (°)	Depth estimated by wire angle (m)	Kind of cloth	Flowmeter No.	Reading	Estimated volume of water filtered (m^3)	Remark
St. 68	68	0.83	167	52.23 W	27 Oct	16:35	41	8	41	GG54	3994	798	11.11	
CTD037										150 µm	3993	650	9.86	
										63 µm	3998	578	7.96	
										63 µm				for experiment, remaining ethanol
St. 70	67	47.02	168	36.15 W	27 Oct	21:10	40	4	40	GG54	3994	552	7.69	
CTD038										150 µm	3993	469	7.11	
										63 µm	3998	400	5.51	
										63 µm				for experiment, remaining ethanol
St. 71	67	30.03	168	45.08 W	27 Oct	23:22	39	2	39	GG54	3994	480	6.68	
CTD039										150 µm	3993	400	6.07	
										63 µm	3998	370	5.09	
										63 µm				for experiment, remaining ethanol
St. 72	67	0.03	168	44.69 W	28 Oct	3:26	35	9	35	GG54	3994	498	6.94	
CTD040										150 µm	3993	419	6.35	
										63 µm	3998	359	4.94	
										63 µm				for experiment, remaining ethanol

S.M.T. is UTC-11h
1) phytoplankton abundant
2) clione&limacina abundant

Table 4.13-2. Data on plankton samples collected by vertical hauls with 80 cm ring net.
GG54: 0.335 mm mesh.

Station no.	Position Lat. (N)		Lon.		S.M.T. Date	Hour	Length of wire (m)	Angle of wire (°)	Depth estimated by wire angle (m)	Kind of cloth	Remark
St. 39-01 (CTD019)	77	0.01	164	59.86 W	15 Oct	17:43	300	1	300	GG54	for experiments
St. MIZ-01 (RINKO 011)	78	3.95	164	53.66 W	16 Oct	13:20	300	5	299	GG54	for experiments
St. 040-02 (CTD020-02)	77	14.95	164	59.57 W	16 Oct	19:34	300	1	300	GG54	for experiments
St. MIZ-02 (RINKO 013)	78	0.26	164	59.61 W	17 Oct	11:47	300	0	300	GG54	for experiments
St. 040-03 (CTD020-03)	77	15.14	164	59.8 W	17 Oct	18:46	300	6	298	GG54	for experiments
St. MIZ-03 (CTD023)	78	2.63	164	57.41 W	18 Oct	10:21	300	15	290	GG54	for experiments
St. 39-02 (CTD019-02)	77	0.11	164	59.79 W	18 Oct	20:37	300	0	300	GG54	for experiments
St. MIZ-04 (RINKO 017)	78	3.40	164	57.68 W	19 Oct	13:36	300	13	292	GG54	for experiments
St. 39-03 (CTD019-03)	77	0.18	164	59.78 W	19 Oct	21:17	600	7	596	GG54	for experiments
St. MIZ-05 (RINKO 020)	78	0.64	164	59.14 W	20 Oct	11:49	300	14	291	GG54	for experiments
St. 43 (CTD024)	77	15.14	166	0.01 W	20 Oct	18:13	710	3	709	GG54	for experiments
St. 39-04 (CTD019-04)	77	0.19	164	59.74 W	21 Oct	1:06	300	5	299	GG54	for experiments
St. MIZ-06 (RINKO 022)	78	1.17	164	58.78 W	21 Oct	11:55	300	8	297	GG54	for experiments
St. 44 (CTD025)	77	0.32	166	0.09 W	21 Oct	19:26	500	8	495	GG54	for experiments
St. 39-05 (CTD019-05)	77	0.08	164	59.78 W	22 Oct	0:52	300	0	300	GG54	for experiments
St. MIZ-07 (RINKO 024)	77	46.6	164	4.28 W	22 Oct	13:39	250	0	250	GG54	for experiments
St. 45 (CTD026)	77	0.13	164	0.16 W	22 Oct	18:56	400	0	400	GG54	for experiments
St. 39-06 (CTD019-06)	77	0.02	164	59.75 W	22 Oct	23:59	300	0	300	GG54	for experiments
St. MIZ-08 (RINKO 026)	77	47.02	163	35.49 W	23 Oct	11:50	250	0	250	GG54	for experiments
St. 46 (CTD027)	77	15.15	163	59.29 W	23 Oct	16:42	300	0	300	GG54	for experiments
St. 39-07 (CTD019-07)	77	0.29	164	59.71 W	24 Oct	0:32	300	2	300	GG54	for experiments
St. MIZ-09 (RINKO 028)	77	50	163	0 W	24 Oct	13:55	250	9	247	GG54	for experiments
St. 49 (CTD028)	77	0.13	168	45.56 W	25 Oct	0:09	300	1	300	GG54	for experiments
St. 52 (CTD029)	74	0.02	168	44.46 W	25 Oct	18:06	150	4	150	GG54	for experiments
St. 54 (CTD031)	73	0	168	44.99 W	26 Oct	2:48	51	2	51	GG54	for experiments
St. 58 (RINKO 032)	70	59.99	168	45.03 W	26 Oct	15:52	34	4	34	GG54	for experiments
St. 60 (CTD034)	70	0	168	44.98 W	26 Oct	22:31	30	2	30	GG54	for experiments
St. 61 (CTD035)	69	30.04	168	45.26 W	27 Oct	1:43	41	3	41	GG54	for experiments
St. 62 (CTD036)	69	0.09	168	41.27 W	27 Oct	5:56	42	7	42	GG54	for experiments
St. 63 (RINKO 033)	68	30.15	168	45.17 W	27 Oct	9:12	43	2	43	GG54	for experiments
St. 68 (CTD037)	68	0.83	167	52.23 W	27 Oct	16:44	41	0	41	GG54	for experiments
St. 70 (CTD038)	67	47.02	168	36.15 W	27 Oct	21:20	40	3	40	GG54	for experiments

S.M.T. is UTC-11h

Table 4.13-3. Data on plankton samples collected by vertical hauls with closing PCP net. The number in the parenthesis means the number of sorted from the sample.

Station no.	Position Lat. (N)	Position Lon.	S.M.T. Date	S.M.T. Hour	Length of wire (m)	Angle of wire (°)	Depth estimated by wire angle (m)	Closed net depth (m)	Kind of cloth	Flowmeter No.	Flowmeter Reading	Estimated volume of water filtered (m^3)	Remark
St.014	67 0.72	168 42.61 W	8 Oct	6:10	20	3	20	0	63 µm	2374	169	2.54	No record of sorted species
CTD004				6:16	34	2	34	21	63 µm	2374	274	4.12	No record of sorted species
St. 021	70 29.81	168 46.26 W	9 Oct	7:02	20	3	20	0	63 µm	2374	205	3.09	
CTD008				7:07	28	10	28	18	63 µm	2374	142	2.14	
St. 024	71 59.23	163 30.98 W	9 Oct	22:05	20	1	20	0	63 µm	2374	202	3.04	Sorted *L. helicina* (1)
CTD009				22:11	28	5	28	18	63 µm	2374	179	2.69	
St. FP2	74 46.19	150 30.79 W	14 Oct	7:42	50	6	50	0	63 µm	2374	593	8.92	Sorted *Themisto libellua* (1)
CTD017				7:51	100	4	100	50	63 µm	2374	443	6.67	Sorted *P. glacialis* C5F (1), C4F (2), C3 (3)
				8:03	250	0	250	103	63 µm	2374	890	13.39	Sorted *Aetideopsis multiserrata* C5F (1), *Chiridius obtusifrons* C6F (1), *C. hyperboreus* C6F (1), *Gaetanus tenuispinus* C5M (1), *Heterorhabdus norvegicus* C6F (1), C6M (1), *Scaphocalanus magnus* C5M (1), Appendicularia (1)
				8:19	500	2	500	259	63 µm	2374	1505	22.65	Sorted *C. obtusifrons* C6F (3), *C. hyperboreus* C6F (2), *H. norvegicus* C6F (3), C6M (2), *S. magnus* C6F (1), C5F (4), C5M (2), Amphipoda (1), *Boroecia maxima* (15), *Eukrohnia hamata* (2)
				8:41	1001	1	1001	503	63 µm	2374	2809	42.27	Sorted *A. multiserrata* C6F (1), *G. brevispinus* C6F (2), *S. magnus* C5M (1), Appendicularia (5), Amphipoda (4), Decapoda (1)

S.M.T. is UTC-11h

(6) Preliminary results

As a preliminary results, we present following items.

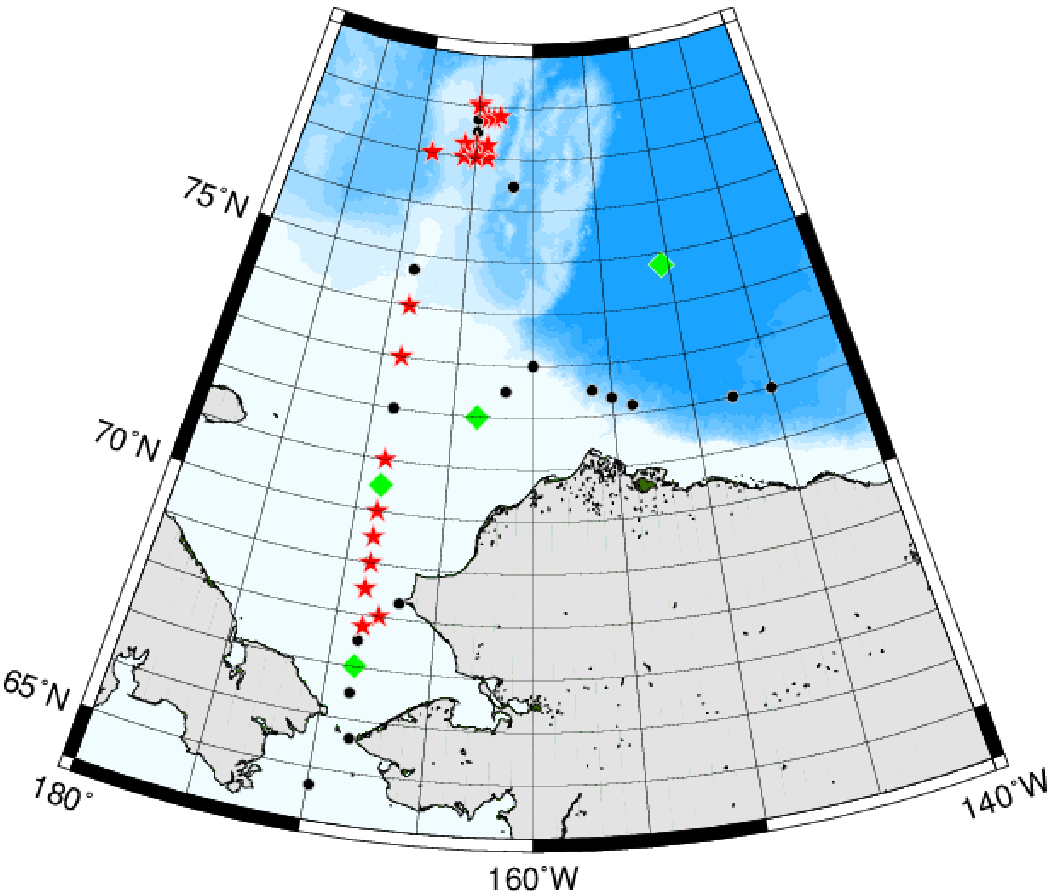

Figure 4.13: Location of the sampling stations in the Pacific sector of Arctic Ocean (circles: NORPAC net, diamonds: NORPAC net + closing nets, stars: NORPAC net + Ring net).

4.14 Zooplankton incubation

(1) Personnel

Kohei Matsuno	Hokkaido University	- PI
Atsushi Yamaguchi	Hokkaido University	
Yoshiyuki Abe	Tokyo University	
Koki Tokuhiro	Hokkaido University	
Yuri Fukai	Hokkaido University	
Fumihiko Kimura	Hokkaido University	
Nao Sato	Hokkaido University	

(2) Objective

The goals of this study are following:

1) Evaluate the effect of temperature on growth rate and Sr/Ca ratio for pteropods in the Arctic Ocean

(3) Sampling and treatment

Fresh pterapods (Figure 4.14) were collected by bucket net with large size cod-end (mesh: 63 µm, mouth diameter: 45 cm) or ring net (mesh: 335 µm, mouth diameter: 80 cm) in the Pacific sector of Arctic Ocean. The bucket net and ring net were towed between surface and 150-300 m depth or bottom -10 m (stations where the bottom shallower than 150 m) at 58 and 32 stations, respectively (Table 4.13-1, 4.13-2). Fresh pterapods specimens (*Limacina helicina*) were immediately sorted and poured into a 500 mL bottle filled filtered seawater for acclimation. At same station, water samples from chlorophyll *a* maximum were collected with niskin sampler as reference of in-situ Sr/Ca ratio and oxygen stable isotope (Table 4.14). After acclimation, alive pterapods incubated in seawater with calcein (50 mg L^{-1}) during one hour, and then the specimens were rinsed with Milli-Q water gently, and incubated in 500 mL bottles filled with filtered seawater at 3, 4, 5 and 6ºC in incubators. After three-weeks incubation, the specimens were checked alive or dead, and preserved in -80ºC.

In the land laboratory, the growth part of the shell will be measured under an epifluorescence microscope with UV light excitation, and Sr/Ca ration and stable isotope in the part will also be measured.

(4) Station list

Sampling station of net samplings is described Table 4.13-1 and 4.13-2 in previous section.

Table 4.14: List of water samples for Sr/Ca ratio and oxygen stable isotope.

Date	St.	Sampling depth (m)
2019/10/8	St. 011 (CTD001)	30
2019/10/8	St. 014 (CTD004)	10,30
2019/10/8	St. 021 (CTD008)	10,30
2019/10/9	St. 024 (CTD009)	10,30
2019/10/14	St. FT2 (CTD017)	30,75,150
2019/10/19	St. 39-03 (CTD019-03)	5,10
2019/10/20	St. 41-04 (CTD021-04)	5
2019/10/20	St. 43 (CTD024)	5
2019/10/20	St. 39-04 (CTD019-04)	5
2019/10/21	St. 44 (CTD025)	20
2019/10/22	St. 39-05 (CTD019-05)	20
2019/10/22	St. 45 (CTD026)	10,20
2019/10/23	St. 46 (CTD027)	10
2019/10/24	St. 49 (CTD028)	20
2019/10/25	St. 52 (CTD029)	20
2019/10/26	St. 54 (CTD031)	20
2019/10/26	St. 60 (CTD034)	20
2019/10/27	St. 61 (CTD035)	20
2019/10/27	St. 62 (CTD036)	20
2019/10/27	St. 68 (CTD037)	20

(5) Preliminary results

As a preliminary results, we present following items.

Figure 4.14: The picture of alive pterapods.

4.15. Sea bottom sediments

(1) Personnel

Kohei Matsuno	Hokkaido University	-PI
Atsushi Yamaguchi	Hokkaido University	
Yoshiyuki Abe	Tokyo University	
Koki Tokuhiro	Hokkaido University	
Yuri Fukai	Hokkaido University	
Fumihiko Kimura	Hokkaido University	
Nao Sato	Hokkaido University	

(2) Objective

The goals of this study are following:

1) Clarify the spatial distribution of diatom resting cells in sediment in the Pacific sector of Arctic Ocean

(3) Sampling

Sea bottom sediments were collected by Smith-McIntyre sampler at 8 stations in the Pacific sector of Arctic Ocean (Figure 4.15). We inserted a liner tube (diameter:3.6 cm) and cut the sediment from surface to 3 cm depth, and the samples were sorted in dark and cool (~4ºC) condition. More than one-month later, their containing resting cells will be quantified by incubation (most probable number method). Other aliquot (0-1 cm) were cut and preserved in dark and cool condition for dinoflagellates analysis (investigator: Dr. So-Young Kim [KOPRI]). Additionally, surface sediments (0-3 cm) and short core samples (0-3-6 cm) were cut and sorted in dark and cool condition for isolation of diatom *Skeletonema* spp. (investigator: Dr. Satoshi Nagai [AFFRC]).

(4) Station list

Table 4.15: Station list of sediments samples collected with Smith-McIntyre sampler at 8 stations in the Pacific sector of Arctic Ocean during October 2019.

St.	Date	Latitude (N)		Longitude			Bottom depth (m)
FP1 (RINKO 001)	2019/10/7	64	40.11	169	55.12	W	47
St. 14 (CTD 004)	2019/10/8	67	0.72	168	42.61	W	44
St. 18 (CTD 005)	2019/10/8	69	0.62	168	45.63	W	52
St. 21 (CTD 008)	2019/10/9	70	29.81	168	46.26	W	38
St. 24 (CTD 009)	2019/10/9	71	59.23	163	30.98	W	38
St. 60 (CTD 034)	2019/10/26	70	0	168	44.98	W	40
St. 68 (CTD 037)	2019/10/27	68	0.83	167	52.23	W	51
St. 70 (CTD 038)	2019/10/27	67	47.02	168	36.15	W	50

(5) Preliminary results

As a preliminary results, we present following item.

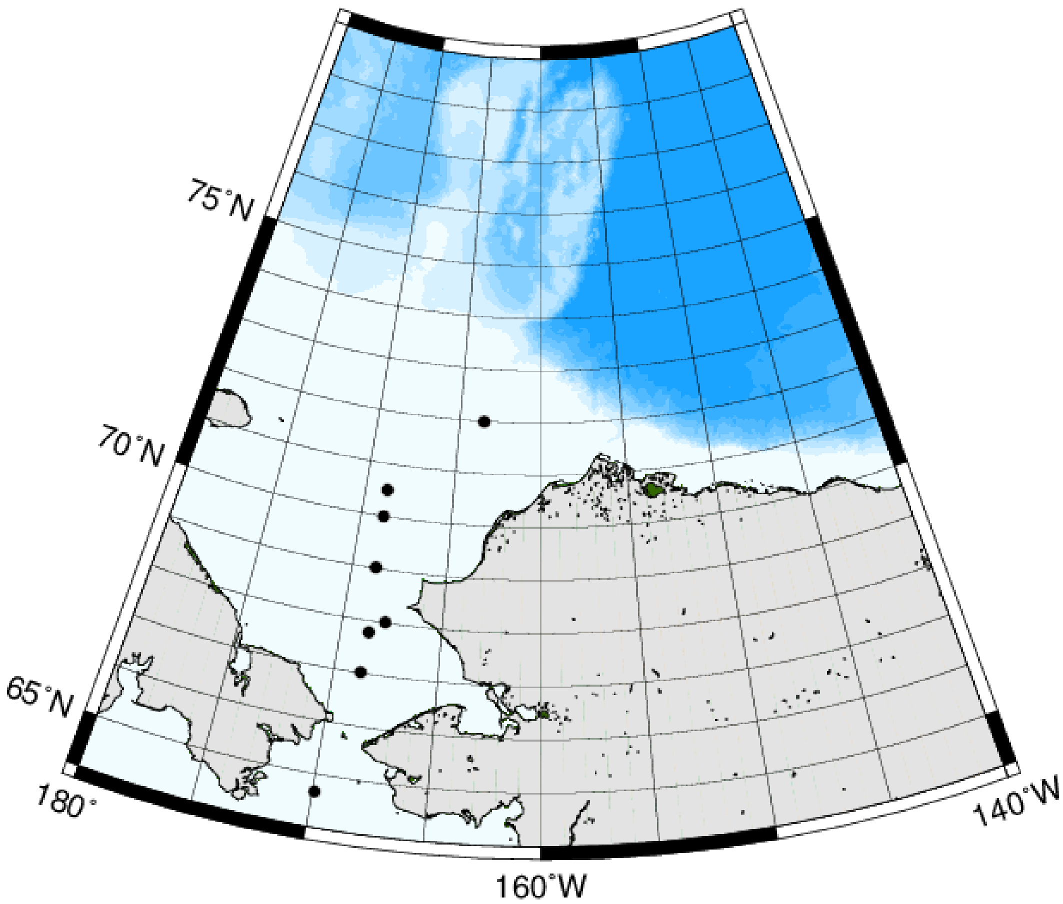

Figure 4.15: Location of the sampling stations for collecting bottom sediments in the Pacific sector of Arctic Ocean during October 2019. Black dots indicates the sampling stations.

5. Geology

5.1. Sea Bottom Topography Measurement

(1) Personnel

Kazutoshi Sato	KIT	-PI
Ryo Ohyama	NME	
Souichiro Sueyoshi	NME	
Shinya Okumura	NME	
Kazuho Yoshida	NME	
Yutaro Murakami	NME	
Takehito Hattori	MIRAI Crew	

(2) Objective

R/V MIRAI is equipped with the Multi Beam Echo Sounding system (MBES; SEABEAM 3012 (L3 Communications ELAC Nautik)). The objective of MBES is collecting continuous bathymetric data along ship's track except shallow depth, to contribute to geological and geophysical studies.

(3) Instruments and Methods

The "SEABEAM 3012" on R/V MIRAI was used for bathymetry mapping during this cruise. To get accurate sound velocity of water column for ray-path correction of acoustic beams, we determined sound velocities at the depth of 6.62m, the bottom of the ship, by a surface sound velocimeter. We made sound velocity profiles based on the observations of CTD, XCTD and Argo float conducted in this cruise by the equation in Del Grosso (1974).

The system configuration and performance are shown in Table 5.1.

Table 5.1: SEABEAM 3012 System configuration and performance

Frequency:	12 kHz
Transmit beam width:	2.0 degree
Transmit power:	4 kW
Transmit pulse length:	2 to 20 msec.
Receive beam width:	1.6 degree
Depth range:	50 to 11,000 m
Number of beams:	301 beams (Spacing mode: Equi-angle)
Beam spacing:	1.5 % of water depth (Spacing mode: Equi-distance)
Swath width:	60 to 150 degrees
Depth accuracy:	< 1 % of water depth (average across the swath)

(4) Preliminary Results

The results will be published after the primary processing.

(5) Data archives

These data obtained in this cruise will be submitted to the Data Management Group of JAMSTEC, and will be opened to the public via “Data Research System for Whole Cruise Information in JAMSTEC (DARWIN)” in JAMSTEC web site.

http://www.godac.jamstec.go.jp/darwin/e

(6) Remarks

1. The following periods, data acquisition was suspended due to the work station trouble.

13:07UTC 06 Nov. 2019 - 13:23UTC 06 Nov. 2019
19:17UTC 06 Nov. 2019 - 19:24UTC 06 Nov. 2019

2. The following periods, data acquisition was suspended due to the shallow sea area.

01:00UTC 07 Oct. 2019 - 23:43UTC 10 Oct. 2019
09:49UTC 26 Oct. 2019 - 07:10UTC 30 Oct. 2019

3. The following periods, data acquisition was suspended due to the observation of microstructure measurement (T-MAP).

18:00UTC 18 Oct. 2019 - 18:20UTC 18 Oct. 2019
23:24UTC 18 Oct. 2019 - 00:09UTC 19 Oct. 2019
06:43UTC 19 Oct. 2019 - 07:13UTC 19 Oct. 2019
10:18UTC 19 Oct. 2019 - 11:10UTC 19 Oct. 2019
14:58UTC 19 Oct. 2019 - 15:29UTC 19 Oct. 2019
23:44UTC 19 Oct. 2019 - 00:09UTC 20 Oct. 2019
07:15UTC 20 Oct. 2019 - 08:08UTC 20 Oct. 2019
11:13UTC 20 Oct. 2019 - 12:18UTC 20 Oct. 2019
16:08UTC 20 Oct. 2019 - 16:33UTC 20 Oct. 2019
21:56UTC 20 Oct. 2019 - 22:22UTC 20 Oct. 2019
04:17UTC 21 Oct. 2019 - 04:42UTC 20 Oct. 2019
09:57UTC 21 Oct. 2019 - 10:30UTC 20 Oct. 2019
14:59UTC 21 Oct. 2019 - 15:28UTC 20 Oct. 2019
16:59UTC 21 Oct. 2019 - 17:21UTC 20 Oct. 2019
05:29UTC 22 Oct. 2019 - 05:55UTC 22 Oct. 2019
09:31UTC 22 Oct. 2019 - 10:06UTC 22 Oct. 2019
14:53UTC 22 Oct. 2019 - 15:18UTC 22 Oct. 2019
16:45UTC 22 Oct. 2019 - 17:09UTC 22 Oct. 2019
23:45UTC 22 Oct. 2019 - 00:12UTC 23 Oct. 2019
05:00UTC 23 Oct. 2019 - 05:41UTC 23 Oct. 2019
08:39UTC 23 Oct. 2019 - 09:16UTC 23 Oct. 2019
12:38UTC 23 Oct. 2019 - 13:09UTC 23 Oct. 2019
15:46UTC 23 Oct. 2019 - 16:13UTC 23 Oct. 2019
21:59UTC 23 Oct. 2019 - 22:26UTC 23 Oct. 2019
02:53UTC 24 Oct. 2019 - 03:16UTC 24 Oct. 2019

09:14UTC 24 Oct. 2019 - 09:51UTC 24 Oct. 2019

14:29UTC 24 Oct. 2019 - 14:50UTC 24 Oct. 2019

16:18UTC 24 Oct. 2019 - 16:43UTC 24 Oct. 2019

00:02UTC 25 Oct. 2019 - 00:29UTC 25 Oct. 2019

08:03UTC 25 Oct. 2019 - 08:44UTC 25 Oct. 2019

00:02UTC 25 Oct. 2019 - 00:29UTC 25 Oct. 2019

23:45UTC 25 Oct. 2019 - 00:06UTC 26 Oct. 2019

22:58UTC 02 Nov. 2019 - 23:29UTC 02 Nov. 2019

5.2. Sea Surface Gravity Measurement

(1) Personnel

Kazutoshi Sato	KIT	-PI
Ryo Oyama	NME	
Souichiro Sueyoshi	NME	
Shinya Okumura	NME	
Kazuho Yoshida	NME	
Yutaro Murakami	NME	
Takehito Hattori	MIRAI Crew	

(2) Objective

The local gravity is an important parameter in geophysics and geodesy. We collected gravity data during this cruise.

(3) Parameters

Relative Gravity [CU: Counter Unit]

[mGal] = (coefl: 0.9946) * [CU]

(4) Instruments and Methods

We measured relative gravity using LaCoste and Romberg air-sea gravity meter S-116 (Micro-g LaCoste, LLC) during the cruise. To convert the relative gravity to absolute one, we measured gravity, using portable gravity meter (Scintrex gravity meter CG-5), at Sekinehama and Hachinohe port as the reference points.

(5) Preliminary Results

Absolute gravity table is shown in Table 5.2

Table 5.2: Absolute gravity table of the MR19-03C cruise

No.	Date	UTC	Port	Absolute Gravity [mGal]	Sea Level [cm]	Ship Draft [cm]	Gravity at Sensor * [mGal]	S-116 Gravity [mGal]
#1	26-Sep-19	06:50	Sekinehama	980371.86	248	622	980372.83	12655.67
#2	11-Nov-19	00:24	Hachinohe	980353.29	262	618	980354.30	12632.49

*: Gravity at Sensor

= Absolute Gravity + Sea Level*0.3086/100 + (Draft-530)/100*0.2222

(6) Observation Log

26 Sep. 2019 to 11 Nov. 2019

(7) Data archives

These data obtained in this cruise will be submitted to the Data Management Group of JAMSTEC, and will be

opened to the public via “Data Research System for Whole Cruise Information in JAMSTEC (DARWIN)” in JAMSTEC web site.
<http://www.godac.jamstec.go.jp/darwin/e>

(8) Remarks

i) The following periods, Depth and Gyro in GRV data were invalid due to the server error.
05:36UTC 29 Sep. 2019
21:48UTC 14 Oct. 2019

ii) The following period, data acquisition were suspended due to the operation PC trouble.
07:43UTC 04 Oct. 2019 - 08:45UTC 04 Oct. 2019

iii) The following period, data were invalid due to the Spring Motor trouble.
15:29UTC 08 Oct. 2019 - 01:00UTC 09 Oct. 2019

5.3. Surface Magnetic Field Measurement

(1) Personnel

Kazutoshi Sato	KIT	-PI
Ryo Oyama	NME	
Souichiro Sueyoshi	NME	
Shinya Okumura	NME	
Kazuho Yoshida	NME	
Yutaro Murakami	NME	
Takehito Hattori	MIRAI Crew	

(2) Objective

Measurement of magnetic force on the sea is required for the geophysical investigations of marine magnetic anomaly caused by magnetization in upper crustal structure. We measured geomagnetic field using a three-component magnetometer during this cruise.

(3) Instruments and Methods

A shipboard three-component magnetometer system (SFG2018, Tierra Tecnica) is equipped on-board R/V MIRAI. Three-axes flux-gate sensors with ring-cored coils are fixed on the fore mast. Outputs from the sensors are digitized by a 20-bit A/D converter (1 nT/LSB), and sampled at 8 times per second. Yaw (heading), Pitch and Roll are measured by the Inertial Navigation System (INS) for controlling attitude of a Doppler radar. Ship's position (Differential GNSS), speed over ground and gyro data are taken from LAN every second.

The relation between a magnetic-field vector observed on-board, Hob, (in the ship's fixed coordinate system) and the geomagnetic field vector, F, (in the Earth's fixed coordinate system) is expressed as:

$$\mathbf{H}_{\mathrm{ob}} = \widetilde{\mathbf{A}}\ \widetilde{\mathbf{R}}\ \widetilde{\mathbf{P}}\ \widetilde{\mathbf{Y}}\ \mathbf{F} + \mathbf{H}_{\mathrm{p}} \qquad \text{(a)}$$

where $\widetilde{\mathbf{R}}$, $\widetilde{\mathbf{P}}$ and $\widetilde{\mathbf{Y}}$ are the matrices of rotation due to roll, pitch and heading of a ship, respectively. $\widetilde{\mathbf{A}}$ is a 3 x 3 matrix which represents magnetic susceptibility of the ship, and $\mathbf{H}_{\mathrm{p}}$ is a magnetic field vector produced by a permanent magnetic moment of the ship's body. Rearrangement of Eq. (a) makes

$$\widetilde{\mathbf{B}}\,\mathbf{H}_{\mathrm{ob}} + \mathbf{H}_{bp} = \widetilde{\mathbf{R}}\ \widetilde{\mathbf{P}}\ \widetilde{\mathbf{Y}}\ \mathbf{F} \qquad \text{(b)}$$

where $\widetilde{\mathbf{B}} = \widetilde{\mathbf{A}}^{-1}$, and $\mathbf{H}_{bp} = -\widetilde{\mathbf{B}}\,\mathbf{H}_{\mathrm{p}}$. The magnetic field, $\mathbf{F}$, can be obtained by measuring , $\widetilde{\mathbf{R}}$, $\widetilde{\mathbf{P}}$, $\widetilde{\mathbf{Y}}$ and $\mathbf{H}_{\mathbf{ob}}$, if $\widetilde{\mathbf{B}}$ and $\mathbf{H}_{bp}$ are known. Twelve constants in $\widetilde{\mathbf{B}}$ and $\mathbf{H}_{\mathbf{bp}}$ can be determined by measuring variation of $\mathbf{H}_{\mathbf{ob}}$ with $\widetilde{\mathbf{R}}$, $\widetilde{\mathbf{P}}$, and, $\widetilde{\mathbf{Y}}$ at a place where the geomagnetic field, $\mathbf{F}$, is known.

(4) Preliminary Results

The results will be published after the primary processing.

(5) Data archives

These data obtained in this cruise will be submitted to the Data Management Group of JAMSTEC, and will be opened to the public via “Data Research System for Whole Cruise Information in JAMSTEC (DARWIN)” in JAMSTEC web site.

<http://www.godac.jamstec.go.jp/darwin/e>

(6) Remarks

1. For calibration of the ship's magnetic effect, we made "figure-eight" turns (a pair of clockwise and anti-clockwise rotation) at the following periods and positions.

05:45UTC - 06:15UTC 12 Oct. 2019 around 73-46N, 145-10W

04:46UTC - 05:15UTC 24 Oct. 2019 around 77-15N, 164-00W

04:00UTC - 04:20UTC 07 Nov. 2019 around 40-18N, 145-59E

2. The following period, Navigation data (Position, COG, SOG LOG, Heading, Depth) were not updated due to the server error.

05:36:11 - 05:36:24UTC 29 Sep. 2019

3. The following periods, data acquisition was stopped.

19:39:54 - 19:40:16UTC 14 Oct. 2019

23:41:03 - 23:42:17UTC 14 Oct. 2019

6. Notice on using

This cruise report is a preliminary but final documentation as of the end of the cruise. This report may not be corrected even if changes on contents (e.g. taxonomic classifications) are found after its publication. This report may also be changed without notice. Data on this cruise report may be raw or unprocessed. If you are going to use or refer to the data written on this report, please ask the Chief Scientist for the latest information. Users of data or results on this cruise report are requested to submit their results to Planning Group, Research Fleet Department, Marine Technology and Engineering Center of JAMSTEC.

E-mail：submit-rv-cruise@jamstec.go.jp